Proseminar on Topological Objects in Physics

ETH Zürich, FS 2014

Supervisor: Dr. Philippe de Forcrand

Contribution list

Chapter 1

Homotopy Theory

Author: Paul Steinmann
Supervisor: Tobias Rindlisbacher

Homotopy theory is the point where the abstract mathematical theory of topology meets geometry. We first start with a basic crash course in basic point set topology. This includes the most important definitions around topology. Afterwards we dive deep into homotopy theory and we will learn how to study some geometrical structure of a space using the introduced theory.

1.1 Basic Topology[2]

1.1.1 Introduction

To understand topology it is a good thing to look at the historical motivation of topology. From analysis the notion of open sets on $\mathbb{R}^n$ is well known. We have useful notions as continuity of maps, compactness, connectedness and several other properties. We would like to look at arbitrary sets and define some similar notions there. For this purpose, topology was introduced. We can think of it as a generalization of the structure of $\mathbb{R}^n$ onto arbitrary sets such that we can define properties as continuity of maps. And as we will see, one can find a rather abstract setting such that on $\mathbb{R}^n$ the new defined structure coincides with the one already known.

Today topology is not only the generalization of such a structure but also a theory that looks at "continuous deformations" of spaces. On Wikipedia, topology is described as follows:

> *Topology is the mathematical study of shapes and spaces. It is an area of mathematics concerned with the properties of space that are preserved under continuous deformations including stretching and bending, but not tearing or gluing.*

With this idea of topology in mind one quickly sees that if a space is continuously deformed by just a bit, the main structure of the space stays the same. One can then prove using topology that we can find a general classification of surfaces in $\mathbb{R}^3$. This is a central element of today's topology.

From this description of topology one does not suspect that topology has a lot in common with differential geometry. The truth is that differential geometry uses a lot of topology, but is a more restrictive theory and has in its heart a similar aim. Where in topology we look at continuous deformations of spaces, in differential geometry we look at differentiable deformations. Where in

topology we also look at spaces without metrics, in differentiable geometry metric spaces are of vital importance. In topology $\mathbb{R}^n$ is an example, where in differential geometry it is essential. Of course, in differential geometry, the restrictions made lead to more geometry, where topology is not necessarily geometrical. Our goal in this text is to treat homotopy theory, which is a part of topology, where one can interpret statements geometrically.

1.1.2 Definitions

The first definition in topology is clearly the one of a topology:

Definition 1.1.1. *A **topology** on a set X is a collection τ of subsets of X having the following properties:*

1. $\emptyset, X \in \tau$
2. $\forall\ (A_\alpha)_{\alpha\in I} \subset \tau\ \Rightarrow\ \bigcup_{\alpha\in I} A_\alpha \in \tau$
3. $\forall\ A_1, \ldots, A_n \in \tau\ \Rightarrow\ \bigcap_{i=1}^{n} A_i \in \tau$

*Then (X, τ) is called a **topological space**.*

With this definition we directly find some examples:

Example 1.1.1.

- *X arbitrary, then $\tau := \{X, \emptyset\}$ is a topology, called the trivial topology.*
- *X arbitrary, then $\tau := \mathcal{P}(X) = \{A \subset X\}$ is a topology, called discrete topology.*

To construct topologies, in particular a useful topology on $\mathbb{R}$, without stating every element explicitly, we need another definition:

Definition 1.1.2. *Let X be a set. A family $\mathfrak{B}$ of subsets of X is called a **basis of a topology** on X if:*

1. $\forall x \in X\ \exists B \in \mathfrak{B}\colon\ x \in B$
2. $B_1, B_2 \in \mathfrak{B},\ x \in B_1 \cap B_2 \Rightarrow \exists B \in \mathfrak{B}\colon\ x \in B \subset B_1 \cap B_2$

Then define $\tau_{\mathfrak{B}} := \{U \subset X | \forall x \in U\ \exists B \in \mathfrak{B}\colon x \in B \subset U\}$.

One can easily proof that $\tau_{\mathfrak{B}}$ is a topology on X. Now we can define the standard topology on $\mathbb{R}^n$:

Example 1.1.2.

- *Let $X = \mathbb{R}^n$ and define $\mathfrak{B} := \{B_r(x) | r > 0,\ x \in X\}$ where $B_r(x)$ is the open ball of radius r around x. $\mathfrak{B}$ is a basis of a topology on X and $\tau_{\mathfrak{B}}$ is called the **standard topology** on $\mathbb{R}^n$.*

One realizes, that for the above example of $\mathbb{R}^n$, the standard topology is exactly the family of open sets of $\mathbb{R}^n$. This follows directly from the definition of an open set in analysis. This leads then to the general definition of an open set:

Definition 1.1.3. *Let (X, τ) be a topological space. An element $A \in \tau$ is called **open** and every set of the form $A^c = X \setminus A$ for $A \in \tau$ is said to be **closed**.*

With this definition we see that we can think of a topology just as the family of open sets. We often denote the topology on a set X as $Open(X)$ so we don't need to mention the topology explicitly.

Another definition that is useful is the one of an open neighbourhood:

Definition 1.1.4. *Let $x \in X$. An **open neighbourhood** of x in X is a $U \in Open(X)$ such that $x \in U$.*

And we can generalize the notions of interior and closure:

Definition 1.1.5. *Let $A \subset X$. The **interior** of A is defined as $A^\circ := \bigcup_{B \subset A,\, B\ open} B$. The **closure** of A is defined as $\overline{A} := \bigcap_{B \supset A,\, B\ closed} B$*

Indeed, the interior is open and the closure is closed.

An important property of a space is compactness. We already know what a compact set in $\mathbb{R}^n$ is from analysis and as a matter of fact we can generalize this notion to arbitrary spaces. The following definitions show that compactness (as every topological property) depends a lot on the topology that we endow our space with.

Definition 1.1.6. *Let X be a topological space. An **open cover** of X is a collection of open subsets $(U_\alpha)_{\alpha \in I} \subset Open(X)$ such that $\bigcup_{\alpha \in I} U_\alpha = X$.*

Definition 1.1.7. *A topological space X is called **compact** if for every open cover $(U_\alpha)_{\alpha \in I}$ of X there is a finite subcover $U_{i_1}, \dots, U_{i_n} \subset (U_\alpha)_{\alpha \in I}$ that still covers X: $\bigcup_{k=1}^{n} U_{i_k} = X$.*

On $\mathbb{R}^n$ this notion of compactness is (as required) equivalent to the one already known (closed and bounded). As said before, compactness depends on the topology. This gets clear as we endow an arbitrary space X with the trivial topology $Open(X) = \{\emptyset, X\}$. Then the space is compact.

We can find several other examples:

Example 1.1.3.

- *Every finite space X with an arbitrary topology is compact, because the topology has only finitely many elements.*
- *A space X with the discrete topology is compact iff X is finite, as points are open in the discrete topology.*
- *$\mathbb{R}$ is not compact: define $U_n = (-n, n)$. Then $\bigcup_{n \in \mathbb{N}} U_n = \mathbb{R}$, but one obviously can't find finitely many U_n that still cover $\mathbb{R}$.*

One of the most important definitions in topology is the one of a continuous map:

Definition 1.1.8. *Let X, Y be two topological spaces. A map $f\colon X \to Y$ is called **continuous** if the preimage of every open set is an open set, so if $\forall\, U \in Open(Y)\colon\ f^{-1}(U) \in Open(X)$*

Example 1.1.4.

- *For a map between two copies of $\mathbb{R}$ with the standard topology, this is equivalent to the other definitions of continuity (see analysis, e.g. [1]).*
- *Let τ_1, τ_2 be two topologies on a space X. $id\colon (X, \tau_1) \to (X, \tau_2)$, $x \mapsto x$ is continuous if and only if $\tau_2 \subset \tau_1$, because for any $U \in \tau_2$ is $id^{-1}(U) = U$, so id is continuous $\Leftrightarrow \forall U \in \tau_2\colon\ U \in \tau_1 \Leftrightarrow \tau_2 \subset \tau_1$.*
- *If X is compact, $f\colon X \to Y$ continuous, then $f(X)$ is compact, too. This statement is very important and powerful for proving compactness of a lot of spaces. It for instance also means that we can't find a continuous surjective map from $[0,1] \subset \mathbb{R}$ to $(0,1) \subset \mathbb{R}$.*

As in algebra with isomorphisms, we look for a notion of "equality" in topology, so for bijective maps that respect the structure. We find it in homeomorphisms:

Definition 1.1.9. *A map $f\colon X \to Y$ between two topological spaces X and Y is called a* ***homeomorphism*** *if it is bijective and if both, f and f^{-1} are continuous.*

A topological property is a property of topological spaces that is preserved under homeomorphisms. Every property we have seen so far is such a topological property. We can use that fact to prove several interesting facts such as the following:

Example 1.1.5.

- *There is no homeomorphism between $S^2 = \{x \in \mathbb{R}^3 | \|x\| = 1\}$ and $\mathbb{R}^2$, as S^2 is compact, where $\mathbb{R}^2$ is not. But there is one between $S^2 \setminus \{(0,0,-1)\}$ and $\mathbb{R}^2$ (even a diffeomorphism): the stereographic projection.*

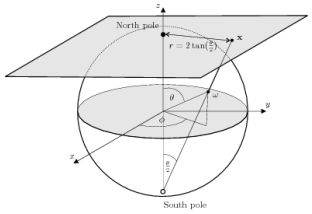

Finally let us introduce paths in topological spaces:

Definition 1.1.10. *Let X be a topological space. A* ***path*** *between $x, y \in X$ is a continuous function $\gamma\colon [0,1] \to X$ such that $\gamma(0) = x,\ \gamma(1) = y$. x is called* ***start point*** *and y is called* ***end point****.*

Definition 1.1.11. *A topological space X is called* ***path connected*** *if for every pair of points $x, y \in X$ there is a path in X connecting x and y.*

It is useful to work in a path connected space, but not every space is path connected. For this purpose we can look at path connected components, so maximally path connected subsets of the space. For instance if we have two disjoint open balls in $\mathbb{R}^n$, this space is not path connected, but we can look at the path connected components - the single balls - separately.

With these basic definitions in topology we can now move on to homotopy theory.

1.2 Homotopy Theory[2],[3]

1.2.1 Definition

Definition 1.2.1. *Let X, Y be two topological spaces and let $f, g\colon X \to Y$ be continuous maps. f and g are called* ***homotopic*** *if there is a continuous map $H\colon [0,1] \times X \to Y$ such that:*

- $\forall\ x \in X\colon\ H(0,x) = f(x)$ *and* $H(1,x) = g(x)$

Then H is called a ***homotopy*** *between f and g.*

One can think of a homotopy as a continuous deformation of the map f to the map g. This idea gets clearer with the following special notion for paths:

Definition 1.2.2. *Two paths $\gamma_0,\ \gamma_1\colon [0,1] \to X$ with $x := \gamma_0(0) = \gamma_1(0)$, $y := \gamma_0(1) = \gamma_1(1)$ are called* ***path homotopic*** *if there is a continuous map $H\colon [0,1] \times [0,1] \to X$ such that:*

1. $\forall\ t \in [0,1]\colon\ H(0,t) = \gamma_0(t),\ H(1,t) = \gamma_1(t)$
2. $\forall\ s \in [0,1]\colon\ H(s,0) = x,\ H(s,1) = y$

Then H is called a ***path homotopy*** *between γ_0 and γ_1.*

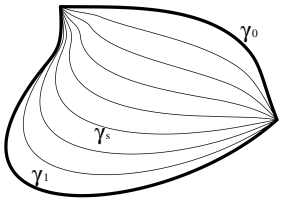

The first condition just means that H is a regular homotopy between γ_0 and γ_1 as maps. The second condition however, is special for paths and means that the starting and ending points are fixed during the homotopy. With the following picture this should get clear:

One can really think of the path homotopy as a continuous family of paths $\gamma_s(t) = H(s,t)$. With this picture in mind we also can understand the more general notion above of homotopy for arbitrary continuous maps.

For two paths where the ending point of the first is the starting point of the second we can define their product:

Definition 1.2.3. *Let $x_0, x_1, x_2 \in X$. If γ_1 is a path from x_0 to x_1 and γ_2 a path from x_1 to x_2 then we define the **product** of γ_1 and γ_2 as:*

$$(\gamma_1 * \gamma_2)(t) = \begin{cases} \gamma_1(2t), & \text{for } t \in [0, \frac{1}{2}] \\ \gamma_2(2t-1), & \text{for } t \in [\frac{1}{2}, 1] \end{cases}$$

A special kind of paths are loops:

Definition 1.2.4. *A **loop** based at $x \in X$ is a path that both starts and ends at x.*

1.2.2 The Fundamental Group

The aforementioned path homotopy is an equivalence relation. We denote the equivalence classes as $[\gamma]$ for a path $\gamma\colon [0,1] \to X$.

Now, as loops are paths too, we can look at equivalence classes of loops. Let $\gamma_1, \gamma_2, \gamma_3$ be loops of X at $x_0 \in X$.

- Define the product on equivalence classes as: $[\gamma_1] * [\gamma_2] = [\gamma_1 * \gamma_2]$. This map is well defined, so it is independent of the representatives of the equivalence classes.
- We have associativity: $([\gamma_1] * [\gamma_2]) * [\gamma_3] = [\gamma_1] * ([\gamma_2] * [\gamma_3])$
- We have an identity: Let $e_{x_0}\colon [0,1] \to X,\ t \mapsto x_0$ be the constant loop. Then we have that $[\gamma_1] * [e_{x_0}] = [\gamma_1] = [e_{x_0}] * [\gamma_1]$.
- We have inverses: define $\gamma_1^{-1}(t) := \gamma_1(1-t)$. This is just the loop going backwards. Then we have that $[\gamma_1] * [\gamma_1^{-1}] = [e_{x_0}] = [\gamma_1^{-1}] * [\gamma_1]$.

Looking at these properties, we see that they are the properties of a group. This justifies the following definition:

Definition 1.2.5. *Let X be a topological space. Let $x_0 \in X$. The group containing all equivalence classes of loops based at x_0 together with the product $*$ is called the **fundamental group** of X at x_0 and is denoted $\pi_1(X, x_0)$.*

Proposition 1.2.1.

- *If X is path connected, $x_0, x_1 \in X$ then $\pi_1(X, x_0) \cong \pi_1(X, x_1)$.*
- *Let X, Y be two homeomorphic spaces with homeomorphism $\varphi\colon X \to Y,\ x \in X,\ y \in Y$ with $\varphi(x) = y$. Then $\pi_1(X, x) \cong \pi_1(Y, y)$.*

The first statement means that the fundamental group is a property of the path connected components of a space. The second one shows us that the fundamental group is another topological property and thus invariant under homeomorphisms.

Definition 1.2.6. *A topological space X is said to be **simply connected** if it is path connected and if for any $x \in X$, the fundamental group is trivial $\pi_1(X, x) \cong \{0\}$.*

Remark 1.2.1.

- *The path connectedness in the definition is important. We don't speak of a simply connected space if it is not path connected, irrespectively of the fundamental group.*
- *A trivial fundamental group is equivalent to the statement that every two paths with the same endpoints are homotopic.*
- *Note that because we require path connectedness, the fundamental group needs to be trivial only at one point in the space to be trivial everywhere.*

To get a feeling of simply connectedness consider the following examples:

Example 1.2.1.

- *$\mathbb{R}^2$ and S^2 are simply connected. For S^2 imagine that if we have a loop going once around the sphere, we can pull it to the side and contract it to a point.*
- *$\mathbb{R}^2 \setminus \{0\}$ and S^1 are not simply connected. For $\mathbb{R}^2 \setminus \{0\}$ a loop around zero can't be continuously deformed into a loop that does not go around zero without passing at some time the point zero. For the circle it is intuitively clear that a loop going once around the circle can't be deformed continuously into the constant loop.*

As an example how to actually use simple connectivity in a proof let us prove the following claim:

Claim. *$\mathbb{R}^2$ is not homeomorphic to $\mathbb{R}^3$.*

Proof. If it were, then $\mathbb{R}^2 \setminus \{0\}$ would be homeomorphic to $\mathbb{R}^3 \setminus \{0\}$. But then, the fundamental groups would coincide, which is not true, as $\mathbb{R}^3 \setminus \{0\}$ is simply connected where $\mathbb{R}^2 \setminus \{0\}$ isn't. □

An important theorem that shows us how to calculate the fundamental group of a space out of the fundamental groups of other spaces says the following:

Theorem 1.2.1. *Let X, Y be two topological spaces and $x_0 \in X,\ y_0 \in Y$.*
Then $\pi_1(X \times Y, (x_0, y_0)) \cong \pi_1(X, x_0) \times \pi_1(Y, y_0)$.

Here we put the product topology on $X \times Y$.

A very important example that uses this fact is the torus:

Example 1.2.2. *The standard torus is defined as $T^2 = S^1 \times S^1$, so we know from the above theorem that $\pi_1(T^2, (x_0, y_0)) \cong \pi_1(S^1, x_0) \times \pi_1(S^1, y_0)$. How to calculate the fundamental group of the circle is shown in the part with covering maps further below.*

The following definition gives rise to a useful concept when dealing with fundamental groups:

Definition 1.2.7. *Two topological spaces X, Y are called **homotopy equivalent**, if there are continuous maps $f\colon X \to Y$ and $g\colon Y \to X$ such that $g \circ f$ is homotopic to $id_x\colon X \to X$ and $f \circ g$ is homotopic to $id_Y\colon Y \to Y$. Then, f and g are called **homotopy equivalences**.*

Homotopy equivalence is an equivalence relation. We say that two spaces that are homotopy equivalent are of the same homotopy type. The notion of homotopy equivalence is a more general one than homeomorphism. Here, spaces don't really look the same but we can deform them such that they look similar. Being more general, it still is enough to show the following:

Theorem 1.2.2. *Let X, Y be two topological spaces of the same homotopy type (i.e. homotopy equivalent) with a homotopy equivalence $f\colon X \to Y$. Then $\pi_1(X, x_0) \cong \pi_1(Y, f(x_0))$ for all $x_0 \in X$.*

That means that we don't need homeomorphisms of spaces to have the same fundamental group. It's enough to have a homotopy equivalence.

1.2.3 Deformation Retract

A special kind of homotopy equivalences are deformation retracts:

Definition 1.2.8. *Let X be a topological space. A subspace $A \subset X$ is called a **deformation retract** of X if there is a continuous map $H\colon [0,1] \times X \to X$ such that:*

1. $\forall\ x \in X\colon\ H(0, x) = x$
2. $\forall\ x \in X\colon\ H(1, x) \in A$
3. $\forall\ s \in [0,1],\ \forall\ a \in A\colon\ H(s, a) = a$

And as a special case of a homotopy equivalence it still holds:

Theorem 1.2.3. *Let X be path connected and let $A \subset X$ be a deformation retract of X and let $x_0 \in A$. Then $\pi_1(A, x_0) \cong \pi_1(X, x_0)$.*

To get a clearer understanding of this rather abstract definition we look at some examples.

Example 1.2.3.

- *Let $X := \mathbb{R}^3 \setminus \{(0,0,z) | z \in \mathbb{R}\}$ and let $A := (\mathbb{R}^2 \setminus \{0\}) \times \{0\}$. Then A is a deformation retract of X with the map $H(s, x, y, z) = (x, y, (1-s)z)$. This is just a sort of collapse of the whole space to the x-y-plane.*
- *Let $X := \mathbb{R}^2 \setminus \{0\}$ be the punctured plane and $A := S^1 \subset X$ be the circle. Then A is a deformation retract of X. We can illustrate the retraction map in the following picture:*

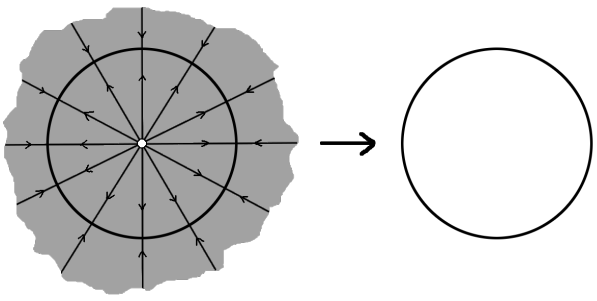

- *The two statements above, together with theorem 1.2.3, show that $\pi_1(\mathbb{R}^3 \setminus \{(0,0,z) | z \in \mathbb{R}\}, x_0) \cong \pi_1(\mathbb{R}^2 \setminus \{0\}, x_0) \cong \pi_1(S^1, x_0)$ for any $x_0 \in S^1$.*

We now can show that a space is simply connected by writing the explicit homotopy, that two spaces have the same fundamental group and we can construct the fundamental groups for products of spaces with known fundamental groups. But until now, we can't calculate a simple non-trivial fundamental group directly. One way to do that uses covering maps.

1.2.4 Covering Maps

Definition 1.2.9. *Let E, B be two spaces. A map $p\colon E \to B$ is called a **covering map** if p is surjective, continuous and there is a discrete space S (e.g. $\mathbb{Z}$) such that for every $b \in B$ there is:*

1. *an open neighbourhood U of b*
2. *a homeomorphism $\varphi\colon p^{-1}(U) \to U \times S$*

such that the following diagram commutes:

$$\begin{array}{ccc} p^{-1}(U) & \xrightarrow{\varphi} & U \times S \\ {\scriptstyle p}\downarrow & \swarrow & \\ U & & \end{array}$$

first proj.

To illustrate this definition consider the following example:

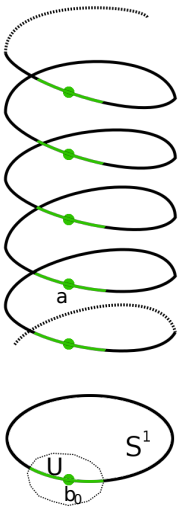

Example 1.2.4.

- *Covering of S^1 with $\mathbb{R}$:*

  We define $p\colon \mathbb{R} \to S^1$ as $p(x) = (\cos(2\pi x), \sin(2\pi x))$. Then p is a covering map: take $b_0 \in S^1$ with $p(a) = b_0$. Then $U = S^1 \cap B_1(b_0)$ is an open neighbourhood and for some $c > 0$: $p^{-1}(U) = \{(a - c + 2\pi n, a + c + 2\pi n) | n \in \mathbb{Z}\}$ which is homeomorphic to $U \times \mathbb{Z}$.

To actually calculate the fundamental group of the circle we need some more definitions:

Definition 1.2.10. *Let $p\colon E \to B$ be a covering map and let $f\colon [0,1] \to B$ be a loop in B. A **lift** of f w.r.t. p is a path $\tilde{f}\colon [0,1] \to E$ such that $p \circ \tilde{f} = f$.*

In general the lift is not a loop itself. It can be only a path. It is very important to have the following proposition:

Proposition 1.2.2. *For a loop $f\colon [0,1] \to B$ with $f(0) = b_0 = p(e_0) \in B$ there is a unique lift with $\tilde{f}(0) = e_0$.*

The proposition justifies the following definition:

Definition 1.2.11. *Let $p\colon E \to B$ be a covering map and let $p(e_0) = b_0 \in B$. The map*

$$\begin{aligned} \phi_{e_0}\colon \pi_1(B, b_0) &\to p^{-1}(b_0) \\ [f] &\mapsto \tilde{f}(1) \end{aligned}$$

*where the lifts start at e_0 is called the **lifting correspondence**.*

This map is well defined, as lifts are uniquely determined by their starting point and the lifting of homotopies is also possible and unique in the above sense.

The main statement of covering maps is then the following theorem.

Theorem 1.2.4. *Let E be simply connected, $p\colon E \to B$ be a covering map and let $p(e_0) = b_0 \in B$. Then the lifting correspondence $\phi_{e_0}\colon \pi_1(B, b_0) \to p^{-1}(b_0)$ is bijective.*

Note that we only have bijectivity here, because $p^{-1}(b_0)$ might not have a special structure on it. But as the following example shows us, there are a lot of situations where we can go further than bijectivity.

Example 1.2.5.

- *Back to the covering of S^1 with $\mathbb{R}$:*

  Let $b_0 = (1, 0) \in S^1, e_0 = 0$. We know already that $p^{-1}(b_0) = \{b_0\} \times \mathbb{Z} \cong \mathbb{Z}$.

- ***Claim**: $\phi_{e_0}\colon \pi_1(S^1, b_0) \to p^{-1}(b_0)$ is a homomorphism*
  ***Proof**: Let $[f], [g] \in \pi_1(S^1, b_0)$ with $\phi_{e_0}([f]) = n$, $\phi_{e_0}([g]) = m$. Now define $\tilde{g}' := n + \tilde{g}$. Then $\tilde{f} * \tilde{g}'$ is a lift of $f * g$ and it ends at $n + m$. Thus $\phi_{e_0}([f * g]) = n + m = \phi_{e_0}([f]) + \phi_{e_0}([g])$.*

□

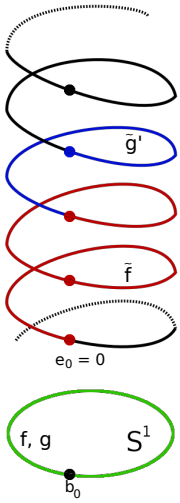

This now means that $\pi_1(S^1, b_0) \cong \mathbb{Z}$

Here are some more examples for spaces and their fundamental groups:

Example 1.2.6.

- *$SU(2)$ is a covering space of $SO(3)$ with the discrete space $S = \{1, -1\}$. As above with the circle, one can show that the lifting correspondence is a homomorphism and thus $\pi_1(SO(3), 1) \cong \{1, -1\}$.*

- *$\pi_1(\mathbb{R}P^1, x_0) = \mathbb{Z}$ and for $n \geq 2$: $\pi_1(\mathbb{R}P^n, x_0) = {}^{\mathbb{Z}}\!/_{2\mathbb{Z}}$*

- *fundamental group of the n-torus: $\pi_1(T^n, x_0) \cong \mathbb{Z}^n$*

- *fundamental group of the n-fold torus:*
  $\pi_1(T^2 \# \ldots \# T^2, x_0) \cong < A_1, \ldots, A_n, B_1, \ldots, B_n \mid (A_1, B_1) \cdot \ldots \cdot (A_n, B_n) = 1 >$[1]

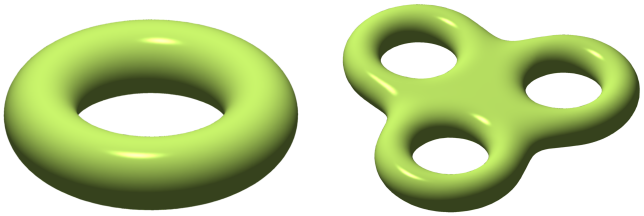

Figure 1.1: The 1-fold and the 3-fold torus

1.2.5 Higher Homotopy Groups[3]

Beside the fundamental group one can define higher homotopy groups that show more of the structure of a space. To define higher homotopy groups we need some more definitions:

Let X be a top. space and $x_0 \in X$ a point. Define $I := [0, 1]$.

[1] The free group with 2n generators modulo the relation on the right hand side.

Definition 1.2.12. *Let $M_n(X, x_0)$ denote the collection of maps $f : I^n \to X$ that collapse the boundary of I^n to x_0 i.e. $f(\partial I^n) = x_0$.*

Definition 1.2.13. *Two maps f, g in $M_n(X, x_0)$ are called **homotopic** in $M_n(X, x_0)$ if there is a homotopy $H\colon [0,1] \times I^n \to X$ of f and g such that $H(s, \cdot)\colon I^n \to X$ is a map in $M_n(X, x_0)$ for every $s \in [0, 1]$ i.e. it also collapses the boundary of I^n to x_0.*

Note that if we have $n = 1$, a map collapsing the boundary is just a loop and the homotopy in $M_n(X, x_0)$ is path homotopy. So the above definition is just a generalization of the concept that lead us to the fundamental group.

As before we define a product:

Definition 1.2.14. *We define the product of two maps f, g in $M_n(X, x_0)$ as follows: for $(t_1, ..., t_n) \in I^n$ let*

$$(f * g)(t_1, ..., t_n) := \begin{cases} f(2t_1, t_2, ..., t_n), & \text{for } t_1 \in [0, \frac{1}{2}] \\ g(2t_1 - 1, t_2, ..., t_n), & \text{for } t_1 \in [\frac{1}{2}, 1] \end{cases}$$

to obtain a new map in $M_n(X, x_0)$.

And again, the notion of homotopy in $M_n(X, x_0)$ is an equivalence relation and the product extends to a product of equivalence relations: $[f] * [g] := [f * g]$.

Definition 1.2.15. *The collection of homotopy classes of $M_n(X, x_0)$, i.e. the equivalence classes w.r.t. being homotopic in $M_n(X, x_0)$ is denoted $\pi_n(X, x_0)$ and is called the **n-th homotopy group** of X at x_0.*

One can easily check that $\pi_n(X, x_0)$ is indeed a group. We notice some facts:

Remark 1.2.2.

- *The first homotopy group is indeed the fundamental group.*
- *Contrary to $n = 1$ higher homotopy groups (i.e. $n \geq 2$) are always abelian. This is not so trivial to see, but the reason lies in the definition of the product, where we only look at the first variable and the others are kept.*

Calculating higher homotopy groups is a lot harder than calculating the fundamental group. Some examples of spaces are provided below.

Example 1.2.7.

- *For $n < k$:* $\pi_n(S^k, x_0) = 0,\ \pi_n(S^n, x_0) \cong \mathbb{Z},\ \pi_{n+2}(S^n, x_0) \cong {}^{\mathbb{Z}}\!/_{2\mathbb{Z}}$
- $\pi_7(S^4, x_0) \cong \mathbb{Z} \times {}^{\mathbb{Z}}\!/_{12\mathbb{Z}}$
- $\pi_n(\mathbb{R}P^n, x_0) \cong \mathbb{Z}$

As a matter of fact, there is until now no formula known to calculate $\pi_m(S^n, x_0)$ for arbitrary $m > n \in \mathbb{N}$.

Bibliography

[1] Vladimir A. Zorich, übersetzt von J. Schüle, *Analysis I*, Springer-Verlag 2006.

[2] James R. Munkres, *Topology, 2nd ed.*, Pearson Education Inc. 2000.

[3] Allen Hatcher, *Algebraic Topology*, Cambridge University Press 2001.

[4] R. Kenna, *Homotopy in statistical physics*, 2008, cond-mat/0602459.

Chapter 2

An introduction to Lie algebras

Author: Oliver Baldacchino
Supervisor: Jonathan Skowera

An elementary introduction to Lie algebras is provided, through coverage of both basic theory notions and several examples. The presentation of the material follows a (hopefully) clear logical and deductive path, which mainly focuses on the conceptual underlying ideas, rather than on mathematical rigour and formalism. That is the reason why many proofs were wittingly omitted or presented in abbreviated form.
In the first section we establish the fundamental relationship between a Lie group and the corresponding Lie algebra, by showing how an analysis of the latter enormously simplifies that of the former, and therefore considering the possibility of characterizing both objects on a "local" level. This connection is made somewhat more quantitative by the discourse on the exponential map, which we examine next.
The second section first introduces some necessary definitions about particular types of Lie algebras, and then turns to the important case of simple and semisimple Lie algebras, which, by virtue of the relevant properties they have, allow a further simplification of the original problem of studying general Lie groups and associated Lie algebras.
In the third and final section we examine a particular example of semisimple Lie algebra, namely $\mathfrak{su}(2)$, and determine all its finite dimensional irreducible representations, basing on the results outlined in the previous paragraphs.

2.1 Lie groups and Lie algebras: basic facts

2.1.1 The route from Lie groups to Lie algebras

Definition 2.1.1 (Lie group)**.** *A real (resp. complex) Lie group G is a C^∞-differentiable manifold (resp. complex manifold), with the additional structure of a group, whose binary product $* : G \times G \to G$ and inverse operation $a \mapsto a^{-1}$ $(a \in G)$ are differentiable (resp. holomorphic) maps.*

Probably the most important and familiar example of a Lie group is given by:

Example 2.1.1 (General linear group)**.** The general Linear group, defined as

$$GL_n(\mathbb{K}) := \{A \in M(n, \mathbb{K}) : \det A \neq 0\}$$

endowed with the usual matrix product, is a Lie group.
Here $\mathbb{K}$ is some field (usually but not necessarily $\mathbb{K} = \mathbb{R}$ or $\mathbb{C}$), and $M(n, \mathbb{K})$ denotes the set of $n \times n$ matrices with entries in this field.

If V is a finite n-dimensional $\mathbb{K}$-vector space, the set of its automorphisms

$$\mathrm{Aut}(V) = \{f \in \mathrm{End}(V) : f \text{ is invertible}\},$$

endowed with the composition operation, is also a Lie group. Since $V \cong \mathbb{K}^n$, a choice of a basis for V brings us back to $GL_n(\mathbb{K})$ itself (because of the connection between an abstract linear map and the associated matrix in a given basis).

Other examples of Lie groups can be readily obtained by considering subsets of the general linear group:

Example 2.1.2 (Other Lie groups)**.**

- the special linear group

$$SL_n(\mathbb{R}) := \{A \in M(n, \mathbb{R}) : \det A = 1\};$$

- the orthogonal and special orthogonal matrices

$$O(n) := \{A \in M(n, \mathbb{R}) : AA^T = A^T A = \mathbb{I}\}$$
$$SO(n) := \{A \in O(n) : \det(A) = 1\}$$

  as well as their complex counterparts, namely the unitary and special unitary groups:

$$U(n) := \{A \in M(n, \mathbb{C}) : AA^\dagger = A^\dagger A = \mathbb{I}\}$$
$$SO(n) := \{A \in U(n) : \det(A) = 1\}.$$

- the upper-triangular matrices;
- the Euclidean space $(\mathbb{R}^n, +)$ with the usual vector addition;
- the Lorentz group of linear isometries of the Minkowski space;
- the n-dimensional sphere S^n, for $n = 0, 1, 3$, i.e. $S^0 = \{\pm 1\}$, $S^1 = \{z \in \mathbb{C} : |z| = 1\}$ and $S^3 \cong \{z \in \mathbb{H} : |z| = 1\}$ (with the usual product of real numbers, complex numbers and quaternions respectively).

A relevant branch of modern Lie theory is concerned with the study of how Lie groups act on and transform geometrical objects like (in the simplest cases) differentiable manifolds or vector spaces. From an historical point of view, this problematic is consistent, and perhaps even followed, the central point of F. Klein's *Erlangen program* (1872), according to which understanding geometry essentially consisted in characterizing those transformations with respect to which an object of interest is left invariant (i.e. when there is a "symmetry").
This task can be greatly simplified in the particular case of Lie groups by examining their action at a local level or, in other words, by looking at the *infinitesimal generators* of this very action. This strikingly innovative approach was suggested and introduced by Sophus Lie (1842-1899), after which the theory we are dealing with is named.

In fact, as we are going to show in the following pages, certain classes of Lie groups and homomorphisms between them can be fully described in a local way, i.e. with no loss of information (for our purposes) occurring in the global–local passage.

Proposition 2.1.1 (Local generation of Lie groups)**.** *If G is a connected Lie group and $U_e \subset G$ is a neighbourhood of the identity, then U_e generates G.*

Definition 2.1.2 (Lie group homomorphism)**.** *A homomorphism ρ between two Lie groups G and H is a map $\rho : G \to H$ which is C^∞ and satisfies $\rho(g\,h) = \rho(g)\,\rho(h)$ for every $g, h \in G$.*

Theorem 2.1.1 (Local characterizability of homomorphisms)**.** *A Lie group-homomorphism $\rho : G \to H$ with G connected, is uniquely determined by its differential $\mathrm{d}\rho_e : T_eG \to T_eH$ at the identity e.*

Remark 2.1.1.

1) Proposition 1.1.1 can be understood in the usual group–theoretical sense: every element $g \in G$ can be written as a finite product $a_1 * a_2 * \cdots * a_n$ with $a_i \in U_e$.
   Also notice the connectedness assumption.

2) For a homomorphism as in definition 1.1.2, the identity element in G is mapped onto the identity element in H, as

$$\rho(e_G) = \rho(e_G)\,\rho(e_G) \;\Rightarrow\; \rho(e_G) = e_H.$$

   Hence (if the groups are connected) we can reconstruct $H \supseteq \mathrm{Image}(\rho)$ from $\rho(U_{e_G}) = U_{e_H}$.

3) The ambiguous expression "is uniquely determined" in theorem 1.1.1 will be clarified in section 1.1.2. For now it simply means that a knowledge of the differential $\mathrm{d}\rho_e$ permits to fully reconstruct the homomorphism ρ.

A new problematic naturally arises now that we have acknowledged the local characterizability of both (connected) Lie groups and their homomorphisms: if we just consider the tangent spaces at the identity of the involved Lie groups, which linear maps $L : T_eG \to T_eH$ actually originate from a homomorphism $\rho : G \to H$ between the corresponding Lie groups?
The answer to this question, which is provided below, will let the structure of a Lie algebra emerge gradually, and that will eventually lead us to the its very definition.

(i) Let $\Psi_g : G \to G$ with $\Psi_g(h) = g\,h\,g^{-1}$ be the family of conjugation automorphisms.
For an homomorphism ρ as above the following clearly holds:

$$\rho \circ \Psi_g = \Psi_{\rho(g)} \circ \rho \tag{2.1}$$

(this follows from $\rho(ghg^{-1}) = \rho(g)\rho(h)\rho(g)^{-1}$).

(ii) We now differentiate (1.1) at the identity:

$$\mathrm{d}\rho_e \circ \mathrm{d}\Psi_g|_e = \mathrm{d}\Psi_{\rho(g)}|_e \circ \mathrm{d}\rho_e \tag{2.2}$$

(iii) Define the **adjoint representation** as

$$\mathrm{Ad} : G \to \mathrm{Aut}(T_eG) \quad \text{s.t.} \quad \mathrm{Ad}(g) = \mathrm{d}\Psi_g|_e$$

and rewrite condition (1.2) accordingly:

$$\mathrm{d}\rho_e \circ \mathrm{Ad}(g) = \mathrm{Ad}(\rho(g)) \circ \mathrm{d}\rho_e.$$

(iv) Define the differential at the identity of Ad as:

$$\mathrm{ad} := \mathrm{d}(\mathrm{Ad})|_e : T_eG \to T_e\left(\mathrm{Aut}(T_eG)\right) \cong \mathrm{End}(T_eG).$$

This can be seen as a bilinear map $T_eG \times T_eG \to T_eG$, for which we employ the notation:

$$\mathrm{ad}(X, Y) =: [X, Y] \qquad \forall X, Y \in T_eG$$

(v) Differentiate (1.1) a second time (or (1.2) just once) to obtain:

$$\mathrm{d}\rho_e \circ \mathrm{ad}(X) = \mathrm{ad}\big(\mathrm{d}\rho_e(X)\big) \circ \mathrm{d}\rho_e$$

from which, evaluating in $Y \in T_eG$ and using the previous definition, we get

$$\boxed{\mathrm{d}\rho_e([X,Y]) = [\mathrm{d}\rho_e(X), \mathrm{d}\rho_e(Y)].} \tag{2.3}$$

Equation (1.3) is finally the relation we were looking for, and which in turns answer our earlier question about a linear map L deriving from a homomorphism ρ.

Remark 2.1.2.

1. Condition (1.3) is usually referred to as "preservation of the brackets" property of some function (in our case $\mathrm{d}\rho_e$). Furthermore it is equivalent to the commutativity of the following diagram:

$$\begin{array}{ccc} T_eG & \xrightarrow{\mathrm{d}\rho_e} & T_eH \\ \Big\downarrow{\scriptstyle \mathrm{ad}} & & \Big\downarrow{\scriptstyle \mathrm{ad}(\mathrm{d}\rho_e)} \\ T_eG & \xrightarrow[\mathrm{d}\rho_e]{} & T_eH \end{array}$$

2. The role of L in the previous derivation is played, of course, by the differential $\mathrm{d}\rho_e$. Notice that we have reduced ourselves to a condition involving this latter only, since this, according to theorem 1.1.1, has to provide complete information about the underlying homomorphism.

3. The conclusion we were led to, is merely a necessary condition. It turns out, but we will not prove it here, that it is also a sufficient one, or equivalently that

$$\begin{gathered} L \text{ satisfies (1.3)} \\ \Longleftrightarrow \\ \exists\, \text{hom. } \rho : G \to H \text{ s.t. } L = \mathrm{d}\rho_e \end{gathered}$$

Our previous discussion motivates the introduction of the object of our main interest:

Definition 2.1.3 (Lie algebra)**.** *A Lie algebra V is a finite dimensional vector space endowed with a bilinear map $[\cdot,\cdot] : V \times V \to V$ (the so-called "brackets") such that for every $X, Y, Z \in V$*

- $[X,Y] = -[Y,X]$ *(skew-symmetry)*
- $[X,[Y,Z]] + [Z,[X,Y]] + [Y,[Z,X]] = 0$
  (Jacobi identity).

Remark 2.1.3. As we have seen, the tangent space at the identity of a Lie group G naturally possesses the structure of a Lie algebra $\mathfrak{g}$, whose brackets are given by the previously defined $\mathrm{ad}(\cdot,\cdot)$, and which satisfy (even though that might not be obvious at first sight) both of the above requirements [1]. Hence we reasonably speak of a Lie algebra *associated* to a Lie group.
The standard notation for Lie algebras employs the Fraktur typeface, e.g. $\mathfrak{g}, \mathfrak{h}, \mathfrak{m}, \ldots$ for Lie algebras associated to Lie groups $G, H, M, \ldots$

[1] actually, as we will see in section 1.2, the Jacobi identity is introduced as a sort of ad hoc hypothesis motivated by reasons of self-consistency.

2.1.2 The exponential map

Given some Lie group G with corresponding Lie algebra $\mathfrak{g}$, we have seen how to pass from the former to the latter, namely by simply determining the tangent space at the identity of G and employing the adjoint map as bracket operation. The inverse transition is also possible and is expressed quantitatively through the exponential map.

Definition 2.1.4 (Exponential map)**.** *Let G be a Lie group and $\mathfrak{g}$ its Lie algebra. The exponential map is given by:*

$$\begin{aligned} \exp : \mathfrak{g} &\to G \\ X &\mapsto \exp(X) := \varphi_X(1) \end{aligned}$$

where $\varphi_X : I \subset \mathbb{R} \to G$ is the unique geodesic through $\mathbb{I} = \varphi_X(0)$ s.t. $\varphi'_X(0) = X$.

The heuristic idea which lies behind this definition is that to every straight line in $\mathfrak{g}$ – which is a vector space (and hence flat)–, i.e. a vector X, we can associate a straight line in G (seen as a manifold), i.e. a geodesic. This association is possible in general only locally; however the additional group structure of G, allows us to extend it to a global level, so as to be able to enlarge the domain of definition to the whole Lie algebra $\mathfrak{g}$ (rather than to a neighbourhood of the origin $0 \in \mathfrak{g}$).

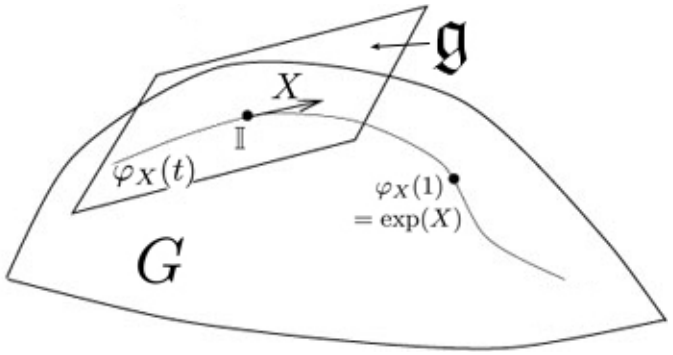

Figure 2.1: Visual explanation of definition 1.1.4. φ_X is the unique geodesic in G (i.e. locally the shortest path between two points), satisfying $\varphi_X(0) = \mathbb{I} \in G$ and $\varphi'_X(0) = X \in \mathfrak{g}$. The choice of $t = 1$ in the definition is just a matter of convention.

Next we examine the most relevant properties of the exponential map. Among them, the following one formalizes the association argument we have just mentioned.

Theorem 2.1.2 (Fundamental property of exp)**.** *The exponential map is the unique map from $\mathfrak{g}$ to G taking 0 to $\mathbb{I}$, whose differential at 0, namely $(\exp_*)_0 : T_0\mathfrak{g} = \mathfrak{g} \to T_{\mathbb{I}}G = \mathfrak{g}$, is the identity map, and whose restriction to lines through the origin $0 \in \mathfrak{g}$ are geodesics trough $\mathbb{I} \in G$.*

A major consequence of this theorem is that, by virtue of a standard result in differential geometry, there is a neighbourhood U of $0 \in \mathfrak{g}$ and a neighbourhood V of $\exp(0) = \mathbb{I}$ such that

$$\exp\big|_U : U \subseteq \mathfrak{g} \to V \subseteq G$$

is a diffeomorphism (i.e. a bijective and differentiable map with differentiable inverse).
This in turn implies the (local) commutativity of the following diagram.

$$\begin{array}{ccc} \mathfrak{g} & \xrightarrow{\psi_*} & \mathfrak{h} \\ \exp \downarrow & & \downarrow \exp \\ G & \xrightarrow[\psi]{} & H \end{array}$$

Other properties of the exponential map are listed hereunder.

Proposition 2.1.2 (Properties of exp)**.**

- $\exp\big((s+t)X\big) = \exp(sX)\exp(tX)$
- $\exp(-X) = \big(\exp(X)\big)^{-1}$
- *If G is a compact Lie group, then* exp *is surjective onto its identity component.*

Proposition 2.1.3 (exp for a matrix Lie group)**.** *If $G \subseteq GL_n(\mathbb{K})$ is a Lie group* [2]*, then, for all $X \in G$*

$$e^X := \exp(X) = \sum_{k=0}^{\infty} \frac{X^k}{k!} = \mathbb{I} + X + \frac{X^2}{2!} + \frac{X^3}{3!} + \dots$$

$$\det(e^X) = e^{trX}.$$

Remark 2.1.4. The last equality in proposition 1.1.3 is of great importance, especially in deriving concrete examples of Lie algebras, as we are going to do in the next section. It can be proved by the following argument: if $A \in M(n,\mathbb{K})$ is diagonalizable, and M is the change of basis matrix from some arbitrary basis to the diagonalizing one, then $\exp(A) = M^{-1}\operatorname{diag}(e^{\lambda_1}, e^{\lambda_2}, \dots, e^{\lambda_n})\, M$ (λ_i: eigenvalues of A). Therefore $\det(e^A) = e^{\operatorname{tr}A}$. The set $\{A \in M(n,\mathbb{K}) : A \text{ is diagonalizable}\}$ is dense in $M(n,\mathbb{K})$ and the function $\det(e^{(\cdot)}) - e^{\operatorname{tr}(\cdot)}$ is continuous. Finally, the identity principle for continuous functions completes the proof.

2.1.3 Examples of Lie algebras

Among the examples covered in this section we are going to deal only with Lie algebras associated to subgroups of $GL_n(\mathbb{K})$ (see examples 1.1.1 and 1.1.2), both because their exemplification is particularly accessible, and because they are probably the most relevant for applications.

Example 2.1.3 (Real general linear group)**.** The Lie algebra associated to $G := GL_n(\mathbb{R})$ is given by $\mathfrak{gl}_n(\mathbb{R}) = \operatorname{End}(\mathbb{R}^n)$, with the bracket operation $[X,Y] = XY - YX$ for all $X, Y \in \mathfrak{gl}_n(\mathbb{R})$.

Proof.

- By construction $\mathfrak{gl}_n(\mathbb{R}) = T_{\mathbb{I}}G$. Moreover, $\dim G = \dim T_eG = n^2 = \dim\big(\operatorname{End}\big(\mathbb{R}^n\big)\big)$, and $T_eG \subset \operatorname{End}(\mathbb{R}^n)$. Therefore, since both T_eG and $\operatorname{End}(\mathbb{R}^n)$ are vector spaces, they must coincide (inclusion and equal dimensions).
- Following the general steps outlined in the previous section (points (i)–(v)), we first compute the adjoint representation (Ad) of G, and the adjoint map (ad) it induces on $T_{\mathbb{I}}G$.
  In what follows we employ the definition of differential of a map φ between two (differentiable) manifolds M and N: the differential of φ at $x \in M$, is given by

$$\begin{aligned} \mathrm{d}\varphi_x : T_xM &\to T_{\varphi(x)}N \\ \gamma'(0) &\mapsto (\varphi \circ \gamma)'(0) \end{aligned}$$

  where $\gamma : I \subset \mathbb{R} \to M$ is a differentiable path such that $\gamma(0) = x$. A simple calculation shows that if $\Psi_g(M) = gMg^{-1}$ for $g, M \in G$, then $\operatorname{Ad}(g)(M) = \mathrm{d}(\Psi_g)|_{\mathbb{I}}(M) = gMg^{-1}$.
  Differentiating a second time at $\mathbb{I}$ we get:

$$\begin{aligned} [X,Y] := \operatorname{ad}(X)(Y) &= \frac{\mathrm{d}}{\mathrm{d}t}\big(\operatorname{Ad}(\gamma(t))(Y)\big)\Big|_{t=0} \\ &= \gamma'(0)\, Y\, \gamma(0) + \gamma(0)\, Y\, (-\gamma(0)^{-1}\, \gamma'(0)\, \gamma(0)^{-1}) \\ &= XY - YX \end{aligned}$$

  where γ is a path as above with $M = G$, $x = \mathbb{I}$ and additionally $\gamma'(0) = X \in T_{\mathbb{I}}G$.

[2] in which case it is called a *matrix Lie group.*

□

As regards the determination of Lie algebras relative to subgroups of $GL_n(\mathbb{K})$, we make use of the procedure described hereunder.

1) Let $M = \{A \in M(n,\mathbb{K}) : P(A) = 0\}$ be a Lie group whose elements are defined through the property $P(A) = 0$.

2) Choose a differentiable path
$$\gamma : I \subseteq \mathbb{R} \to M$$
such that $\gamma(0 \overset{!}{\in} I) = \mathbb{I}$.

3) Differentiate the defining relation $P(A) = 0$:
$$0 = \frac{\mathrm{d}}{\mathrm{d}t} P\big(\gamma(t)\big)\Big|_{t=0} = \gamma'(0)\, \frac{\mathrm{d}P}{\mathrm{d}A}\Big|_{\gamma(0)=\mathbb{I}}$$
$$\overset{\text{def.}}{\iff} \quad \mathfrak{p}\big(\gamma'(0)\big) = 0$$
obtaining a new defining relation $\mathfrak{p}$ which is a function of $\gamma'(0)$ only (for that we also use $\gamma(0) = \mathbb{I}$). Define a new set accordingly:
$$\mathfrak{m} = \{A \in M(n,\mathbb{K}) : \mathfrak{p}(A) = 0\}$$

4) The Lie algebra $\mathrm{Lie}(M)$ of M consists of the tangent vectors at the identity in M. Hence the previous steps imply $A \in \mathrm{Lie}(M) \Rightarrow A \in \mathfrak{m}$, i.e. $\mathrm{Lie}(M) \subseteq \mathfrak{m}$.

5) We now prove the opposite inclusion. Let $A \in \mathfrak{m}$ and define another path:
$$\begin{aligned} \gamma_A : I_A \subseteq \mathbb{R} &\to M \\ t &\mapsto e^{tA} \end{aligned}$$
Now first check that indeed $\gamma_A(t) \in M$, i.e. that $P(\gamma_A(t)) = 0$ using the defining relation of $\mathfrak{m}$, i.e. $\mathfrak{p}(A) = 0$. Finally notice that A can be written as a tangent vector to the identity in M, as
$$\frac{\mathrm{d}}{\mathrm{d}t}\big(\gamma_A(t)\big)\Big|_{t=0} = Ae^{tA}\Big|_{t=0} = A.$$
Thus it follows: $\mathfrak{m} \subseteq \mathrm{Lie}(M)$.

6) Final result:
$$\mathrm{Lie}(M) = \mathfrak{m} = \{A \in M(n,\mathbb{K}) : \mathfrak{p}(A) = 0\}$$

We now apply the outlined procedure to the cases of the "normal" and special (both real and complex) orthogonal groups, i.e. to $O(n)$, $U(n)$, $SO(n)$, $SU(n)$.

Example 2.1.4 (Special orthogonal groups)**.** The Lie algebras associated to $SO(n)$ and to $SU(n)$ are given by
$$\mathfrak{so}(n) = \{A \in M(n,\mathbb{R}) : A + A^T = 0\}$$
$$\mathfrak{su}(n) = \{A \in M(n,\mathbb{C}) : A + A^\dagger = 0,\ \mathrm{tr}(A) = 0\}$$
respectively.

Proof. Let $\# = T, \dagger$ denote the operation of either transposition or of conjugate transposition of a matrix (with real or complex entries respectively). Then the special orthogonal groups mentioned in the example 1.1.2, have a defining property

$$P(A) = \begin{pmatrix} AA^{\#} - \mathbb{I} = A^{\#}A - \mathbb{I} \\ \det(A) - 1 \end{pmatrix} = \begin{pmatrix} 0 \\ 0 \end{pmatrix}.$$

Let's now consider each row separately. For the first one we have, with $\gamma : I \subset \mathbb{R} \to G$ (where $G = SO(n) \vee SU(n)$) and $\gamma(0) = \mathbb{I}$,

$$\begin{gathered} \gamma(t)\gamma(t)^{\#} = \mathbb{I} \quad \Rightarrow \\ \frac{\mathrm{d}}{\mathrm{d}t}\big(\gamma(t)\gamma(t)^{\#}\big)\Big|_{t=0} = \gamma'(0) + \gamma'(0)^{\#} = 0. \end{gathered}$$

For the second one we get:

$$\begin{gathered} \det\big(\gamma(t)\big) = 1 \quad \Rightarrow \\ \frac{\mathrm{d}}{\mathrm{d}t}\Big(\det\big(\gamma(t)\big)\Big)\Big|_{t=0} = \frac{\mathrm{d}}{\mathrm{d}t}\Big(\sum_{\sigma\in S_n} \operatorname{sgn}(\sigma) \prod_{i=1}^{n} \gamma_{i,\sigma(i)}(t)\Big)\Big|_{t=0} \\ = \sum_{\sigma\in S_n} \operatorname{sgn}(\sigma) \sum_{j=1}^{n} \gamma'_{j,\sigma(j)}(0) \prod_{\substack{i=1 \\ i\neq j}}^{n} \underbrace{\gamma_{i,\sigma(i)}(0)}_{=\delta_{i,\sigma(i)}} = \sum_{j=1}^{n} \gamma'_{j,j}(0) \\ = \operatorname{tr}\big(\gamma'(0)\big) = 0. \end{gathered}$$

Hence we obtain:

$$\mathfrak{p}(A) = \begin{pmatrix} A + A^{\#} \\ \operatorname{tr}(A) \end{pmatrix} = \begin{pmatrix} 0 \\ 0 \end{pmatrix}$$

and accordingly $\mathfrak{g}_{\#} := \{A \in M(n, \mathbb{K}) : \mathfrak{p}(A) = 0\}$.

Now let $A \in \mathfrak{g}_{\#}$ and define $\tilde{\gamma} : \tilde{I} \ni t \mapsto e^{tA} \in G$.
Indeed $e^{tA} \in G$, as

$$\begin{gathered} e^{tA}\big(e^{tA}\big)^{\#} = e^{tA}e^{tA^{\#}} = e^{tA}e^{-tA} = \mathbb{I} \\ \text{and} \quad \det(e^{tA}) = e^{t\operatorname{tr}(A)} = e^{0} = 1 \end{gathered}$$

Moreover

$$\frac{\mathrm{d}}{\mathrm{d}t}\big(\tilde{\gamma}(t)\big)\Big|_{t=0} = Ae^{tA}\Big|_{t=0} = A$$

We conclude $\mathfrak{g}_{\#}$ = Lie algebra of G.
Notice that in the case of $SO(n)$ the condition on the trace is redundant, as it is already implied by the antisimmetry, which requires all the (real) diagonal terms of every $A \in \mathfrak{so}(n)$ to vanish.

□

Example 2.1.5 (Orthogonal groups)**.** The Lie algebras associated to $O(n)$ and to $U(n)$ are given by

$$\begin{gathered} \mathfrak{o}(n) = \mathfrak{so}(n) = \{A \in M(n, \mathbb{R}) : A + A^{T} = 0\} \\ \mathfrak{u}(n) = \{A \in M(n, \mathbb{C}) : A + A^{\dagger} = 0\} \end{gathered}$$

respectively.

Proof. The same as the previous one, neglecting the condition on the determinant/trace. □

Remark 2.1.5.

1. All of the above mentioned Lie algebras have the commutator of matrices as bracket operation (see example 1.1.3).

2. The found Lie algebras are real vector spaces with dimensions given by:

$$\dim_{\mathbb{R}}\big(\mathfrak{so}(n)\big) = \dim_{\mathbb{R}}\big(\mathfrak{o}(n)\big) = \frac{n(n-1)}{2}$$
$$\dim_{\mathbb{R}}\big(\mathfrak{u}(n)\big) = n^2\,, \quad \dim_{\mathbb{R}}\big(\mathfrak{su}(n)\big) = n^2 - 1.$$

Example 2.1.6 (Symplectic group)**.** The symplectic group (which is a real Lie group) is defined as

$$Sp(2n,\mathbb{R}) = \{A \in M(2n,\mathbb{R}) : A^T J A = J\}$$
$$\text{where } J = \begin{pmatrix} 0 & \mathbb{I}_n \\ -\mathbb{I}_n & 0 \end{pmatrix}$$

and the corresponding Lie algebra is given by:

$$\mathfrak{sp}(2n) = \{A \in M(2n,\mathbb{R}) : A^T J + JA = 0\}.$$

Proof. Apply the described general procedure taking the following into account:

$$J^{-1} = -J = J^T \quad \text{and} \quad Je^M J^{-1} = \exp(JMJ^{-1}).$$

□

2.2 Representation theory of Lie algebras

2.2.1 Definitions and first results

Definition 2.2.1 (Representation of a group)**.** *A representation (ρ, V) of a group G on the vector space V is a map*

$$\rho : G \to Aut(V)$$

such that $\rho(gh) = \rho(g)\rho(h)$ for every $g, h \in G$.

Definition 2.2.2 (Representation of a Lie algebra)**.** *A representation (π, V) of a Lie algebra $(\mathfrak{g}, [\cdot, \cdot])$ on the vector space V is a linear map*

$$\pi : \mathfrak{g} \to \mathfrak{gl}(V) = End(V)$$

which preserves the brackets, i.e. such that,

$$\pi[X, Y] = [\pi(X), \pi(Y)]$$

for every $X, Y \in \mathfrak{g}$.

A connection between the two kinds of representation can be established by making use of the results about the exponential map (section 1.1.2), and assuming a couple of extra conditions are satisfied.

Proposition 2.2.1 (Correspondence of representations)**.** *Let V be a finite dimensional $\mathbb{K}$-vector space with char$(\mathbb{K}) = 0$, and G a simply connected Lie group with associated Lie algebra $\mathfrak{g}$.*
Then there is a one-to-one correspondence between the representations of G and those of $\mathfrak{g}$.

Proof. Aut(V) is a Lie group since it is both a vector space (and therefore a "flat" manifold), and a group with respect to the composition operation.
End(V) is, of course, a vector space. Moreover, since V is finite dimensional, we have Aut$(V) \cong GL_n(\mathbb{K})$, and hence the bracket operation on End(V) is induced by the commutator of matrices in $GL_n(\mathbb{K})$, i.e. $[X, Y] = X \circ Y - Y \circ X$ for all $X, Y \in$ End(V) ($\circ$ = composition of endomorphisms).
So we only need apply theorem 1.1.2 and the resulting implications to the particular case in which $H =$ Aut(V) and $\mathfrak{h} =$ End(V). If ρ and π are representations of G and $\mathfrak{g}$ respectively, then the commutative diagram associated to theorem 1.1.2 takes the form:

$$\begin{array}{ccc} \mathfrak{g} & \xrightarrow{\pi = \mathrm{d}\rho_e} & \mathrm{End}(V) \\ \Big\downarrow \exp & & \Big\downarrow \exp \\ G & \xrightarrow[\rho]{} & \mathrm{Aut}(V) \end{array}$$

what finally allows us to state the sought correspondence between the two types of representations. □

We now present a very special case of representation of Lie algebras, and which we are going to make extensive use of in the next section.

Example 2.2.1 (Adjoint representation)**.** The adjoint map "ad" (defined in section 1.1.1) induces the so-called *adjoint representation* of a Lie algebra $\mathfrak{g}$:

$$\begin{array}{rcl} \mathrm{ad} : \mathfrak{g} & \to & \mathfrak{gl}(\mathfrak{g}) \\ X & \mapsto & \mathrm{ad}(X) = [X, \cdot] \in \mathrm{End}(\mathfrak{g}) \end{array}$$

The requirement $\mathrm{ad}[X,Y] = [\mathrm{ad}(X), \mathrm{ad}(Y)]$ is equivalent to the Jacobi identity (which we have postulated to hold for all Lie algebras).
In regard to the above *correspondence* argument, this representation corresponds to the representation "Ad" of the Lie group G:

$$\mathrm{Ad} : G \to \mathrm{Aut}(\mathfrak{g})$$

Notice that for both ad and Ad the representation space is given by the Lie algebra itself: $V = \mathfrak{g}$.

We are now ready to take a step forward in the analysis of Lie algebras, and, indirectly, of the associated Lie groups, by performing a further simplification of our original problem, whose treatment has been greatly facilitated, as mentioned already, by the local study of the involved structures. In what follows, we will concentrate on a special class of Lie algebras, namely (complex) simple and semisimple Lie algebras, whose useful "regularity" properties permit us to more easily classify their structure and representations.

Definition 2.2.3 (Lie subalgebra and ideal)**.** *Let $\mathfrak{g}$ be a Lie algebra. A set $\mathfrak{h} \subset \mathfrak{g}$ is a Lie subalgebra if*

$$[X,Y] \in \mathfrak{h} \quad \forall X, Y \in \mathfrak{h}$$

(i.e. it is closed under the brackets).
The set $\mathfrak{h}$ is called an ideal if the above closure relation holds for every $X \in \mathfrak{h}$ and $Y \in \mathfrak{g}$.

Remark 2.2.1. In regards to the $\mathfrak{g} - G$ *correspondence* framework discussed earlier, an ideal $\mathfrak{h}$ is equivalent to a normal subgroup $H \subset G$ (if G is simply connected).

Definition 2.2.4 (Simple Lie algebra)**.** *A Lie algebra $\mathfrak{g}$ is simple if $\dim \mathfrak{g} > 1$ and if it contains no nontrivial ideals, i.e. for any ideal $\mathfrak{h} \subset \mathfrak{g}$ we have $\mathfrak{h} = \{0\} \vee \mathfrak{h} = \mathfrak{g}$.*

Complex simple Lie algebras are extremely important because we have at our disposal a complete classification of them, meaning that each of them is either isomorphic to one in the following list:

- $A_n = \mathfrak{sl}(n+1, \mathbb{C}) = \{A \in M(n+1, \mathbb{C}) : \mathrm{tr}(A) = 0\}$
- $B_n = \mathfrak{so}(2n+1, \mathbb{C})$
- $C_n = \mathfrak{sp}(2n, \mathbb{C})$
- $D_n = \mathfrak{so}(2n, \mathbb{C})$

or to one of the so-called *exceptional* Lie algebras: $\mathfrak{g}_2, \mathfrak{f}_4, \mathfrak{e}_6, \mathfrak{e}_7, \mathfrak{e}_8$, about which we will not say more.

The importance of classifying simple Lie algebras was first realized by W. Killing (1847-1923), whose initial and partial results thereabout were refined by E. Cartan (1869-1851). In his 1894 doctoral thesis, Cartan obtained the definitive classification mentioned above, and later, in 1914, also managed to classify the real simple Lie algebras, by appropriately "restricting" the statements about the former case to the latter one.

2.2.2 Semisimple Lie algebras

Definition 2.2.5 (Chains of subalgebras and related concepts)**.** *Let $\mathfrak{g}$ be a Lie algebra.*
The lower central series $\{\mathscr{D}_k\mathfrak{g}\}_k$ is defined as

$$\mathscr{D}_1\mathfrak{g} = [\mathfrak{g}, \mathfrak{g}]$$
$$\mathscr{D}_k\mathfrak{g} = [\mathfrak{g}, \mathscr{D}_{k-1}\mathfrak{g}]$$

The derived series $\{\mathscr{D}^k\mathfrak{g}\}_k$ is defined as:

$$\mathscr{D}^1\mathfrak{g} = [\mathfrak{g}, \mathfrak{g}]$$
$$\mathscr{D}^k\mathfrak{g} = [\mathscr{D}^{k-1}\mathfrak{g}, \mathscr{D}^{k-1}\mathfrak{g}]$$

Furthermore $\mathfrak{g}$ is said to be

- *nilpotent if* $\mathscr{D}_k\mathfrak{g} = 0$ *for some* k*;*
- *solvable if* $\mathscr{D}^k\mathfrak{g} = 0$ *for some* k*;*
- *perfect if* $\mathscr{D}^1\mathfrak{g} = \mathscr{D}_1\mathfrak{g} =: \mathscr{D}\mathfrak{g} = \mathfrak{g}$.

Definition 2.2.6 (**Semisimple Lie algebra**)**.** *A Lie algebra* $\mathfrak{g}$ *is semisimple if it contains no nonzero solvable ideals.*
Equivalently, if $\mathfrak{h} \subset \mathfrak{g}$ *is an ideal such that* $\mathscr{D}^k\mathfrak{h} = 0$ *for some* k*, then* $\mathfrak{h} = \{0\}$.

Proposition 2.2.2 (Equivalent definitions of semisimple Lie algebras)**.** *All of the following statements are equivalent to the above definition of semisimplicity:*

1) $Rad(\mathfrak{g}) = \{0\}$*, where*

$$Rad(\mathfrak{g}) := \sum_{\substack{\text{solvable} \\ \text{ideals of } \mathfrak{g}}} \mathfrak{h} \quad (= \textit{maximal solvable ideal})$$

is (by definition) the radical of $\mathfrak{g}$.

2) $\mathfrak{g}$ *has no nonzero abelian ideals, i.e. if* $\mathfrak{h} \subset \mathfrak{g}$ *is an ideal s.t.* $[X, Y] = 0$ *for every* $X, Y \in \mathfrak{h}$ *then* $\mathfrak{h} = \{0\}$.

3) The Killing form associated to $\mathfrak{g}$*, i.e. the bilinear form*

$$\begin{aligned} B : \mathfrak{g} \times \mathfrak{g} &\to \mathbb{K} \\ (X, Y) &\mapsto B(X, Y) := tr\big(ad(x) \circ ad(Y)\big) \end{aligned}$$

is non degenerate. [3]

4) $\mathfrak{g}$ *is the (finite) direct sum of simple Lie algebras* $\mathfrak{g}_\mathfrak{i}$*:*

$$\mathfrak{g} = \mathfrak{g}_1 \oplus \cdots \oplus \mathfrak{g}_n = \bigoplus_{i=1}^{n} \mathfrak{g}_\mathfrak{i}$$

Remark 2.2.2. A different yet similar definition of the Killing form as

$$\mathfrak{gl}(V) \times \mathfrak{gl}(V) \ni (X, Y) \mapsto B_V(X, Y) := \operatorname{tr}\big(X \circ Y\big) \in \mathbb{K},$$

allows us to provide a sufficient condition for the solvability of a Lie algebra (definition 1.2.5), namely through

Theorem 2.2.1 (Cartan's criterion)**.** *If* $\mathfrak{g} \subseteq \mathfrak{gl}(V)$ *is a subalgebra and* $B_V(X, Y) = 0$ *for every* $X, Y \in \mathfrak{g}$*, then* $\mathfrak{g}$ *is solvable.*

We now come to the presentation of those two properties of semisimple Lie algebras, which make them most useful and effective, especially as regards the study of their representation theory.

Proposition 2.2.3 (**Complete reducibility**)**.** *Let* (π, V) *be a representation of the Lie algebra* $\mathfrak{g}$*. Then if* $W \subseteq V$ *is an invariant subspace for* $\pi(\mathfrak{g})$*, then there exists another invariant subspace* $W' \subseteq V$ *such that* $V = W \oplus W'$.

[3] a bilinear form $\phi : V \times V \to \mathbb{K}$ is said to be non degenerate if $\phi(v, w) = 0 \ \forall v \in V \Rightarrow w = 0$.

Remark 2.2.3.

1. If (π, V) is a representation of $\mathfrak{g}$, and if (π_i, V_i) $(i = 1, 2)$ are two subrepresentations of it, i.e. $\pi(\mathfrak{g})(V_i) \subseteq V_i$, then we can define their direct sum representation $(\pi_1 \oplus \pi_2, V_1 \oplus V_2)$.
   In terms of matrices, this would amount to build, for all $X \in \mathfrak{g}$, a block diagonal matrix of the form
   $$(\pi_1 \oplus \pi_2)(X) = \begin{pmatrix} \pi_1(X) & 0 \\ 0 & \pi_2(X) \end{pmatrix},$$
   from which the invariance requirement on the subspaces V_i results evidently.

2. The "atomic" representations as regards the mentioned decomposition in direct sums, are the so-called *irreducible* representations. They are atomic, because their only invariant subspaces are the trivial ones (i.e. $\{0\}$ or V_i itself), and therefore admit no further decomposition.

3. Complete reducibility always holds for representations of finite groups. In the continuous case of Lie groups and algebras, a sufficient condition for its validity is semisimplicity.

Proposition 2.2.4 (**Preservation of Jordan decomposition**). *Let (π, V) and $\mathfrak{g}$ as before. Then for any element $X \in \mathfrak{g}$ there are $X_s, X_n \in \mathfrak{g}$ such that the following holds:*

$$\pi(X)_s = \pi(X_s) \quad \textit{and} \quad \pi(X)_n = \pi(X_n)$$

where the subscripts s and n denote the diagonalizable and nilpotent parts respectively.

Remark 2.2.4. Every endomorphism $F \in \mathrm{End}(V)$ can be decomposed as a sum of a diagonalizable and a nilpotent endomorphism: $F = F_s + F_n$.
Since $\pi(X) \in \mathfrak{gl}(V) = \mathrm{End}(V)$,

$$\pi(X) = \underbrace{\pi(X)_s + \pi(X)_n}_{\text{actual}} \overset{\text{pr.1.2.4}}{=} \pi(\underbrace{X_s + X_n}_{\text{formal}}).$$

The last equality is ensured by proposition 1.2.4; in particular semisimplicity allows one to say that if $X \in \mathfrak{g}$ then also $X_s, X_n \in \mathfrak{g}$ (which is not always the case otherwise!).
Moreover $X = X_s + X_n \in \mathfrak{g}$ is in general a formal notation justified by the above proposition. If, as a particular case, $\mathfrak{g} \subseteq \mathfrak{gl}(V)$, then the usual decomposition for endomorphisms can be applied, and therefore this notation stops, so to speak, being just formal.

In the next section we are going to apply the general definition and results outlined above, to study a concrete case of a Lie algebra and of the representation theory which characterizes it.

2.3 Example: finite dimensional representations of $\mathfrak{su}(2)$

Our main goal here is to classify all the finite dimensional irreducible representations of the semisimple Lie algebra

$$\mathfrak{su}(2) = \{A \in M(2,\mathbb{C}) : A + A^\dagger = 0,\ \mathrm{tr}(A) = 0\}.$$

1^{st} Step: We complexify the real Lie algebra $\mathfrak{su}(2)$ and exploit the following isomorphism:

$$\begin{aligned}\mathfrak{su}(2) \otimes \mathbb{C} =: \mathfrak{su}(2)_{\mathbb{C}} &\cong \mathfrak{sl}(2,\mathbb{C}) \\ &= \{A \in M(2,\mathbb{C}) : \mathrm{tr}(A) = 0\}\end{aligned}$$

Proof. Every element in $\mathfrak{sl}(2)$ can be written as a complex (i.e. with coefficients in $\mathbb{C}$) linear combination of elements in $\mathfrak{su}(2)$ as:

$$\mathfrak{sl}(2) \ni X = \underbrace{\frac{X - X^\dagger}{2}}_{X_-} + i\ \underbrace{\frac{X + X^\dagger}{2i}}_{X_+}.$$

Both of the summands are skew-symmetric and traceless, which directly follows from $X_\pm = -X_\pm^\dagger$ and from $\mathrm{tr}(X) = \mathrm{tr}(X^\dagger)$. Thus $X_\pm \in \mathfrak{su}(2)_{\mathbb{C}}$. □

Hence it suffices to study the representations of $\mathfrak{sl}(2)$ instead of those of $\mathfrak{su}(2)_{\mathbb{C}}$. Finally, the representations π of the non complexified algebra $\mathfrak{su}(2)$ can be obtained by restriction to real linear combinations of elements in $\mathfrak{sl}(2)_{\mathbb{C}}$, meaning that π takes arguments of the form $\sum_{i=1}^{2} \alpha_i v_i$, where $\alpha_i \in \mathbb{R} \subset \mathbb{C}$ and $\{v_i\}_i$ is a basis of $\mathfrak{sl}(2)_{\mathbb{C}}$.

2^{nd} Step: A basis of $\mathfrak{g} := \mathfrak{sl}(2,\mathbb{C})$ is given by the vectors

$$H = \begin{pmatrix} 1 & 0 \\ 0 & -1 \end{pmatrix} \quad X = \begin{pmatrix} 0 & 1 \\ 0 & 0 \end{pmatrix} \quad Y = \begin{pmatrix} 0 & 0 \\ 1 & 0 \end{pmatrix},$$

which obey the commutation relations:

$$[H,X] = 2X \quad [H,Y] = -2Y \quad [X,Y] = H.$$

3^{rd} Step: As already mentioned, $\mathfrak{g}$ is semisimple, what can be at best proved through the non-degeneracy of the associated Killing form (see proposition 1.2.2).
Let $\pi : \mathfrak{g} \to \mathfrak{gl}(V)$ be a finite dimensional irreducible representation of $\mathfrak{g}$. Therefore, since the Jordan decomposition must be preserved, and $H = H_s + H_n = H_s + 0$ is diagonal, we have:

$$\pi(H)_s = \pi(H) \quad \text{and} \quad \pi(H)_n = \pi(0) = 0.$$

This implies that $\pi(H) \in \mathrm{End}(V)$ is diagonalizable for every $x \in \mathfrak{h} := \mathrm{Span}(H)$, and consequently that the representation space V can be decomposed as a direct sum of corresponding eigenspaces (usually called *weight spaces*) relative to $\pi(H)$, i.e.

$$V = \bigoplus_\alpha V_\alpha \qquad (= \bigoplus \text{weight spaces}) \tag{2.4}$$

where $\pi(H)(v) = \alpha(H)\, v$ for $v \in V_\alpha$ and $\alpha \in \mathfrak{h}^*$.

4^{th} Step: Consider the adjoint representation (example 1.2.1), noticing that the commutation relations in step 1 can be written as eigenvalue equations:

$$\begin{aligned} \mathrm{ad}(H)(H) &= 0 \quad (\text{eigenvector } H, \text{ eigenavalue } 0) \\ \mathrm{ad}(H)(X) &= 2X \quad (\text{——"—— } X, \text{ ——"—— } 2) \\ \mathrm{ad}(H)(Y) &= -2Y \quad (\text{——"—— } Y, \text{ ——"—— } -2). \end{aligned}$$

The corresponding eigenspaces in $\mathfrak{g}$ are $\mathfrak{h}$, $\mathfrak{g}_2 := \mathrm{Span}(X)$ and $\mathfrak{g}_{-2} := \mathrm{Span}(Y)$. All of these eigenspaces are one dimensional; hence the linear map $\mathrm{ad}(H) \in \mathrm{End}(\mathfrak{g})$ can be diagonalised, and in turn the Lie algebra $\mathfrak{g}$ itself can be written as:

$$\begin{gathered} \mathfrak{g} = \mathfrak{h} \oplus \mathfrak{g}_2 \oplus \mathfrak{g}_{-2} \\ (=: \text{cartan subalgebra} \oplus \text{root spaces}) \end{gathered} \tag{2.5}$$

which is usually referred to as *Cartan decomposition* of the Lie algebra [4].

5^{th} Step: Look at how each "component" of $\mathfrak{g}$ (i.e. $\mathfrak{h}$ and $\mathfrak{g}_{\pm 2}$), acts on each component of V (i.e. on the V_α's).
• The action of $\mathfrak{h}$ on a V_α is completely defined by:

$$\pi(H)(v) = \alpha(H)v \quad \text{for } v \in V_\alpha.$$

• As regards the action of $\mathfrak{g}_2$ consider ($v \in V_\alpha$):

$$\begin{aligned} &\big(\pi(H) \circ \pi(X)\big)(v) = \big(\pi(X) \circ \pi(H)\big)(v) + \\ &[\pi(H), \pi(X)](v) = \alpha(H)\,\pi(X)(v) + 2\,\pi(X)(v) \\ &= \big(\alpha(H) + 2\big)\,\pi(X)(v) \ \in V_{\alpha+2}. \end{aligned}$$

Analogously, for the action of $\mathfrak{g}_{-2}$ we have:

$$\big(\pi(H) \circ \pi(Y)\big)(v) = \big(\alpha(H) - 2\big)\,\pi(Y)(v) \ \in V_{\alpha-2}.$$

Hence we conclude:

$$\begin{aligned} \pi(\mathfrak{g}_{\pm 2}) &: V_\alpha \to V_{\alpha \pm 2} \\ \pi(\mathfrak{h}) &: V_\alpha \to V_\alpha \end{aligned}$$

Figure 2.2: Schematic representation of the action of the vectors $X, Y, H \in \mathfrak{g}$ on the eigenspaces V_{n-2k}. These actions basically produce a shift in the eigenvalues – and hence in the related eigenspaces – either by 0 (H) or by ± 2 (X respectively Y). For the sake of clarity, here H stands for $\pi(H)$ and likewise for X and Y.

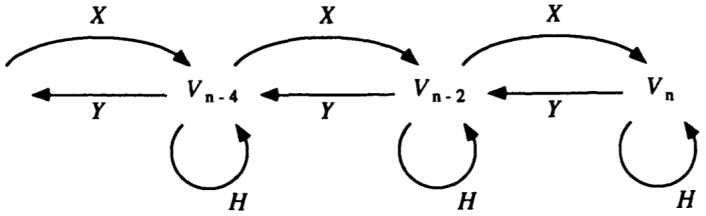

[4] in a general case this decomposition would read $\mathfrak{g} = \mathfrak{h} \oplus (\bigoplus_\alpha \mathfrak{g}_\alpha)$ where $\mathfrak{h}$ (the *Cartan subalgebra*) is a subalgebra of maximally commuting elements, and the $\mathfrak{g}_\alpha$ (*root spaces*) are the eigenspaces relative to $\mathrm{ad}(\mathfrak{h}) \in \mathrm{End}(\mathfrak{g})$.

6^{th} Step: As we have seen, each subspace is sent through the action of $\mathfrak{g}$ into another subspace with eigenvalue differing either by 0 or by ± 2. Hence decomposition (1.4) can be written as:

$$V = \bigoplus_{k\in\mathbb{Z}} V_{\alpha_0+2k} \qquad (\alpha_0 \in \mathbb{C}).$$

Now, since V was assumed to be finite dimensional, this direct sum must be finite, and consequently the α's have to form a bounded sequence of complex numbers like the following

$$\underbrace{\beta}_{\text{min.}}, \beta+2\,, \beta+4\,, \ldots, \underbrace{\beta+2K}_{\text{max.}} =: n,$$

and whose biggest element we call n.

7^{th} Step: We now reconstruct all of the V_α (and from them V itself) starting from the extremal – i.e. the n^{th} – eigenspace, and by repeatedly applying the "lowering operation" induced by $\pi(Y)$. This construction we formalize through the following:

Lemma 2.3.1. *Let $v \in V_n$, then*

$$W := \mathit{Span}\{v, \pi(Y)(v), \pi(Y)^2(v), \ldots\} = V$$

Proof. (just a sketch)
We need to show that W is an invariant subspace with respect to the action of $\mathfrak{g}$ (or equivalently of each of its components), namely that $\pi(\mathfrak{g})(W) \subseteq W$. Subsequently we can directly infer from the irreducibility of the representation π (step 3), that $W = V$.

- Clearly $\pi(\mathfrak{g}_{-2})(W) \subseteq W$ as

$$\pi(Y)\big(\pi(Y)^m(v)\big) = \pi(Y)^{m+1}(v) \in W$$

- From the previous calculation and inductively:

$$\pi(H)\big(\pi(Y)^m(v)\big) = (n-2m)\pi(Y)^m(v).$$

  Hence $\pi(\mathfrak{h})(W) \subseteq W$.

- Again inductively and using $[X,Y] = H$ and $\pi(X)(v) = 0$ we have:

$$\begin{aligned} &\pi(X)\big(\pi(Y)^m(v)\big) \\ &= m(n-m+1)\,\pi(Y)^{m-1}(v) \end{aligned} \tag{2.6}$$

  Hence $\pi(\mathfrak{g}_2)(W) \subseteq W$.

□

8^{th} Step: The finite dimensionality of V again implies that there exists a smallest integer $m \in \mathbb{Z}$ such that the m^{th} action of Y on some $v \in V_n$ vanishes. Applying the condition

$$\begin{cases} \pi(Y)^m(v) = 0 \\ \pi(Y)^k(v) \neq 0 \quad \text{for } 0 \leqslant k \leqslant m-1 \end{cases}$$

to equation 1.6 in the previous step we get:

$$\begin{aligned} \pi(X)(0) = 0 &= m(n-m+1)\,\pi(Y)^{m-1}(v) \\ \Rightarrow \quad & n-m+1 = 0. \end{aligned}$$

This last result, together with lemma 1.3.1, leads to several important consequences:

- $n \in \mathbb{C}$ is a non-negative integer, as $n = m - 1$ and $m \in \mathbb{Z}_{\geqslant 1}$.
- The sequence of basis vectors in lemma 1.3.1 reads: $v, \pi(Y)(v), \pi(Y)^2(v), \ldots, \pi(Y)^n(v)$. In fact the number of steps required to pass from V_n to the other extremal eigenspace (i.e. the one with eigenvalue β in step 6) is given by $m - 1 = n$.
- $\dim(V_\alpha) = 1$ for all α (each V_α is spanned by a single $\pi(Y)^k(v)$), and $\dim(V) = n + 1$.
- The eigenvalues of the operator $\pi(H)$ (i.e. the mentioned $\beta + 2k$) turn out to be:

  $$-n\,,\ -n+2\,,\ \ldots\,,\ n-2\,,\ n$$

  since $n - \big(2 \times (\#\,\text{of steps})\big) = n - 2n = -n$. Also notice the symmetry about the origin in $\mathbb{Z}$ of the above string of numbers.
- A choice of an $n \in \mathbb{N}$ uniquely determines an irreducible representation $V^{(n)}$ with the above properties. The converse is also necessarily true: any finite dimensional representation of $\mathfrak{g}$, whose action $\pi(H)$ has eigenvalues satisfying the above conditions, is irreducible.

Example 2.3.1 (Irreducible representations of $\mathfrak{sl}(2, \mathbb{C})$)**.**

1. (Trivial representation) Let $V = \mathbb{C}$ and $\pi(H)(z) := 0$ for all $z \in \mathbb{C}$. Then $n = 0$ and $V^{(0)} = \text{Span}(z \in \mathbb{C}) = \mathbb{C}$ is the corresponding irreducible representation.
2. (Standard representation) Let $V = \mathbb{C}^2$ and $\{x, y\}$ be a basis of V. Now define:

   $$\pi(H)(x) := x \qquad \pi(H)(y) := -y$$

   whence it follows that $n = 1$ and that

   $$\mathbb{C}^2 = \underbrace{\text{Span}(y)}_{V_{-1}} \oplus \underbrace{\text{Span}(x)}_{V_1} = V^{(1)}$$

   is the 2-dimensional associated irreducible representation.
3. (N^{th} Symmetric power of (2)) Let

   $$W = \text{Sym}^N(\mathbb{C}^2) \cong \mathbb{C}[x, y]_N$$

   i.e. the space of N-times contravariant symmetric tensors [5], which is isomorphic to the space of the homogeneous polynomials of degree N.
   The set $\{x^N, x^{N-1}y, \ldots, y^N\}$ clearly forms a basis for $\mathbb{C}[x, y]_N$. Now define:

   $$\pi(H)(x^{N-k}y^k) := (N - 2k) \cdot x^{N-k}y^k$$

   The eigenvalues $N - 2k$ all have multiplicity 1, and form a string $N, N-2, \ldots, -N$.
   Hence we have that $n = N$ and that $\text{Sym}^N(\mathbb{C}^2)$ is an irreducible representation with

   $$\text{Sym}^N(\mathbb{C}^2) = \bigoplus_{k=0}^{N} \underbrace{\text{Span}\big(x^{N-k}y^k\big)}_{V_{N-2k}} = V^{(N)}.$$

By virtue of the uniqueness property discussed previously, we can actually state that all the finite dimensional irreducible representations of $\mathfrak{sl}(2, \mathbb{C})$ coincide with a symmetric power of the standard representation, namely are of the form $\text{Sym}^N(\mathbb{C}^2)$ for $N \in \mathbb{Z}_{\geqslant 0}$ [6].
So we have finally accomplished our goal of classifying all the (finite dimensional) irreducible representations of $\mathfrak{sl}(2, \mathbb{C})$, and in turn this would in principle allow us to determine the corresponding representations of our original algebra, namely $\mathfrak{su}(2, \mathbb{C})$. This can be done as specified at the end of step 1.

[5] namely those tensors for which $v^1 \otimes v^2 \otimes \ldots \otimes v^N = v^{\sigma(1)} \otimes v^{\sigma(2)} \otimes \ldots \otimes v^{\sigma(N)}$ for every permutation $\sigma \in S_N$.
[6] notice that $\text{Sym}^0(\mathbb{C}^2) = \mathbb{C}$ (trivial representation), and $\text{Sym}^1(\mathbb{C}^2) = \mathbb{C}^2$ (standard representation).

Bibliography

[1] William Fulton and Joe Harris *Representation theory, A first course*. Springer-Verlag, Graduate texts in mathematics, 2004.

[2] Matthias R. Gaberdiel. *Symmetries in Physics* (lecture notes). ETH Zuerich, 2013.

[3] Cyril Stark, *Lie Algebras: a crash course* (in *Topology in Physics*). Proseminar in Theoretical Physics, ETH Zuerich, 2006.

[4] Veeravalli S. Varadarajan, *Historical review of Lie theory*. UCLA Department of Mathematics. `http://www.math.ucla.edu/~vsv/liegroups2007/historical%20review.pdf`

[5] Giuseppe De Marco, *Analisi due, secondo corso di analisi matematica*. Decibel editrice, Padova, 2nd Edition, 1999.

[6] Antonio Machí, *Gruppi, Una introduzione a idee e metodi della Teoria dei Gruppi*. Springer-Verlag, Unitext, 2007.

[7] Steven Roman, *Advanced linear algebra*. Springer-Verlag, Graduate texts in mathematics, 3rd Edition, 2008.

[8] Benjamin Steinberg, *Representation Theory of finite groups, An introductory approach*. Springer-Verlag, Universitext, 2012.

[9] Wikipedia, *Lie algebra* — Wikipedia, The Free Encyclopedia. `http://en.wikipedia.org/wiki/Lie_algebra`.

[10] Wikipedia, *Lie group* — Wikipedia, The Free Encyclopedia. `http://en.wikipedia.org/wiki/Lie_group`.

[11] Wikipedia, *Exponential map* — Wikipedia, The Free Encyclopedia. `http://en.wikipedia.org/wiki/Exponential_map`.

Chapter 3

Solitons in KdV Equation

Author: Oliver Rietmann
Supervisor: Cristian Vergu

In this chapter, we will study the properties of some solutions to the KdV equation. It is a non-linear partial differential equation, whose solutions describe propagating waves and wavepackets. Some of these solutions have several "particle-like" properties. They are called solitons. In the context of Lagrangian formalism, we will determine the obvious constants of motion and relate them in a natural way to the momentum, mass, etc. of the solutions to the KdV equation. Amongst a few quantitative studies of several (solitonic) solutions, we will systematically construct the interesting "cnoidal" solution.

3.1 Introduction

The Korteweg-de-Vries equation (KdV equation) is given by

$$\partial_t \phi = 6\phi\partial_x\phi - \partial_x^3\phi, \quad \text{where } \phi : \mathbb{R}\times\mathbb{R} \longrightarrow \mathbb{R}. \tag{3.1}$$

It is a non-linear, partial differential equation, named after Diederik Korteweg und Gustav de Vries, who introduced it in 1895. They used it to describe the propagation of water waves of long wavelength in a narrow, shallow water channel. Such waves were first observed by John Scott Russell in 1834 [3]. Furthermore, the KdV equation (3.1) has infinitely many independent constants of motion and it can be solved analytically [1] by means of the inverse scattering transform [4], but we will not go into that.

A soliton is a localized wave packet that moves at constant speed. It does not lose its shape, even after colliding with other solitons. Moreover, solitons are solutions to non-linear differential equations of systems with infinitely many constants of motion [1]. One such system is described by the KdV equation (3.1).

3.2 Some Examples

The simplest solution to Equation (3.1) that describes a soliton, is the one-soliton solution

$$\phi(x,t) = 2\,\mathrm{sech}^2(x-4t). \tag{3.2}$$

It describes a single soliton, moving in positive x-direction with constant velocity 4. Figure 3.1 shows a plot of this solution.

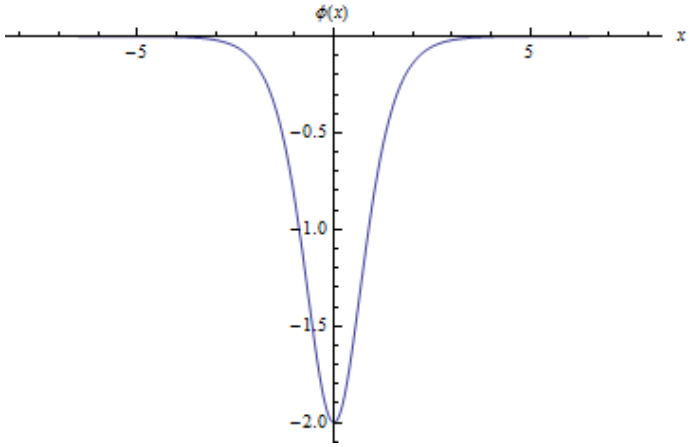

Figure 3.1: The one-soliton solution (3.2) of (3.1) at time $t = 0$.

More generally, the solution of (3.1) to the initial condition

$$\phi(x, 0) = -n(n+1)\,\mathrm{sech}^2(x),\ n \in \mathbb{N}$$

describes n solitons propagating in positive x-direction [2]. For $n = 2$, we obtain the two-soliton solution

$$\phi(x,t) = -\frac{12(3 + \cosh(64t - 4x) + 4\cosh(8t - 2x))}{(\cosh(36t - 3x) + 3\cosh(28t - x))^2}, \tag{3.3}$$

that describes two-solitons propagating in positive x direction (see Figure 3.2).

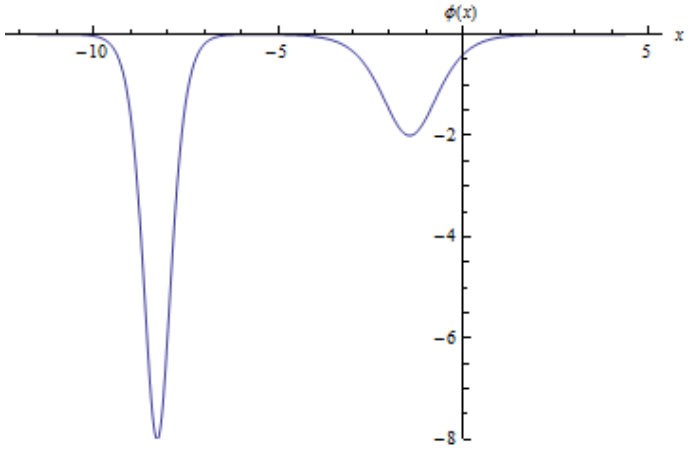

Figure 3.2: The two-soliton solution (3.3) and (3.1) at time $t = -0.5$.

The larger peak travels faster than the smaller one and they intersect at $x = 0$ and $t = 0$. During the overlap of the two peaks, the larger one increases its velocity, while the other one travels in negative x direction. This can be observed in Figure 3.3.

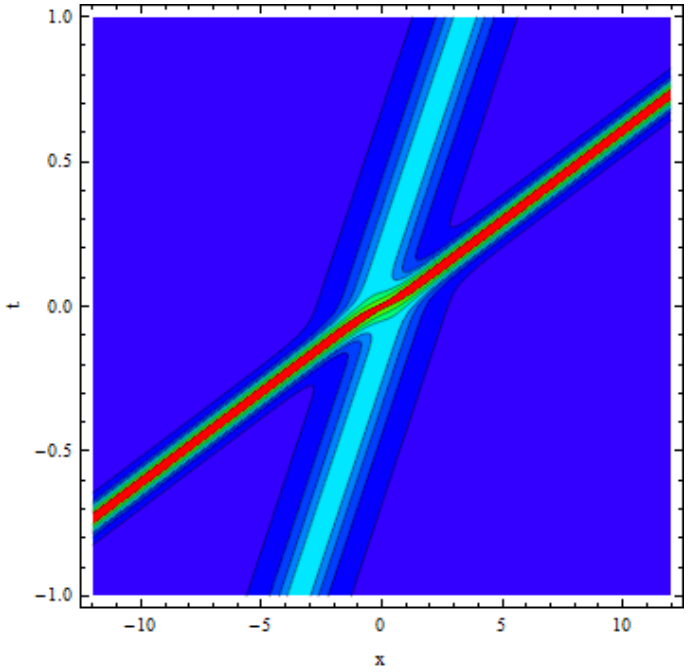

Figure 3.3: The two-soliton solution (3.3) of (3.1).

Moreover, the peak during the collision is smaller than the larger peak before the intersection. Long time after the collision, the two peaks have again the same shape and velocity as before the overlap, as we would expect for solitons.

From the initial- and (periodic) boundary condition

$$\phi(x,0) = -4\,\mathrm{sech}^2(x),\ \ \phi(-2,t) = \phi(2,t), \tag{3.4}$$

we obtain the numerical solution of (3.1) shown in Figure 3.4.

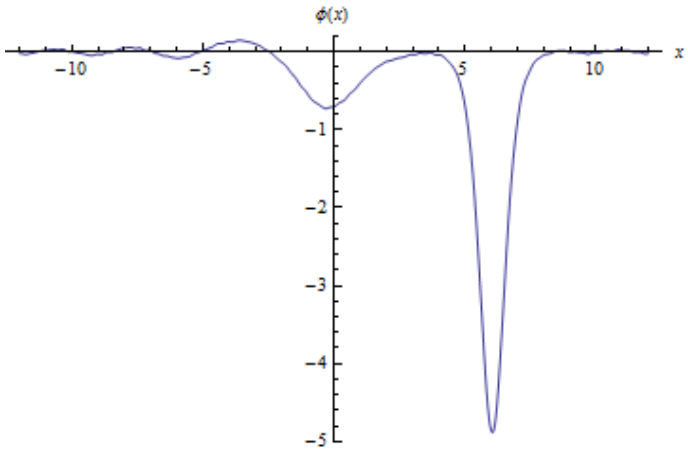

Figure 3.4: The solution of (3.1) under (3.4).

This describes a large peak moving in positive x direction, that leaves small dispersive peaks behind, that travel in negative x direction.

3.3 Derivation of the KdV Equation

We want to describe water waves in a long, shallow water channel.

Let x be the position along the channel, t the time coordinate, U the potential energy and ρ a constant with no explicit dependence on x and t. Let $y(x,t)$ the displacement. Furthermore, we

define: $v := \partial_t y$. Consider the Navier-Stokes equation:

$$\rho(\partial_t v + v\partial_x v) = -\partial_x U[y] \tag{3.5}$$

Expanding the right-hand side at $y \equiv 0$ in derivatives of y yields

$$-\partial_x U = f_2\partial_x^2 y + f_4\partial_x^4 y + ..., \tag{3.6}$$

where $\{f_i\}_{i=2}^{\infty}$ are constants. We assumed that the odd derivatives vanish. Any odd derivative term would contribute a heat-equation-like term in the final result. Since this describes a diffusion rather than a propagating wave, we make this assumption. We can choose new constants $\{\tilde{f}_i\}_{i=2}^{\infty}$ such that by plugging Equation (3.6) into Equation (3.5), we obtain:

$$\partial_t^2 y = (\partial_t y)\partial_x\partial_t y + \tilde{f}_2\partial_x^2 y_2 + \tilde{f}_4\partial_x^4 y + ... \tag{3.7}$$

Since we are interested in waves of a shallow, long water channel, we go to the limit of small amplitudes and long wavelength. If we assume, that the solutions to Equation (3.7) are wave-like, thus

$$y(x,t) = e^{i(kx-\omega t)},\ k = \frac{2\pi}{\lambda}, \tag{3.8}$$

the high order derivatives w.r.t. x will become small, which means we can neglect them. Furthermore, the non-linear terms in Equation (3.7) become small due to the small amplitude assumption. Thus we have a weak non-linearity of Equation (3.7) in this limit:

$$\partial_t^2 y = \tilde{f}_2\partial_x^2 y_2 + \underbrace{(\partial_t y)\partial_x\partial_t y}_{\text{small}} + \underbrace{\tilde{f}_4\partial_x^4 y}_{\text{small}} \tag{3.9}$$

By suitable choice of units for x, t and y, Equation (3.9) turns into

$$\partial_t^2 y = \partial_x^2 y_2 - 12\epsilon(\partial_t y)\partial_x\partial_t y + 2\epsilon\partial_x^4 y \tag{3.10}$$

and by changing our frame of reference with the substitutions $y(x-t,\epsilon t) = y(\xi,\tau),\ \xi := x-t,\ \tau := \epsilon t$ in the limit $\epsilon \to 0$, we get from Equation (3.10):

$$0 = \partial_\xi\partial_\tau y(\xi,\tau) - 6\partial_\xi y(\xi,\tau)\partial_\xi^2 y(\xi,\tau) + \partial_\xi^4 y(\xi,\tau) \tag{3.11}$$

Under the simple substitutions $\phi := \partial_\xi y(\xi,\tau), x := \xi$ and $t := \tau$, Equation (3.11) turns into the KdV equation (3.1):

$$\partial_t\phi = 6\phi\partial_x\phi - \partial_x^3\phi$$

3.4 Lagrangian Formalism and Noether's Theorem

From now on, we assume that $y(x,t)$ and all its derivatives vanish at $\pm\infty$.

3.4.1 Lagrangian of the KdV System

We will denote the partial derivatives with a subscript, thus $y_t := \partial_t y,\ y_x := \partial_x y$ and so on. Furthermore, remember the definition $\phi := y_x$. The Lagrangian of the KdV system is

$$L[y, y_t] = \frac{1}{2}\int_{-\infty}^{\infty}\left(y_x y_t - 2y_x^3 - y_{xx}^2\right)dx. \tag{3.12}$$

To verify this, we compute the Euler-Lagrange equation:

$$\begin{aligned}
0 &= \frac{d}{dt}\frac{\delta L}{\delta y_t} - \frac{\delta L}{\delta y} = \frac{d}{dt}\left(\frac{1}{2}\int_{-\infty}^{\infty} y_x \delta(x-x')dx\right) - \frac{1}{2}\int_{-\infty}^{\infty}\left(y_t\partial_x - 6y_x^2\partial_x - 2y_{xx}\partial_x^2\right)\delta(x-x')dx \\
&= \frac{d}{dt}\left(\frac{1}{2}\int_{-\infty}^{\infty} y_x \delta(x-x')dx\right) - \frac{1}{2}\int_{-\infty}^{\infty}\left(-y_{tx} + 2\cdot 6y_x y_{xx} - 2y_{xxxx}\right)\delta(x-x')dx \\
&= y_{xt} - 6y_x y_{xx} + y_{xxxx} = \phi_t - 6\phi\phi_x + \phi_{xxx}
\end{aligned}$$

This is exactly the KdV equation (3.1).

3.4.2 Noether's Theorem

We formulate Noether's theorem:

Let L be a Lagrangian and $y := y(\tilde{y}, \alpha)$ a family of functional transformations, parametrized by $\alpha \in (-\epsilon, \epsilon),\ \epsilon > 0$, where $\tilde{y}$ and y satisfy the Euler-Lagrange equation. If $L[y(\tilde{y},\alpha), \partial_t y(\tilde{y},\alpha)] = L[\tilde{y}, \tilde{y}_t] + dF(\tilde{y},\alpha)/dt$, then:

$$\frac{d}{dt}\left(\int_{-\infty}^{\infty}\frac{\delta L}{\delta y_t}\partial_\alpha y dx - \partial_\alpha F\right)\Big|_{\alpha=0} = 0. \tag{3.13}$$

Thus the term in the brackets (at $\alpha = 0$) is a constant of motion.

Now we give a proof for this statement.
By the Leibniz rule, we have:

$$\frac{d}{dt}\left(\frac{\delta L}{\delta y_t}\partial_\alpha y\right) = \left(\frac{d}{dt}\frac{\delta L}{\delta y_t}\right)\partial_\alpha y + \frac{\delta L}{\delta y_t}\partial_\alpha y_t \tag{3.14}$$

Then we compute:

$$\begin{aligned}
&\frac{d}{dt}\left(\partial_\alpha F\right) = \partial_\alpha\left(\frac{dF}{dt}\right) = \partial_\alpha(L[y,\partial_t y] - L[\tilde{y},\tilde{y}_t]) = \partial_\alpha L[y,\partial_t y] = \int_{-\infty}^{\infty}\left(\frac{\delta L}{\delta y}\partial_\alpha y + \frac{\delta L}{\delta y_t}\partial_\alpha y_t\right)dx \\
&\overset{(3.14)}{=} \int_{-\infty}^{\infty}\left(\frac{\delta L}{\delta y}\partial_\alpha y - (\frac{d}{dt}\frac{\delta L}{\delta y_t})\partial_\alpha y + \frac{d}{dt}(\frac{\delta L}{\delta y}\partial_\alpha y)\right)dx = \int_{-\infty}^{\infty}\Bigg(\underbrace{(\frac{\delta L}{\delta y} - \frac{d}{dt}\frac{\delta L}{\delta y_t})}_{=0 \text{ (Euler-Lagrange)}}\partial_\alpha y + \frac{d}{dt}(\frac{\delta L}{\delta y}\partial_\alpha y)\Bigg)dx \\
&= \frac{d}{dt}\int_{-\infty}^{\infty}\frac{\delta L}{\delta y}\partial_\alpha y dx \\
&\Longrightarrow \frac{d}{dt}\left(\int_{-\infty}^{\infty}\frac{\delta L}{\delta y}\partial_\alpha y dx - \partial_\alpha F\right) = 0 \Longrightarrow \frac{d}{dt}\left(\int_{-\infty}^{\infty}\frac{\delta L}{\delta y}\partial_\alpha y dx - \partial_\alpha F\right)\Big|_{\alpha=0} = 0
\end{aligned}$$

This is exactly what we wanted to show.

3.5 Conservation Laws

Using Noether's theorem, we can now compute several constants of motion. This will allow us to assign a mass, a momentum, etc. to a soliton of the KdV equation.

3.5.1 Conservation of Total Momentum

Consider the spacial translation $y(x) := \tilde{y}(x-\alpha)$, then the Lagrangian transforms as $L[y, y_t] = L[\tilde{y}, \tilde{y}_t]$ (note: $F \equiv 0$). By Noether's theorem, we get the following constant of motion, which we call the total momentum:

$$P := -\frac{1}{2}\int_{-\infty}^{\infty} \phi^2 dx = -\frac{1}{2}\int_{-\infty}^{\infty} \phi^2 dx + \Big[\frac{1}{6}\phi_x\Big]_{-\infty}^{\infty} = \int_{-\infty}^{\infty} \Big(-\frac{1}{2}\phi^2 + \frac{1}{6}\phi_{xx}\Big) dx \tag{3.15}$$

We define the integrand as the total momentum density

$$j := -\frac{1}{2}\phi^2 + \frac{1}{6}\phi_{xx}. \tag{3.16}$$

3.5.2 Conservation of Total Mass

Consider the shift of the equilibrium position $y := \tilde{y}+\alpha$, then the Lagrangian transforms as $L[y, y_t] = L[\tilde{y}, \tilde{y}_t]$ (note: $F \equiv 0$). By Noether's theorem,

$$m := \frac{1}{6}\int_{-\infty}^{\infty} \phi dx \tag{3.17}$$

is a constant of motion. We can think of this quantity as the total mass of our system and of

$$\rho := \frac{1}{6}\phi \tag{3.18}$$

as the density. This is due to the following continuity equation:

$$0 \overset{(3.1)}{=} \frac{1}{6}(\phi_t - 6\phi\phi_x - \phi_{xxx}) = \frac{1}{6}\big(\phi_t + \partial_x \underbrace{(-3\phi^2 + \phi_{xx})}_{6j=}\big) \overset{(3.18),(3.16)}{=} \rho_t + \mathrm{div} j$$

If we think of m as the mass, then by the divergence theorem, the change of mass in a certain volume is given by the momentum density "flux" j, that flows through the surface of that volume. (Note that we are still in one space dimension, although talking about volume.)

3.5.3 Conservation of Total Energy

Consider the time translation $y(x,t) = \tilde{y}(x, t-\alpha)$, then the Lagrangian transforms as:

$$\begin{aligned} L[y, \partial_t y] &= L[\tilde{y}, \tilde{y}_t] - (L[\underbrace{y(x,t+\alpha)}_{\tilde{y}(x,t)\ =}, \underbrace{\partial_t y(x,t+\alpha)}_{\tilde{y}_t(x,t)\ =}] - L[y(x,t), \partial_t y(x,t)]) \\ &= L[\tilde{y}, \tilde{y}_t] - \int_0^{\alpha} \frac{d}{dt} L[y(x,t+\beta), \partial_t y(x,t+\beta)] d\beta \\ &= L[\tilde{y}, \tilde{y}_t] + \frac{d}{dt}F, \quad \text{where } F := -\int_0^{\alpha} L[y(x,t+\beta), \partial_t y(x,t+\beta)] d\beta \end{aligned}$$

By Noether's theorem, we get the conservation of energy:

$$E := \frac{1}{2}\int_{-\infty}^{\infty} \big(2\phi^3 + (\phi_x)^2\big) dx \tag{3.19}$$

3.5.4 Center of Mass

The Galilei transformation $y(x,t) = \tilde{y}(x+\alpha t, t) + \frac{\alpha x}{t}$ leads to the following conservation law:

$$M_{CM} := \frac{1}{2}\int_{-\infty}^{\infty}\left(\phi^2 t + \frac{1}{3}\phi x\right)dx = t\underbrace{\int_{-\infty}^{\infty}\frac{1}{2}\phi^2\,dx}_{=-P} + \int_{-\infty}^{\infty}\underbrace{\frac{1}{6}\phi}_{=\rho}\,x dx = \underbrace{\int_{-\infty}^{\infty}\rho x dx}_{\text{center of mass}} - tP = constant \quad (3.20)$$

This means that the center of mass moves at constant speed.

3.5.5 Infinitely Many Constants of Motion

The KdV system has a countably infinite number of independent constants of motion. Let $n \in \mathbb{N}$ and P_n polynomials, defined recursively by

$$P_1 := \phi,\ P_n := \frac{dP_{n-1}}{dx} + \sum_{i=1}^{n-2} P_i P_{n-1-i},\ n \geq 2,$$

then the following are independent constants of motion [4]:

$$F_n := \int_{-\infty}^{\infty} P_{2n-1}(\phi, \phi_x, \phi_{xx}, ...)dx \quad (3.21)$$

We are not going to prove this, but note that the constants of motion (3.15), (3.17), (3.19) are of the same form as the F_n's in Equation (3.21). However, the constant of motion (3.20) is not. So although we have found infinitely many constants of motion, not all constants of motion are of this form.

Everything we have done so far still holds if we assume periodic boundary conditions instead of the vanishing at infinity assumption, since we only need this to get rid of the boundary terms when we do integration by parts.

3.5.6 Examples Revisited

As an application of what we just derived, we are going to assign a mass, momentum, etc. to the solitonic solutions from the very beginning.

Remember the one-soliton solution (3.2) of the KdV equation (3.1):

$$\phi(x,t) = 2\,\mathrm{sech}^2(x-4t)$$

It has the following properties:

v	m	P	E	M_{CM}
4	$-\frac{2}{3}$	$-\frac{8}{3}$	-4.6	0

Table 3.1: Properties of the one-soliton solution (3.2).

For the two-soliton solution (3.3), we calculate these properties for each peak separately. The index 1 corresponds to the larger peak and 2 to the smaller one (see Figure 3.2).

v_1	m_1	P_1	E_1	$M_{CM,1}$
16	$-\frac{4}{3}$	$-\frac{64}{3}$	-204.8	21.7

v_2	m_2	P_2	E_2	$M_{CM,2}$
2	$-\frac{2}{3}$	$-\frac{8}{3}$	-6.4	2.3

Table 3.2: Properties of the two-soliton solution (3.3) for each peak.

3.6 Hamiltonian Formalism

3.6.1 Hamiltonian of the KdV System

We define the Hamiltonian as the Legendre transformation of the Lagrangian:

$$H[\phi] := \int_{-\infty}^{\infty} \underbrace{\frac{\delta L}{\delta(y_t)}}_{\pi(x):=} y_t) dx - L[y, y_t] = \frac{1}{2} \int_{-\infty}^{\infty} \left(2\phi^3 + \phi_x^2\right) dx \tag{3.22}$$

We think of $\pi(x)$ as the continuous analogue of the momentum of a particle in the discrete case. However, π and y are not independent and thus we can't use them to derives the Hamilton equations [1]. Nevertheless, we obtain similar equations:

$$\delta H = 0,\ 2y_t = \frac{\delta H(\pi)}{\delta \pi},\ 2\pi_t = -\frac{\delta H(y)}{\delta y}$$

3.6.2 Poisson Brackets

Let $F_1[\phi]$, $F_2[\phi]$, $F_2[\phi]$ and $F[\phi]$ be functionals on the phase space. We define the Poisson bracket by:

$$[F_1, F_2] := \int_{-\infty}^{\infty} \left(\frac{\delta F_1}{\delta \phi} \partial_x \frac{\delta F_2}{\delta \phi} \right) dx \tag{3.23}$$

This gives us the right time evolution:

$$\begin{aligned} \frac{dF}{dt} &\overset{\text{(chain rule)}}{=} \int_{-\infty}^{\infty} \frac{\delta F}{\delta \phi} \phi_t dx \overset{(3.1)}{=} \int_{-\infty}^{\infty} \frac{\delta F}{\delta \phi} (6\phi\phi_x - \phi_{xxx}) dx = \int_{-\infty}^{\infty} \frac{\delta F}{\delta \phi} \partial_x (3\phi^2 - \phi_{xx}) dx \\ &= \int_{-\infty}^{\infty} \frac{\delta F}{\delta \phi} \partial_x \left(\frac{\delta}{\delta \phi} \frac{1}{2} \int_{-\infty}^{\infty} \left(2\phi^3 + \phi^2\right) \right) dx \overset{(3.22)}{=} \int_{-\infty}^{\infty} \frac{\delta F}{\delta \phi} \partial_x \frac{\delta H}{\delta \phi} dx \overset{(3.23)}{=} [F, H] \end{aligned}$$

In addition, our Poisson brackets form a Lie Algebra on the phase space:

$$\begin{aligned} &\text{anti-symmetry: } [F_1, F_2] = -[F_2, F_1] \\ &\text{Jacobi: } [F_1, [F_2, F_3]] + [F_2, [F_3, F_1]] + [F_3, [F_2, F_1]] = 0 \end{aligned}$$

3.7 The Cnoidal Wave

In this chapter, we are going to construct a solution to the KdV equation, the so called cnoidal solution [1]. Substituting the propagating wave ansatz $\phi = \phi(z)$, where $z := x - vt$ into the KdV equation (3.1) yields:

$$\begin{aligned} 0 &\overset{(3.1)}{=} 6\phi\phi_z - \partial_t \phi - \phi_{zzz} = 6\phi\phi_z + v\phi_z - \phi_{zzz} = \partial_z (3\phi^2 + v\phi - \phi_{zz}) \\ \Longrightarrow 0 &= \phi_{zz} - (3\phi^2 + v\phi + C_1) \\ \Longrightarrow \frac{1}{2}\phi_z^2 &= C_0 + (\phi^3 + \frac{1}{2} v\phi^2 + C_1\phi) = C_0 - V[\phi], \\ &\text{where } C_1, C_2 = \text{const. and } V[\phi] := -(\phi^3 + \frac{1}{2} v\phi^2 + C_1\phi) \end{aligned} \tag{3.24}$$

We can think of the LHS of Equation (3.24) as a kinetic energy of an infinitesimal mass point and of V as a potential [1]. From now on, we assume that V has a local minimum and a local maximum and that C_0 lies between them (see Figure 3.5). In this case, we have a bounded solution, just like a particle in a potential in classical mechanics.

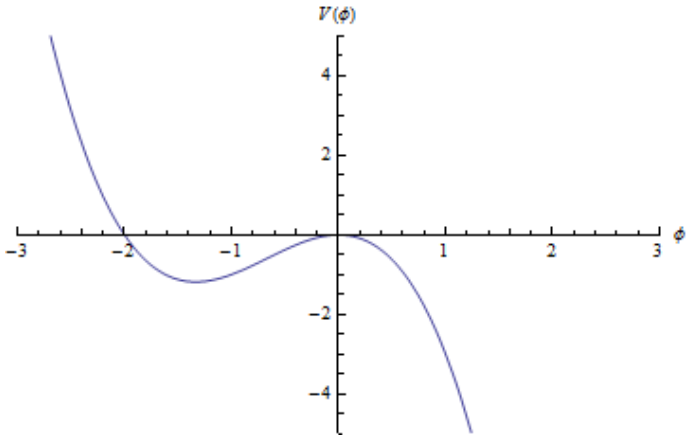

Figure 3.5: The potential $V[\phi]$.

For such a potential, we can find $a_1, a_2, a_3 \in \mathbb{R}, a_1 < a_2 < a_3$ such that (3.24) factorizes:

$$\phi_z^2 = 2(\phi - a_1)(\phi - a_2)(\phi - a_3). \tag{3.25}$$

Now we substitute $\phi(z) = (a_2 - a_1)f(z)^2 + a_1$ into (3.25) and obtain

$$f_z^2 = \frac{a_3 - a_1}{2}(1 - f^2)(1 - kf^2) \ , \quad k := \frac{a_2 - a_1}{a_3 - a_1}. \tag{3.26}$$

The Jacobi elliptic function $\mathrm{sn}(z, k)$ is a solution to the differential equation (3.27) [6]:

$$w_z^2 = (1 - w^2)(1 - kw^2) \tag{3.27}$$

Thus the solutions to Equation (3.26) and (3.25) are:

$$f(z) = \mathrm{sn}(\sqrt{\frac{a_3 - a_1}{2}}z, k), \tag{3.28}$$

$$\phi(x,t) = a_1 + (a_2 - a_1)\,\mathrm{sn}^2\left(\sqrt{\frac{a_3 - a_1}{2}}(x - vt), k\right) \tag{3.29}$$

Note that the constants a_1, a_2, a_3 still depend on v and k. To determine them, we plug Equation (3.29) into the KdV equation (3.1). Using the identity $\mathrm{sn}^2 + \mathrm{cn}^2 = 1$ and choosing new constants, we finally obtain the cnoidal solution

$$\underline{\underline{\phi(x,t) = \frac{C}{3}\left(2 - \frac{1}{k}\right) - \frac{v}{6} - C\,\mathrm{cn}^2\left(\sqrt{\frac{C}{2k}}(x - vt), k\right),}} \tag{3.30}$$

where $k \in (0, 1)$ and $C, v \in \mathbb{R}$ are (independent!) constants.

In the limit $k \to 1$ and $C = \frac{v}{2}$, we get the one-soliton solution

$$\phi(x,t) = -\frac{v}{2}\,\mathrm{sech}^2\left(\frac{\sqrt{v}}{2}(x - vt)\right), \tag{3.31}$$

with corresponding potential:

$$V(\phi) = -\phi^3 - \frac{v}{2}\phi^2 \ , \quad C_0 = 0 \tag{3.32}$$

Figure 3.5 shows the potential (3.32) of the one-soliton solution (3.31) for $v = 4$. Note that the soliton of Equation (3.31) increases its speed v with increasing amplitude.

Consider the family of solutions (3.33) to the KdV equation (3.1), parametrized by $k \in (0, 1]$. It describes a continuous transition from a periodic cnoidal wave ($k < 1$) to the non-periodic one-soliton solution ($k = 1$) [5].

$$\phi_k(x,t) = \frac{2}{3}\left(1 - \frac{1}{k}\right) - 2\,\mathrm{cn}^2\left(\frac{x-t}{\sqrt{k}}, k\right) \tag{3.33}$$

The Figures 3.6, 3.7 and 3.8 show the plots of (3.33) for several values of k.

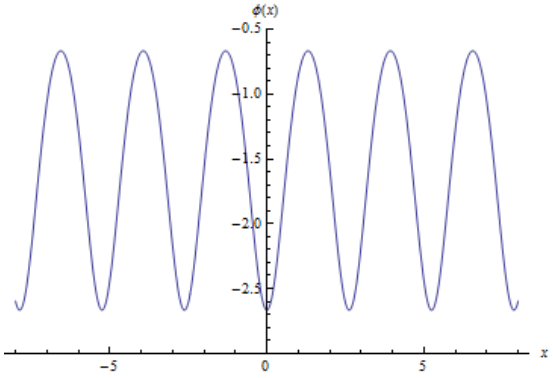

Figure 3.6: The cnoidal wave (3.33) for $k = 0.5$

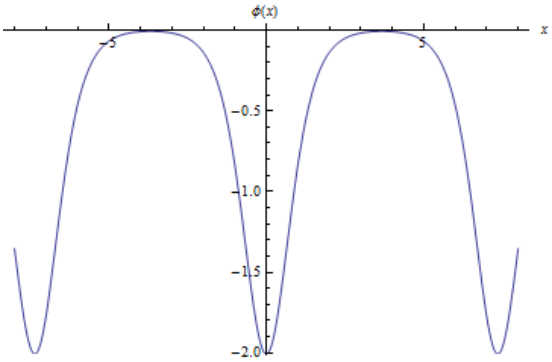

Figure 3.7: The cnoidal wave (3.33) for $k = 0.99$.

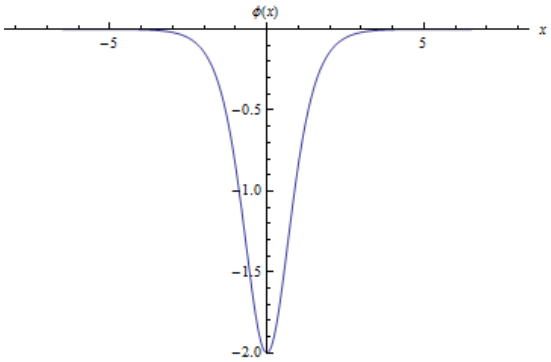

Figure 3.8: The one-soliton limit $k = 1$ of (3.33).

Bibliography

[1] Gert Eilenberger, Solitons, 1983.

[2] Peter Young, http://young.physics.ucsc.edu/ 250/mathematica/soliton.nb.pdf, 2007.

[3] http://de.wikipedia.org/wiki/Korteweg-de-Vries-Gleichung, 17.03.2014.

[4] http://en.wikipedia.org/wiki/Korteweg-de_Vries_equation, 17.03.2014.

[5] Andrei Ludu, Nonlinear Waves and Solitons on Contours and Closed Surfaces, 2012.

[6] http://functions.wolfram.com/EllipticFunctions/JacobiSN/ 13/01/02/, 2014.

Chapter 4

Kinks in ϕ^4 and in Sine-Gordon Theory

Author: Djordje Pantic
Supervisor: Dr. Marius de Leeuw

The following text deals with the derivation of kink solutions in ϕ^4 and in sine-Gordon theory. In addition, several important properties of kinks will be shown, as well as a systematic method of generating higher-order kink solutions.

4.1 Introduction

Solitons are solitary wave packets that maintain their shape while traveling at a constant speed, and that can collide against each other without being perturbed. Kinks are a type of soliton solutions in scalar field theories, such as ϕ^4 and sine-Gordon theory, which will be investigated here. Sine-Gordon theory is in fact related to ϕ^4, and it describes a system of coupled pendula in a gravitational field.

4.2 ϕ^4 Theory

4.2.1 Kink solutions

In order to find kink solutions, we shall start by looking at a more general case. The action for a real scalar field ϕ in its relativistically covariant form in D space-time dimensions $(t, x^1, x^2, ..., x^{D-1})$:

$$S_\phi = \int \mathrm{d}^D x \left\{ \frac{1}{2}(\partial_\mu \phi)(\partial_\nu \phi)\eta^{\mu\nu} - V(\phi) \right\} \ ,$$

where $\eta^{\mu\nu}$ is the (inverse) Minkowski metric. The corresponding equation of motion follows from the variation principle:

$$\frac{\delta S_\phi}{\delta \phi} = 0 \ \Rightarrow \ -\partial^2\phi - \frac{\mathrm{d}V}{\mathrm{d}\phi} = 0, \ \partial^2 = \eta^{\mu\nu}\partial_\mu\partial_\nu \ .$$

The Hamiltonian of a configuration $\phi = \phi(x^\mu)$ is given by:

$$H[\phi] = \int \mathrm{d}^{D-1} x \left\{ \frac{1}{2}(\partial_t \phi)^2 + \frac{1}{2}(\nabla\phi)^2 + V(\phi) \right\},$$

where $(\nabla\phi)^2 = \sum_{i=1}^{D-1}(\partial_i\phi)^2$.

Let us now consider the case where $D = 2$, i.e. with space-time coordinates (t, x). Further, we may take a static limit in order to find time-independent solutions $\phi = \phi(x)$. As a result, the equation of motion simplifies to $\frac{d^2\phi}{dx^2} = \frac{dV}{d\phi}$. Integrating this, we get:

$$\int_{\phi_0}^{\phi} \frac{\mathrm{d}\phi'}{\sqrt{2V(\phi')}} = x - x_0, \quad \phi_0 \equiv \phi(x_0), \tag{4.1}$$

where x_0 is the lower bound of integration with respect to the space coordinate.
At this point we introduce the ϕ^4 theory by considering a quartic potential

$$V(\phi) = \frac{\lambda}{4}(\phi^2 - \alpha^2)^2 \ , \quad \alpha^2 \equiv \frac{\mu^2}{\lambda} \ , \tag{4.2}$$

where α is a parameter that measures the strength of the field, and μ is a mass parameter. Upon inserting (5.2) into (5.1) and setting $\phi_0 = 0$ for simplicity, we get the *static kink solutions* of ϕ^4:

$$\phi_{\pm}(x) = \pm\frac{\mu}{\sqrt{\lambda}} \tanh\left(\frac{\mu}{\sqrt{2}}(x - x_0)\right) \ . \tag{4.3}$$

Moving kinks can be obtained by performing a Lorentz boost:

$$\phi_{\pm,v}(t, x) = \pm\frac{\mu}{\sqrt{\lambda}} \tanh\left(\frac{\mu}{\sqrt{2}}\gamma(x - x_0 - vt)\right) \ , \tag{4.4}$$

where $\gamma = \frac{1}{\sqrt{1-v^2/c^2}}$.

An example of a ϕ^4 kink is shown in figure 5.1.

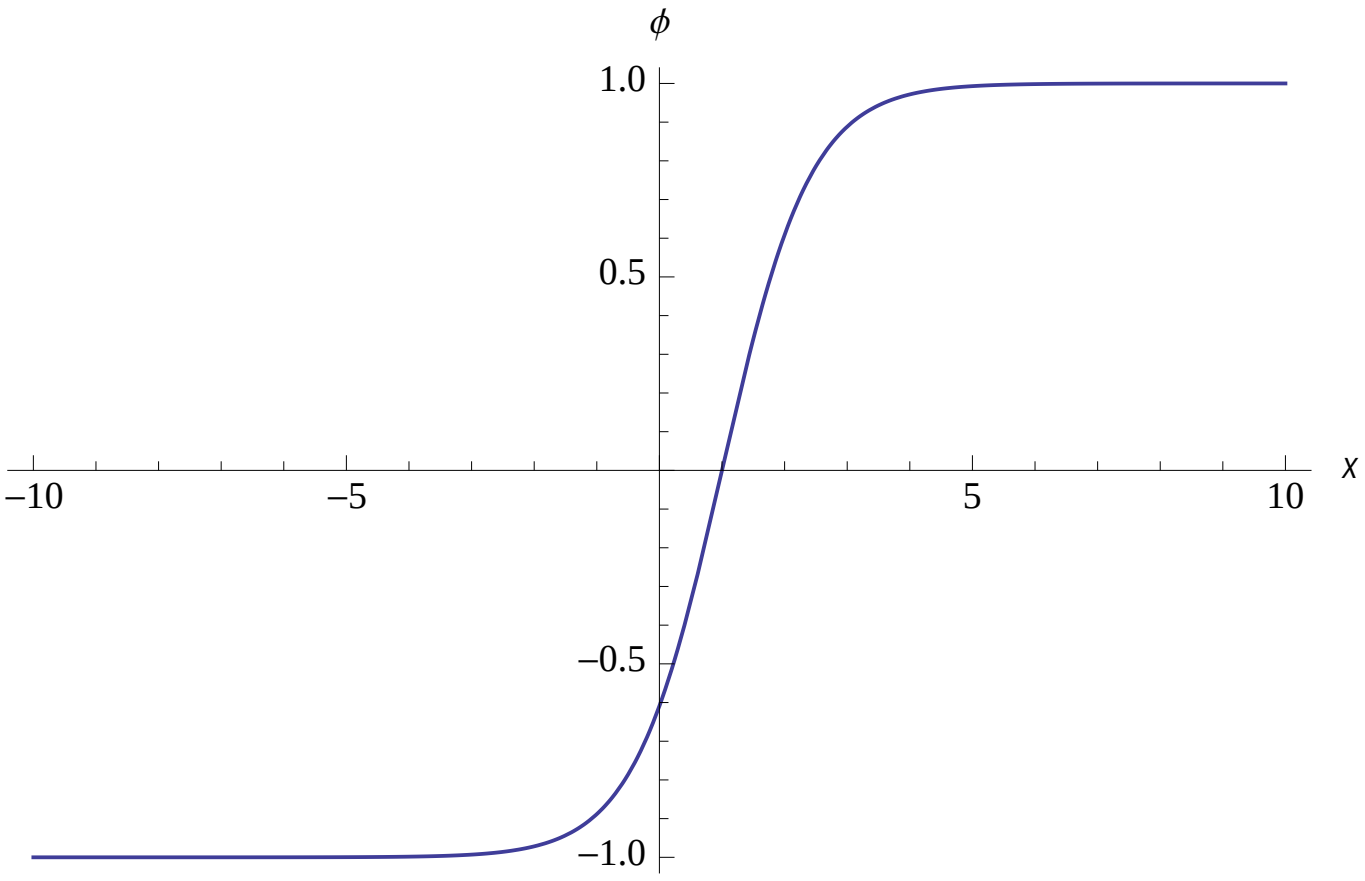

Figure 4.1: A ϕ^4 kink corresponding to the previously calculated $\phi_+(x)$.

Furthermore, the value of a kink for a certain value of x describes the position of a massive point particle moving from one minimum of the potential (5.2) to the other one. Hence, by rotating the graph of the potential by 90°, its point of intersection with a moving kink corresponds to the position of the aforementioned particle. This is illustrated in figure 5.2.

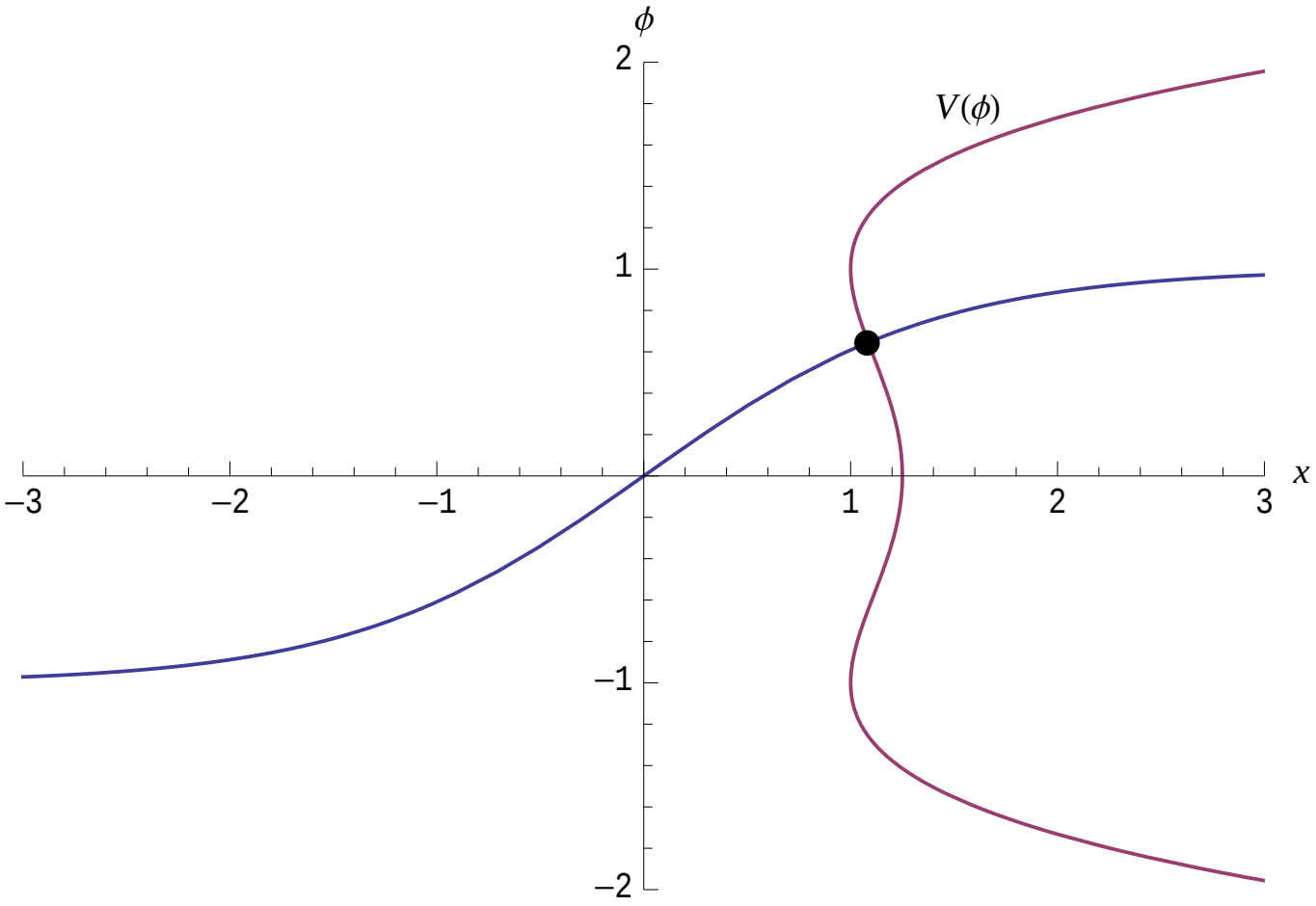

Figure 4.2: Point of intersection of a (moving) ϕ^4 kink (blue curve) with the corresponding quartic potential (5.2) (purple curve).

4.2.2 Properties of Kinks

Having established what kinks in ϕ^4 theory are, we shall now take a look at a few interesting properties that they possess.

i) The energy density of a static kink is given by the Hamiltonian density

$$\begin{aligned}\mathscr{H}[\phi_\pm] &= \frac{1}{2}(\partial_t\phi_\pm)^2 + \frac{1}{2}(\partial_x\phi_\pm)^2 + V(\phi_\pm) \\ &= \frac{\mu^4}{2\lambda}\frac{1}{\cosh^4[\frac{\mu}{\sqrt{2}}(x-x_0)]} \ .\end{aligned}$$

From this, we can conclude that the total energy (which can be identified with the mass) of a static kink is

$$M_{\text{kink}} = H[\phi_\pm] = \int_{-\infty}^{\infty} \mathrm{d}x \ \mathscr{H}[\phi_\pm] = \frac{2\sqrt{2}\mu^3}{3\lambda} \ .$$

A straightforward calculation yields

$$H[\phi_{\pm,v}] = \gamma M_{\text{kink}} \ .$$

Therefore, a moving kink obeys the relativistic energy-mass relation for point particles.

ii) Due to the nonlinearity of ϕ^4, a superposition of two kinks with different velocities and positions is in general *not* a solution. However, linear superpositions of kinks are approximate solutions to the theory, provided the separation between the individual kinks is large enough. This will later be illustrated graphically in the case of two-kink solutions.

iii) Kinks are non-perturbative: in the limit $\lambda \to 0$, (5.3) and (5.4) become ill-defined and thus meaningless. In other words, they cannot be obtained by perturbing around $\lambda = 0$.

iv) To investigate the stability of kinks, consider the current associated with a moving kink:

$$k^\mu_\pm = \frac{\sqrt{\lambda}}{2\mu}\epsilon^{\mu\nu}\partial_\nu\phi_{\pm,v} \ ,$$

where $\epsilon^{\mu\nu}$ is the Levi-Civita symbol. Due to the antisymmetry of $\epsilon^{\mu\nu}$, we have that

$$\partial_\mu k^\mu_\pm = 0 \ ,$$

which means that $k^\mu_\pm$ is conserved.
The charge associated with k^μ is

$$Q = \int_{-\infty}^{\infty} \mathrm{d}x \ k^0_\pm = \frac{\sqrt{\lambda}}{2\mu}[\phi_{\pm,v}(t,\infty) - \phi_{\pm,v}(t,-\infty)] = \pm 1 \ .$$

If $Q = 1$, the underlying object is a kink, whereas for $Q = -1$ it is called an *antikink*.

The quantity Q is also called the *topological index*, since it only depends on the boundaries of the kink. It can easily be seen that Q is conserved by the time evolution:

$$\frac{dQ}{dt} = \int \mathrm{d}x \partial_\mu k^\mu = 0 \ ,$$

since k^μ is conserved. Therefore, since the topological index of a kink is $\neq 0$ and is conserved, it cannot be converted by time evolution to a zero energy state (vacuum state), which has a different topological index $Q_{\text{vac}} = 0$. In other words, once a moving kink is created, it will travel forever without being destroyed.

4.3 Sine-Gordon Theory

The sine-Gordon field theory is defined by the Lagrangian density

$$\mathscr{L} = \frac{1}{2}(\partial_\mu\phi)^2 - \frac{m^2}{\beta^2}(1-\cos\beta\phi) = \frac{1}{2}(\partial_\mu\phi)^2 - \frac{m^2}{2!}\phi^2 + \frac{\beta^2 m^2}{4!}\phi^4 \pm \dots \ .$$

As it contains a ϕ^4 term itself, sine-Gordon theory can be seen as a deformation of ϕ^4 theory.

The Hamiltonian is given by

$$H[\phi,\dot{\phi}] = \int \mathrm{d}x \left[\frac{1}{2}(\dot{\phi}^2+\phi_x^2) + \frac{m^2}{\beta^2}(1-\cos\beta\phi)\right], \tag{4.5}$$

and thus the equation of motion, namely the sine-Gordon equation, is

$$\ddot{\phi} = \phi_{xx} - \frac{m^2}{\beta}\sin\beta\phi \ ,$$

where $\dot{\phi} \equiv \frac{\partial\phi}{\partial t}$, $\phi_x \equiv \frac{\partial\phi}{\partial x}$.

4.3.1 One-Kink Solutions

We shall use the same strategy as for ϕ^4 kinks: in order to find one-kink solutions to the theory, let us first look for static solutions $\phi = \phi(x)$, and then perform a Lorentz boost. In the static limit, the equation of motion simplifies to

$$\phi_{xx} = \frac{m^2}{\beta}\sin\beta\phi \ . \tag{4.6}$$

We shall further assume the boundary conditions $\phi_x(\pm\infty) = 0$, which correspond to a localization of the kink.

Taking a closer look at (5.6), one can see that it is also the equation of motion of the classical mechanical system

$$h = \frac{1}{2}\phi_x^2 + \underbrace{\frac{m^2}{\beta^2}(\cos\beta\phi - 1)}_{V(\phi)} \ , \tag{4.7}$$

which describes motion of particle in a periodic potential $V(\phi)$. Further, the boundary conditions $\phi_x(\pm\infty) = 0$ are equivalent to the requirement that the particle approaches one of the maxima of $V(\phi)$ at "time" $x \to \infty$, i.e. $\beta\phi(\pm\infty) \in 2\pi\mathbb{Z}$.

The total energy h of the solution can therefore be evaluated at $x \to \pm\infty$:

$$h = \frac{1}{2}\underbrace{\phi_x^2}_{\to 0} + \frac{m^2}{\beta^2}(\underbrace{\cos\beta\phi}_{\to 1} - 1)\Big|_{x\to\pm\infty} = 0.$$

Hence, by integrating (5.7), we get

$$x - x_0 = \pm\int \frac{\mathrm{d}\phi}{\sqrt{2(h-V(\phi))}} = \pm\frac{1}{m}\ \log\ \tan\frac{\beta\phi}{4} \ .$$

Inverting the dependence of x on ϕ and boosting it, we get the moving kink and antikink solution to the sine-Gordon theory, which are illustrated in figure 5.3:

$$\phi_k(x,t) = \frac{4}{\beta}\ \tan^{-1}e^{\gamma m(x-vt-x_0)}, \tag{4.8}$$

$$\phi_{\bar{k}}(x,t) = \frac{4}{\beta}\ \tan^{-1}e^{-\gamma m(x-vt-x_0)} \tag{4.9}$$

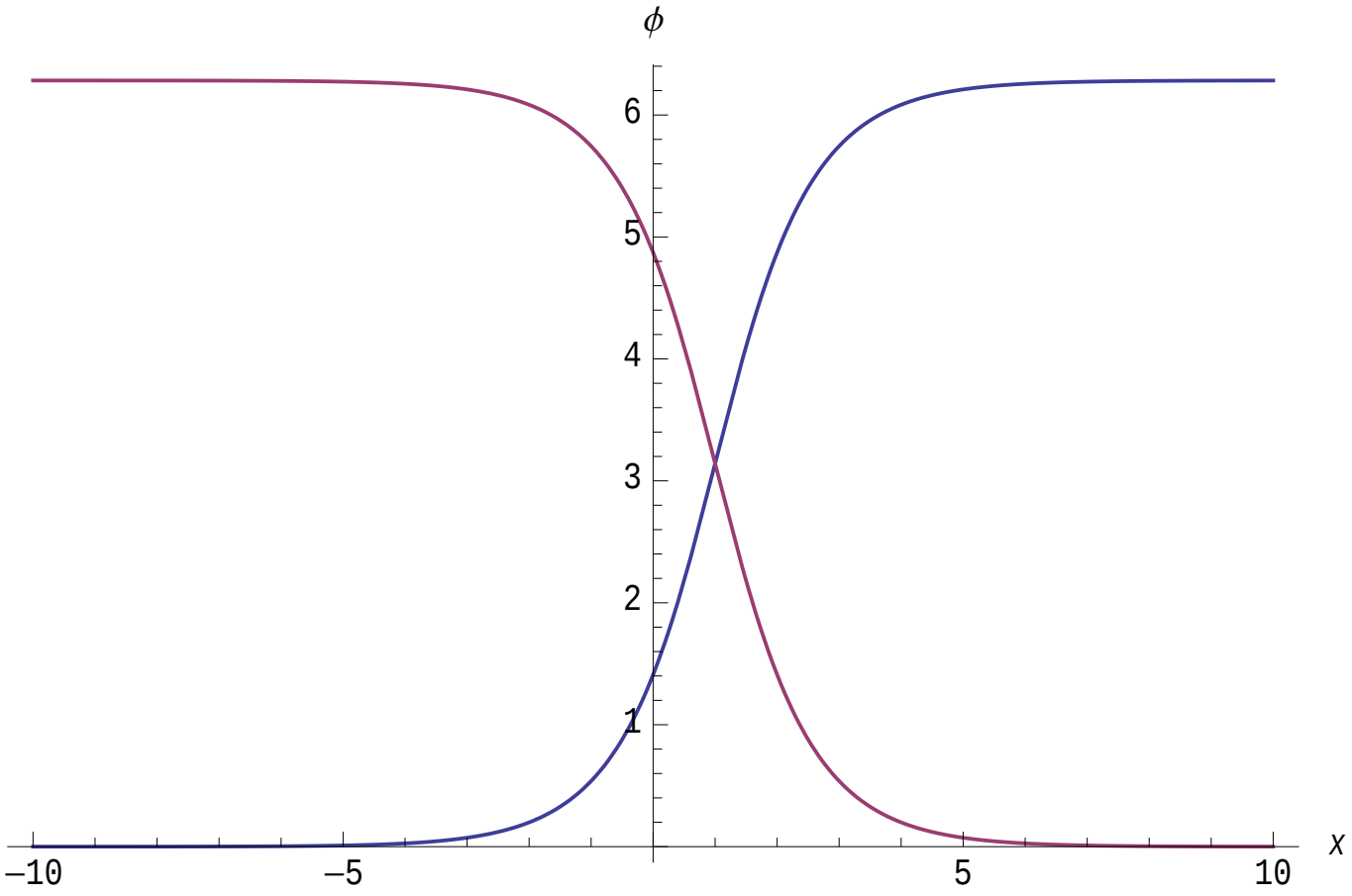

Figure 4.3: A sine-Gordon kink (blue curve) and antikink (purple curve).

We have introduced the energy of $\phi(x,t)$ in (5.5). The momentum is given by the component T_{01} of the energy momentum tensor

$$T_\mu{}^\nu = \partial_\mu\phi\frac{\delta\mathscr{L}}{\delta\partial_\nu\phi} - \delta^\nu_\mu\mathscr{L} \ ,$$

namely

$$P[\phi,\dot\phi] = \int \mathrm{d}x \ \dot\phi\phi_x \ . \tag{4.10}$$

By inserting (5.8) into (5.5) and (5.10) and integrating explicitly, we get

$$H[\phi_k] = \frac{M}{\sqrt{1-v^2}} \ , \quad P[\phi_k] = \frac{Mv}{\sqrt{1-v^2}} \ ,$$

which coincides with the energy and momentum of a relativistic particle of mass

$$M = M_k = M_{\bar k} = \frac{8m}{\beta^2} \ .$$

Since it will be of use later, recall that the energy and momentum of a relativistic particle with mass M can be written as

$$E = M\cosh\theta \ , \quad P = M\sinh\theta \ ,$$

where the rapidity θ is defined by $v = \tanh\theta$.

Note that the antikink solution can be obtained from the kink solution by the transformation

$$\theta \mapsto \theta + i\pi \ .$$

4.3.2 Multikink Solutions

When looking for multikink solutions, it is beneficial to introduce light cone coordinates:

$$\tau = \frac{t+x}{2} \ , \quad \partial_\tau = \partial_t + \partial_x \ ,$$
$$\sigma = \frac{t-x}{2} \ , \quad \partial_\sigma = \partial_t - \partial_x \ .$$

A way to generate multikink solutions is via the *Bäcklund transformation*:

$$\partial_\tau \phi_2 = \partial_\tau \phi_1 + \frac{2m\eta}{\beta} \ \sin\frac{\beta}{2}(\phi_1 + \phi_2)$$
$$\partial_\sigma \phi_2 = -\partial_\sigma \phi_1 + \frac{2m}{\beta\eta} \ \sin\frac{\beta}{2}(\phi_1 - \phi_2) \ ,$$

which maps a solution ϕ_1 to another solution ϕ_2 with a spectral parameter η.
One can prove that this transformation indeed maps a solution to another one by acting with ∂_σ on the first equation and then using the second one to evaluate it:

$$\partial_\sigma \partial_\tau \phi_2 = \partial_\sigma \left(\partial_\tau \phi_1 + \frac{2m\eta}{\beta} \ \sin\frac{\beta}{2}(\phi_1 + \phi_2) \right)$$
$$\Leftrightarrow \ \partial_\sigma \partial_\tau (\phi_2 - \phi_1) = m \ \eta \ \cos\frac{\beta}{2}(\phi_1 + \phi_2) \ \partial_\sigma(\phi_1 + \phi_2)$$
$$= \frac{2m^2}{\beta} \ \cos\frac{\beta}{2}(\phi_1 + \phi_2) \ \sin\frac{\beta}{2}(\phi_1 - \phi_2)$$
$$= \frac{m^2}{\beta}(\sin\beta\phi_1 - \sin\beta\phi_2)$$
$$\Leftrightarrow \ (\partial_t^2 - \partial_x^2)(\phi_2 - \phi_1) = \frac{m^2}{\beta}(\sin\beta\phi_1 - \sin\beta\phi_2) \ ,$$

and since per assumption ϕ_1 is a solution, we get

$$(\partial_t^2 - \partial_x^2)\phi_2 = -\frac{m^2}{\beta}\sin(\beta\phi_2) \ ,$$

so ϕ_2 is indeed a solution. □

We can generate multikink solutions by acting with the Bäcklund transformation iteratively on the trivial solution $\phi = 0$. Therefore, the one-kink solution can be recovered by setting $\phi_1 = 0$ in the Bäcklund transformation and integrating:

$$\eta^{-1}\partial_\tau \phi_2 = -\eta \partial_\sigma \phi_2 = \frac{2m}{\beta}\sin\frac{\beta\phi_2}{2} \ .$$

The most general solution to these equations is

$$\phi_2 = \frac{4}{\beta} \ \tan^{-1}\exp \ m(\eta^{-1}\tau - \eta\sigma - x_0) \ ,$$

where x_0 is a constant of integration.
Setting $\eta = e^\theta$ and using the definition of light cone coordinates and the rapidity θ, we recover the one-kink solution (5.8):

$$\phi_k = \frac{4}{\beta} \ \tan^{-1}\exp(x \ \cosh\theta - t \ \sinh\theta - x_0) \ .$$

We can generate two-kink solutions by performing a Bäcklund transformation on (5.8) and integrating for ϕ_2. However, the integration turns out to be not quite trivial. Therefore, we shall introduce a more elegant, purely algebraic way to generate multikink solutions due to *Bianchi*:
Starting with a classical solution ϕ of the sine-Gordon equation, we can generate two new solutions ϕ_1 and ϕ_2 by integrating the Bäcklund transformation of ϕ with spectral spectral parameter η_1 and η_2, respectively. Further, if we integrate the Bäcklund transformation of ϕ_1 with the spectral parameter η_2 which was used in the calculation of ϕ_2, we get a new, higher-order solution that we shall denote by ϕ_{12}. Similarly, another solution ϕ_{21} can be obtained by integrating the Bäcklund transformation of ϕ_2 with the spectral parameter η_1. This is demonstrated in figure 5.4.

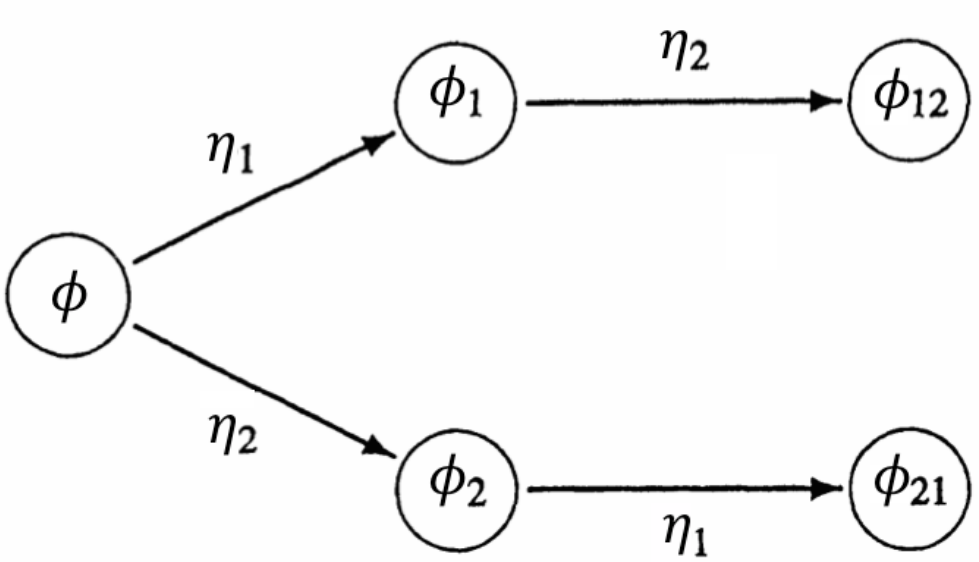

Figure 4.4: Two possibilities to perform two consecutive Bäcklund transformations of a solution ϕ with spectral parameters η_1 and η_2.

In general, the solutions ϕ_{12} and ϕ_{21} will depend not only on the spectral parameters η_1 and η_2, but also on some integration constants. As can be seen in figure 5.4, this means that in general $\phi_{12} \neq \phi_{21}$. However, *Bianchi's permutability theorem* states that it is possible to choose the integration constants in a way that $\phi_{12} = \phi_{21} = \Phi$.

To prove the theorem, notice that if the solution Φ exists, then the commutativity of the Bäcklund transformations requires that

$$\partial_\tau \phi_{12} = \partial_\tau \phi_1 + \frac{2m\eta_2}{\beta} \sin\frac{\beta}{2}(\Phi + \phi_1) = \partial_\tau \phi + \frac{2m\eta_1}{\beta} \sin\frac{\beta}{2}(\phi + \phi_1) + \frac{2m\eta_2}{\beta} \sin\frac{\beta}{2}(\Phi + \phi_1) \ ,$$
$$\partial_\tau \phi_{21} = \partial_\tau \phi_2 + \frac{2m\eta_1}{\beta} \sin\frac{\beta}{2}(\Phi + \phi_2) = \partial_\tau \phi + \frac{2m\eta_2}{\beta} \sin\frac{\beta}{2}(\phi + \phi_2) + \frac{2m\eta_1}{\beta} \sin\frac{\beta}{2}(\Phi + \phi_2) \ . \quad (4.11)$$

Subtracting the two equations we get an equation which can be solved for Φ. One of the solutions is given by

$$\Phi = \phi + \frac{4}{\beta} \tan^{-1}\left[\frac{\eta_1 + \eta_2}{\eta_1 - \eta_2} \tan\frac{\beta}{4}(\phi_1 - \phi_2)\right] \ . \quad (4.12)$$

To finish the proof, one checks that (5.12) satisfies (5.11) together with

$$\partial_\sigma \phi_{12} = -\partial_\sigma \phi_1 + \frac{2m}{\eta_2 \beta} \sin\frac{\beta}{2}(\phi_1 - \Phi) = \partial_\sigma \phi - \frac{2m}{\eta_1 \beta} \sin\frac{\beta}{2}(\phi - \phi_1) + \frac{2m\eta_2}{\beta} \sin\frac{\beta}{2}(\phi_1 - \Phi) \ ,$$
$$\partial_\sigma \phi_{21} = -\partial_\sigma \phi_2 + \frac{2m}{\eta_1 \beta} \sin\frac{\beta}{2}(\phi_2 - \Phi) = \partial_\sigma \phi - \frac{2m}{\eta_2 \beta} \sin\frac{\beta}{2}(\phi - \phi_2) + \frac{2m\eta_1}{\beta} \sin\frac{\beta}{2}(\phi_2 - \Phi) \ .$$

□

Setting $\phi = 0,\ \eta_1 = e^{\theta},\ \eta_2 = e^{-\theta}$ and

$$\phi_i = \frac{4}{\beta}\,\tan^{-1}\exp\, m(\eta_i^{-1}\tau - \eta_i\sigma)$$

in (5.12), we get the kink-antikink solution in the center of mass frame:

$$\phi_{k\bar{k}}(x,t) = -\frac{4}{\beta}\,\tan^{-1}\frac{\sinh\, m\gamma v t}{v\,\cosh\, m\gamma x}\ . \tag{4.13}$$

On the other hand, for $\eta_1 = e^{\theta}$, $\eta_2 = -e^{-\theta}$, we get the kink-kink solution in the center of mass frame:

$$\phi_{kk}(x,t) = \frac{4}{\beta}\,\tan^{-1}\frac{v\,\sinh\, m\gamma x}{\cosh\, m\gamma v t}\ . \tag{4.14}$$

A plot of (5.13) and (5.14) is shown in figure 5.5 for a small time t.

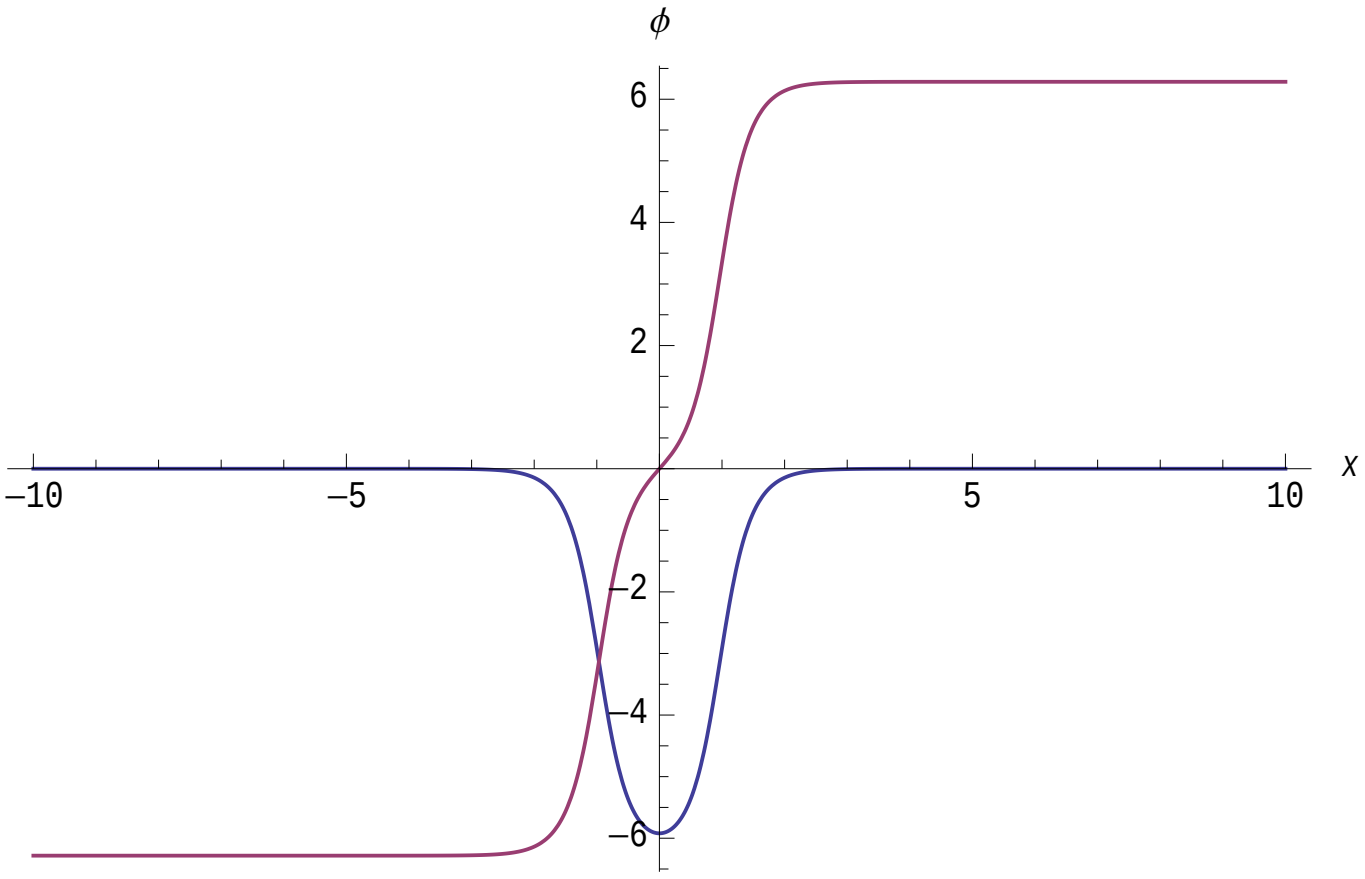

Figure 4.5: A sine-Gordon kink-antikink (blue curve) and kink-kink (red curve) for a small time t.

For large t, (5.13) and (5.14) become a superposition of a kink and an antikink, or two kinks, respectively.
The energy and momentum of $\phi_{k\bar{k}}$ in the center of mass frame can be calculated by inserting (5.13) into (5.5) and (5.10) and calculating the integrals explicitly:

$$H[\phi_{k\bar{k}}] = 2M\,\cosh\,\theta\ , \quad P[\phi_{k\bar{k}}] = 0\ .$$

In fact, the total momentum vanishes only because we chose the spectral parameters in a way that the individual kink and the antikink travel in opposite directions with the same velocity. Moreover, the total energy is simply the sum of the energies of the individual kinks. In this sense, kinks behave like massive particles.

By treating v in (5.13) as a formal variable instead of as a velocity, we can generate a new type of solution by setting $v = i\ \tan\vartheta_b$ $(\vartheta_b \in \mathbb{R} \Rightarrow v \in i\mathbb{R})$:

$$\phi_b(x,t) = -\frac{4}{\beta}\ \tan^{-1}\frac{\sin(tm\ \sin\vartheta_b)}{\tan\vartheta_b\ \cosh(xm\ \cos\vartheta_b)}\ .$$

This solution is called a *breather*. Its energy

$$H[\phi_b] = 2M\ \cos\vartheta_b \leq 2M$$

suggests that it is a $k\bar{k}$ bound state. Indeed, its time evolution is different from that of the two-kink solutions we have seen previously. A breather is localized in a neighborhood of a fixed point x in space, in this case $x = 0$. Clearly, this is an oscillating system.

4.4 Conclusion

We have seen that moving kinks obey the relativistic energy-mass relation for point particles: $E_{\text{kink}} = \gamma M_{\text{kink}}$. Moreover, kinks are characterized by their topological index $Q = \pm 1$, which is conserved in time. Hence, a moving kink travels forever without being destroyed. Multikink solutions can be generated by iterating the Bäcklund transformation on the trivial solution $\phi = 0$. A more elegant method arises from Bianichi's permutability theorem. Lastly, the energy and momentum of a multikink are the sums of the energies and momenta of the individual kinks by which it is generated. This is another feature that kinks share with particles.

Bibliography

[1] Gleb Arutyunov, Utrecht University, *Classical Field Theory*,
http://www.staff.science.uu.nl/∼proko101/CFTnotesGleb.pdf

[2] Tomislav Prokopec, Utrecht University, *Classical field theory 2013 (NS-364B) - Supplementary lecture notes*,
http://www.staff.science.uu.nl/ proko101/AdditionalNotes2013.pdf

[3] Constantin Candu, ETH Zürich, *Introduction to Integrability*,
http://www.itp.phys.ethz.ch/research/qftstrings/archive/13FSInt/CFT

Chapter 5

Spontaneous symmetry breaking, Goldstone's theorem

Author: Steffen Arnold
Supervisor: Christian Vergu

The idea of spontaneous symmetry breaking is a crucial concept in quantum field theory. As will be shown, the spontaneous breaking of a global continuous symmetry results in the emergence of massless modes, the so-called Goldstone bosons. Goldstone's theorem then examines the number of these Goldstone bosons when dealing with certain physical systems and their underlying symmetries. This report introduces the concept of spontaneous symmetry breaking in terms of complex ϕ^4 theory and provides a brief derivation of Goldstone's theorem in the classical as well as in the quantum mechanical case.

5.1 Introduction

Our nature is full of asymmetries, and the concept of symmetry breaking is illustrated at this point by means of the chirality of snail shells. The reader may already be aware of the fact that the vast majority of snail shells have a spiral structure that is *right*-coiling. Actually, snails with differing orientations of their spiral structure are, generally, not able to mate. While this explains why a certain chirality dominates within the population, however, it does not explain why this should be just the *right*-coiling shells, and there is no plausible reason for this specific preference in nature. This is an example on symmetry breaking in nature: The underlying system is, in principle, symmetric. However, it *appears* to be asymmetric and could be described by asymmetric laws. Obviously, one would not base a study of the morphology of snail shells on the prevalent chirality but rather understand it as some variable in such a theory. Imagine now we were missing the information that there do exist *left*-coiling shells in nature and we had based our theory on the exclusive existence of right-coiling shells. The challenge then lies in recognizing the underlying symmetry that possibly prevents us from gaining further insight into the theory and its unity.

This report deals with the spontaneous breaking of a continuous symmetry in physical theories, a fundamental concept in quantum field theory, that is, the physics of subatomic particles or quasiparticles. For a long time it was assumed that the weak and electromagnetic interactions need to be considered as two processes basically independent from each other. In fact, the spontaneous breaking of the $SU(2) \times U(1)$ symmetry gives rise to a *unified* theory of weak and electromagnetic interactions

together. The same concept also provides the basis for the famous Higgs mechanism that attributes mass to the so-called Higgs gauge bosons.

The concept of the spontaneous breaking of a global continuous symmetry will, in this report, be familiarized in terms of the simple yet instructive complex ϕ^4 theory, that is, for the time being neglecting quantum field theory. It will then be shown that, and for which reason, the spontaneous breaking of a global continuous symmetry results in the emergence of massless modes that we refer to as the so-called Goldstone bosons. Goldstone's theorem, whose proof will be outlined in the further course of this report, then examines how the number of these massless modes is related to the generators of the symmetries when dealing with a particular physical system. The main findings from these considerations will be summarized at the end of this report.

5.2 Spontaneous symmetry breaking

5.2.1 Examples

We will start to explore the spontaneous breaking of a global symmetry by considering two illustrative physical examples, the first one being the rod bent through applying a force along its length, and the second one being the spin orientations of an infinitely large ferromagnet depending on its temperature. From these examples, then, their common features will be summarized, which already provide a first vague characterization of spontaneous symmetry breaking.

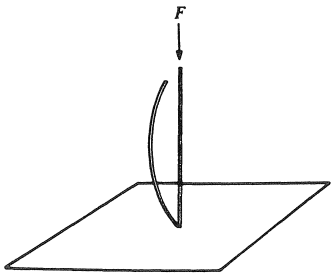

Figure 5.1: A thin rod will bend when a force F is applied along its length. Source: [1]

Bent rod First, think of a thin rod of circular cross-section that we place vertically on a table as illustrated in Figure 5.1. This physical system possesses a global rotational symmetry, we would not be able to distinguish a second arrangement of this rod that was rotated along its length from the initial one. Now, we push down along its length with a force F. When F exceeds a critical value, the rod will certainly bend into a *random* direction. This new arrangement of the rod bent into a *particular* direction consequently lost its rotational symmetry. By rotation, however, we would still be able reach each of the *imaginable* outcomes of this little thought experiment.

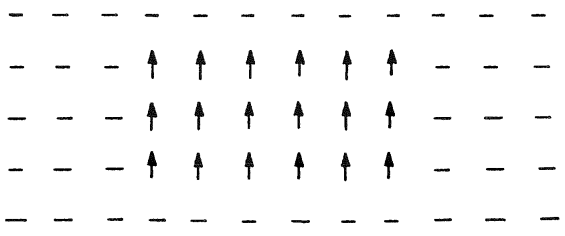

Figure 5.2: At low temperatures T the spins of a ferromagnet are aligned. Source: [1]

Infinitely large ferromagnet The second example addresses the idealized and infinitely large ferromagnet. As should be known, the behavior of this particular physical system stems from spin-spin interaction, and its Hamiltonian is therefore given by

$$H = -\sum_{i,j} J_{i,j}\, S_i \cdot S_j \,,$$

with $J_{i,j}$ being the coupling tensor. In the simplified Ising model, $S_i = \pm 1$ and only interaction between nearest neighbors is considered. In the ground state, i.e. the state of minimal energy, all spins are aligned within one domain as illustrated in Figure 5.2, and obviously this state is not invariant under rotation. At high temperatures T, however, the spins become randomly oriented and the ground state therefore becomes symmetric.

Important features The important features exhibited by both of these examples include that (a) there exists a parameter, e.g. the force F or the temperature T, that exceeds some *critical value*, and subsequently (b) the symmetric configuration of the physical system becomes unstable. A new *ground state* is then reached (c) that is is *degenerate*, and this particular ground state – not to be confused with the set of equally possible ground states – does no longer share the symmetry of the initial symmetric configuration of the physical system.

5.2.2 Symmetries

Before we are ready to translate the findings from the previous examples into a profound concept, we need an understanding of global symmetries. A global symmetry is present when a physical system is invariant under application of one or more global transformations.

Global transformations A *global* transformation is independent of the point in space-time, as opposed to a local transformation. An example for a common global and continuous symmetry is the rotation by a certain angle. Substantial parts of physics may be expressed in terms of invariant Lagrangians and their underlying symmetries.

We can generalize the operators of a Lie group in the form

$$U(\alpha) = \mathrm{e}^{-\mathrm{i}\alpha_k Q_k} \,,$$

where a_k are parameters and Q_k are the basic operator functions. We may then identify the *generators* of the transformation Q_k by partial derivatives, i.e.

$$-\mathrm{i}Q_k = \frac{\partial}{\partial \alpha_k} U(\alpha = 0) \,.$$

5.2.3 Breaking

Equipped with an understanding of global symmetries, we are now ready to turn to their breaking. The following considerations will be based on classical scalar field theory, and the reader may find a more general treatment within the framework of quantum field theory in [1]. First, some subsequently used terminology is clarified, thus setting up the framework. Then, the concept of spontaneous symmetry breaking will be examined and formalized in terms of the simple yet instructive ϕ^4 theory. Based on this theory, the emergence of massless modes, the so-called Goldstone bosons, that arise from the breaking of the symmetry, will be demonstrated and interpreted.

Framework From classical mechanics one might be used to deal with point-like particles and the generalized coordinates $q_i(t)$ at a time t associated with them. From the Lagrangian L of the physical system one may then easily deduce the equations of motion that allow us to find expressions for the behavior of the system. In field theory, we regard excitations of a physical field rather than point-like particles, and the generalized coordinates $q_i(t)$ are consequently replaced by the field amplitude $\phi(x^\mu)$ at some point x^μ in space-time. Instead of the Lagrangian L that characterizes the state of the *overall* system, we formulate the physical system through a Lagrangian density $\mathcal{L}$, thus introducing locality as necessary for physical fields, and the action $\mathcal{S}$ is then given through

$$\mathcal{S} = \int \mathrm{d}^{D-1}x \, \mathrm{d}t \, \mathcal{L} \,,$$

where the explicit form of $\mathcal{L}$ depends on the field theory under consideration. It can be shown that the equations of motion for a field theory are indeed corresponding to those in classical mechanics by replacing $t \mapsto x^\mu$ and $q_i(t) \mapsto \phi(x^\mu)$. Upon quantization of the field we arrive at the particle interpretation. For a complex scalar field, $\mathcal{L}$ is given by

$$\mathcal{L} = (\partial_\mu \phi)(\partial^\mu \phi^*) - V(\phi, \phi^*) \,,$$

and the ground state, that is, the state of lowest energy, is consequently found by minimizing the potential $V(\phi, \phi^*)$ and may be identified with the notion of the vacuum in the particle interpretation.

We already get the idea that a particular ground state solution does not share the same symmetry of the Lagrangian density in the case of a spontaneously broken symmetry. The term 'spontaneous' refers the broken symmetry of a particular ground state solution depending on some parameter, although the Lagrangian density $\mathcal{L}$ (and its potential) is still symmetric.

Complex ϕ^4 theory Consider the Lagrangian density

$$\mathcal{L} = (\partial_\mu \phi)(\partial^\mu \phi^*) - \underbrace{\left[m^2 \phi^* \phi + \lambda (\phi^* \phi)^2\right]}_{V(\phi, \phi^*)} , \tag{5.1}$$

of complex ϕ^4 theory which owes its name to the quartic self-interaction term $(\phi^* \phi)^2 = |\phi|^4$ in the potential $V(\phi, \phi^*)$. Quantization of the field ϕ yields particles of mass m, but m^2 is regarded within the following considerations as a parameter only. This Lagrangian density has a global $U(1)$ symmetry, i.e. it is invariant under any transformations of the form

$$\phi \mapsto \phi' = \mathrm{e}^{\mathrm{i}\Lambda} \, \phi \,, \; \Lambda = \text{const.}$$

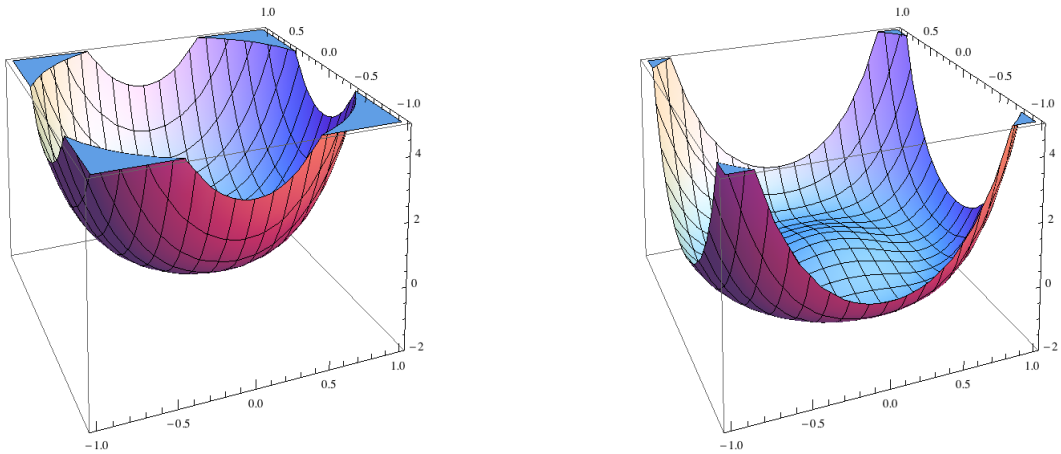

Figure 5.3: The potential $V(\phi, \phi^*)$ from Equation 5.1 for $m^2 > 0$ (left) and $m^2 < 0$ (right).

The appearance of the potential $V(\phi, \phi^*)$ for the two interesting cases $m^2 < 0$ and $m^2 > 0$ is illustrated in Figure 5.3. The latter potential is sometimes referred to as *Mexican hat potential*.

We may then obtain the ground state solutions for this potential as its minima from

$$\frac{\partial V}{\partial \phi} = m^2 \phi^* + 2\lambda\, \phi^* (\phi^* \phi) \quad \& \text{ complex conjugate.}$$

For $m^2 > 0$ there exists a single minimum at $\phi^* = \phi = 0$. In the more interesting case of $m^2 < 0$ we obtain two different extrema, the former minimum at $\phi^* = \phi = 0$ has now become a maximum, and in addition we surprisingly find new minima for

$$\phi^* \phi = -\frac{m^2}{2\lambda} =: a^2 \,. \tag{5.2}$$

In other words, the minima of $V(\phi, \phi^*)$ lie along the circle $|\phi| = a$, thus forming a set of degenerate ground states that are related to each other by the symmetry of $\mathcal{L}$. A particular ground state does not share the global symmetry of the physical system, hence, the symmetry is spontaneously broken for $m^2 < 0$. Physical fields, i.e. excitations above the ground state, are then realized as perturbations about the *chosen* ground state at $|\phi| = a$.

Goldstone boson We will now try to find these physical fields by finding a representation of ϕ for which the new fields are corresponding to foresaid perturbations. Put

$$\phi = [\rho + a]\, \mathrm{e}^{\mathrm{i}\theta},$$

i.e. the field ϕ is expressed in terms of two *real* scalar fields ρ and θ and such that both ρ and θ have *vanishing* vacuum expectation values in the particle interpretation. Plugging the new expression for ϕ into $V(\phi, \phi^*)$ and using Equation 5.2 $\Leftrightarrow m^2 = -2a^2\lambda$ we obtain

$$\begin{aligned} V(\phi, \phi^*) &= m^2 \left[\rho + a\right]^2 + \lambda \left[\rho + a\right]^4 \\ &= -2\, a^2 \lambda \left[\rho + a\right]^2 + \lambda \left[\rho + a\right]^4 \\ &= -2\, a^2 \lambda \left[\rho^2 + 2\, a\rho + a^2\right] \\ &\quad + \lambda \left[\rho^4 + 4\, a\rho^3 + 6\, a^2 \rho^2 + 4\, a^3 \rho + a^4\right] \\ &= \lambda \rho^4 + 4\, \lambda a \rho^3 + \boxed{4\, \lambda a^2 \rho^2} - \lambda a^4 \,. \end{aligned} \tag{5.3}$$

Similarly, the new expression for $(\partial_\mu \phi)(\partial^\mu \phi^*)$ yields

$$(\partial_\mu \phi)(\partial^\mu \phi^*) = (\partial_\mu \rho)(\partial^\mu \rho) + \left[\rho + a\right]^2 (\partial_\mu \theta)(\partial^\mu \theta) \,.$$

In particular, a term in ρ^2 appears in the Lagrangian density $\mathcal{L}$, and consequently the field ρ has a mass associated with it that is given by (cf. Equation 5.3)

$$m_\rho^2 = 4\lambda a^2 \,.$$

At the same time, there is no such term in θ^2, and we conclude that θ is a *massless* field.

From the spontaneous breaking of the global $U(1)$ symmetry of complex ϕ^4 theory we obtain a massive and a massless field from what would otherwise be two massive fields. One may imagine that if we placed a ball inside the potential it would obviously cost energy to displace it along ρ, that is, against the restoring forces of the potential, whereas there are no restoring forces along $|\phi| = a$, that is, for θ. The massless θ particle is referred to as Goldstone boson.

5.3 Goldstone's theorem

As was shown previously for complex ϕ^4 theory, the spontaneous breaking of a global continuous symmetry results in the emergence of massless modes which we refer to as Goldstone bosons. This section deals with the question of the general validity of this observation, the number of Goldstone bosons which we may expect when dealing with certain physical systems and their underlying symmetries, and the status of this concept in quantum field theory.

The number of Goldstone bosons can be derived from group theoretical considerations and forms the key part of Goldstone's theorem as formulated in the following.

5.3.1 Number of Goldstone bosons

We will now try to find a relation between the result of a group transformation and the mass of the associated field ϕ_a. Assume, we had some Lagrangian density $\mathcal{L}$ that is globally invariant under a symmetry group G. Furthermore, we have a set of N real fields ϕ_a, $a = 1, 2, 3, ..., N$ and that the potential $V(\phi)$ is invariant under a group transformation $g \in G$. Next, we try to construct the subgroup H of G that contains all elements of G that leave the ground state ϕ_0 invariant. This could basically be everything between (a) the trivial case, that is, *all* symmetries are spontaneously broken, or (b) the full group, that is, *no* symmetries are spontaneously broken.

Derivation Since ϕ_0 is the ground state, it must hold that

$$\left.\frac{\partial V}{\partial \phi}\right|_{\phi=\phi_0} = 0\,,$$

and we may expand the potential $V(\phi_a)$ around the ground state

$$V(\phi) = V(\phi_0) + \frac{1}{2}\left(\frac{\partial^2 V}{\partial\phi_i \partial\phi_j}\right)_{\phi=\phi_0} \chi_i\,\chi_j + \mathcal{O}(\chi^3)\,, \quad \chi_i(x) = \phi_i(x) - \phi_0\,.$$

The *mass tensor* $M_{i,j}$ is therefore given through

$$M_{i,j} = \left(\frac{\partial^2 V}{\partial\phi_i \partial\phi_j}\right)_{\phi=\phi_0}\,,$$

and, in particular, $M_{i,j}$ must be positive or zero because $V(\phi_0)$ is the minimum.

Next we apply a group transformation to the potential,

$$\phi \mapsto \phi' = U(g)\phi$$

where $U(g)$ is the unitary matrix corresponding with the group element $g \in G$, resulting in

$$V(\phi_0') = V(U(g)\phi_0) = V(\phi_0) + \frac{1}{2}\left(\frac{\partial^2 V}{\partial\phi_i \partial\phi_j}\right)_{\phi=\phi_0} \delta\phi_i\,\delta\phi_j + ...$$

where $\delta\phi_i$ is the variation in ϕ_i under the transformation and we have used the assumption, that the potential V is invariant under a group transformation. Obviously, it must hold

$$\left(\frac{\partial^2 V}{\partial\phi_i \partial\phi_j}\right)_{\phi=\phi_0} \delta\phi_i\,\delta\phi_j = 0\,, \tag{5.4}$$

otherwise, ϕ_0 would not be the ground state in contradiction with our assumptions.

Case 1: If g belongs to the subgroup H of G, that is, it leaves the ground state ϕ_0 invariant, then it follows from $\phi_0' = \phi_0$, immediately, that

$$\delta\phi_i = [U(g)\phi_0 - \phi_0]_i = 0$$

in full correspondence with the claim in Equation 5.4.

Case 2: If, however, g does *not* belong to the subgroup H of G, that is, $\phi_0' \neq \phi_0$, then the variation $\delta\phi_i$ may be approximated through

$$\delta\phi_i = \underbrace{\left[\left(\frac{\partial U}{\partial \alpha_k}\right)_{\alpha_k=0} \phi_0\right]_i}_{=:U'(0)\phi_0} \delta\alpha_k \neq 0\,.$$

Consequently, it must hold from Equation 5.4

$$M_{i,j}\,[U'(0)\phi_0]_j = 0\,,$$

i.e. the fields $U'(0)\phi_0$ are massless. These are the Goldstone bosons.

Conclusion The number of fields that are not required to be massless is simply the dimension of the Lie algebra of H. The elements $g \notin H$ do not form a group, instead we may then derive the number of Goldstone bosons from the dimension of the coset G/H, that is, the number of generators of the symmetry group G that are not also generators of the subgroup H.

In particular, this result does not depend on the actual representation of G nor on the form of the potential. Note that this conclusion even holds in the case that the symmetry is *not* broken.

5.3.2 Goldstone's theorem

We now have all the information needed to formulate the classical version of Goldstone's theorem.

Assume, the Lagrangian density $\mathcal{L}$ is invariant under a symmetry group G, and that the ground state solution is invariant under a subgroup H of G. Then, for each generator of G that is not a generator of H, there will emerge massless particles that we call Goldstone bosons.

5.3.3 Status in quantum mechanics

A rigorous proof of Goldstone's theorem in the framework of quantum mechanics turns out to be quite complicated and requires the consideration of some subtleties. Therefore, the proof is only outlined in the following. The reader may be referred to [3] for an extensive proof.

- Start by recalling that we have, due to the invariance of $\mathcal{L}$ under G, divergenceless Noether currents j_μ^a and that the corresponding charges Q^a are conserved.
- The conserved charges Q^a are the generators of the global transformations.
- Assume that the field operator $\phi(x)$ has a non-vanishing vacuum expectation value, i.e.

$$\langle 0|\phi(x)|0\rangle \neq 0\,.$$

- Assume that the field operator $\phi(x)$ is not a singlet under the transformation and, therefore, there must exist another operator $\phi'(x)$ such that

$$[Q^a, \phi'(x)] = \phi(x)\,.$$

- We thus arrive, by plugging in the expression for Q^a, at

$$0 \neq \langle 0|\phi(x)|0\rangle = \langle 0|\left[Q^a, \phi'(x)\right]|0\rangle = \int \mathrm{d}^3y \, \langle 0|\left[j_0^a(y), \phi'(x)\right]|0\rangle \,, \tag{5.5}$$

  and it can be shown that this expression implies the existence of massless particles.

- Continue by inserting the completeness relation into Equation 5.5, yielding

$$0 \neq \sum_n \int \mathrm{d}^3y \, \left(\langle 0|j_0^a(y)|n\rangle\langle n|\phi'(x)|0\rangle - \langle 0|\phi'(x)|n\rangle\langle n|j_0^a(y)|0\rangle\right) . \tag{5.6}$$

- Using translation invariance and performing the spatial integral, we arrive at

$$0 \neq (2\pi)^2 \sum_n \delta^3(\boldsymbol{p}_n) \left(\langle 0|j_0^a(0)|n\rangle\langle n|\phi'(x)|0\rangle \, \mathrm{e}^{\mathrm{i}M_n y_0} - \langle 0|\phi'(x)|n\rangle\langle n|j_0^a(0)|0\rangle \, \mathrm{e}^{-\mathrm{i}M_n y_0}\right) . \tag{5.7}$$

- It can be shown that Equation 5.7 is independent of y_0 using that j_μ^a is divergenceless and integrating its Taylor expansion. We may then conclude that $M_n = 0$, i.e. that there must exist states that are massless, and these are indeed the Goldstone bosons.

5.3.4 Another example

As a last example we will consider the Lagrangian density

$$\mathcal{L} = \frac{1}{2}(\partial_\mu\phi_i)(\partial^\mu\phi_i) - \frac{m^2}{2}\phi_i\phi_i - \lambda(\phi_i\phi_i)^2 \,,$$

where $\phi_i, i = 1, 2, 3$ is an isovector Lorentz-scalar field. This Lagrangian density $\mathcal{L}$ is invariant under $SO(3)$, that is, under global transformations of the form

$$G : \phi_i \mapsto \phi_i' = \left(\mathrm{e}^{\mathrm{i}T_k\alpha_k}\right)_{i,j} \phi_j = U_{i,j}\phi_j = \left[U(g)\phi\right]_i \,.$$

Again, we obtain different ground state solutions as the minima of the potential and depending on m^2. For $m^2 > 0$ we have a minimum at $\phi_i = 0$. For $m^2 < 0$ we find degenerate ground states at $|\phi_0|^2 = -m^2/(4\lambda) =: a^2$, similar to the minimum found in complex ϕ^4 theory.

We choose $\phi_0 = a\, e_3$ as our ground state for the following considerations. This particular ϕ_0 is not invariant under the full group G but under the subgroup H that is found to be

$$H : \phi_0 \mapsto \phi_0' = U(h)\phi_0 = \phi_0, U(h) = \mathrm{e}^{\mathrm{i}T_3\alpha_3} \,.$$

If we put $\phi_3 = \chi + a$ such that ϕ_1, ϕ_2, and χ are the physical fields, we find for the potential

$$V = \boxed{4a^2\lambda\chi^2} + 4a\lambda\chi\left(\phi_1^2 + \phi_2^2 + \chi^2\right) + \lambda\left(\phi_1^2 + \phi_2^2 + \chi^2\right)^2 - \lambda a^4 \,,$$

from which we can deduce that the χ field can be associated with a mass

$$m_\chi^2 = 4a^2\lambda \,,$$

while the fields ϕ_1, ϕ_2 appear to be massless for the same argument as before.

Indeed, the full symmetry group G has three generators, of which only the one generator of H leaves the chosen ground state ϕ_0 invariant. From Goldstone's theorem we would have, therefore, expected precisely one massive field – that we found to be χ – and two massless fields.

5.4 Summary

The two examples of the rod bent through applying a force and of the spin orientations of an infinitely large ferromagnet served as motivation for studying the breaking of a symmetry. Starting from complex ϕ^4 theory the concept of spontaneous symmetry breaking in case of global continuous symmetries was derived. It was shown that the spontaneous breaking of a global continuous symmetry, as in the case of the Mexican hat potential, leads to degenerate vacua that we may associate with the massless Goldstone bosons. In the general case, when a Lagrangian density $\mathcal{L}$ is invariant under a symmetry group G and a chosen ground state ϕ_0 is only invariant under a subgroup H, the number of Goldstone bosons is just the dimension of the coset G/H, i.e. the number of generators of G that are not also generators of H. This statement is known as Goldstone's theorem. In particular, this statement does not depend on the representation of G or H nor on the explicit form of the potential, and it even applies to the case when there is *no* spontaneous symmetry breaking ($H = G$).

Bibliography

[1] L. H. Ryder. *Quantum Field Theory*. Cambridge University Press, 1996.

[2] Proseminar in Theoretical Physics. Topology in Physics. *ETH Zürich*, 2006.

[3] J. Bernstein. Spontaneous symmetry breaking, gauge theories, the Higgs mechanism and all that. Rev. Mod. Phys. **46**, 7 (1974), 7-48.

[4] J. Zierenberg. Spontaneous Symmetry Breaking. Bachelor thesis, University of Leipzig, 2008.

Chapter 6

Bose-Einstein-Condensation and the U(1) symmetry breaking

Author: Maximilian Seyrich
Supervisor: Cristian Vergu

The existence of a condensed phase for Bosons at low temperature was first predicted by Albert Einstein in 1925 in his paper "Quantentheorie des einatomigen Gases". A macroscopic fraction of particles occupy the ground state in the so-called Bose-Einstein-Condensate, making quantum physics macroscopically visible. The order parameter of the corresponding spontaneous symmetry breaking and the underlying U(1) symmetry will be connected to the Bose-Einstein-Condensate with the help of the 2nd Quantization formalism in this paper.

6.1 Introduction

If steam reaches a critical pressure for a given temperature, a fraction of the steam will be condensed. Einstein compares this process in his above-mentioned paper with the condensation taking place if a bosonic gas has reached a critical number of particles. All the energy levels different from the ground state will be saturated and with increasing particle number an increasing macroscopic fraction will occupy the ground state. A macroscopic clump of particles, described by only one wave function, have now all zero momentum. Figure 6.4 shows the density distribution of Rb-Atoms in momentum space. Instead of talking of critical particle numbers, it is nowadays common to separate the two phase by the Temperature. If you think of an experimental realization, it is easier to fix the particle number and to cool down the particles than vice versa. Consequently, one sees in the high- temperature phase $T > T_C$ a broaden distribution in the order of the theoretically predicted range of the Bose-Einstein-distribution function, for $T \sim T_C$ a peak in the middle for the zero momentum and an even sharper peak (theoretically a delta-peak) for the condensed low temperature phase $T << T_C$.

6.2 Quantum Statistics for the Ideal Bose Gas

To understand Einstein's reasoning, one needs the theory of Quantum Statistics for the Ideal Bose Gas. In this section the Bose-Einstein-distribution is showed via the Grand-Partition function. The thereof derived equation of state for fixed particle number will raise problems for particle numbers

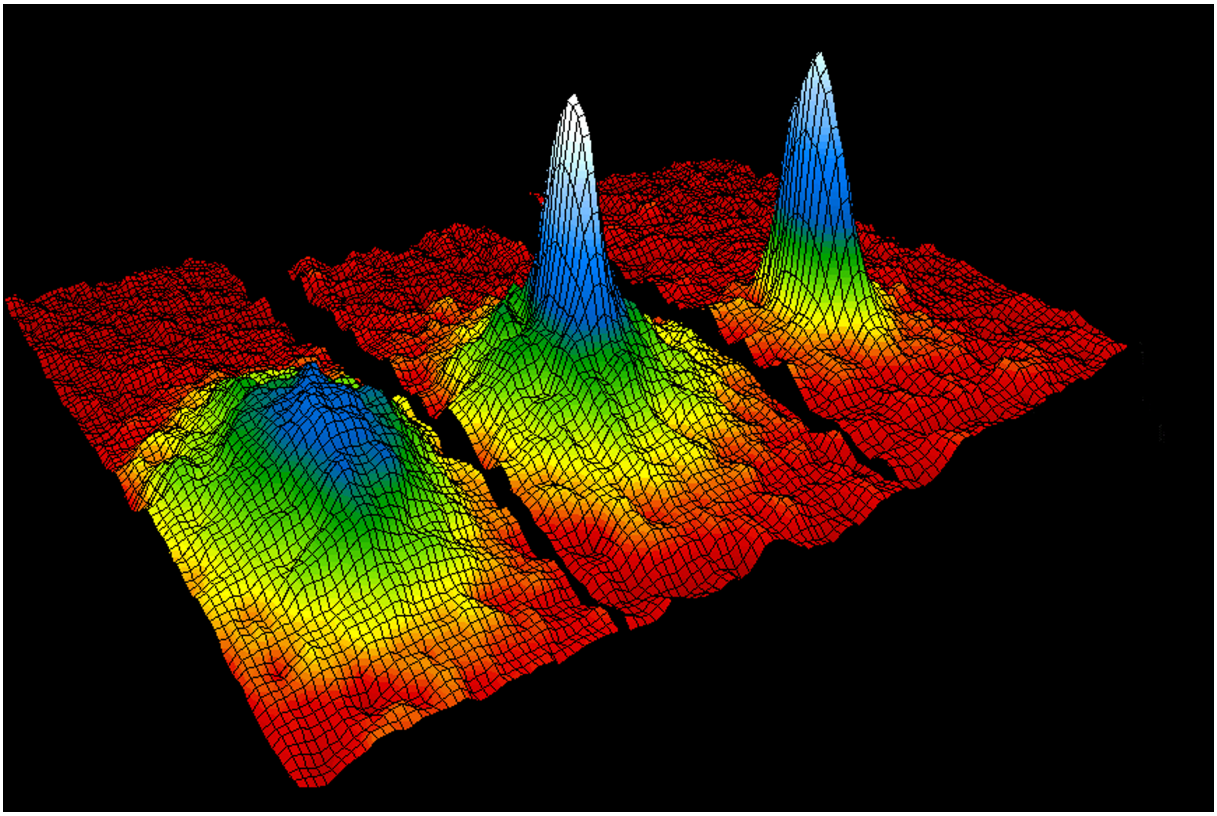

Figure 6.1: Distribution of Rb-atoms in momentum space. Left panel: T $> T_C$, middle panel: $T \sim T_C$, right panel $T << T_C$: Peak for p=0 state while the number of atoms with finite momentum shrinks.

greater than the critical particle number (or for $T \ll T_C$ when the particle number is held constant instead of the temperature), before some logical considerations will lead us to the only explanation of how this contradiction is solved.

6.2.1 Bose-Einstein-distribution

A gas of free particle in a in a box of volume V with boundary condition has to solve the time-independent Schrödinger equation of the tensor product of all the states of each particle.

$$\hat{H}\Psi = E\Psi = \sum_p n_p e_p \Psi \tag{6.1}$$

where n_p is the occupation number per momentum state and e_p the according energy.

The grand partition function is then known as

$$\begin{aligned} \Xi(T,V,\mu) &= tr(\hat{\rho}) && (6.2)\\ &= tr(e^{-\beta(\hat{H}-\mu\hat{N}}) && (6.3)\\ &= \sum_{n_p} e^{-\beta\sum_p (n_p e_p - \mu n_p)} && (6.4)\\ &= \prod_p \frac{1}{1-e^{-\beta(e_p-\mu)}} && (6.5) \end{aligned}$$

The limit of a geometric series was used in the last step.

Expectation values of an operator are defined via the trace of the operator's product with the density matrix. The expected value of the occupation number $\langle n_p \rangle$ is now obtained via

$$\langle n_p \rangle = tr(\hat{\rho}\hat{n}_p) \tag{6.6}$$

$$= \frac{\sum_{n_p} n_p e^{-\beta \sum_p (n_p e_p - \mu n_p)}}{\sum_{n_p} e^{-\beta \sum_p (n_p e_p - \mu n_p)}} \tag{6.7}$$

$$= -k_B T \partial_{e_p} \log(\Xi) \tag{6.8}$$

$$= \frac{1}{e^{\beta(\epsilon_p - \mu)} - 1} \tag{6.9}$$

The last equation is the well-known Bose-Einstein-Distribution.

6.2.2 Limited particle number in the Equation of state

If one comes now back to Einstein's problem of a Bosonic gas in a fixed volume at fixed temperature, one has to introduce boundary condition for the solution of the Schrödinger-Equation. These boundary conditions (e.g. for simplicity periodic) leads to discrete states of momenta that the atoms can be in. Einstein equation of limited particle number is easily derived form the Bose-Einstein-Distribution. The particle number N must be equal to the number that one obtains if one sums the occupation number per momentum state over all momenta

$$N = \sum_p n_p = \sum_p \frac{1}{e^{\beta(\epsilon_p - \mu)} - 1} \tag{6.10}$$

Taking now the continuous limit one can exchange the sum $\sum_p$ by the integral $\frac{V}{h^3} \int d^3p$. $\frac{V}{h^3}$ is the cell volume of our density function in momentum space and ϵ_p the energy to the momentum p. Applying this and switching to spherical momentum coordinates one gets

$$N = 4\pi \int \frac{p^2}{e^{\beta(\epsilon_p - \mu)} - 1} dp \tag{6.11}$$

After a substitution, the integral term can be described by a series as function of the fugacity $z = e^{\beta\mu}$, more precisely:

$$\int \frac{x^2}{\frac{e^{x^2}}{z} - 1} dx = \frac{\sqrt{\pi}}{4} \sum_{s=1}^{\infty} \frac{z^s}{s^{\frac{3}{2}}} := \frac{\sqrt{\pi}}{4} g_{\frac{3}{2}}(z) \tag{6.12}$$

This series obviously diverges for $z > 1$, or putting it in other words for $\mu > 0$
Adding everything together one finally arrives at the equation of state:

$$N = V(\frac{2\pi m k_B T}{h^2})^{\frac{3}{2}} g_{\frac{3}{2}}(z) \tag{6.13}$$

That is the equation Einstein used to predict the condensation. Since the function $g_{\frac{3}{2}}(z)$ is monotonously in z, its maximum is the Zeta-function: $g_{\frac{3}{2}}(1) = \zeta(\frac{3}{2}) \simeq 2.612$. The particle number N has got a maximum value in our calculus.

$$N_{max} = V(\frac{2\pi m k_B T}{h^2})^{\frac{3}{2}} \zeta(\frac{3}{2}) \tag{6.14}$$

6.2.3 Continuous Limit and the Ground state

Let one consider a simple thought experiment. In a box of given volume V at given temperature T the particle number of a gas can be chosen arbitrary. The theory should then determine the pressure of the gas.

However, equation (6.14) stands in contradiction to this simple issue. There is a maximum for the particle number according to the calculus, the right hand side has a clear maximum for given temperature and volume if z approaches 1. That means the chemical potential goes to zero in order to maximizes the right-hand-side. But since $g_{\frac{3}{2}(z)}$ has this maximum for $z = 1$, the particle number cannot be chosen arbitrarily high.

A first hint of what happens can be seen in the Bose-Einstein-Distribution.

$$n_p = \frac{1}{e^{\beta(\epsilon_p - \mu)} - 1} \tag{6.15}$$

For N reaching the maximum value, the chemical potential μ goes to 0. The term in the denominator gets to $e^{\beta(\epsilon_p - \mu)} - 1$, which has a singularity for the ground state $\epsilon_p = 0$. The occupation number for the ground state is not finite.

Where is the mistake?

It is in equation (6.11). Taking the continuous limit of the density in momentum space, the contributions of the occupation of the ground state is neglected. For $p = 0$ the integrand gets due to the p^2-term zero and N no longer contains the particle that are in the ground state. The limit for the particle number derived above must therefore be interpreted slightly differently. The particle number for particles that are not in the ground state is limited, not the total particle number.

If there are more particles in the excited states than the limit value, these states get saturated. The simple answer is that a fraction of particles condenses to the ground state. It is common to call the fraction of particles in the ground state the condensed particles and the particles in all the other states are in the saturated state. As the Bose-Einstein-Distribution already hinted, the occupation number gets macroscopic big if one reaches the critical number of particles. More precisely, the fraction of condensed particles is growing with the total particle number.

Instead of holding the temperature T constant respectively raising the particle number N in our thought experiment, one can alternatively fix N and lower T. One gets the same issues in equation (6.14) which leads also to the conclusion that at a critical temperature T_C the condensation starts to take place. The critical Temperature can be calculated

$$T_C = \frac{h^2}{2\pi m k_B} \left(\frac{N}{V \zeta(\frac{3}{2})}\right)^{\frac{3}{2}} \tag{6.16}$$

which is in the range of several nano Kelvins for example given Rubidium atoms. The advantage here is that one can calculate the condensed particle number N_0 more easily and in dependence of the temperature.

$$N_0 = N_{tot}\left(1 - \frac{T}{T_C}\right)^{\frac{3}{2}} \tag{6.17}$$

Also the phenomena of phase transition takes place. In figure(6.3) one can see a cusp for the specific heat capacity at $T = T_C$. In fact, the specific heat has a non-continuous derivative at this point. Since the specific heat is proportional to the second temperature derivative of the free energy, the Bose-Einstein condensate phase transition is of 3rd order according to the Ehrenfest classifications of phase transition.

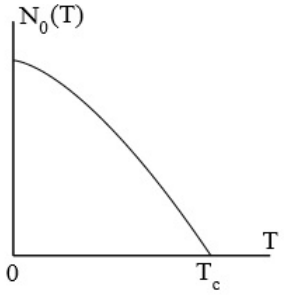

Figure 6.2: Fraction of condensed particles as function of the temperature.

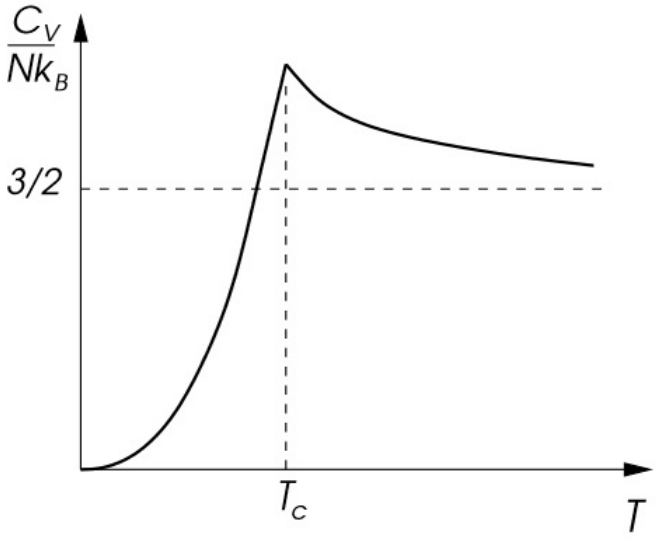

Figure 6.3: Heat capacity as a function of temperature. There is a continuous cusp for $T = T_C$ with a noncontinuous derivative.

6.2.4 Experimental Proof and Physical Explanation

It took more than 70 years to prove experimentally that Bose and Einstein's prediction was right. Cornell, Wiemann und Ketterle showed among some others the existence of the Bose-Einstein-Condensation for Rb-Atoms. They won the Nobel prize for this discovery in 2001.

The common method consists of mainly two phases.

- The atoms are caught in a magneto-optical trap and cooled down by lasers. Temperatures in the range of μ m can be reached. To cool the atoms down to the critical temperature, Evaporative cooling is needed.

- Evaporative cooling means that one sorts the atoms with the highest energy out. Almost 99,9 per cent of the atoms are taken out in this step in order to reach temperatures in the range of nK.

Physically one can understand it like this: atoms are particles, that are described by a wave packet. The size of this package is the thermal de-Broglie wave length

$$\lambda = (\frac{2\pi m k_B T}{h^2})^{\frac{3}{2}} \tag{6.18}$$

The wave length raises for falling temperatures. If the wave length reaches the range of the median distances d between the particles, quantum effects come into play. Overlapping wave-functions of indistinguishable particles in almost the same mode posses now a critical phase space density which leads then to the Bose-Einstein-Condensation.

$$\lambda \simeq (\frac{N}{V})^{\frac{1}{3}} \tag{6.19}$$

Equation (6.19) shows one again, that for Bose-Einstein-condensation high particle density and low temperatures are needed.

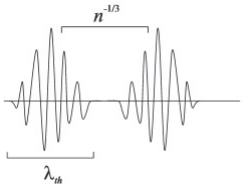

Figure 6.4: Wavelength and the median distance of atoms $n^{\frac{1}{3}}$.

6.3 2nd Quantization and the link to the U(1) symmetry breaking

The Ginzburg-Landau theory of phase transition in solid state physics states that there is an underlying broken symmetry for each phase transition. It is a generalization of the Landau expansion of the free energy. The Landau expansion is based on the symmetry and spontaneous broken symmetry of an order parameter. The order parameter possesses a certain symmetry in the high-temperature disordered phase which can be described by a Group G of symmetry operations leaving the system invariant. At the phase transition a form of order appears. It reduces the symmetry group of operations leaving the system invariant G' to a subgroup of G, $G' \subset G$. This change of symmetry is called *spontaneous symmetry breaking*.
Reaching Bose-Einstein-Condensate by lowering the temperature, one gets a phase transition of 3rd order. What is the broken symmetry? In the following chapter the formalism of second quantization is introduced in order to show that the broken symmetry is the U(1) symmetry of the order parameter $\hat{\Psi}_0$, the field operator for states in the ground state.

6.3.1 Formalism of 2nd Quantization

Atoms filled in a box of given volume V were described above by tensor products of wave-functions. The "first" quantization was induced by the commutator rules for momentum p_i and space variable q.

$$[p_i, q_j] = i\hbar\delta_{ij} \tag{6.20}$$

The same can now be done for fields, more precisely for the momentum $\pi(\vec{x})$ and the space variable $\Psi(\vec{x})$ at a point $\vec{x}$.

$$[\pi(\vec{x}), \Psi(\vec{y})] = i\hbar\delta^3(\vec{x} - \vec{y}) \tag{6.21}$$

Why is one interested in fields? If one goes back to the particles filled in the box, ϕ_i shall be the one-particle function as in the section above. This wave-function is one mode of a set of discrete

modes for the i-th particle due to the boundary condition. Therefor, one gets discrete values in k-space.

Each mode can now be described as a harmonic oscillator with states in the Fock space and the creation and annihilation operators $\hat{a}^\dagger$ respectively $\hat{a}$. One can then define the field operators

$$\hat{\Psi}(\vec{x}) = \sum_i \phi_i(\vec{x})\hat{a}_i \tag{6.22}$$

$$\hat{\Psi}^\dagger(\vec{x}) = \sum_i \phi_i(\vec{x})\hat{a}_i^\dagger \tag{6.23}$$

The two can be interpreted as annihilating respectively creating operator of a particle at a point $\vec{x}$ when acting on a tensor product of Fock states. The probability of removing a particle at point $\vec{x}$ and then putting it back is then

$$\langle i|\hat{\Psi}^\dagger(\vec{x})\hat{\Psi}(\vec{x})|i\rangle = |\phi_i(\vec{x})|^2 \tag{6.24}$$

This is nothing else than the probability of finding one particle in a one-particle system or the number of particles in state $\langle i\rangle$ in a box of n particles.

6.3.2 Bogeliubov Approximation

If a lowest energy state (ground state $i = 0$) has a macroscopic occupation N_0, one can separate the field operator in a condensed term ($i = 0$) and non-condensed components.

$$\hat{\Psi}^\dagger(\vec{x}) = \psi_0(\vec{x})a_0 + \sum_{i=0} \phi_i(\vec{x})\hat{a}_i \tag{6.25}$$

$$with \;\; a_0 = \sqrt{N_0} \tag{6.26}$$

The entropy for all the particles in the ground state is zero, since one knows that there are all in the ground state. One substitutes the operator for the ground state by a constant, a complex number a_0. Intuitively, the constant a_0 has to be equal to the square root of N_0.

The so-called Bogeljubov-Ansatz is then:

$$\hat{\Psi}(\vec{x}) = \Psi_0(\vec{x}) + \delta\hat{\Psi}(\vec{x}) \tag{6.27}$$

The field $\Psi_0(\vec{x})$ is called the wavefunction of the condensate and is the order parameter to the Bose-Einstein phase transition.

6.3.3 Order parameter and broken symmetry

The order parameter $\Psi_0(\vec{x})$ has an absolute value $\Psi_0(\vec{x})$ and a phase $S(r)$.

$$\Psi_0(\vec{x}) = \Psi_0(\vec{x})e^{iS(r)} \tag{6.28}$$

$|\Psi_0(\vec{x})|$ determines the particle density of the condensate $n(\vec{x}) = |\Psi_0(\vec{x})|^2$ at a point $\vec{x}$ and the phase $S(r)$ characterizes the coherence and super-fluidity phenomena. Mathematically, $\Psi_0 = \sqrt{N_0}\phi_0$ is only defined up to a particular phase factor. Physically, the system chooses a random phase at the phase transition which can be measured. This means nothing else than a spontaneous symmetry breaking. What is the underlying symmetry?

The expectation value for the order parameter $\hat{\Psi}_0$ is defined as.

$$\langle\hat{\Psi}_0(\vec{x})\rangle = \langle n_0|\hat{\Psi}_0(\vec{x})|n_o\rangle \tag{6.29}$$
$$\tag{6.30}$$

In equation (6.29) the spontaneous symmetry can be verified by comparing the results for the high-temperature phase and the condensed phase.

$$T \ll T_C \qquad \langle\hat{\Psi}_0(\vec{x})\rangle = \langle n_0|\hat{\Psi}_0(\vec{x})|n_0\rangle = \langle n_0|\sqrt{N_0}\phi_0|n_0\rangle = \sqrt{N_0}\phi_0 \neq 0 \tag{6.31}$$
$$T \gg T_C \qquad \langle\hat{\Psi}_0(\vec{x})\rangle = \langle n_0|\hat{\Psi}_0(\vec{x})|n_0\rangle = \langle n_0|\phi_0\hat{a_0}|n_0\rangle = \langle n_0|n_0 - 1\rangle = 0 \tag{6.32}$$

The expectation value for the wave function of the condensate in the high-temperature phase is clearly U(1) invariant. Transforming $\Psi \to \Psi e^{i\Delta}$ gives one still $\langle\Psi\rangle = 0$. Obviously, the Group G of the system's symmetries contains U(1). In the condensed phase, however, the expectation value of the wave function of the condensate is no longer U(1) invariant. The system chooses randomly a particular phase S(r) which can be measured by interferometer. This spontaneous symmetry breaking causes the phase transition of 3^{rd} order for the Bose-Einstein-Condensation.

6.3.4 Coherent states

The expectation value of the wave function of the condensate cannot be finite if the system is in a number state. The Bogeliubov-Ansatz giving one the finite value is just an approximation, so also the original term including the annihilation operator of the ground state should provide a finite value. As one has seen in the calculation for the expectation value for high temperatures, applying it to the number states will give 0 since the different number states for each mode are orthogonal. Thereof one can conclude that one cannot represent the condensate by the number states.

Consequently, the condensate has to be described by an eigenfunction of the annihilation operator of the ground state mode.

$$\hat{a}_0|\alpha\rangle = \alpha|\alpha\rangle \tag{6.33}$$

where α is a complex number. Such an eigenstate is known from the harmonic oscillator, the state that describes best the classical oscillation: The coherent state, consisting of a linear superposition of all the number states multiplied by a phase.

$$|\alpha\rangle = e^{-\frac{|\alpha|^2}{2}} \sum_{n=0}^{\infty} \frac{\alpha^n}{\sqrt{n!}}|n\rangle \tag{6.34}$$

Bibliography

[1] Einstein, Quantentheorie des einatomigen Gases, Zweite Abhandlung, 1925

[2] MOKA Secs 4.1-42, Helsinki

[3] Cohen-Tannoudji: BEC: An Introduction, Poincaré Seminar 1998, Paris

[4] Sigrist, Statistical Physics, Lecture notes autumn semester 2013, Zurich

Chapter 7

Superfluidity : Vortices & BKT transition

Author: Vetterli Samir
Supervisor: Jens Langelage

'This report aims at giving a short insight in the topics of superfluidity vortices and BKT transition. In particular, it is the superfluid transition of 4He which is highlighted, namely by using the Two-Fluid model, but also through the Fermi liquid theory of Landau *and the* Bogobuliov *theory. In a second part, the* Gross-Pitaevskii *equation leads to solution of the problem taking into account interaction as well as spatial variation of the potential. This leads to vortex -solutions of the problem which have a winding number and are topological defects of the superfluid. The appearance of these excitations bears several consequences, amongst which is the BKT transition. The latter explains the formation of Bose − Einstein condensate within two-dimensional films by considering the correlation functions of the system under scope.*

7.1 Helium

Superfluidity is a state of matter characterized by an absence of viscosity at temperatures close to absolute zero. Superfluidity is overall a phase transition which happens at low temperature, within quantum liquids and in a specific range of pressure. It has principally been observed by Helium isotopes, which perfectly embody the phenomenon. This remarkable property of Helium is the consequence of weak Van der Waals interaction combined with low atomic mass. In the case of Helium, it is a second-order phase transition, because the specific heat is discontinuous (see Figure 1) and which differentiate the high temperature liquid phase He-I from the low temperature liquid phase He-II. This phase transition of Helium is overall a matter of ordering of a liquid system. In fact, it corresponds to the transition to a state with less symmetries. Two different main isotopes of Helium were discovered to become superfluid at low temperature: 4He and 3He. Although they only differ by the number of neutrons in their respective atom-core, the phase transition that occurs for both elements is quite different. 4He is a boson, because it consists of 2 neutrons and 2 protons and thus has a total zero spin. 3He, on the other side, has 2 neutrons and only one proton, which makes it a half-spin particle and therefore a fermionic particle [8]. 4He has He-I and He-II separated by the lambda-line which intersects the saturated pressure curve at the λ-point given by

$$\begin{aligned} T_\lambda &= 2.17\text{K} \\ P_\lambda &= 29.8\text{atm.} \end{aligned} \tag{7.1}$$

Near T_λ, the specific heat behaves like $A|T - T_\lambda|^{-\alpha}$ and the peculiar shape of this divergence is the reason for the name λ.

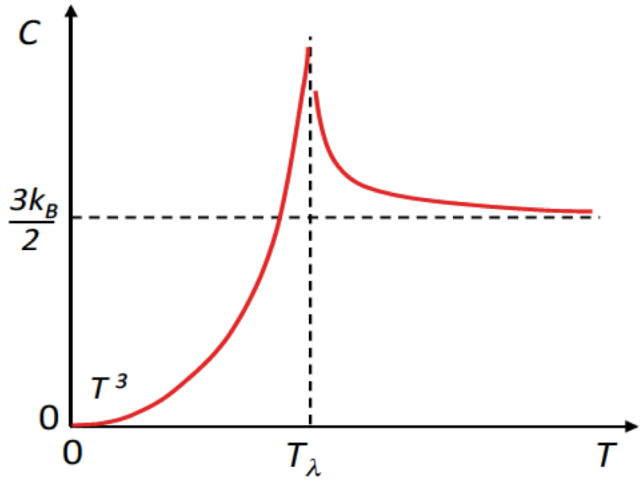

Figure 1 - Specific heat at the superfluid transition temperature T_λ. Note how C behaves in a T^3 power law in the region near absolute zero [1].

3He only becomes liquid at 0.1 K and superfluid at a few mK (see Figure 2) for the following reason; the difference between both of these isotopes mainly stems from the distributions they obey to, 3He and 4He respectively to Fermi and Bose statistics, and their total spin. 3He has to first form Cooper pairs, as in a superconductivity transition, in order to become bosonic and then undergo the same phase transition as 4He. Therefore, it requires additional cooling of the system in order for the long-range binding to establish.

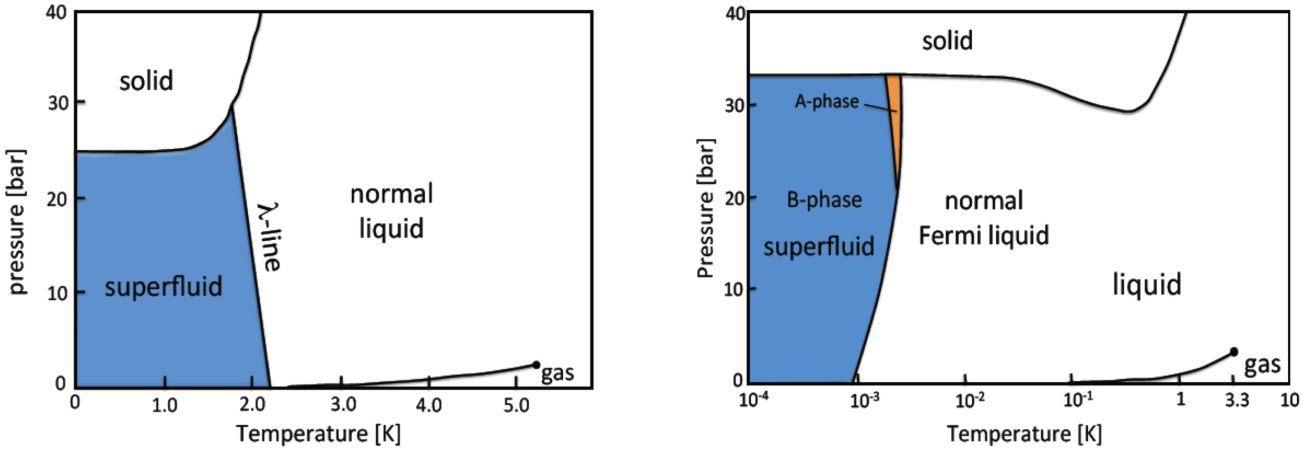

Figure 2 - Phase diagrams of Helium. Left panel : bosonic 4He. Right panel : fermionic 3He. Note the logarithmic temperature scale in the right panel. While 4He has one superfluid phase, there are two, the A- and B-phase, for 3He [1].

Whereas other systems of particles would form a solid lattice at temperatures near absolute zero and thereby minimize their potential energy, Helium does not undergo this transition. If one considers the interatomic potential within Helium particles, it consists of two main components. The first one is a short-ranged strongly repulsive interatomic interaction, whereas the second is a long-range interatomic Van der Waals potential. A close approximation [1] of the total potential would

be of the form

$$V(r) = Ae^{-r/r_1} - B\left(\frac{r_2}{r}\right)^6, \tag{7.2}$$

with A = 4.89 eV, B = 9.3 $\cdot 10^{-5}$ eV, $r_1 = 0.22$ $\mathring{A}$, $r_2 = 4.64$ $\mathring{A}$. This fit presents a minimum at $r_0 \simeq 3\mathring{A}$ with a minimal potential $V(r_0) = -7.8 \cdot 10^{-4}$ eV. A condition for a solid not to become liquid is established by the Lindemann criterion, which is an attempt to predict the bulk melting point of crystalline materials. The idea that lies behind this phenomenological law is that the average amplitude of thermal vibrations increases with increasing temperature. In the situation considered, we have

$$\frac{\Delta r}{d} \leq \ L_m, \text{ with } \mathrm{L_m} \approx 0.1 \tag{7.3}$$

Δr represents here the fluctuation around the 0-point position, d is the lattice constant at T= 0, which for Helium is about $d \simeq 4.4\mathring{A}$. We conclude that for fluctuations of about 5 $\mathring{A}$, the criterion is no more verified and therefore the system becomes fluid. Using Heisenberg's uncertainty principle $\Delta r \Delta p \approx \hbar$, we can deduce an approximation of the energy of the system in the liquid phase. We thus have

$$\Delta E = \frac{\Delta p^2}{2m} = \frac{1}{2m}\left(\frac{\hbar}{\Delta r}\right)^2 \approx 8.6 \cdot 10^{-4}\text{eV} \tag{7.4}$$

which is in absolute value slightly greater than the potential minimum. It follows that the potential well which results from the total potential of interaction is smaller than the actual energy of the Helium particle in the fluid phase, therefore allowing it to move freely. In other words, the wave function is not localized in a specific region of the system. This, however, applies only in a range of pressure below 25 bar around 0 K.

7.2 Two-Fluid model

A suitable model that lies behind superfluidity is the Two-Fluid model imagined by Tisza in 1938 and developed by Landau later. It considers the superfluid He-II as made of two different components, one of which is called the normal fluid, the other the superfluid. Both parts of the system have different densities which evolve as temperature varies under T_λ and whose sum is equal to the total density of the liquid Helium. For $T \to T_\lambda$, the density of the superfluid component ρ_s vanishes, whereas at T = 1 K the density of the normal component ρ_n is already close to the one of the liquid.

The excitation spectrum $\epsilon(k)$ of He-II is made of two regions, which describe two different types of quasiparticles :

- The linear phonon region near 0, where

$$\epsilon(\vec{k}) = c\hbar|\vec{k}|, \ |\vec{k}| << |\vec{k_0}|; \tag{7.5}$$

- the quadratic roton region, where

$$\epsilon(\vec{k}) = \Delta + \frac{\hbar^2}{2\mu}|\vec{k} - \vec{k_0}|^2, \ |\vec{k}| \sim |\vec{k_0}|. \tag{7.6}$$

where $c = 226m/s$ is the sound velocity and $\Delta/k_B = 9$ K are the roton parameters and $\mu = 0.25m_{He}$ [2].

The two-fluid model can be understood by considering an ideal noninteracting Bose gas that undergoes a phase transition called a $Bose-Einstein$ condensation (BEC) at the critical temperature T_{BE} given by

$$k_B T_{BE} = \frac{2\pi\hbar^2}{m}\left(\frac{N}{2.6V}\right)^{2/3}. \tag{7.7}$$

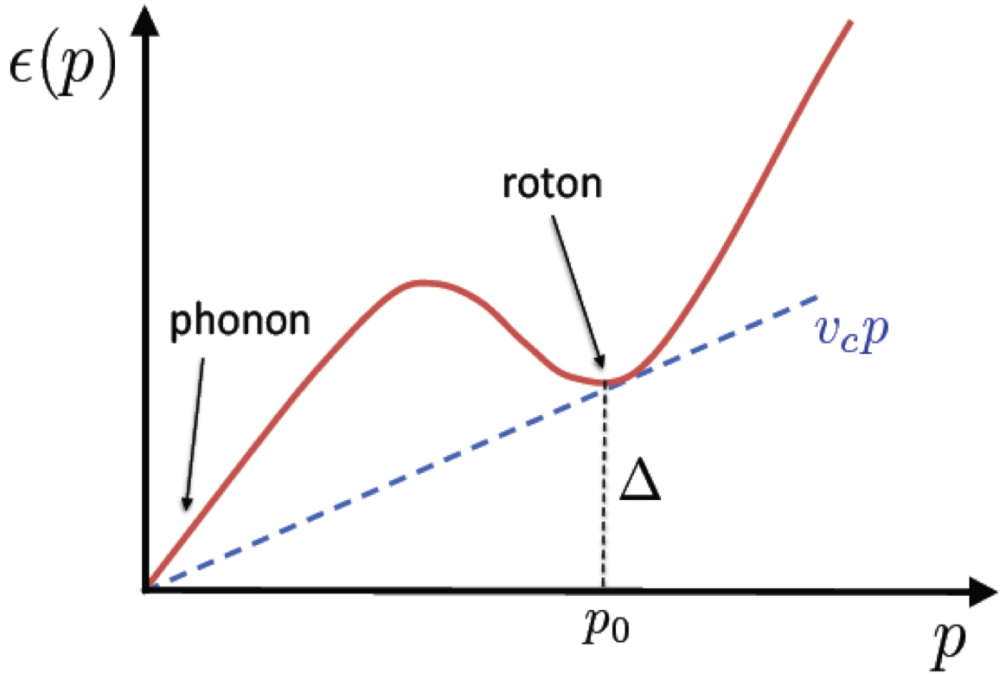

Figure 3 - Spectrum of a superfluid with a linear sound-like behavior at low energy and a local minimum around p_0 due to roton excitations. The dashed line ($v_c p$) indicates the maximal velocity of the superfluid to sustain frictionless flow. $\epsilon(k)$ is not quadratic as it would be the case for a non-interacting Bose gas [1].

The critical temperature T_{BE} is however slightly different from T_λ. Furthermore, the specific heat of a Bose-gas has a power law $T^{3/2}$, whereas it is a T^3 for 4He. The density of the superfluid component ρ_s increases at $T \to 0$ K, whereas the number of condensate particles stays more or less constant with respect to the total number of particles. Especially, this model allow one to justify the linear photon dispersion relation of the energy spectrum for small wave vectors k.

7.3 Bogobuliov Theory

Let us write down the Hamiltonian of this system by considering that the interaction can be described by a two-body potential $V(\vec{q})$

$$\mathcal{H} = \sum_{\mathbf{k}} E_0(\vec{k}) \hat{a}^\dagger_{\mathbf{k}} \hat{a}_{\mathbf{k}} + \frac{1}{2\Omega} \sum_{\mathbf{k}_1, \mathbf{k}_2, \mathbf{q}} V(\vec{q}) \hat{a}^\dagger_{\mathbf{k}_1+\mathbf{q}} \hat{a}^\dagger_{\mathbf{k}_2-\mathbf{q}} \hat{a}_{\mathbf{k}_1} \hat{a}_{\mathbf{k}_2} \tag{7.8}$$

where $E_0(\vec{k}) = \frac{\vec{k}^2}{2m} - \mu$ and μ is the chemical potential [3]. The field operator in this equation is expressed in the phase space using

$$\hat{\Psi}(\vec{r}) = \frac{1}{\sqrt{\Omega}} \sum_{\vec{k}} e^{i\vec{k}\vec{r}} \hat{a}_{\vec{k}} \ , \ \hat{\Psi}^\dagger(\vec{r}) = \frac{1}{\sqrt{\Omega}} \sum_{\vec{k}} e^{-i\vec{k}\vec{r}} \hat{a}^\dagger_{\vec{k}} \tag{7.9}$$

and $\hat{a}^\dagger_{\vec{k}}$, $\hat{a}_{\vec{k}}$ are respectively the creation and annihilation operators in the Fock-space spanned by vectors $|n_1, n_2, \ldots\rangle = \frac{(a_1^\dagger)^{n_1}(a_2^\dagger)^{n_2}\ldots}{\sqrt{n_1! n_2! \ldots}} |0\rangle$ with $|0\rangle$ being the vacuum state . At a temperature below T_{BE} the lowest energy one-particle state ψ_0 which is an eigenstate with momentum equal to zero in a uniform system is occupied by

$$N_0(T) = N \left(1 - \left(\frac{T}{T_{BE}} \right)^{3/2} \right) \tag{7.10}$$

particles. Therefore the number of particles occupying their lowest energy state vanishes as the temperature tends to the critical temperature T_{BE}. This is similar to the way the superfluid component behaves in He-II as the temperature approaches T_λ for 4He. Thus, the part of the system $N_0(T)$ in the ψ_0 state, which is called the condensate, is really similar to the superfluid component. Let's take $|C; N, N_0\rangle$ as a superfluid state with a total number of N particles, N_0 of which are constituting the condensate. If $\hat{a}_0^\dagger$ and $\hat{a}_0$ are respectively the creation and annihilation operators for the ground state, applying them on a vector yields

$$\begin{aligned} \hat{a}_0 |C; N, N_0\rangle &= \sqrt{N_0}\, |C; N, N_0 - 1\rangle \\ \hat{a}_0^\dagger |C; N, N_0\rangle &= \sqrt{N_0 + 1}\, |C; N, N_0 + 1\rangle \end{aligned} \tag{7.11}$$

and the subsequent relations follow

$$\begin{aligned} \hat{a}_0^\dagger \hat{a}_0 |C; N, N_0\rangle &= N_0 |C; N, N_0\rangle \\ \hat{a}_0 \hat{a}_0^\dagger |C; N, N_0\rangle &= (N_0 + 1) |C; N, N_0 + 1\rangle . \end{aligned} \tag{7.12}$$

For $N \to \infty$, $N_0 + 1 \simeq N_0$ so that we can replace both products of operators $\hat{a}_0^\dagger \hat{a}_0$ and $\hat{a}_0 \hat{a}_0^\dagger$ by N_0. Therefore, N_0 will be later used as a large parameter for describing the problem. The number operator $\mathbf{N}$ acts upon the state as follows

$$\mathbf{N} |C; N, N_0\rangle = N_0 |C; N, N_0\rangle , \tag{7.13}$$

where $\mathbf{N} = \sum_{\mathbf{k}} \hat{a}_{\mathbf{k}}^\dagger \hat{a}_{\mathbf{k}}$ which we can also write as $\mathbf{N} = \hat{a}_0^\dagger \hat{a}_0 + \sum_{\mathbf{k}\neq 0} \hat{a}_{\mathbf{k}}^\dagger \hat{a}_{\mathbf{k}}$. Neglecting the terms of 0 order in N_0, the square of the number operator is

$$\mathbf{N}^2 \simeq N_0^2 + 2N_0 \sum_{\mathbf{k}\neq 0} \hat{a}_{\mathbf{k}}^\dagger \hat{a}_{\mathbf{k}} \tag{7.14}$$

when acting upon the state $|C; N, N_0\rangle$. As far as the potential part of the Hamiltonian $\mathcal{H}_V$ is concerned, we consider and regroup the terms in function of the number of operator $\hat{a}_0, \hat{a}_0^\dagger$ they contain. We have

$$\mathcal{H}_V^{(0)} = \frac{1}{2\Omega} V(0) \hat{a}_0^\dagger \hat{a}_0^\dagger \hat{a}_0 \hat{a}_0 = \frac{1}{2\Omega} V(0) N_0^2 \simeq \frac{1}{2\Omega} V(0) \left(\mathbf{N}^2 - 2N_0 \sum_{\mathbf{k}\neq 0} \hat{a}_{\mathbf{k}}^\dagger \hat{a}_{\mathbf{k}} \right) \tag{7.15}$$

for the zero-order term. The next order term contains two zero-momentum operators $\hat{a}_0, \hat{a}_0^\dagger$. These are displayed beneath

$$\begin{aligned} \vec{k_1} + \vec{q} = \vec{k_2} - \vec{q} = 0 \quad &: \quad \frac{N_0}{2\Omega} \textstyle\sum_{\mathbf{q}\neq 0} V(\vec{q}) \hat{a}_{-\mathbf{q}} \hat{a}_{\mathbf{q}} \\ \vec{k_1} + \vec{q} = \vec{k_1} = 0 \quad &: \quad \frac{N_0}{2\Omega} \textstyle\sum_{\mathbf{k_2}\neq 0} V(0) \hat{a}_{\mathbf{k_2}}^\dagger \hat{a}_{\mathbf{k_2}} \\ \vec{k_1} + \vec{q} = \vec{k_2} = 0 \quad &: \quad \frac{N_0}{2\Omega} \textstyle\sum_{\mathbf{q}\neq 0} V(\vec{q}) \hat{a}_{-\mathbf{q}}^\dagger \hat{a}_{-\mathbf{q}} \\ \vec{k_1} = \vec{k_2} - \vec{q} = 0 \quad &: \quad \frac{N_0}{2\Omega} \textstyle\sum_{\mathbf{q}\neq 0} V(\vec{q}) \hat{a}_{\mathbf{q}}^\dagger \hat{a}_{\mathbf{q}} \\ \vec{k_2} = \vec{k_2} - \vec{q} = 0 \quad &: \quad \frac{N_0}{2\Omega} \textstyle\sum_{\mathbf{q}\neq 0} V(0) \hat{a}_{-\mathbf{k_1}}^\dagger \hat{a}_{\mathbf{k_1}} \\ \vec{k_1} = \vec{k_2} = 0 \quad &: \quad \frac{N_0}{2\Omega} \textstyle\sum_{\mathbf{q}\neq 0} V(\vec{q}) \hat{a}_{-\mathbf{q}}^\dagger \hat{a}_{\mathbf{q}}^\dagger . \end{aligned} \tag{7.16}$$

Since at low temperatures, we expect small momenta to dominate, we make the following approximation $V(\vec{k}) \simeq V(0)$. Taking account only of terms in $O(N_0)$ we have

$$\mathcal{H}_V \simeq \frac{1}{2\Omega}V(0)\left(\mathbf{N}^2 - 2N_0\sum_{\mathbf{k}\neq 0}\hat{a}^\dagger_{\mathbf{k}}\hat{a}_{\mathbf{k}}\right) + \frac{N_0}{2\Omega}\sum_{\mathbf{k}\neq 0}V(0)(\hat{a}^\dagger_{\mathbf{k}}\hat{a}^\dagger_{-\mathbf{k}} + \hat{a}_{\mathbf{k}}\hat{a}_{-\mathbf{k}}) + \frac{V(0)}{2\Omega}4N_0\sum_{\mathbf{k}\neq 0}\hat{a}^\dagger_{\mathbf{k}}\hat{a}_{\mathbf{k}} \equiv \mathcal{H}^B_V, \tag{7.17}$$

and the total Hamiltonian can therefore be approximated with the *Bogoliubov Hamiltonian* $\mathcal{H}^B$

$$\mathcal{H}^B = \sum_{\mathbf{k}}\left(\frac{\vec{k}^2}{2m} - \mu\right)\hat{a}^\dagger_{\mathbf{k}}\hat{a}_{\mathbf{k}} + \mathcal{H}^B_V. \tag{7.18}$$

Whereas initially the Hamiltonian $\mathcal{H}$ commuted with the number operator $\mathbf{N}$ and thereby had well-defined energy eigenvalues, with the *Bogoliubov Hamiltonian*, the energy states are no more well-defined, which is why we must set $\mu = 0$. We further define the effective Hamiltonian by omitting the non-operator parts of $\mathcal{H}^B_V$

$$\mathcal{H}^B_{eff} = \sum_{\mathbf{k}\neq 0}\left(\frac{\vec{k}^2}{2m} + \frac{V(0)}{\Omega}N_0\right)\hat{a}^\dagger_{\mathbf{k}}\hat{a}_{\mathbf{k}} + \frac{V(0)N_0}{2\Omega}\sum_{\mathbf{k}\neq 0}(\hat{a}^\dagger_{\mathbf{k}}\hat{a}^\dagger_{-\mathbf{k}} + \hat{a}_{\mathbf{k}}\hat{a}_{-\mathbf{k}}). \tag{7.19}$$

In order to determine the energy eigenvalues of this Hamiltonian, we want to take appropriate linear combinations of the creation and annihilation operators, so as to diagonalize $\mathcal{H}^B$ in a form that would look alike

$$\mathcal{H}^B = \sum_{\mathbf{k}\neq 0}\epsilon(\vec{k})\hat{b}^\dagger_{\mathbf{k}}\hat{b}_{\mathbf{k}}. \tag{7.20}$$

Let $\hat{b}_{\mathbf{k}}, \hat{b}^\dagger_{\mathbf{k}}$ be the linear combinations defined by

$$\begin{aligned}\hat{b}_{\mathbf{k}} &= \alpha(\vec{k})\hat{a}_{\mathbf{k}} - \beta(\vec{k})\hat{a}^\dagger_{-\mathbf{k}}\\ \hat{b}^\dagger_{\mathbf{k}} &= \alpha(\vec{k})\hat{a}^\dagger_{\mathbf{k}} - \beta(\vec{k})\hat{a}_{-\mathbf{k}},\end{aligned} \tag{7.21}$$

where $\alpha(\vec{k}), \beta(\vec{k})$ are real valued functions of $|\vec{k}|$ called *Bogoliubov coefficients*. If we impose that $[\hat{b}_{\mathbf{k_1}}, \hat{b}^\dagger_{\mathbf{k_2}}\,] = \delta_{\mathbf{k_1},\mathbf{k_2}}$, this leads to

$$\alpha(\vec{k})^2 - \beta(\vec{k})^2 = 1,\ \forall\vec{k}, \tag{7.22}$$

in terms of the real valued coefficients. By inverting the equations for the initial operators, we obtain

$$\begin{aligned}\hat{a}_{\mathbf{k}} &= \alpha(\vec{k})\hat{b}_{\mathbf{k}} + \beta(\vec{k})\hat{b}^\dagger_{-\mathbf{k}}\\ \hat{a}^\dagger_{\mathbf{k}} &= \alpha(\vec{k})\hat{b}^\dagger_{\mathbf{k}} + \beta(\vec{k})\hat{b}_{-\mathbf{k}}.\end{aligned} \tag{7.23}$$

We can then substitute these expressions in the effective Hamiltonian, define $h(\vec{k})$ and $g(\vec{k})$ respectively as $\frac{N_0V(0)}{2\Omega}$ and $g(\vec{k}) = \frac{|\vec{k}|^2}{2m} + \frac{N_0V(0)}{\Omega}$ and it follows that

$$\begin{aligned}H^B_{eff} \;&= \textstyle\sum_{\mathbf{k}\neq 0}[g(\vec{k})(\beta(\vec{k})^2 + \alpha(\vec{k})^2) + 4h(\vec{k})\alpha(\vec{k})\beta(\vec{k})]\hat{b}^\dagger_{\mathbf{k}}\hat{b}_{\mathbf{k}}\\ &\quad + \textstyle\sum_{\mathbf{k}\neq 0}[g(\vec{k})\alpha(\vec{k})\beta(\vec{k}) + h(\vec{k})(\alpha(\vec{k})^2 + \beta(\vec{k})^2)][\hat{b}_{\mathbf{k}}\hat{b}_{-\mathbf{k}} + \hat{b}^\dagger_{\mathbf{k}}\hat{b}^\dagger_{-\mathbf{k}}]\\ &\quad + \text{terms not involving operators.}\end{aligned} \tag{7.24}$$

In order to diagonalize H^B we must therefore cancel the second term, that is, set

$$g(\vec{k})\alpha(\vec{k})\beta(\vec{k}) + h(\vec{k})(\alpha(\vec{k})^2 + \beta(\vec{k})^2) = 0. \tag{7.25}$$

We must then determine the *Bogoliubov coefficients* in terms of the known functions $h(\vec{k}), g(\vec{k})$ making sure that $\alpha(\vec{k})^2 - \beta(\vec{k})^2 = 1$ is satisfied. It results that

$$\begin{aligned} \beta(\vec{k})^2 &= \tfrac{1}{2}\left\{\sqrt{\tfrac{g^2(\vec{k})}{g^2(\vec{k})-4h^2(\vec{k})}} - 1\right\} \\ \alpha(\vec{k})^2 &= \tfrac{1}{2}\left\{\sqrt{\tfrac{g^2(\vec{k})}{g^2(\vec{k})-4h^2(\vec{k})}} + 1\right\} \end{aligned} \tag{7.26}$$

We finally have obtained $H^B_{eff} = \sum_{\mathbf{k}\neq 0} \epsilon(\vec{k}) \hat{b}^\dagger_{\mathbf{k}} \hat{b}_{\mathbf{k}}$ with

$$\epsilon(\vec{k}) = g(\vec{k})(\beta(\vec{k})^2 + \alpha(\vec{k})^2) + 4h(\vec{k})\alpha(\vec{k})\beta(\vec{k}) = \sqrt{\frac{\vec{k}^2}{2m}\left(\frac{\vec{k}^2}{2m} + \frac{2N_0V(0)}{\Omega}\right)}. \tag{7.27}$$

This energy is that of a quasiparticle. As said before, the normal fluid consists of the thermal excitations with kinetic energy $\frac{\vec{k}^2}{2m}$and momentum $\vec{p}$. For $\vec{k} \to 0$ the dispersion relation of a quasiparticle is

$$\epsilon(k) \simeq \frac{|\vec{k}|}{m}\sqrt{\frac{N_0V(0)m}{\Omega}} = c|\vec{k}|, \tag{7.28}$$

where c is the sound velocity and $V(0) > 0$ must be positive in order for the total energy to be real. It follows that the interaction between the quasiparticles has a repulsive nature. So this hereby proves the linear dispersion relation for small wave vectors and the appearance of excitations destroy the frictionless character of the flow [3]. We define the critical velocity as the minimum of previous quantity, that is $v_c = \min_k \frac{\epsilon(\vec{k})}{|\vec{k}|}$. For non-interacting systems where no quasiparticles are created, the spectrum of energy is given by the kinetic energy $\epsilon(\vec{k}) = \vec{k}^2/2m \propto \vec{k}^2$, which is why the critical velocity can be made arbitrarily small, i.e. $v_c = 0$ and the flow is not superfluid.

As for the roton region, where $\vec{k} \approx \vec{k_0}$, one can show that the energy spectrum is indeed quadratic and presents a minimum at this point. This is done by doing following Ansatz [4]; the wave function of roton excitations is given by a linear combination of condensate ground state wave functions ϕ as follows

$$\psi_{rot} = \phi \sum_i e^{i\vec{k}\vec{r_i}}. \tag{7.29}$$

Substitution of this result in order to minimize $\dfrac{\langle\psi|\,\mathcal{H}\,|\psi\rangle}{\langle\psi|\,\psi\rangle}$ gives an upper boundary for the energy excitation of momentum $\hbar\vec{k}$. The resulting energy is given by

$$E(\vec{k}) = \frac{\hbar^2\vec{k}^2}{2mS(\vec{k})}, \tag{7.30}$$

where $S(\vec{k})$ is the structure factor from scattering of neutrons in the liquid.

$$S(\vec{k}) = \int e^{i\vec{k}\vec{r}} g(\vec{r}) dr^3, \tag{7.31}$$

and $g(\vec{r})$ is the two-atom zero-temperature correlation function. Taking experimental data results (see Figure 4) into account, we observe that the minimum of the energy spectrum in the roton region corresponds with the maximum of the structure factor at the wavelength of the nearest neighbor distance.

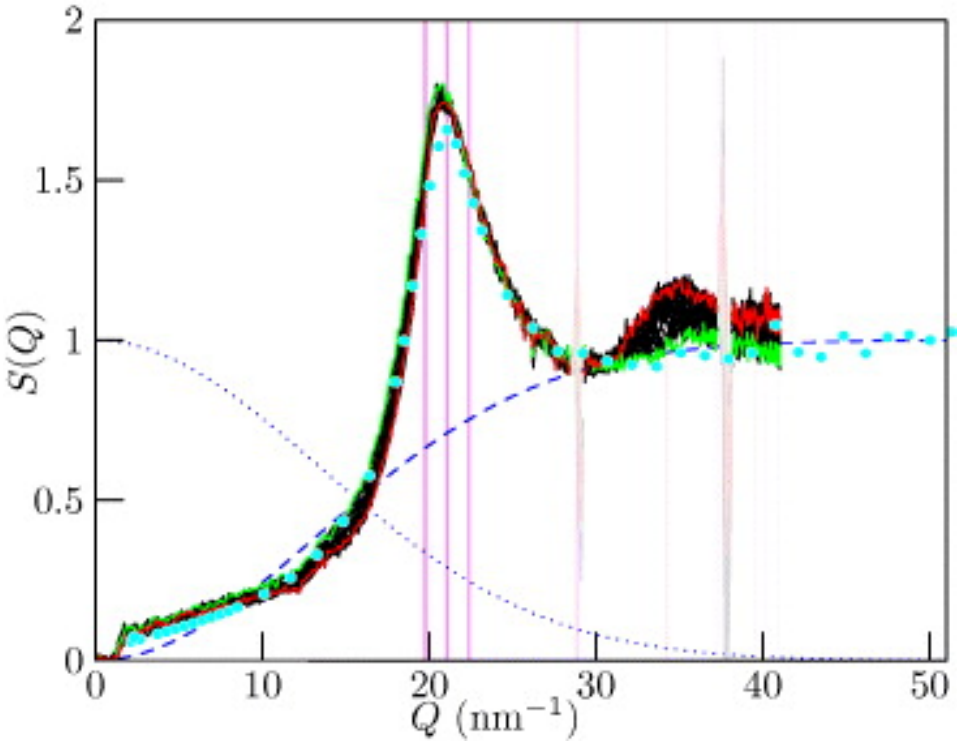

Figure 4 - $S(\vec{k})$ presents a sharp maximum near $k = 20\text{nm}^{-1}$ which correspond to the wavelength of the nearest neighbor distance in the liquid. The maximum in $S(\vec{k})$ correspond to a minimum in $E(\vec{k})$. This confirms that rotons excitations have a wavenumber that matches that of the nearest neighbor [5].

7.4 Landau Fermi liquid theory

Although Landau Fermi liquid theory is mainly intended for strongly interacting Fermi liquids, it can be extended to elementary excitation of superfluid 4He as well as dilute solutions of 3He in 4He. We consider a fluid which flows at a constant velocity v in a capillary and has momentum $\vec{p}$. Friction between the tube and the fluid create quasiparticles. Let's consider one of these excitation with energy $\epsilon(\vec{k})$ and momentum $\vec{k}$. In the lab frame, the tube is at rest. Conservation of momentum during the interaction yields

$$\vec{p} = \vec{p'} + \vec{k} \tag{7.32}$$

where $\vec{p'}$ represents the momentum of a fluid particle after the collision. Therefore, if no excitation takes place, it follows that $\vec{p} = \vec{p'}$. Nevertheless, because a quasiparticle is created, the conservation of energy can be written as

$$\frac{\vec{p}^2}{2m} = \frac{\vec{p'}^2}{2m} + \epsilon(\vec{k}), \tag{7.33}$$

where m describes the mass of the fluid particle. Taking the square of momentum conservation relation yields

$$|\vec{p'}|^2 = |\vec{p}|^2 + |\vec{k}|^2 - 2\vec{p}\cdot\vec{k} \tag{7.34}$$

and if θ represents the angle between $\vec{p}$ and $\vec{k}$, we have

$$|\cos\theta| = \frac{|\vec{p}|^2 - |\vec{p'}|^2 + |\vec{k}|^2}{2|\vec{p}||\vec{k}|}. \tag{7.35}$$

In particular, it follows that

$$\frac{|\vec{p}|^2 - |\vec{p'}|^2}{|\vec{p}||\vec{k}|} \leq |\cos\theta| \leq 1, \tag{7.36}$$

which, if combined with the expression of the energy conservation yields

$$\frac{m\epsilon(\vec{k})}{2|\vec{p}||\vec{k}|} \leq 1. \tag{7.37}$$

Using the energy spectrum relation (7.28), we get that

$$v_0 := \frac{1}{m}\sqrt{\frac{N_0 V(0) m}{\Omega}} \leq \frac{|\vec{p}|}{m} = |\vec{v}|. \tag{7.38}$$

More precisely, if $|\vec{v}| > v_0$ thermal excitation will happen. However, if the velocity $|\vec{v}|$ is in a specific range given by $0 < |\vec{v}| < v_0$, no dissipation takes place and therefore the fluid behaves in a superfluid manner. The theoric value $v_0 \simeq \frac{\epsilon(k_0)}{k_0} = \frac{\Delta}{k_0} = 60\text{m/s}$, according to (7.6), does not correspond with the experimental one, which lies around 1m/s. This illustrates the limit of the two-body potential model used for describing the BEC, which assumes that the gas is dilute or weakly non-ideal. The actual theory of superfluidity treats the fluid as a highly correlated and strongly interacting system.

7.5 Gross-Pitaevskii equation

Let's consider the Hamiltonian of the $Bose - Einstein$ condensate, this time taking also spatial variations into account in addition to interactions

$$\begin{aligned}\mathcal{H} = \int dr^3 \{\frac{\hbar^2}{2m}(\nabla\hat{\Psi}^\dagger(\vec{r})\cdot\nabla\hat{\Psi}(\vec{r})) + [V(\vec{r})-\mu]\hat{\Psi}^\dagger(\vec{r})\hat{\Psi}(\vec{r})\} \\ +\frac{1}{2}\int dr^3 \int dr'^3 \hat{\Psi}^\dagger(\vec{r})\hat{\Psi}^\dagger(\vec{r'})U\delta(\vec{r}-\vec{r'})\hat{\Psi}(\vec{r})\hat{\Psi}(\vec{r'}).\end{aligned} \tag{7.39}$$

The equation of motion for the field operator $\hat{\Psi}$ can be written as

$$i\hbar\frac{\partial\hat{\Psi}(\vec{r},t)}{\partial t} = [\hat{\Psi}(\vec{r},t),\mathcal{H}] = [\frac{-\hbar^2\nabla^2}{2m} + V(\vec{r}) - \mu + U\hat{\Psi}^\dagger(\vec{r},t)\hat{\Psi}(\vec{r},t)]\hat{\Psi}(\vec{r},t). \tag{7.40}$$

We further use that the field operator can be written as

$$\hat{\Psi}(\vec{r}) = \frac{1}{\sqrt{\Omega}}\sum_{\mathbf{k}}\hat{a}_{\mathbf{k}}e^{i\vec{k}\cdot\vec{r}} = \frac{\hat{a}_0}{\sqrt{\Omega}} + \frac{1}{\sqrt{\Omega}}\sum_{\mathbf{k}\neq 0}\hat{a}_{\mathbf{k}}e^{i\vec{k}\cdot r}. \tag{7.41}$$

Provided the interaction is sufficiently weak, one may employ only the first term as an approximation for a dilute Bose gas. Also, for a BEC we may replace the operator $\hat{a}_0$ by a complex number $a_0 = \sqrt{N_0}$ because $N_0 \simeq N_0 - 1$, such that

$$\hat{\Psi}(\vec{r}) \longrightarrow \hat{\Psi}(\vec{r}) = \psi_0(\vec{r}) + \delta\hat{\Psi}(\vec{r}), \tag{7.42}$$

and the state $\psi_0(\vec{r})$ can then be determined by Hartree approximation, namely by minimizing the energy $E = \langle\psi_0|\,\mathcal{H}\,|\psi_0\rangle$. By variation of the energy functional

$$E = \int dr^3[\frac{\hbar^2}{2m}|\nabla\psi_0(\vec{r})|^2 + [V(\vec{r})-\mu]|\psi_0(\vec{r})|^2 + \frac{U}{2}|\psi_0(\vec{r})|^4] \tag{7.43}$$

we obtain exactly what in the Ginzburg-Landau theory of $2^n d$ order phase transition is considered as a form of the free energy, i.e.

$$f(\vec{r}) = f_n + \alpha|\psi_0(\vec{r})|^2 + \frac{1}{2}\beta|\psi_0(\vec{r})|^4 + \frac{1}{2}|\nabla\psi_0(\vec{r})|^2, \tag{7.44}$$

where $\hbar = m = 1$, $\alpha, \beta \in \mathbb{R}$ and $\psi_0(\vec{x})$ is known as the order parameter. Let's write

$$\tilde{U} \equiv \tilde{U}(\psi_0) = f_n + \alpha|\psi_0(\vec{r})|^2 + \frac{1}{2}\beta|\psi_0(\vec{r})|^4. \tag{7.45}$$

In order for $\tilde{U}$ to have a unique minimum, we must require that β is positive, in our situation, $U > 0$. Further, we can notice that the functional E is invariant under a global U(1) phase rotation

$$\psi_0(\vec{x}) \longrightarrow e^{i\alpha}\psi_0(\vec{x}). \tag{7.46}$$

If $\alpha < 0$ is chosen, that is if $V(\vec{r}) < \mu$, then $\tilde{U}$ can be re-expressed as

$$\tilde{U} = \frac{1}{2}\beta(n_0 - |\psi_0|^2)^2 \Rightarrow \int dr^3 f(\vec{r}) = \int dr^3[\frac{1}{2}|\nabla\psi_0(\vec{r})|^2 + \frac{1}{2}\beta(n_0 - |\psi_0(\vec{r})|^2)^2] \tag{7.47}$$

Variation of this quantity with respect to $\psi_0(\vec{r})^*$ yields

$$\nabla^2\psi_0(\vec{r}) + \frac{\beta}{2}(n_0 - |\psi_0(\vec{r})|^2)\psi_0(\vec{r}) = 0 \tag{7.48}$$

whose vacuum solutions are $\psi_0(\vec{r}) = \sqrt{n_0}e^{i\phi}$ provided that the phase ϕ is constant in space. Defining the phase spontaneously breaks the U(1) symmetry. In the homogeneous state, i.e. $\nabla\psi_0(\vec{r}) = 0$, we require that $\psi_0(\vec{r}) = \sqrt{n_0}$ and fix the potential V to zero. In the initial situation considered, through derivation

$$i\hbar\frac{\partial\psi_0(\vec{r},t)}{\partial t} = \frac{\delta E}{\delta\psi_0(\vec{r},t)} \tag{7.49}$$

we obtain the so-called $Gross - Pitaevskii$ equation

$$i\hbar\frac{\partial\psi_0(\vec{r},t)}{\partial t} = \left(-\frac{\hbar^2\nabla^2}{2m} + V(\vec{r}) - \mu + U|\psi_0(\vec{r},t)|^2\right)\psi_0(\vec{r},t). \tag{7.50}$$

Multiplying the $Gross - Pitaevskii$ equation by $\psi_0^*(\vec{r},t)$ and subtracting the complex conjugate yields

$$\begin{aligned}\frac{\partial|\psi_0(\vec{r},t)|^2}{\partial t} &= -\frac{\hbar}{2mi}\{\psi_0^*(\vec{r},t)\nabla^2\psi_0(\vec{r},t) - \psi_0(\vec{r},t)\nabla^2\psi_0^*(\vec{r},t)\} \\ &= -\boldsymbol{\nabla}\cdot\frac{\hbar}{2mi}\{\psi_0^*(\vec{r},t)\nabla\psi_0(\vec{r},t) - \psi_0(\vec{r},t)\nabla\psi_0^*(\vec{r},t)\}\end{aligned} \tag{7.51}$$

which we may rewrite in the form of the continuity equation $\frac{\partial\rho}{\partial t} + \boldsymbol{\nabla}\cdot\vec{j}(\vec{r},t) = 0$ with

$$\begin{aligned}\rho(\vec{r},t) &= |\psi_0(\vec{r},t)|^2 \\ \vec{j} &= \frac{\hbar}{m}\mathrm{Im}[\psi^*\nabla\psi].\end{aligned} \tag{7.52}$$

As a consequence, the current density is linked with the phase of the condensate wave function $\psi(\vec{r}) = \sqrt{n_0}e^{i\phi(\vec{r})}$ through

$$\vec{j}(\vec{r}) = \frac{\hbar}{m}n_0\nabla\phi(\vec{r}) = n_0\vec{v_s}(\vec{r}), \tag{7.53}$$

therewith defining the superfluid component's velocity v_s as $\vec{v_s} = \frac{\hbar}{m}\nabla\phi$. In addition, the velocity of the superfluid component derives from a scalar field and as a consequence

$$\nabla\times\vec{v_s} = 0 \tag{7.54}$$

the velocity field is irrotational. Properties of the superfluid component include that it is irrotational and carries zero entropy.

7.6 Vortices

We now show that the solution of $Gross-Pitaevskii$ equation can, under certain conditions, represent a vortex. In fluid dynamics, a vortex is a region of a fluid in which the particles have a rotary motion around an imaginary axis that can be straight or curved [6]. It takes place in the absence of external forces, when viscous friction is present and the flow is turbulent. Heuristically speaking, a vortex is a soliton solution of the field equation (7.48) which satisfies following criteria : the field configuration ψ_0 vanishes at a point $\vec{r} \in \mathbb{R}^3$ and the phase ϕ increases by $2\pi N$, $N \in \mathbb{Z}^*$, along a circle around $\vec{r}$. The solution of the *Gross-Pitaevskii* equation then has the form

$$\psi_0(r_\perp, \theta, z) = \sqrt{n_0}\rho_s(r_\perp)e^{i\theta n} \tag{7.55}$$

for zero line along the z-axis with $(r_\perp, \theta, z)$ being the cylindrical coordinates. The function $\rho_s(r_\perp)$ has following properties :

$$\begin{cases} \lim\limits_{r_\perp \to 0} \rho_s(r_\perp) = 0 \\ \\ \lim\limits_{r_\perp \to a_0} \rho_s(r_\perp) = 1, \end{cases} \quad \text{with } a_0 = \sqrt{\frac{\hbar^2}{2mUn_0}}. \tag{7.56}$$

A vortex is also characterized by its vorticity, that is, a vector $\vec{\omega}$ which describes the local spinning motion at a point near the axis from a frame moving along with it. This characteristic is defined as the rotational of the velocity field of the fluid

$$\vec{\omega} = \boldsymbol{\nabla} \times \vec{v}, \tag{7.57}$$

whose direction is the direction of the axis and intensity is proportional to a particle's angular velocity. It is greater near the axis of the vortex and almost zero outside of this region. There are usually two main velocity profiles to be taken into account. The first has a velocity proportional to the radius r, the fluid rotates in the same manner as a rigid body around its axis. The vorticity is equal to two times the angular velocity of the whole fluid and its gradient vanishes. The second profile is inversely proportional to the radius and the vorticity vanishes only along a vortex line. A vortex line is a curve within the vortex region which is parallel to the vorticity vector and is either a closed loop or finishes at the boundary of the fluid. In this case, the flow is irrotational as it was illustrated in (7.54). This implies that the circulation along any closed contour is zero if it does not include the axis, i.e. it is simply connected, or has a fixed value Γ in the opposite case. Therefore, the tangential component of the velocity is given by $v_\theta = \frac{\Gamma}{2\pi r}$ and the angular momentum rv_θ is constant. Quantum vortices have additionally quantized angular momentum [7].

We consider a classical fluid within a spinning bucket at constant angular velocity Ω. It's surface profile is given by

$$z(r) = \frac{\Omega^2 r^2}{2g} \tag{7.58}$$

in cylindrical coordinates. In this case, the vorticity agrees with the linear velocity profile if the velocity is purely tangential to the rotation axis, i.e.

$$\vec{\omega} = \boldsymbol{\nabla} \times \vec{v} = 2\Omega\hat{e}_z, \tag{7.59}$$

the vorticity is twice the angular velocity of the whole fluid. We now consider He-II instead of a classical fluid. According to the Two-Fluid Model, the superfluid component is irrotational and therefore has a velocity profile that is inversely proportional to the radial coordinate r. Thus, for any closed contour C that is not simply connected the circulation of the superfluid velocity is not zero but rather,

$$\oint \vec{v_s} \cdot \vec{dl} = \frac{\hbar}{m} \oint \nabla\phi \cdot \vec{dl} = \frac{\hbar}{m}\Delta\phi, \tag{7.60}$$

where the superfluid component's velocity was used in the expression of the velocity field and $\Delta\phi$ represents the phase difference around the vortex center. Because of its periodicity, $\Delta\phi = 2\pi n,\ n \in \mathbb{Z}^*$. The superfluid illustrates thereby the quantization of the circulation and especially that of the angular momentum, since

$$\oint \vec{v}\cdot\vec{dl} = rv_\theta \int_0^{2\pi} d\theta = \frac{\hbar}{m}\Delta\phi, \Rightarrow rv_\theta = \frac{h}{m}n \equiv \kappa n, \tag{7.61}$$

where $\kappa = h/m_{He} = 9.97\cdot 10^{-4}$ cm^2/s is known as the quantum of circulation. That the velocity field can have a non-zero circulation corresponds to a region within the contour C which is not superfluid, i.e. where ρ_s has to vanish. This, in turn, explains why the velocity does not become asymptotically large close the vortex axis as would

$$v_\theta = \frac{\kappa}{2\pi r} \tag{7.62}$$

suggest and confirms the existence of a vortex as a solution of the $Gross - Pitaevskii$ equation. Thus, there exist some value a_0 such that (7.62) only applies for $r \geq a_0$. As seen previously, if the velocity of the fluid is superior to a critical velocity v_0, the superfluid component disappears, the flow becomes turbulent and viscous friction is observed. In a rotary region, this velocity is replaced by a critical angular velocity, written Ω_c at which the first vortex is formed. We can show that this critical value depends actually on the vortex core radius a_0. In order for the fluid to reach a thermodynamic equilibrium, it requires to minimize its free energy given by

$$F = E - TS. \tag{7.63}$$

In the rotating frame of reference, where the fluid is at rest, the free energy of the system becomes

$$F' = F - \vec{\Omega}\cdot\vec{L} = E - TS - \vec{\Omega}\cdot\vec{L}, \tag{7.64}$$

where E denotes the internal energy of the vortex, $\vec{L}$ the angular momentum. Let's now consider He-II at 0 Kelvin in a rotating cylinder. The total internal energy of the vortex is a sum of the core energy due to the local depletion of the condensate and of that of the circular flow of the superfluid around the core. Because the first one is negligible we restrict the computation to the energy of the rotating fluid. The first vortex appears only if the free energy of the fluid is reduced by the creation of the vortex, that is, if

$$F_{no\ vortex} = -TS \Rightarrow \Delta F' = F'_{vortex} - F'_{no\ vortex} = E - \Omega L < 0, \tag{7.65}$$

where we used that condensate ground state is the state with zero angular momentum. Using the classical model of a fluid in a bucket, the energy and angular momentum can be written as

$$E = \int d\Omega \int dr\rho_s g z(r) = \int_0^{2\pi} d\theta \int_{a_0}^{R} dr\rho_s g \frac{\Omega^2 r^2}{2g} r = \frac{\rho_s \kappa^2}{4\pi}\ln(R/a_0) \tag{7.66}$$

$$L = \int_0^{2\pi} d\theta \int_{a_0}^{R} dr\rho_s v_s r^2 = \frac{\rho_s\kappa}{2}(R^2 - a_0^2) \simeq \frac{\rho_s\kappa}{2}R^2. \tag{7.67}$$

Therefore, the critical angular momentum is found to be

$$\Omega_c = \frac{E}{L} = \frac{\kappa}{2\pi R^2}\ln(R/a_0), \tag{7.68}$$

and thus dependent from the core radius $a_0 \simeq 10^{-8}$ cm. If the angular velocity goes beyond this limit, more and more vortex lines will appear, thereby forming a vortex lattice. The number of vortex lines per unit area can be determined using relation (7.59) and Stokes' theorem

$$\oint_{\partial S} \vec{ds}\cdot\vec{v} = \int_S dx^2 \vec{n}\cdot\vec{\omega} \ \Rightarrow\ n = \frac{2\Omega}{\kappa} \tag{7.69}$$

and is therefore dependent of the rigid body's vorticity $\omega = 2\Omega$ [2].

7.7 BKT transition

A peculiar behavior appears in 2 dimensional superfluids. Due to phase fluctuations of the condensate wave function a new type of phase transition appears [1].

Independent classical particles do not have any correlation among each other. This is different for quantum particles. We consider a general occupation number state for free spineless bosons,

$$|\Phi\rangle = \left|n_{\vec{k_0}}, n_{\vec{k_1}}, \ldots\right\rangle = \ldots (\hat{a}^\dagger_{\vec{k_1}})^{n_{\vec{k_1}}} (\hat{a}^\dagger_{\vec{k_0}})^{n_{\vec{k_0}}} |0\rangle \,. \tag{7.70}$$

The ground state would be the state with all bosons occupying the lowest-energy single-particle state. The correlation function is expressed by

$$\left\langle \Phi \right| \hat{\Psi}^\dagger(\vec{r}) \hat{\Psi}(\vec{r'}) \left| \Phi \right\rangle = \frac{1}{\Omega} \sum_{\vec{k},\vec{k'}} e^{-i\vec{k}\vec{r}+i\vec{k'}\vec{r'}} \underbrace{\left\langle \Phi \right| \hat{a}^\dagger_{\vec{k}} \hat{a}_{\vec{k'}} \left| \Phi \right\rangle}_{n_{\vec{k}}\delta_{\vec{k},\vec{k'}}} = \frac{1}{\Omega} \sum_{\vec{k}} n_{\vec{k}} e^{-i\vec{k}(\vec{r}-\vec{r'})}, \tag{7.71}$$

which in the limit $\vec{r'} \to \vec{r}$ approaches the constant density n and vanishes at very large distances.

The pair correlation function given by

$$n^2 g(\vec{r}-\vec{r'}) = \left\langle \Phi \right| \hat{\Psi}^\dagger(\vec{r}) \hat{\Psi}^\dagger(\vec{r'}) \hat{\Psi}(\vec{r'}) \hat{\Psi}(\vec{r}) \left| \Phi \right\rangle \tag{7.72}$$

can be used to show that

$$n^2 g(\vec{r}-\vec{r'}) = n^2 + \left| \int \frac{dk^3}{(2\pi)^3} e^{-i\vec{k}(\vec{r}-\vec{r'})} n_{\vec{k}} \right|^2 + O\Big(\frac{1}{\Omega}\Big) = n^2(1 + e^{-A^2(\vec{r}-\vec{r'})^2/2}) + O\Big(\frac{1}{\Omega}\Big), \tag{7.73}$$

using the approximation according to which $n_{\vec{k}}$ follows a Gaussian distribution which corresponds to the classical Maxwell-Boltzmann distribution. Note that the probability of finding two bosons at the same position is twice as large as for long distances. Thus, bosons like to cluster together. In the limit where the distance becomes large, i.e. $|\vec{R}| = |\vec{r} - \vec{r'}| \to \infty$,

$$\begin{aligned} g(\vec{R}) = \int \frac{dk^2}{(2\pi)^2} \frac{e^{-i\vec{k}\vec{R}}}{e^{\beta(\epsilon(\vec{k})-\mu)} - 1} &\approx \frac{2mk_BT}{\hbar^2} \int \frac{dk^2}{(2\pi)^2} \frac{e^{-i\vec{k}\vec{R}}}{k^2 + k_0^2} \\ &= 2\frac{K_0(k_0R)}{\lambda^2} \approx \frac{1}{(2\pi)^2\lambda^2|\vec{R}|} e^{-k_0|\vec{R}|}. \end{aligned} \tag{7.74}$$

with $k_0^2 = -\frac{2m\mu}{\hbar^2}$ ¿ 0, $\lambda = \frac{h}{\sqrt{2\pi m k_B T}}$ and $K_0(x)$ the modified Bessel function. The correlation function goes to zero like $|\vec{R}|^{-1}$. However this is not true, because our integral approach neglects the macroscopic occupation of the $\vec{k} = 0$ state. Thus,

$$\langle \hat{n}_{\vec{k}} \rangle = n_0 \delta(\vec{k}) + \frac{1}{(2\pi)^3} \frac{1}{e^{\beta(\epsilon(\vec{k})-\mu)} - 1} \tag{7.75}$$

such that for $|\vec{R}| \to \infty$,

$$g(\vec{R}) = n_0 + \frac{1}{(2\pi)^3\lambda^2|\vec{R}|}. \tag{7.76}$$

The correlation function approaches a finite value on long distances. Now let's consider the correlation function in high temperature limit. In this situation,

$$g(\vec{R}) = \int \frac{dk^2}{(2\pi)^2} \frac{e^{-i\vec{k}\vec{R}}}{e^{\beta(\epsilon(\vec{k})-\mu)} - 1} \approx \frac{2mk_BT}{\hbar^2} \int \frac{dk^2}{(2\pi)^2} \frac{e^{-i\vec{k}\vec{R}}}{k^2 + k_0^2} = 2\frac{K_0}{\lambda^2} k_0 R \approx \frac{1}{\lambda^2} \sqrt{\frac{2\pi}{k_0 R}} e^{-k_0 R}. \tag{7.77}$$

Thus, the correlation presents an exponential decay. This is however not the case in the low temperature limit. If we keep n_0 constant, use the energy functional given by (7.43) and restrict to the phase fluctuations

$$E[\phi] = Un_0^2 \int dr^2 [a_0^2 |\nabla\phi|^2 + \frac{1}{2}] = Un_0^2 [\sum_{\vec{q}} a_0^2 q^2 \phi_{\vec{q}} \phi_{-\vec{q}} + \frac{\Omega}{2}], \tag{7.78}$$

with the Fourier transform

$$\phi(\vec{r}) = \frac{1}{\sqrt{\Omega}} \sum_{\vec{q}} \phi_{\vec{q}} e^{i\vec{q}\vec{r}} \tag{7.79}$$

and Ω the normalization constant. With gaussian averaging, it follows that

$$g(\vec{R}) = n_0 \langle e^{i(\phi(0)-\phi(\vec{R}))} \rangle = n_0 e^{-\langle(\phi(0)-\phi(\vec{R}))^2\rangle} = \left(\frac{\pi R}{r_o}\right)^{-\eta(T)} \tag{7.80}$$

with $\eta(T) = \frac{2}{k_0 \lambda^2}$ being a function linear in T and $r_o^{-3} = n$ being a characteristic length. Here $g(\vec{R})$ still decays but now algebraically (see Figure 5) and the correlation length is, as a consequence, infinitely larger for low temperatures.

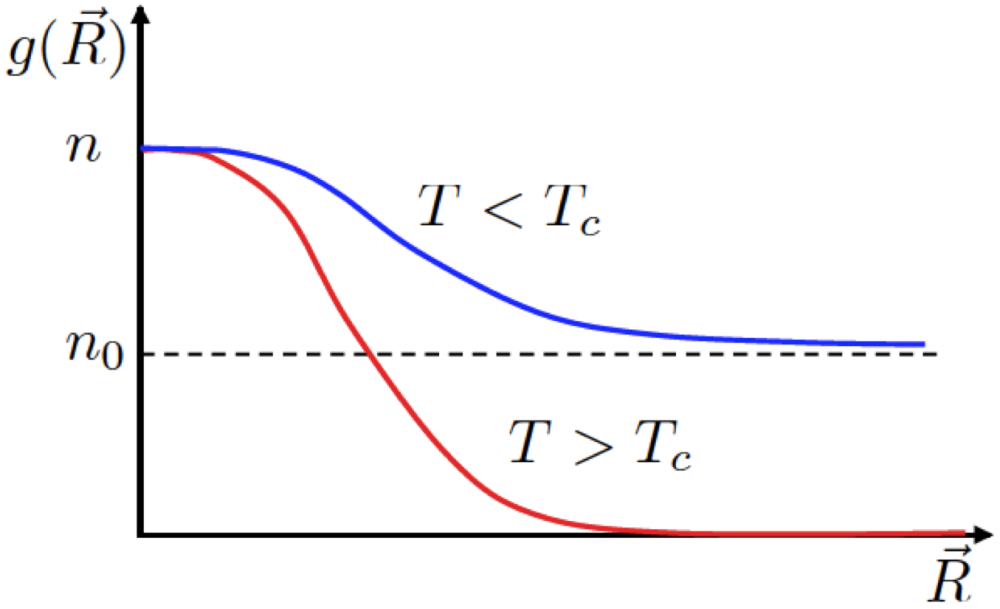

Figure 5 - Schematic behavior of the single-particle correlation function in the normal ($T > T_c$) and the $Bose - Einstein$ condensed phase ($T < T_c$). n is the overall particle density and n_0 the density of the condensed particles [1].

In uniform two dimensional systems, $Mermin - WagnerHohenberg$'s theorem claim that off-diagonal long range order is destroyed by thermal fluctuations at finite temperature. In other words, continuous symmetry cannot be spontaneously broken at finite temperatures with sufficiently short-range interactions. This is why a $Bose - Einstein$ condensation cannot occur in systems with dimensions smaller than two, in contrast to three-dimensional fluids. However, previous theorem does not prevent the existence of phase transition. The two-dimensional system can indeed form a quasi-condensate and become superfluid below a finite critical temperature. This is the so-called BKT transition named after Berezinskii, Kosterlitz and Thouless. And it is illustrated here by the correlation length, which diverges at temperature below T_{KT} in comparison to that above the critical temperature. In a 2-dimensional superfluid, vortices act as topological excitations and cause the change of the correlation function. The critical temperature of the phase transition can be determined by considering the free energy at equilibrium [1]. Using the energy of a single vortex

$$E = \frac{\rho_s \kappa}{4\pi} \ln(R/a_0), \tag{7.81}$$

and given the entropy $S = k_B \ln \left(\frac{R}{a_0}\right)^2$ - where $\left(\frac{R}{a_0}\right)^2$ is the probability of the possible microstates - the expression of the free energy of the system is given as

$$F = E - TS = \left\{ \frac{\hbar^2 n_0 \pi}{m} - 2k_B T \right\} \ln \left(\frac{R}{a_0} \right). \tag{7.82}$$

This suggest a phase transition at the critical temperature

$$T_{KT} = \frac{\hbar^2 n_0 2\pi}{2mk_B}. \tag{7.83}$$

Above T_{KT}, vortices are favored whereas below they are suppressed. High temperature's exponential decay of the correlation function correspond with unbound free vortices destroying the phase coherence. Near absolute zero, vortices bind into pairs of opposite winding number such that there is no phase winding of bound pairs. Vortex and anti-vortex can therefore be created spontaneously without the change of the overall phase of the system. The total winding number is conserved

$$n^{tot} = \sum_i n_i. \tag{7.84}$$

7.8 Conclusion

To sum up, many different properties define what a superfluid is. The use of a $Bose - Einstein$ condensate is a good model to describe and demonstrate that these properties exist. However, this model also shows its limits when it comes down to specific heat, critical temperature, etc. and does not account for a unique and global explanation of the superfluidity. In particular, the energy spectrum is still described by two different approaches in order to prove the existence of phonon and roton excitations. The $Gross - Pitaevskii$ equation allows to describe the formation of vortices within the superfluid, namely the irrotational and dissipationless flow. The critical velocity also applies in this case and defines the limit at which the lattice of vortex forms. Finally, the $Berezinskii - Kosterlitz - Thouless$ transition describes the phase transition within two-dimensional fluids. It wonderfully fits together with the appearance of a lattice of bound vortices which minimize the total energy of the system. Here also, a critical temperature can be defined and theoretically computed as a limit which correspond with a phase transition.

Bibliography

[1] *Statistical physics*, Manfred Sigrist, ETH Zürich, Herbstsemester 2013.

[2] *Vortices and Turbulence at Very Low Temperatures*, Carlo F. Barenghi, Yuri A. Sergeev, SpringerWienNewYork, CISM, 2008.

[3] *Elements of Statistical Mechanics*, Ivo Sachs, Siddhartha Sen, James Sexton, Cambridge University Press, 2006.

[4] *Energy Spectrum of the Excitations in Liquid Helium*, R.P. Feynman and Michael Cohen, Phys. Rev. Vol. 102 No. 5, 1956.

[5] *Static and dynamic structure factor in solid 4He: Absence of a glassy phase*, Y. Mukharsky et al 2013 EPL 101 26002.

[6] en.wikipedia.org/wiki/vortex Wikipedia page.

[7] en.wikipedia.org/wiki/Quantum_vortex Wikipedia page.

[8] en.wikipedia.org/wiki/Superfluid_helium_4 Wikipedia page.

Chapter 8

Aharonov-Bohm Effect

Author: Cyril Welschen
Supervisor: Oscar Åkerlund

This chapter deals with the Aharonov-Bohm effect, a fundamental phenomena of quantum physics. The aim is to introduce the AB-effect, to describe its topological and geometrical aspects and to discuss three interpretations of it. More precisely, it is shown that the AB-phase is a topological phase, in the sense that it depends on topological quantities, and also that it is a special case of Berry's geometrical phase. The presented interpretations are the most common one based on the gauge potentials, the B interpretation based on electromagnetic field strengths and the C interpretation based entirely on gauge invariant quantities, the holonomies. Also a theoretical example showing the periodicity of the AB-effect is discussed.

8.1 Introduction

The AB-effect is a fundamental phenomena of quantum mechanics. It is so deeply engrained in quantum physics that it can be described in the most basic formalism of quantum mechanics. In a nutshell, the AB-effect shows that charged particles are influenced by electromagnetic fields even if they are never in a region where the field is non-zero.

In their paper from 1959 Yakir Aharonov and David Bohm presented two possible experiments to test the hypothesis that charged particles are influenced by electric and magnetic fields even if they are never in direct contact with them [1][2]. The first experiment describing the electric Aharonov-Bohm effect was never experimentally tested. Also it's mathematical description is not as clean as the one of the second experiment, the magnetic Aharonov-Bohm effect. Therefore most of today's literature and scientific papers deal only with the magnetic AB-effect.

The AB-effect represents one of the deep quantum mechanical mysteries and there are, more than fifty years after it's discovery, still a lot of unanswered questions. Like in quantum mechanics itself it is not the prediction of an outcome of a certain experiment which is troublesome, but the fundamental question on how to interpret it. To give the reader the possibility to choose the last two sections of this chapter provide three interpretations of the AB-effect and their strengths and weaknesses.

In the first section the magnetic AB-effect will be introduced and some important properties are noted. After some preparations and general considerations about the momentum operator the topological aspects of the AB-effect are derived. The importance of the topology of the configuration

space is investigated and it will be shown that the effect depends only on the winding number of the curve which describes the path of the particle and the magnetic flux through a surface bound by this curve, but not specifically on the shape of the curve. Because the AB-phase therefore depends only on topological quantities it can be called a topological phase.

In the third section the relation of the AB-phase to Berry's geometrical phase is described, namely that the AB-phase is a special case of the Berry phase. This is done by using a relation between the Berry phase and the so called Mead-Berry connecting one-form, which is a general result of Berry's theory on geometrical phases. After that an example of the periodicity of the Aharonov-Bohm effect is given before the different interpretations are discussed.

8.2 The AB-Effect

In this section the AB-effect is described following [3]. To derive it one needs to know how wave functions transform under gauge transformations. Consider first the classical Hamiltonian of a charged particle with mass m and charge e in the electromagnetic potentials $\mathbf{A}(\mathbf{x},t)$ and $\varphi(\mathbf{x},t)$, i.e.

$$H = \frac{1}{2m}\left(\mathbf{p} - \frac{e}{c}\mathbf{A}(\mathbf{x},t)\right)^2 + e\varphi(\mathbf{x},t) + V(\mathbf{x},t)\,, \tag{8.1}$$

where the potential V stands for non-electromagnetic influences. The Schrödinger equation in this case is

$$\left[\frac{1}{2m}\left(\frac{\hbar}{i}\nabla - \frac{e}{c}\mathbf{A}(\mathbf{x},t)\right)^2 + e\varphi(\mathbf{x},t) + V(\mathbf{x},t)\right]\psi(\mathbf{x},t) = i\hbar\partial_t\psi(\mathbf{x},t)\,. \tag{8.2}$$

If the potentials undergo a gauge transformation, $\varphi \to \varphi' = \varphi - \frac{1}{c}\partial_t\chi$ and $\mathbf{A} \to \mathbf{A}' = \mathbf{A} + \nabla\chi$, the solution to the SE with the primed potentials is given by

$$\psi'(\mathbf{x},t) = \psi(\mathbf{x},t)\exp\left(\frac{ie}{\hbar c}\chi(\mathbf{x},t)\right)\,, \tag{8.3}$$

where $\psi(\mathbf{x},t)$ is the solution of (8.2). This can be seen by multiplying (8.2) from the left by $\exp\left((ie/\hbar c)\chi(\mathbf{x},t)\right)$ and using the identity

$$e^{f(y)}\frac{\partial}{\partial y} = \left(\frac{\partial}{\partial y} - \frac{\partial f}{\partial y}\right)e^{f(y)} \tag{8.4}$$

twice. The next step is to study the wave function in a field free region. Consider an electron travelling in a space region G where the magnetic field $\mathbf{B} = \mathbf{B}(\mathbf{x})$ vanishes. Because $\mathbf{B} = \nabla\wedge\mathbf{A} \equiv 0$ in G the vector potential can be written as the gradient of a scalar field, i.e. $\mathbf{A} = \nabla\Lambda$. Thus

$$\Lambda(\mathbf{x}) = \int_{\mathbf{x}_0}^{\mathbf{x}} \mathrm{d}\mathbf{s}\cdot\mathbf{A}(\mathbf{s})\,, \tag{8.5}$$

where $\mathbf{x}_0$ is an arbitrary point in G. The wave function in the field free region can now be calculated out of (8.2) with $\mathbf{A} = \nabla\Lambda$ or easier with the gauge transformation $\chi = -\Lambda$ yielding $\mathbf{A}' = \nabla\Lambda + \nabla(-\Lambda) = 0$ and the corresponding SE, which now reads

$$\frac{1}{2m}\left(\frac{\hbar}{i}\nabla\right)^2\psi' + V\psi' = i\hbar\partial_t\psi'\,. \tag{8.6}$$

(Where we have set $\varphi = 0$.) With the result of Eq. (8.3) this leads to

$$\psi = \psi'\exp\left(\frac{ie}{\hbar c}\Lambda\right) = \psi'\exp\left(\frac{ie}{\hbar c}\int_{\mathbf{x}_0}^{\mathbf{x}}\mathrm{d}\mathbf{s}\cdot\mathbf{A}(\mathbf{s})\right)\,, \tag{8.7}$$

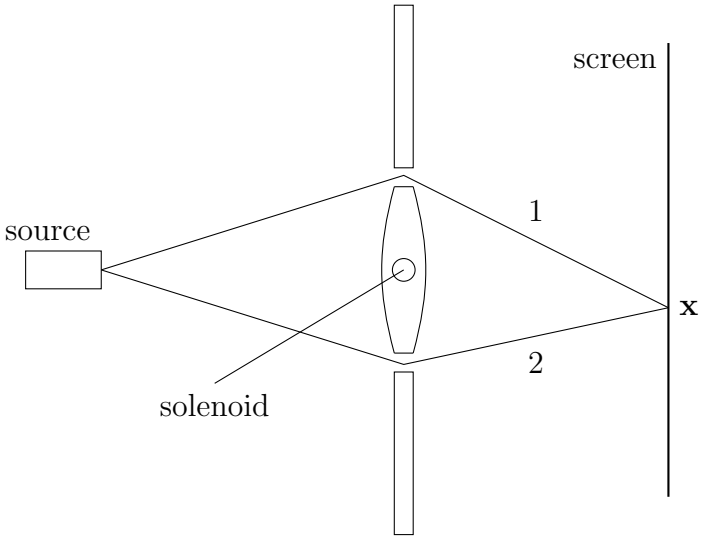

Figure 8.1: Experimental setup of the AB-effect.

where ψ is the wave function in the gauge $\mathbf{A} = \nabla\Lambda$ and ψ' the one in the gauge $\mathbf{A}' = 0$. These are all the preparations needed to describe the AB-effect. One experimental setup for measurements of the AB-effect is shown in Figure 8.2. The setup is similar to the double slit experiment. The difference is that between the slits a solenoid with a magnetic field in it is placed perpendicular to the plane. The magnetic field shall be shielded from the path of the electrons ensuring that they travel only in field free regions. The solution as a function of the field is the superposition of the solutions when only one slit is open. These solutions differ from the solutions without a magnetic field only by a phase:

$$\psi_{i,B} = \psi_{i,0} \exp\left(\frac{ie}{\hbar c}\int_i \mathrm{d}\mathbf{s}\cdot\mathbf{A}(\mathbf{s})\right) \qquad (i = 1, 2)\,. \tag{8.8}$$

The first index denotes the path, the second one denotes whether or not there is a magnetic field in the solenoid. The superposition of these solutions

$$\psi_B = \psi_{1,0} \exp\left(\frac{ie}{\hbar c}\int_1 \mathrm{d}\mathbf{s}\cdot\mathbf{A}(\mathbf{s})\right) + \psi_{2,0} \exp\left(\frac{ie}{\hbar c}\int_2 \mathrm{d}\mathbf{s}\cdot\mathbf{A}(\mathbf{s})\right) \tag{8.9}$$

gives the wave function $\psi_B(\mathbf{x})$ for the case when both slits are open and a magnetic field is in the solenoid. This can be rewritten in a more suitable way. For this notice that with Stokes theorem the relative phase between $\psi_{1,0}$ and $\psi_{2,0}$ becomes

$$\frac{e}{\hbar c}\int_1 \mathrm{d}\mathbf{s}\cdot\mathbf{A}(\mathbf{s}) - \frac{e}{\hbar c}\int_2 \mathrm{d}\mathbf{s}\cdot\mathbf{A}(\mathbf{s}) = \frac{e}{\hbar c}\oint \mathrm{d}\mathbf{s}\cdot\mathbf{A}(\mathbf{s}) = \frac{ie}{\hbar c}\Phi_B\,, \tag{8.10}$$

where Φ_B is the magnetic flux through any surface with boundary corresponding to the paths of integration. Thus equation (8.9) can be written as

$$\psi_B = \left(\psi_{1,0}\exp\left(\frac{ie}{\hbar c}\Phi_B\right) + \psi_{2,0}\right)\exp\left(\frac{ie}{\hbar c}\int_2 \mathrm{d}\mathbf{s}\cdot\mathbf{A}(\mathbf{s})\right)\,. \tag{8.11}$$

This shows that the relative phase depends on the magnetic flux Φ_B. Since the interference pattern on the screen is proportional to $|\psi_B|^2$ this means that the pattern depends on the magnetic flux. This is called the Aharonov-Bohm effect.

Notice that the electron is influenced even though it was never in a region where $\mathbf{B} \neq 0$, which is rather unexpected. Equation (8.11) suggests that in this case in addition to the electromagnetic field strengths the vector potential is also physically relevant. In contrast to the classical case where the electromagnetic potentials are just mathematical aids without any physical meaning. For later considerations notice also that the integration is over a closed path and depends only on the flux through the surface for which it is the boundary. In addition the region where the electron has a non-vanishing wave function is not simply connected.

Electric AB-Effect

In the electric Aharonov-Bohm effect the equations suggest that it is the scalar potential φ which is physically relevant. We do not go into the electrical AB-effect since it gives no additional insight and is theoretically less clean. Moreover it has never been experimentally confirmed [4]. For completeness only the main idea shall be sketched, following [1]. The experimental setup is as follows. A coherent electron beam is split into two parts. The individual beams pass through metal tubes shielding the wave packets from electrical fields. When the wave packets are inside the tubes the tubes are brought on different potentials, say φ_1 and φ_2 and before the packets leave the tubes the electric field is again zero making sure that the wave packets are never in a region with non-vanishing field. Then the beams are brought to interference. Also here, like with the magnetic AB-effect, a shift in the interference pattern is predicted.

To calculate the phase shift consider first a Faraday cage (representing one tube) with a charge inside it. The cage is connected to a generator producing an alternating potential $V(t)$ on it. The Hamiltonian for the region inside the cage is $H = H_0 + V(t)$ where H_0 is the Hamiltonian when there is no fluctuating potential. If $\psi_0(x,t)$ denotes a solution with Hamiltonian H_0, then a solution to H is given by

$$\psi = \psi_0 e^{-iS/\hbar}\,, \quad \text{where} \quad S = \int V(t)\mathrm{d}t\,, \tag{8.12}$$

which follows from

$$i\hbar\frac{\partial\psi}{\partial t} = \left(i\hbar\frac{\partial\psi_0}{\partial t} + \psi_0\frac{\partial S}{\partial t}\right)e^{-iS/\hbar} = \left(H_0 + V(t)\right)\psi = H\psi\,. \tag{8.13}$$

For the two tubes the solution is the superposition

$$\psi = \psi_0^{(1)} e^{-iS_1/\hbar} + \psi_0^{(2)} e^{-iS_2/\hbar}\,, \tag{8.14}$$

where the numbers in the brackets denote which tube is described and as before

$$S_1 = e\int \varphi_1 \mathrm{d}t, \quad \text{and} \quad S_2 = e\int \varphi_2 \mathrm{d}t\,. \tag{8.15}$$

The shift in the interference pattern is thus because of the phase difference $(S_1 - S_2)/\hbar$. Notice that also in the electric AB-effect the electron is split and moves in a non simply connected region and the phase consists also of integrals over the (scalar) potential. Furthermore the electron is also never in a region with non-vanishing (electric) field and the effect is again a pure quantum mechanical one, i.e. interference of the electron with itself is required.

8.3 Topological Aspects

In this section it is shown that the AB-phase is a topological phase. After some preparations the topological phase is introduced and in the end of the section it is shown that the AB-phase meets the requirements to be a topological phase.

Normally the j-th component of the momentum operator is given by $p_j = -i\partial_j$ (from now on we set $\hbar = 1$) where ∂_j denotes the partial derivative with respect to x_j. In general, however, the j-th component is of the form

$$p_j = -i\partial_j + \omega_j(x) \tag{8.16}$$

as argued by Dirac [5]. The $\omega_j(x)$ are real valued functions only depending on the space coordinate. A sketch of Dirac's argumentation for this result is the following.

Dirac's Derivation

A dominant feature of the mathematical description of quantum mechanics is that not all observables commute. A main interest therefore is to present equations (called commutation relations or quantum conditions) to determine the quantities $\xi\eta - \eta\xi$. A fairly general method to obtain these quantities is by classical analogy. To this end consider first the theory of classical mechanics. An important concept is the Poisson Bracket (PB). For two dynamical variables u and v it is denoted by $[u, v]$. The main properties are antisymmetry, linearity, the Jacobi identity and

$$[u_1u_2, v] = [u_1, v]u_2 + u_1[u_2, v]\,, \qquad [u, v_1v_2] = [u, v_1]v_2 + v_1[u, v_2]\,. \tag{8.17}$$

To introduce a quantum PB it is assumed that the same properties hold. As it turns out these properties are sufficient to determine the form of the quantum PB by calculation $[u_1u_2, v_1v_2]$ in two different ways using Eq. (8.17) in different orders. This calculation leads to

$$uv - vu = i\hbar[u, v] \tag{8.18}$$

for the definition of the quantum PB $[u, v]$ of any two variables u and v. Thereby $\hbar$ arises as a new universal constant. The task to find the quantum conditions now reduces to the task to determine the quantum PBs. The strong analogy of classical and quantum PB suggest that at least the basic variables have corresponding Poisson Brackets. This leads to the fundamental quantum conditions

$$x_ix_j - x_jx_i = 0\,, \tag{8.19}$$
$$p_ip_j - p_jp_i = 0\,, \tag{8.20}$$
$$x_ip_j - p_jx_i = i\hbar\delta_{ij}\,. \tag{8.21}$$

In the one dimensional case ($xp - px = i\hbar$), using that by the chain rule the relation

$$\frac{\mathrm{d}}{\mathrm{d}x}x|\psi\rangle = x\frac{\mathrm{d}|\psi\rangle}{\mathrm{d}x} + |\psi\rangle \tag{8.22}$$

holds for any $|\psi\rangle$, we have

$$\frac{\mathrm{d}}{\mathrm{d}x}x - x\frac{\mathrm{d}}{\mathrm{d}x} = 1\,. \tag{8.23}$$

Comparing this with Eq. (8.21) shows that $-i\hbar\mathrm{d}/\mathrm{d}x$ satisfies the same commutation relations with x that p does. In an analogous way it can be seen that the linear operators $-i\hbar\partial_j$ satisfy the same commutation relations with the x's and with each other that the p's do. Therefore the operator p_j *can* be identified with $-i\hbar\partial_j$ without getting any inconsistency. Out of this possibility follows that the x's form a complete commuting set of observables: Any function of the x's and p's can be taken as a function of the x's and the $-i\hbar\partial_{(.)}$'s and then not commute with all the x's unless it is a function of the x's only. The equations $p_j = -i\hbar\partial_j$ do not necessarily hold, but in any case the quantities $p_j + i\hbar\partial_j$ each commute with all the x's thus each is a function of the x's only, say $\omega_j(x)$, which results in Eq. (8.16) (where $\hbar$ is set to one).

The one-form ω

Now back to the considerations about the momentum operator. (The rest of this section follows essentially [6].) For any wave function $\psi(x)$ holds

$$0 = \langle x|p_ip_j - p_jp_i|\psi\rangle = i\psi(x)(\partial_j\omega_i - \partial_i\omega_j) \tag{8.24}$$

using the fundamental quantum condition (8.20) and the chain rule

$$\partial_i(\omega_j f) = (\partial_i\omega_j)f + \omega_j\partial_i f\,. \tag{8.25}$$

Since Eq. (8.24) holds for any wave function one gets the relation $\partial_j\omega_i - \partial_i\omega_j = 0$ for all i, j. Because p_j has a definite transformation behaviour and one term is a derivative ω_j also transforms like a derivative and ω_j can be viewed as the j-th component of a one-form $\omega = \omega_j \mathrm{d}x^j$ (we always use Einstein's sum convention). The above relation between the components now implies that the one-form ω is closed, i.e. the exterior derivative vanishes:

$$\mathrm{d}\omega = \partial_i\omega_j \mathrm{d}x^i \wedge \mathrm{d}x^j = \frac{1}{2}(\partial_i\omega_j - \partial_j\omega_i)\mathrm{d}x^i \wedge \mathrm{d}x^j = 0\,, \tag{8.26}$$

where the antisymmetry of the basis elements of the two-form ($\mathrm{d}x^i \wedge \mathrm{d}x^j = -\mathrm{d}x^j \wedge \mathrm{d}x^i$) was used. After knowing that ω is closed the question is if it is also exact. Remember the definition: an m dimensional from f is called exact if there is an $m-1$ dimensional from η such that $f = \mathrm{d}\eta$. To know when a closed form is also exact Poincaré's lemma states that a closed from on a manifold M is exact if and only if the first de Rham co-homology group of M is trivial. In particular the closed form on M is exact if M is simply connected. This statement provides the mathematical reason why the AB-effect exists as we will see soon. But first consider displacements in the configuration space. The momentum operator is the generator of displacement in the configuration space: for the components ε^j of an infinitesimal displacement ε one gets (by using Taylor expansion and neglecting second-order terms in ε^j)

$$\langle x|\psi\rangle \to \langle x|e^{i\varepsilon^j p_j}|\psi\rangle = (1 + \varepsilon^j\partial_j + i\varepsilon^j\omega_j)\psi(x) \tag{8.27}$$

$$= \left[\psi + \varepsilon^j\partial_j\psi\right](1 + i\varepsilon^j\omega_j) \tag{8.28}$$

$$= \psi(x+\varepsilon)e^{i\varepsilon^j\omega_j}\,. \tag{8.29}$$

Since the p_j commute with each other this result can be generalized to finite displacements. Along a closed curve C ($C(0) = C(T)$) in M this yields

$$\langle x|\psi\rangle \to \langle x|\exp\left(i\oint_C \mathrm{d}x^j p_j\right)|\psi\rangle = \psi(x)\exp\left(i\oint_C \omega\right)\,, \tag{8.30}$$

i.e. in a displacement around a closed curve the wave function picks up a phase with phase angle corresponding to the path integral of the one-form ω over this closed curve.

Dependence on the Topology

Depending on the topology of the configuration space M this path integral vanishes or not. This shall be discussed now. First M is assumed to be trivial, in particular simply connected. Then ω is also exact and can be written as $\omega = \mathrm{d}\eta$. This implies that the path integral over a closed curve vanishes:

$$\oint_C \omega = \oint_C \mathrm{d}\eta = \eta(C(T)) - \eta(C(0)) = 0\,. \tag{8.31}$$

Alternatively the integral also equals zero by applying Stokes' theorem and the fact that ω is closed. The integration of the two-form is thereby over any surface S with boundary ∂S corresponding to the curve C:

$$\oint_C \omega = \int_S \mathrm{d}\omega = 0\,, \quad \text{where} \quad C = \partial S\,. \tag{8.32}$$

It is clear that there is no analogy of the first argumentation to the case where M has non-trivial topology, since then ω is no longer exact. Also the second argumentation fails when trying to apply it to non-trivial configuration spaces. The problem with a non trivial topology of M is that there does not need to be a surface S with $\partial S = C$. The details are explained on the following example.

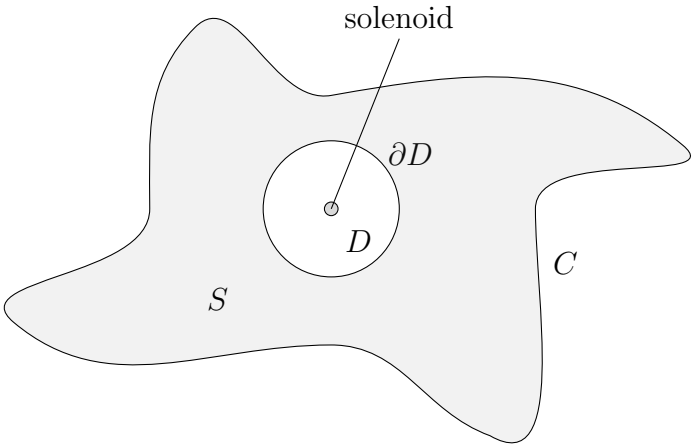

Figure 8.2: Curve C encircling D once with solenoid and surface S.

Non-trivial Topologies

Consider as the configuration space $\mathbb{R}^2 \setminus D$, a disk D removed from the plane. If C is a closed curve, which encircles D once then $\partial S = C + \partial D$ (see Fig. 8.3). Stokes' theorem now gives

$$\oint_C \omega = \int_S \mathrm{d}\omega + \oint_{\partial D} \omega = \oint_{\partial D} \omega \,. \tag{8.33}$$

Therefore the path integral corresponding to the phase angle does not vanish any more. In fact the original phase from (8.30) goes over into the phase

$$\exp\left(i \oint_{\partial D} \omega\right) . \tag{8.34}$$

This phase is called the fundamental phase. This discussion shows that the phase does not depend on the shape of the curve C but on how many times it encircles D. If C encircles D n_+ times counter-clockwise and n_- times clockwise then

$$\oint_C \omega = (n_+ - n_-) \oint_{\partial D} \omega \,. \tag{8.35}$$

The integer number $n_+ - n_-$ is called the winding number of the curve C. Because the original phase depends only on the winding number and the fundamental phase (i.e. topological properties) the phase is called a topological phase. For later considerations notice that there are two requirements for the topological phase

$$\exp\left(i \oint_C \omega\right) = \left[\exp\left(i \oint_{\partial D} \omega\right)\right]^{(n_+ - n_-)} \tag{8.36}$$

to be non-trivial. First the winding number has to be non-zero and second

$$\oint_{\partial D} \omega \neq 2\pi k \quad \text{for} \quad k \in \mathbb{Z} \,. \tag{8.37}$$

This will lead to the periodicity in the AB-effect in the example discussed in Section 8.5.

Dirac Phase

After this mathematical discussion consider again an electron. It shall travel on a closed loop in the configuration space, which is in the first discussed case all of $\mathbb{R}^3$. Let $\mathbf{B} = \nabla \times \mathbf{A}$ ($\mathbf{A} = (A^1, A^2, A^3)$) and define the differential form $A = A_j \mathrm{d}x^j$ (where $A_j = -A^j$) with $\mathrm{d}A = -\frac{1}{2}\varepsilon_{ijk}\mathbf{B}^i \mathrm{d}x^j \wedge \mathrm{d}x^k$. The

generalization of the momentum operator (generator for infinitesimal displacement) is $p_j \to \tilde{p_j} = p_j - \frac{e}{c}A^j$ therefore

$$\langle x|\tilde{p_j}|\psi\rangle = \left(-i\partial_j + \frac{e}{c}A_j + \tilde{\omega}_j(x)\right)\psi(x)\,. \tag{8.38}$$

Because the configuration space is $\mathbb{R}^3$ the one-form $\tilde{\omega}$ is exact. Furthermore the one-form A is defined only up to addition of an exact form: $A \to A' = A + \mathrm{d}f$. Thus $\tilde{\omega}$ can be absorbed into the definition of A. The displacement of the wave function of the electron is now

$$\psi \to \langle x| \exp\left(i \oint_C \mathrm{d}x^j \tilde{p_j}\right)|\psi\rangle = \exp\left(i\frac{e}{c}\oint_C A\right)\psi\,. \tag{8.39}$$

The phase

$$\exp\left(i\frac{e}{c}\oint_C A\right) \tag{8.40}$$

is called the Dirac phase or electromagnetic phase and depends on the path of the electron. For $\mathbf{B} \neq 0$ the phase depends on C and is a Berry phase (see 8.4). If $\mathbf{B} = 0$ A becomes a closed form and because the configuration space is $\mathbb{R}^3$ it is also exact and the phase vanishes.

Topological Phase

For $M \subset \mathbb{R}^3$ with a non-trivial topology the closeness of A does not imply the exactness. With the identification $\omega = \frac{e}{c}A$ the topological phase becomes the AB-phase

$$\exp\left(i\frac{e}{c}\oint_C A\right) \tag{8.41}$$

given by the winding number of the curve C and the fundamental topological phase as before. The fundamental phase in this case is (using again Stokes' theorem)

$$\exp\left(i\frac{e}{c}\int_D \mathrm{d}A\right) = \exp\left(-i\frac{e}{c}\int_D \mathbf{B}\cdot\mathrm{d}\mathbf{S}\right) = \exp\left(-i\frac{e}{c}\Phi_B\right)\,. \tag{8.42}$$

8.4 Geometrical Aspects

In this section the geometrical aspects of the AB-effect will be described following [6]. It will be shown that the AB-phase is a special case of Berry's geometrical phase. For this the definitions of the Mead-Berry connecting one-form and the Berry phase are needed. The motivations for these definitions as well as a central relation between these two will be derived at the beginning of the next chapter about the Berry phase. Here they are only stated and then used to show that the AB-phase is indeed a Berry phase. In Berry's theory the defining properties of a physical system are gathered in a set of parameters $R = (R_1, ..., R_m)$ corresponding to a point on a manifold M. The eigenvalue equation for a Hamiltonian $h = h(R)$ is

$$h(R)|n;R\rangle = E_n(R)|n;R\rangle\,. \tag{8.43}$$

Since the eigenstates $|n;R\rangle$ form a complete set any state vector $\psi(t)$ can be expanded in terms of the eigenstates. With the adiabatic approximation

$$|\psi(t)\rangle\langle\psi(t)| = |n;R(t)\rangle\langle|n;R(t)| \qquad \forall t\,, \tag{8.44}$$

i.e. a state remains an eigenstate of $h(R(t))$ at all times t with the same energy quantum number n, the expansion has only one term:

$$\psi(t) = c_n(t)|n;R(t)\rangle\,. \tag{8.45}$$

It can be shown that the coefficient is given by

$$c_n(t) = \exp\left(-i\int_0^t E_n(t')\mathrm{d}t'\right)\exp\left(i\gamma_n(t)\right)\,, \tag{8.46}$$

where

$$\exp\left(i\gamma_n(t)\right) = \exp\left(\int_0^t i\langle n;R(t')|\frac{\mathrm{d}}{\mathrm{d}t'}|n;R(t')\rangle\mathrm{d}t'\right)\,. \tag{8.47}$$

The Berry's phase angle is $\gamma_n(T)$ and $\exp\left(i\gamma_n(T)\right)$ is called the Berry phase factor. Also needed is the definition of the Mead-Berry connection one-form A^n_{MB}. It is defined as $A^n_{\mathrm{MB}} = A^n_{\mathrm{MB},i}\mathrm{d}R^i := i\langle n;R|\frac{\partial}{\partial R^i}|n;R\rangle\mathrm{d}R^i = i\langle n;R|\mathrm{d}|n;R\rangle$. The relation between the Berry phase angle and the Mead-Berry connection one-from is that

$$\gamma_n(T) = \int_{R(0)}^{R(T)} i\langle n;R(t)|\mathrm{d}|n;R(t)\rangle = \oint_C A^n_{\mathrm{MB}}\,. \tag{8.48}$$

This relation will be needed to demonstrate that the AB-phase is in fact a Berry phase.

AB-Phase as a Berry Phase

We return to the experimental setup of the magnetic AB-effect and want to show the correspondence to the Berry phase. To this end the wave function of an electron shall always stay within a box, which at time t is located at the position $\mathbf{R}(t)$. The box only moves in the region where there is no magnetic field, i.e. outside the solenoid. The eigenvalue equation in this case is

$$H\left(\mathbf{p}-\frac{e}{c}\mathbf{A},\mathbf{x}-\mathbf{R}\right)|n;\mathbf{R}\rangle = E_n(\mathbf{R})|n;\mathbf{R}\rangle\,, \tag{8.49}$$

with respect to a coordinate frame centred in the middle of the box. The eigenvectors of this Hamiltonian can be written as

$$\langle x|n;\mathbf{R}\rangle = \exp\left(i\frac{e}{c}\int_{\mathbf{R}}^{\mathbf{x}} A\right)\psi_n(\mathbf{x}-\mathbf{R})\,, \tag{8.50}$$

where the $\psi_n(\mathbf{x}-\mathbf{R})$ are the energy eigenvectors of the free Hamiltonian $H_0 = H_0\left(\mathbf{p},\mathbf{x}-\mathbf{R}\right)$ shifted into the box. The integration can be done over any path connection $\mathbf{R}$ and $\mathbf{x}$, which is not encircling or intersecting the region where the magnetic field is non-zero. The Mead-Berry connection one-form $A^n_{\mathrm{MB}} := i\langle n;R|\frac{\partial}{\partial R^i}|n;R\rangle\mathrm{d}R^i$ can be calculated to

$$A^n_{\mathrm{MB}} = i\int \mathrm{d}^3x\,\overline{\psi_n}(\mathbf{x}-\mathbf{R})\left[-\frac{ie}{c}A(\mathbf{R})\psi_n(\mathbf{x}-\mathbf{R}) + d\psi_n(\mathbf{x}-\mathbf{R})\right] = \frac{e}{c}A\,. \tag{8.51}$$

With the definition of the Berry phase angle $\gamma_n(T)$ and Eq. (8.48) the AB-phase turns out to be in fact a special case of Berry's phase:

$$\exp\left(i\gamma_n(T)\right) = \exp\left(\frac{ie}{c}\oint_C A\right)\,. \tag{8.52}$$

The integration hereby is along the path of the box. Notice that the right side doesn't depend on n, therefore the formula holds for any wave packet. We have thus shown that the AB-phase is a special case of the Berry phase where the dependence on the geometry is gone and only the topological properties play a role.

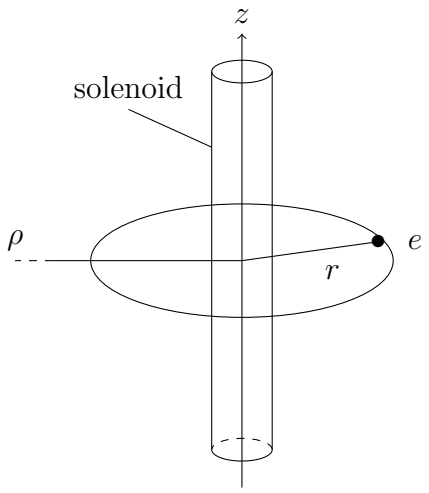

Figure 8.3: Setup of the theoretical bound state AB-effect. An electron circles around the solenoid at fixed distance r.

8.5 Periodicity of the AB-effect

In this section a special feature of the AB-effect, namely its periodicity, shall be demonstrated on an example. As seen before one of the requirements for the fundamental phase to be non-trivial is that

$$\oint_{\partial D} \omega \neq 2\pi k \qquad \forall k \in \mathbb{Z} \tag{8.53}$$

must hold, which gives the fundamental phase of the AB-effect the period $\Phi_0 = 2\pi\frac{c}{e}(\hbar)$. All observable phenomena concerning the AB-effect depend only on the flux Φ_B through the excluded region and are periodic with period Φ_0. As an example we look at the bound state AB-effect [4].

Bound State AB-Effect

An electron shall be bound on a circle with radius r around the solenoid with magnetic field B_z. We assume that the cylinder along which the magnetic flux goes in the negative z-direction has radius $\rho \gg r$ (see Fig. 8.5). In the Coulomb gauge where $\nabla A = 0$ one has in this case $A_\theta = \Phi/2\pi r$ and $A_\rho = A_z = 0$. The Hamiltonian of the electron is

$$H = \frac{1}{2mr^2}\left[L_z + r\frac{e}{c}A_\theta\right]^2 = \frac{1}{2mr^2}\left[L_z + \frac{e\Phi}{2\pi c}\right]^2 , \tag{8.54}$$

where L_z denotes the angular momentum. The bound state wave functions are

$$\psi_\ell(\theta) = \frac{1}{\sqrt{2\pi}}\exp\left(i\ell\theta\right) \tag{8.55}$$

with energies

$$E_\ell = \frac{1}{2mr^2}\left[\ell\hbar + \frac{e\Phi}{2\pi c}\right]^2 = \frac{\hbar^2}{2mr^2}\left[\ell + \frac{\Phi}{\Phi_0}\right]^2 \left(= \frac{K_z^2}{2mr^2}\right) \tag{8.56}$$

and a kinetic angular momentum $K_z = mr^2\dot{\theta}$ of

$$K_z = L_z + \frac{e\Phi}{2\pi c} = \hbar[\ell + \frac{\Phi}{\Phi_0}]\,. \tag{8.57}$$

This example clearly demonstrates, that the eigenvalues are periodic in Φ with period Φ_0: increasing Φ by Φ_0 maps the energy E_ℓ to $E_{\ell+1}$, which is nothing more than a relabelling of the states.

8.6 A versus B Interpretation

Probably the most important question concerning the AB-effect is how to interpret it. In their original paper Aharonov and Bohm proposed that the vector potential is the relevant quantity to describe nature instead of the magnetic field strength. They suggested to look at the electromagnetic potentials as physically real fields since they are needed to describe the AB-effect. The problem with this point of view is that the potentials are gauge variant. In fact, in modern field theories gauge invariance is criterion for a quantity to be considered physically real. This interpretation from Aharonov and Bohm is called the A interpretation since it is build on the vector potential $\mathbf{A}$.

But there is also another interpretation called the B interpretation. The letter B stands for the magnetic field strength $\mathbf{B}$. This interpretation is built on the possibility that quantum mechanics can be described solely in terms of the electromagnetic field strengths. Although the B interpretation would restore the interpretation of the vector potential as just a mathematical aid, it comes at a high price: to explain the AB-effect there would have to be a non-local interaction between ψ outside the solenoid and $\mathbf{B}$ inside it.

First the B interpretation will be described and discussed.

B Interpretation

The aim of the B interpretation is to formulate quantum mechanics solely in terms of field strengths in order to given an alternative interpretation to the A interpretation [7]. The starting point is to have a close look at the usual implementation of an electromagnetic field. This is done by making the replacement

$$\partial_\mu \to \partial_\mu - ieA_\mu \qquad (\mu = 0, 1, 2, 3)\,. \tag{8.58}$$

Here also the speed of light was set to one. As seen above the wave function ψ has to transform under the gauge transformation $A'_\mu = A_\mu + \partial_\mu \Lambda$ according to

$$\psi' = \exp(ie\Lambda)\,\psi \tag{8.59}$$

in order that the SE remains invariant. This means that the wave function is not gauge invariant. The idea therefore is to construct a wave function that is gauge invariant. To this end one takes four arbitrary single-valued differentiable functions $z^\mu(x, \xi)$ of x^μ and ξ, where $-\infty < \xi \leq 0$, which satisfy the boundary conditions

$$z^\mu(x, 0) = x^\mu \qquad \text{and} \qquad \lim_{\xi \to -\infty} z^\mu(x, \xi) = \text{spatial infinity}\,. \tag{8.60}$$

"Spatial infinity" stands for any limit sufficiently remote in a space-like direction from x^μ such that the electromagnetic field vanishes and the potential A_μ is small enough to be negligible. With this conditions Ψ defined as

$$\Psi \equiv \exp\left(-ie \int_{-\infty}^{0} A_\mu(z) \partial_\xi z^\mu \mathrm{d}\xi\right) \psi \tag{8.61}$$

is a gauge-invariant wave function. This follows with Eq. (8.59):

$$\Psi' = \exp\left(-ie \int_{-\infty}^{0} (A_\mu(z) + \partial_\mu \Lambda(z)) \partial_\xi z^\mu \mathrm{d}\xi\right) \psi' \tag{8.62}$$

$$= \Psi \exp\left(-ie \int_{-\infty}^{0} \partial_\mu \Lambda(z) \partial_\xi z^\mu \mathrm{d}\xi\right) \exp(ie\Lambda(x)) \tag{8.63}$$

and

$$\begin{aligned} -ie \int_{-\infty}^{0} \partial_\mu \Lambda(z) \partial_\xi z^\mu \mathrm{d}\xi &= -ie \int_{z(x,-\infty)}^{z(x,0)} \partial_\mu \Lambda(z) \mathrm{d}z^\mu \\ &= -ie\,[\Lambda(z(x,0)) - \Lambda(z(x,-\infty))] = -ie\Lambda(x) \end{aligned} \tag{8.64}$$

with the boundary conditions (8.60). Notice that Ψ differs from ψ only by a phase, thus it can equally well be used to compute probabilities in quantum mechanics. To use the wave function Ψ the replacement (8.58) in the SE from before has to be changed as well. By carrying out an integration by parts and using the boundary conditions (8.60) the operator replacement is changed to

$$\partial_\mu \to \partial_\mu - ie \int_{-\infty}^{0} F_{\nu\sigma}(z) \partial_\xi z^\nu \partial_\mu z^\sigma \mathrm{d}\xi \,, \tag{8.65}$$

where

$$F_{\mu\nu} \equiv \partial_\mu A_\nu - \partial_\nu A_\mu \tag{8.66}$$

is the electromagnetic field strength tensor. Equation (8.65) shows that it is indeed possible to formulate quantum mechanics in terms of the field strength only. However, the price is that the field strengths appear non-locally in line integrals. The calculations needed to explain the the interference effects are now integrals of the field strength over the surface swept out by the curves $z^\mu(x, \xi)$ as x makes a complete circuit of each multiply connected region. These surface integrals give the same results as the line integrals of the A interpretation. Also when the electromagnetic field is quantized it is possible to formulate quantum mechanics in terms of the field strength but this will not be discussed here.

Non-locality

Now the non-local aspects of the B interpretation are discussed. To do so first the term "local action" has to be specified: An interpretation shall meet the criterion of local action if all causes of an event propagate only via continuous physical processes [8]. In this sense the B interpretation clearly is non-local because the wave function vanishes wherever the magnetic field is non-zero. This produces a "gap" between these two which is not bridged by any continuous physical process.

A possible objection to this argument would be that a quantum wave function is never identically zero, i.e. there is always a small part of the wave function intersecting with the region where the magnetic field is non-zero. But if this would be the cause and the interaction took place at the overlap, then the clarity of the effect should depend on the quality of the shielding. However this is not experimentally observed.

A Interpretation

The problem with the A interpretation is that it suggests to consider a gauge variant field as a physically real field. This makes the A interpretation non-separable in the following sense: A physical system S is called separable if it is always possible to decompose it into subsystems with associated observable properties and to retrieve the properties of S from the properties of the subsystems [8]. An example of non-separability in this sense are entangled quantum systems. The state vector of such systems cannot always be factorized into a product of state vectors of the component systems. However the AB-effect is non-separable in a different sense. The explanation of the AB-effect requires knowledge about the underlying space as a whole. The shift in the interference pattern cannot be reduced to observable properties associated to specific spacetime regions since the vector potential has a gauge freedom which is not observable.

On the other hand it is clear that the A interpretation meets the above criterion for local action and also that in the B interpretation the AB-effect is a separable effect. The results of this section can be summarized as shown in Table 8.6.

Besides the A and B interpretation there is also a third one, the C interpretation. This interpretation is discussed in the next section.

	A	B
local action	yes	no
separability	no	yes

Table 8.1: Comparison between the A and B interpretation of the Aharonov-Bohm effect.

8.7 C Interpretation

This third interpretation, called the C interpretation, is based on integrals over closed curves, i.e. the gauge invariant quantities

$$S(C) = \exp\left(i \oint_C A\right) . \tag{8.67}$$

More precisely the AB-effect is the result of the coupling of a section of an associated bundle (the wave function) to a non-trivial flat connection (a non-pure gauge vector potential with zero magnetic field) in a trivial bundle (AB-bundle) with topologically non-trivial (non-simply-connected) base space (ordinary Euclidean space minus a tube). In the following this will be discussed in more detail following [9], [10] and [11].

The AB Bundle

First the AB bundle has to be introduced. Because the system has symmetry along the axis of the solenoid it can be idealised and the configuration space in the AB experiment is $\mathbb{R}^2$ minus a point, say the origin, which is denoted by $\mathbb{R}^{2*}$. This forms the base space of the bundle. The space $\mathbb{R}^{2*}$ is of the same homotopy type as the circle S^1. Since the classification of a principle bundle depends only on the homotopy type of the space one can consider S^1 instead of $\mathbb{R}^{2*}$. The structure group of the bundle is the gauge group of electromagnetism, the Lie group $U(1)$. Thus by Steenrod's theorem for the classification of principle bundles over spheres one has a one-to-one correspondence between the sets

$$\{\text{homotopy classes of } U(1) \text{ bundles over } S^1\} \overset{1to1}{\longleftrightarrow} \{\text{homotopy classes of maps } S^0 \to S^1\} . \tag{8.68}$$

Since the right set consists of only one point there is (up to equivalence) only one $U(1)$-bundle over S^1, namely the product bundle and the AB bundle ξ_{AB} is

$$\xi_{AB} : \underset{\text{fibre}}{U(1)} \longrightarrow \underset{\text{total space}}{\mathbb{R}^{2*} \times U(1)} \longrightarrow \underset{\text{base space}}{\mathbb{R}^{2*}} . \tag{8.69}$$

Gauge Group and Moduli Space of Flat Connections

As mentioned above the vector potential is manifested in this description of the AB-effect as a flat connection on ξ_{AB}. This subsection describes how the gauge group $\mathcal{G}$ acts on the space of flat connections on the AB bundle, denoted by $\mathcal{C}_0$ and discusses the moduli space $\mathcal{C}_0/\mathcal{G}$.

The gauge group of the AB-bundle is $\mathcal{G} = C^\infty(\mathbb{R}^{2*}, U(1))$, the space of smooth functions from the base space to the structure group. The Lie algebra to the structure group is $u(1) = i\mathbb{R}$. The space of flat connections on ξ_{AB} is given by

$$\mathcal{C}_0 = \{\mathcal{A} \in \Omega^1(\mathbb{R}^{2*}, u(1)) | \mathrm{d}\mathcal{A} = 0\} , \tag{8.70}$$

the closed $u(1)$-valued differential one-forms on $\mathbb{R}^{2*}$ and the gauge group $\mathcal{G}$ acts on $\mathcal{C}_0$ through

$$\mathcal{C}_0 \times \mathcal{G} \longrightarrow \mathcal{C}_0 , \tag{8.71}$$

$$(\mathcal{A}, f) \longmapsto \mathcal{A} + f^{-1}\mathrm{d}f . \tag{8.72}$$

Now to the moduli space $\mathcal{C}_0/\mathcal{G}$. In a more general case it can be shown that the moduli space of gauge equivalence classes of flat connections on a bundle $M \times G \to M$ is isomorphic to $H^1_{DR}(M; \mathfrak{g})/[M, G]$,

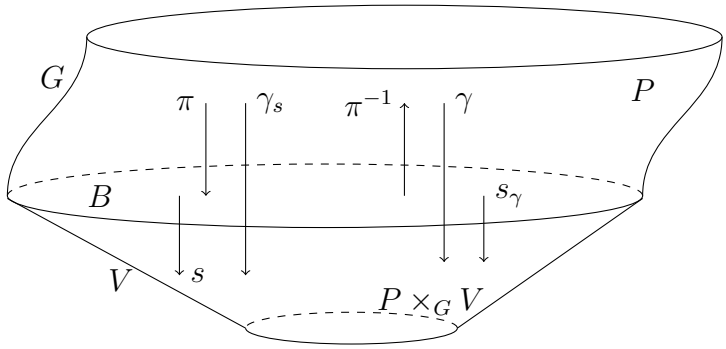

Figure 8.4: Schema of the induced maps between the principle G-bundle with total space P and the associated vector bundle with total space $P \times_G V$ and fibres V.

the quotient of the first de Rham co-homology group of M with coefficients in the Lie algebra $\mathfrak{g}$ of the structure group, modulo the group of smooth homotopy classes of maps from M to G. Applied to the case of the AB bundle this means that the moduli space $\mathcal{C}_0/\mathcal{G}$ is isomorphic to the circle S^1 with length 1.

A sketch on how to see this is the following. The moduli space is

$$\frac{\mathcal{C}_0}{\mathcal{G}} = \{[\mathcal{A}] | \mathcal{A} \in \mathcal{C}_0\}, \quad \text{where} \quad [\mathcal{A}] = \{\mathcal{A} + f^{-1}\mathrm{d}f | f \in \mathcal{G}\}. \tag{8.73}$$

It is the set of gauge equivalence classes of flat connections on ξ_{AB}. The first de Rham co-homology group of $\mathbb{R}^{2*}$ is $H^1_{DR}(\mathbb{R}^{2*}, i\mathbb{R}) = \{\lambda[\mathcal{A}_0]_{DR} | \lambda \in \mathbb{R}\} \cong H^1_{DR}(S^1, i\mathbb{R}) \cong \mathbb{R}$. Where the form

$$\mathcal{A}_0 = \underbrace{i\frac{x\mathrm{d}y - x\mathrm{d}x}{x^2+y^2}}_{\mathrm{d}\varphi} \in \mathcal{C}_0 \subset \Omega^1(\mathbb{R}^{2*}, i\mathbb{R}) \tag{8.74}$$

is closed but not exact and is the connection inducing the flux $-\Phi_0$ when multiplying by $-1/|e|$, since it is equal to $i\mathrm{d}\varphi$ where φ is the angle form (remember that $\Phi_0 = 2\pi c\hbar/|e|$ and set $c = \hbar = 1$). Because $\mathcal{A}_0$ generates the flux $-\Phi_0$ there is no AB-effect. The AB-effect with flux $\Phi = -\lambda\Phi_0$ is produced by the connection $\mathcal{A} = \lambda\mathcal{A}_0$.

To determine the moduli space $\mathcal{C}_0/\mathcal{G}$ one needs to find the smallest σ such that $(\lambda+\sigma)\mathcal{A}_0 \in [\lambda\mathcal{A}_0]$, which is equivalent to $\sigma\mathcal{A}_0 = f^{-1}\mathrm{d}f$ using (8.73). For $\varphi \neq 0$, $\mathcal{A}_0 = i\mathrm{d}\varphi$ and also $\tilde{f}^{-1}\mathrm{d}\tilde{f} = i\mathrm{d}\varphi$ for an $\tilde{f} \in \mathcal{G}$, thus $\sigma = 1$. This means that $(\lambda+1)\mathcal{A}_0 \sim \lambda\mathcal{A}_0$ and in particular $\mathcal{A}_0 \sim 0$. So the moduli space $\mathcal{C}_0/\mathcal{G}$, the space of flat connections on the AB bundle modulo the gauge group, is in fact isomorphic to the circle with length 1.

Covariant Derivative, Parallel Transport and Holonomy groups

The aim of this subsection is to calculate the holonomy group of each equivalence class of flat connections on ξ_{AB}. This can be done by the isomorphism found in the previous section. Every gauge equivalence class is identified with an element of S^1. Then the holonomy group of a connection of this class is the subgroup of S^1 generated by this element. As it will turn out, these subgroups are either finite cyclic groups or an infinite cyclic group which is dense in S^1.

It is useful to study first the more general case to see better what is going on. Let $\xi : G \to P \xrightarrow{\pi} B$ be a principle bundle with a matrix Lie group as the structure group ($\mathfrak{g}$ denotes the Lie algebra) and let $\xi_V : V \to P \times_G V \xrightarrow{\pi_V} B$ be the associated vector bundle. The set of equivariant functions from P to V (i.e. functions satisfying $\gamma(pg) = g^{-1}\gamma(p)$) is denoted by $\Gamma_{eq}(P, V)$ and the sections of ξ_V by $\Gamma(\xi_V)$. A section $s \in \Gamma(\xi_V)$ induces an equivariant function $\gamma_s \in \Gamma_{eq}(P, V)$ by the use of the local trivialization π. $s(\pi(p)) = [p, v] \in P \times_G V$ defines $\gamma_s(p) = v$. Also the reverse is possible, this time by π^{-1}. $s_\gamma(b) = [p, \gamma(p)]$, where $p \in \pi^{-1}(\{b\})$ see Fig. 8.7.

Every connection on ξ can be described by a smooth one-form $\omega \in \Omega^1(P, \mathfrak{g})$. The desired decomposition of the tangent space into horizontal and vertical subspaces, $(TP)_p = H_p \oplus V_p$, is thereby provided algebraically through $H_p = \ker(\omega_p)$. Let $X \in \Gamma(TB)$ and $X^\uparrow \in \Gamma(TP)$ it's horizontal lifting by ω, then the covariant derivative of the section s with respect to ω in the direction of X is defined by

$$\nabla^\omega_X s := s_{X^\uparrow(\gamma_s)} \,. \tag{8.75}$$

In local coordinates the expression is

$$\nabla^{\omega_U}_{X^\mu \partial/\partial x^\mu}(s^i e_i) = X^\mu D^j_{\mu i} s^i e_j \quad \text{with} \quad D^j_{\mu i} = \delta^j_i \frac{\partial}{\partial x^\mu} + \mathcal{A}^j_{\mu i} \,, \tag{8.76}$$

where x^μ ($\mu = 1, \ldots, \dim B$) are local coordinates on $U \subset B$, e_i ($i = 1, \ldots, \dim V$) is a basis of the local sections in $\pi_V^{-1}(U)$ and $D^j_{\mu i}$ is the usual local covariant derivative. And where $\mathcal{A}_U{}^j_i = \mathcal{A}^j_{\mu i} \mathrm{d}x^\mu = (\sigma^* \omega_U)^j_i$, ($\mathcal{A}^j_{\mu i}$ is determined by $\nabla^{\omega_U}_{\partial/\partial x^\mu} e_i = \mathcal{A}^j_{\mu i} e_j$) is the geometrical gauge potential in U. This is given by the pullback of the restricted one-form by $\sigma : U \to \pi^{-1}(U)$, $\sigma(b) = \phi^{-1}(b, 1)$, where $\phi : \pi^{-1}(U) \to U \times G$ is a local trivialization of ξ.

In an overlapping trivialization (8.76) is replaced by

$$\nabla^{\omega'_U}_{X^\mu \partial/\partial x^\mu}(s'^i e'_i) = X^\mu D^j_{\mu i} s'^i e'_j \quad \text{with} \quad D^j_{\mu i} = \delta^j_i \frac{\partial}{\partial x^\mu} + \mathcal{A}'^j_{\mu i} \,, \tag{8.77}$$

where the local potential transforms as

$$\mathcal{A}^j_{\mu l} = g^j_k \mathcal{A}'^k_{\mu i} g^{-1}{}^i_l + (\partial_\mu g^j_k) g^{-1}{}^k_l \tag{8.78}$$

in correspondence to (8.72) for G abelian.

For each smooth curve $c : [0, 1] \to B$ and each $p \in P_{c(0)} = \pi^{-1}(\{c(0)\})$ there is a unique curve $c^\uparrow$ in P such that $\dot{c}^\uparrow(t) \subset H_{c(t)}$ for all $t \in [0, 1]$. The curve $c^\uparrow$ is called the horizontal lifting of c by ω through p. With this horizontal lifting follows that for each connection ω and each curve c there exists a diffeomorphism $P^\omega_c : P_{c(0)} \to P_{c(1)}$ called parallel transport. If c is a loop $P^\omega_c \in \mathrm{Diff}(P_b)$ for $c(0) = c(1) = b$ and is called holonomy of ω at b along c. The space of loops in B with $c(0) = c(1) = b$ is denoted by $\Omega(B, b)$. It gives rise to a subset of the space of diffeomorphism from P_b to itself denoted by $\mathrm{Hol}^\omega_b \subset \mathrm{Diff}(P_b)$. Hol^ω_b is called the holonomy of ω at b.

Now let $c \in \Omega(B, b)$ and β be any lifting of c through $q \in P_b$. Then there is a unique curve $g : [0, 1] \to G$ in the structure group such that by acting on β it gives the horizontal lifting $c^\uparrow$ of c through $p = c^\uparrow(0)$, i.e. $c^\uparrow(t) = \beta(t) g(t)$. The function g satisfies the differential equation

$$\frac{\mathrm{d}}{\mathrm{d}t} g(t) = -\omega_{\beta(t)}(\dot{\beta}(t)) \,, \tag{8.79}$$

which has the solution

$$g(t) g(0)^{-1} = T \exp\left(\int_0^t \mathrm{d}\tau \omega_{\beta(\tau)}(\dot{\beta}(\tau)) \right) \,, \tag{8.80}$$

where $T\exp(\cdot)$ denotes the time-ordered exponential. From $q = p$ follows $g(0) = 1$ and for each $p \in P$ there is a subgroup of G with elements g' such that $c^\uparrow(1) = p g'$ for $c \in \Omega(B, \pi(p))$. This subgroup is called the holonomy of ω at p.

If c is contained in a subspace U of B with a local trivialization ϕ as above and $\beta(t) = \sigma(c(t))$, then one gets the local formula

$$c^\uparrow(t) = \phi^{-1}(c(t), 1) \left(T \exp\left(- \int_{c(0)}^{c(t)} \mathcal{A}_U \right) \right) g(0) \,, \tag{8.81}$$

which goes over into

$$c^\uparrow(t) = \left(c(t), T \exp\left(- \int_{c(0)}^{c(t)} \mathcal{A}_U \right) \right) \tag{8.82}$$

when ξ is a product bundle (by choosing $g(0) = 1$).

Now this general considerations shall be applied to the AB-effect where $V = \mathbb{C}$, $\xi = \xi_{AB}$ (which is in particular a product bundle) and the wave function $\psi = s$ is a global section on the associated vector bundle $\xi_{\mathbb{C}} : \mathbb{C} \to \mathbb{R}^{2*} \times \mathbb{C} \xrightarrow{\pi_{\mathbb{C}}} \mathbb{R}^{2*}$. The structure group and corresponding Lie algebra are as in the previous section, i.e. $G = U(1)$ and $\mathfrak{g} = u(1) = i\mathbb{R}$. Furthermore there is an action defined as follows: $U(1) \times \mathbb{C} \to \mathbb{C}$, $(e^{i\varphi}, z) \mapsto e^{i\varphi} z$. Now one has $\mathcal{A}_\mu = \mathcal{A}_{0\mu} = i a_\mu$ where a_μ is real, which follows from the discussion in the previous subsection. Thus the usual operator for covariant derivatives goes over into

$$D_\mu \psi = \left(\frac{\partial}{\partial x_\mu} + i a_\mu \right) \psi \,. \tag{8.83}$$

The physical gauge potential A_μ is then defined by $a_\mu = q A_\mu$ when ψ carries the charge q. Multiplying Eq. (8.83) by i gives the usual (physical) operator $i D_\mu \psi = (i\partial_\mu - q A_\mu)\psi$ which corresponds to the familiar operators $(i\nabla + q\mathbf{A})\psi$ and $(i\partial_t - q\varphi)\psi$. For $q = -|e|$ results $a_\mu = -(2\pi/\Phi_0) A_\mu$.

For a curve $c \in \Omega(\mathbb{R}^{2*}, (x_0, y_0))$, which turns n times around the solenoid, Eq. (8.82) yields

$$c^\uparrow = \left((x_0, y_0), \exp\left(-n \oint_c \mathcal{A} \right) \right) = \left((x_0, y_0), \exp\left(-in \oint_c a \right) \right) \tag{8.84}$$

$$= \left((x_0, y_0), \exp\left(-i|e| n \oint_c \mathbf{A} \cdot \mathrm{d}\mathbf{x} \right) \right) = \left((x_0, y_0), e^{-2\pi i n \Phi/\Phi_0} \right) . \tag{8.85}$$

Thus for $\Phi/\Phi_0 = \lambda \in [0, 1)$ the holonomy groups

$$\mathrm{Hol}^{\omega(\Phi)}_{((x_0,y_0),1)} = \left(e^{-2\pi i n (\Phi/\Phi_0)} \right)_{n \in \mathbb{Z}} = \begin{cases} \mathbb{Z}_q, & \lambda = p/q,\ p, q \in \mathbb{Z}, (p, q) = 1 \\ \mathbb{Z}, & \lambda \notin \mathbb{Q} \end{cases} \tag{8.86}$$

follow. For $\lambda \notin \mathbb{Q}$ the holonomy group is dense in $U(1)$, which can be seen by contradiction: for $e^{2\pi i n_1 \lambda} = e^{2\pi i n_2 \lambda}$ with $n_1 \neq n_2$ follows $e^{2\pi i (n_1 - n_2)\lambda} = 1$, thus $(n_1 - n_2)\lambda = m$ for some $m \in \mathbb{Z}$ and $\lambda \in \mathbb{Q}$.

This result means that there are two types of potentials. In the case where $\mathrm{Hol}^{\omega(\Phi)}_{((x_0,y_0),1)} = \mathbb{Z}_q$ there are potentials such that the holonomy is zero when going n times around a circle with center at the origin. For $\mathrm{Hol}^{\omega(\Phi)}_{((x_0,y_0),1)} = \mathbb{Z}$ there are potentials such that one can get arbitrary close to any given value of the holonomy phase when going a sufficiently large number of times around the circle.

This closes the discussion of the C interpretation. It is clear that in this interpretation there is like the A interpretation a local action between the gauge potential and the wave function but it is also non-separable. Now the comparison can be summarized as shown in Table 8.7.

	A	B	C
local action	yes	no	yes
separability	no	yes	no

Table 8.2: Comparison between the A, B and C interpretations of the Aharonov-Bohm effect.

8.8 Summary

The goal of this chapter was to explain the AB-effect and to look at it from different perspectives. We have seen that there are reasons to call the AB-phase a topological phase but also reasons to call it a geometrical phase. Also the role of the topology of the configuration space was discussed and an example of one of its properties, the periodicity of the AB-effect, was given. There would be many more interesting examples and many fields of applications where the AB-effect is also seen and used. But since the space was limited the focus was on the theoretical foundations, the origin and the fundamental questions of the effect, like the question about the interpretation which was discussed in the last two sections.

Even today, more then fifty years after its discovery, the AB-effect is subject of many research articles. There are still a lot of interesting and also deep questions to answer and since it is such a fundamental phenomena the AB-effect provides a good starting point when one tries to understand quantum mechanics better. In particular, it would be a ground-breaking achievement if the question of the interpretation, now still a matter of taste, could be solved.

Bibliography

[1] Y. Aharonov and D. Bohm, *Significance of Electromagnetic Potentials in the Quantum Theory*, Phys. Rev **115**, 485 (1959).

[2] Y. Aharonov and D. Bohm, *Further Considerations on Electromagnetic Potentials in the Quantum Theory*, Phys. Rev **123**, 1511 (1961).

[3] F. Schwabl, *Quantenmechanik*, chapter 7.4 and 7.5, Springer-Verlag, Berlin Heidelberg, 2007.

[4] M. Peshkin, *The Aharonov-Bohm effect Part one: Theory*, Lecture Notes in Physics Volume 340, 1-34, Springer-Verlag, Berlin Heidelber, 1989.

[5] P. Dirac, *The Principles of Quantum Mechanics*, The International Series of Monographs on Physics 27, Oxford University Press, 1958.

[6] A. Bohm *et al.*, *The Geometric Phase in Quantum Systems*, chapter 2 and 3, Springer-Verlag, Berlin Heidelberg, 2003.

[7] B. DeWitt, *Quantum Theory without Electromagnetic Potentials*, Phys. Rev **125**, 2189 (1962).

[8] T. Eynck, H. Lyre and N. von Rummell, *A versus B! Topological nonseparability and the Aharonov-Bohm effect*, Preprint, 2001.

[9] M. Socolovsky, *Aharonov-Bohm Effect*, Encyclopedia of Mathematical Physics Volume 1, 191-198, Elsevier Ltd., 2006.

[10] M. Aguilar and M. Socolovsky, *Aharonov-Bohm Effect, Flat Connections, and Green's Theorem*, Int. J. Theor. Phys. **41**, 839 (2002).

[11] Ch. Nash and S. Sen, *Topology and Geometry for Physicists*, Dover Publications, New York, 2011.

Chapter 9

Berry Phase

Author: Hansueli Jud
Supervisor: Jonathan Skowera

Berry's phase is a geometric, gauge invariant property of a quantum mechanical system which appears if an eigenstate is transported slowly around a closed circuit C by varying its parameter-dependent Hamiltonian. The eigenstate can acquire a dynamical phase as well as a Berry phase. An explicit formula for the Berry phase is derived from the spectrum and eigenstates of the Hamiltonian in the limit of the adiabatic approximation. Additionally, the generalization to non-adiabatic evolutions using the theory of principal fibre bundles is briefly discussed. The concepts are then applied to an example of a spinning quantum system in a magnetic field where nuclear magnetic resonance and the Berry phase are used to implement a fault tolerant quantum logic gate.

9.1 Introduction

Within the following pages, the basic formalism describing the Berry phase is discussed including some basic theory which is needed. It will turn out that the Berry phase is a purely geometric object not depending on a specific gauge. The derivations are based on the adiabatic assumption, which may be dropped leading to a more general definition. Furthermore, the Berry phase for a spin particle in an external magnetic field is calculated. The results obtained there are then used to get an idea of how one can implement quantum logic gates using nuclear magnetic resonance. In case of a controlled phase shift gate, experimental results are in high agreement with the theoretic expectations.
Historically, the geometric phase had been ignored for almost half a century, considering it as an unimportant property. It was argued by Fock that such a phase could be set to unity by redefining the phase of the initial wave function [1]. However, Fock's argument did restrict to non-cyclic evolutions only and it will be shown that in general Berry's phase can not be transformed away. Initially the phase has only been calculated in the regime of the adiabatic assumption, however, it took only a year for generalizations to non-adiabatic evolutions to pop up which has also been extended to a "non-abelian" Berry phase.

In the following section the Berry phase in the adiabatic limit is described which is mainly based on [2] and Berry's original paper [3].

9.2 Quantum mechanical background

Consider a non isolated quantum system with underlying Hamiltonian $H(R)$ where the changing environment is described by the varying parameter $R = R(t)$. Furthermore, let the according Hilbert space $\mathcal{H}$ be separable and denote the eigenstates of H by $|n; R\rangle$ where n is the quantum number.

Every change of the environment traces out a curve $\mathbf{C} : [0, T] \to M$ where M is a smooth manifold. The parameter space is described by this manifold which consists of the points labeled by the parameter R. Geometrically the parameter space may be a complicated manifold consisting of several coordinate patches, however the Hamiltonian operator is set to be a "smooth" and single-valued function of $R \in M$, where smoothness is meant in the sense that the Hamiltonian's eigenvalues and eigenvectors are smooth functions of R.

The evolution of a state vector $\psi(t)$ is described by the Schrödinger equation

$$i\frac{d\psi(t)}{dt} = H(R)\psi(t). \tag{9.1}$$

The evolution of density operators is described by the von Neumann equation

$$\frac{d\rho(t)}{dt} = [H(R), \rho(t)]. \tag{9.2}$$

Additionally postulate that the Hilbert space does contain the solutions of the Schrödinger equation for all $R \in M$ and thus also for all times. Therefore there exists a single Hilbert space for all values of R and for each one, it is possible to choose an orthonormal basis of eigenvectors of the parameter-dependent Hamiltonian

$$H(R)\,|n; R\rangle = E_n(R)\,|n; R\rangle\,, \tag{9.3}$$
$$\langle m; R|\,|n; R\rangle = \delta_{nm}. \tag{9.4}$$

9.3 Adiabatic Approximation

Let the system evolve around a closed path $R(t)$ in parameter space between times $t = 0$, such that $R(T) = R(0)$ for $t = T$ with Hamiltonian $H(R(t))$. Consider now the situation where the physical system does not jump from one eigenstate to another due to the interaction with the environment, i.e., when the state remains an eigenstate of $H(R(t))$ with the same quantum number n for all times t. This is also called the adiabatic approximation where a state $\rho = |\psi(t)\rangle\langle\psi(t)|$ evolves such that at all times t

$$|\psi(t)\rangle\langle\psi(t)| \overset{adiabatic}{=} |n; R(t)\rangle\langle n; R(t)|\,. \tag{9.5}$$

For the adiabatic approximation to apply T must be large. This time development, also called *adiabatic time development*, can only be an approximation, unless the evolving state does not change in time.

To derive the condition of validity of the adiabatic approximation express the evolving state vector $\psi(t)$ in the basis $|n; R(t)\rangle$,

$$\psi(t) = \sum_m c_m(t)\,|m; R(t)\rangle \tag{9.6}$$

Choose now the initial condition for solving the Schrödinger equation such that at $t = 0$ the state is an eigenstate of $H(R(0))$ with eigenvalue $E_n(R(0))$, i.e.,

$$|\psi(0)\rangle \langle\psi(0)| = |n; R(0)\rangle \langle n; R(0)|, \tag{9.7}$$

or $\psi(0) = |n; R(0)\rangle$, where the second form follows after fixing an arbitrary phase factor to unity. The adiabatic approximation is a valid approximation to the initial condition given by 9.7 if and only if all the coefficients $c_m(t)$ in 9.6 vanish except $c_n(t)$, or written as an equation:

$$\psi(t) \overset{adiabatic}{=} c_n(t) |n; R(t)\rangle, \tag{9.8}$$

where $c_n(0) = 1$ according to the initial condition.
Substituting the expression 9.8 into the Schrödinger equation 9.1 and using 9.3 the following expression may be obtained:

$$\left(\frac{d}{dt}c_n(t) + iE_n(R(t))c_n(t)\right) |n; R(t)\rangle \overset{adiabatic}{=} -c_n(t)\frac{d}{dt} |n; R(t)\rangle. \tag{9.9}$$

Applying $\langle m; R(t)|$ to that expression yields in view of orthogonality for $m \neq n$

$$\langle m; R(t)| \frac{d}{dt} |n; R(t)\rangle \overset{adiabatic}{=} 0 \quad \forall m \neq n \tag{9.10}$$

Which turns out is a necessary and sufficient condition for the validity of the adiabatic approximation. It is useful to express the left-hand of this equation in terms of the matrix elements of the time derivative of the Hamiltonian. The expression can be derived by taking the differential (exterior derivative) of both sides of 9.3,

$$dH(R) |n; R\rangle + H(R)d |n; R\rangle = dE_n(R) |n; R\rangle + E_n(R)d |n; R\rangle. \tag{9.11}$$

Applying $\langle m, R|$ to both sides of this equation for $m \neq n$ yields

$$\langle m; R| dH(R) |n; R\rangle + E_m(R) \langle m; R| d |n; R\rangle = E_n(R) \langle m; R| d |n; R\rangle, \tag{9.12}$$

using 9.3. Rewrite the expression

$$\langle m; R| \mathrm{d} |n; R\rangle = \frac{\langle m; R| \mathrm{d}H(R) |n; R\rangle}{E_n(R) - E_m(R)}, \quad \forall m \neq n. \tag{9.13}$$

Choosing an environmental process, $R = R(t)$, the differentials can be replaced with ordinary time-derivatives by dividing both sides of the equation by dt

$$\langle m; R(t)| \frac{d}{dt} |n; R(t)\rangle = \frac{\langle m; R| \frac{d}{dt}H(R) |n; R\rangle}{E_n(R) - E_m(R)}, \tag{9.14}$$

for all $m \neq n$. The adiabatic approximation is thus valid if and only if the right-side of this equation can be neglected. Due to the appearance of the time derivative in this equation, the approximation is called adiabatic. Notice that the left-hand side of 9.14 has the dimension of frequency. Therefore to decide if the adiabatic approximation is applicable an intrinsic frequency (or Energy) scale for the quantum system must be known.

9.4 Calculation of Berry's Adiabatic Phase

In the following it will be shown that for a periodic Hamiltonian $H(t) = H(R(t))$, an adiabatically evolving state $W(t) = |\psi(t)\rangle \langle\psi(t)|$ with the initial condition $W(0) = |n; R(0)\rangle \langle n; R(0)|$ traverses a closed path C in the parameter space. However this does in general not apply to the normalized state vector $\psi(t)$, fulfilling the Schrödinger equation 9.1. In general the path

$$\mathbf{C} : [0, T] \ni t \to \psi(t) \in \mathcal{H}, \tag{9.15}$$

with $\langle\psi(t)| |\psi(t)\rangle = 1$, is not closed in $\mathcal{H}$, but satisfies

$$\mathbf{C}(T) = \psi(T) = e^{-i\alpha_\psi}\psi(0). \tag{9.16}$$

As will be shown the phase factor takes the form

$$e^{-i\alpha_\psi} = e^{-i\int_0^t E_n(t')\mathrm{d}t'} e^{i\gamma_n(t)} \tag{9.17}$$

where the first phase factor is called the dynamical phase factor and $\gamma_n(t)$ describes the Berry phase acquired.

In the regime of the adiabatic approximation, express the evolving state vector according to 9.8, where the coefficients c_n satisfy 9.9. Applying $\langle n; R(t)|$ to both sides of 9.9 and using orthogonality the following explicit formula for c_n can be obtained ($E_n(t) := E_n(R(t))$)

$$\left(\frac{d}{dt}c_n(t) + iE_n(R(t))c_n(t)\right)\delta_{nn} = -c_n(t)\langle n; R(t)| \frac{d}{dt}|n; R(t)\rangle, \tag{9.18}$$

and after rearranging

$$\frac{d}{dt}c_n(t) = -c_n(t)(iE_n(t) + \langle n; R(t)| \frac{d}{dt}|n; R(t)\rangle). \tag{9.19}$$

This equation can be integrated obtaining

$$\int_{c_n(0)}^{c_n(t)} \frac{dc_n}{c_n} = -i\int_0^t E_n(t')dt' - \int_0^t \langle n; R(t')| \frac{d}{dt'}|n; R(t')dt'\rangle. \tag{9.20}$$

Using that $c_n(0) = 1$ (initial condition), this yields

$$c_n(t) = e^{-i\int_0^t E_n(t')dt'} e^{i\gamma_n(t)}, \tag{9.21}$$

where

$$e^{i\gamma_n(t)} := e^{i\int_0^t i\langle n;R(t')|\frac{d}{dt'}|n;R(t')\rangle dt'}. \tag{9.22}$$

Since $\psi(t)$ is obtained from $\psi(0)$ by a unitary time development it is a normalized vector. Additionally the coefficient $c_n(t)$ of 9.8 is a phase factor and therefore $\gamma_n(t)$ is a real phase angle defined up to an integer multiple of 2π.

It is important to notice that the phase angle $\gamma_n(t)$ does not depend on the time dependence of the integrand in 9.22. It can in fact be directly defined in terms of a (path) integral over a vector valued function $\mathbf{A}_i^n(R) := i \langle n; R| \nabla |n; R\rangle$

$$\gamma_n(t) = \int_0^t i \langle n; R(t')| \frac{d}{dt'} |n; R(t')\rangle \, \mathrm{d}t' = \int_{R(0)}^{R(t)} i \langle n; R| \frac{\partial}{\partial R^i} |n; R\rangle \, \mathrm{d}R^i = \int_{R(0)}^{R(t)} \mathbf{A}_i^n(R) dR^i. \quad (9.23)$$

Where this vector-valued function is called the *Mead-Berry vector potential*. The equation 9.23 indicates that, the Mead-Berry vector potential $\mathbf{A}^n$ is only defined with the use of the single-valued basis eigenvectors $|n; R\rangle$ of the Hamiltonian $H(R)$. However a smooth single-valued basis may in general not be found on the whole parameter space M, but only on its patches. Therefore the same holds also for $\mathbf{A}^n$ and it is assumed here that the curve C lies in a single patch over which a smooth single-valued basis exists.

Expressed as a (local) differential one-form defined on the same patch as $|n; R\rangle$, the Mead-Berry vector potential reads

$$A^n = A_i^n dR^i := i \langle n; R| \frac{\partial}{\partial R^i} |n; R\rangle \, dR^i = i \langle n; R| \, d \, |n; R\rangle \, . \quad (9.24)$$

The differentials dR^i are the basis differential one-forms (covariant vectors, $i = 1, 2, ..., \mathcal{M} = dim(M)$) and "$d$" is the exterior derivative operator. This one-form is also called the **Mead-Berry connection one-form** and can be used to yield the following expression for the phase angle $\gamma_n(t)$

$$\gamma_n(t) = \int_{R(0)}^{R(t)} i \langle n; R(t)| \, d \, |n; R(t)\rangle = \int_C A^n, \quad (9.25)$$

where C is the curve in the parameter space M.

9.4.1 Gauge Transformations and Mead-Berry Curvature Two-Form

A new set of eigenvectors $|n; R\rangle'$ of the Hamiltonian H can be defined by performing the *phase transformations*

$$|n; R\rangle \to |n; R\rangle' = e^{i\zeta_n(R)} |n; R\rangle \, , \quad (9.26)$$

where $\zeta_n(R)$ are arbitrary real phase angles. *Gauge transformations* are defined by restricting to phase transformation for which the phase factors $e^{i\zeta_n(R(t))}$ are single-valued functions.

In general in going from one patch $O_1 \subset M$ of the parameter space to a neighboring patch $O_2 \subset M$ with a different parametrization, the eigenvectors of $H(R)$ in the overlap region $O_1 \cap O_2$ are related by phase transformations of the form 9.26.

Using the definition of the Mead-Berry vector potential 9.23 the behavior under a gauge transformation is given by

$$\begin{aligned} \mathbf{A}^n(R) \to \mathbf{A'}^n(R) &= i \langle n; R|' (\nabla |n; R\rangle') \\ &= i \langle n; R| \, e^{-i\zeta_n(R)} (\nabla e^{i\zeta_n(R)} |n; R\rangle) \\ &= i \langle n; R| \, \nabla |n; R\rangle + i e^{-i\zeta_n(R)} (\nabla e^{i\zeta_n(R)}) \\ &= \mathbf{A}^n(R) - \nabla \zeta_n(R). \end{aligned} \quad (9.27)$$

In case of the connection one-form this may be written as

$$A^n(R) \to A'^n(R) = A(R) - \mathrm{d}\zeta_n(R). \tag{9.28}$$

The phase angle $\gamma_n(t)$ transforms under a gauge transformation according to

$$\begin{aligned}\gamma_n(t) \to \gamma'_n(t) &= \int_{R(0)}^{R(t)} \mathbf{A}'^n(R) dR \\ &= \gamma_n(t) - \zeta_n(R(t)) + \zeta_n(R(0)).\end{aligned} \tag{9.29}$$

Using gauge transformations it is possible to transform away $\gamma_n(t)$ if it is assumed that $\zeta_n(R(t))$ is arbitrary, which will be discussed in the following. Inserting 9.21 into 9.8 yields an expression for $\psi(t)$

$$\psi(t) \overset{adiabatic}{=} e^{\frac{1}{i}\int_0^t E_n(t')dt'} e^{i\gamma_n(t)} \left|n; R(t)\right\rangle . \tag{9.30}$$

Considering phase transformations the basis eigenvectors $|n; R(t)\rangle$ are only determined up to a phase factor. Therefore, the additional phase factor may be transformed away, and in fact it may be set to one as was shown by Fock. Indeed the fact that you could transform away this additional phase was universally accepted for half a century and in turn the Berry phase was ignored. However Fock did not consider the case of cyclic changes and it will be shown that in general it is not possible to eliminate γ_n.

Doing the calculations that led to 9.30 but using $|n; R\rangle'$ instead of $|n; R\rangle$ yields the same expression with the primed quantities on the right-hand side. Using a phase transformation for the primed quantities the following may be obtained

$$e^{i\gamma'_n(t)} \left|n; R(t)\right\rangle' = e^{i\gamma'_n(t)} e^{i\zeta_n(R(t))} \left|n; R(t)\right\rangle . \tag{9.31}$$

In the case of $\zeta_n(R(t))$ being a single-valued function modulo 2π, it can be chosen such that the phase factor $e^{i\gamma'_n(t)} e^{i\zeta_n(R(t))}$ becomes unity resulting in an expression for $\psi(t)$

$$\psi(t) = e^{\int_0^t E_n(t')dt'} \left|n; R(t)\right\rangle . \tag{9.32}$$

Which also fulfills the initial condition and since $|n; R\rangle'$ is as valid a basis eigenvector as $|n; R\rangle$, the time development of the state vector involves the dynamical phase factor only, which is Fock's result.

However, the above argument holds only if $\zeta_n(R(t))$ can be chosen arbitrarily. If instead the environmental parameters return to their original values after some period T, as described by a closed path C, $\zeta_n(R(t))$ may not be chosen freely to remove $\gamma_n(t)$. Indeed for $R(T) = R(0)$ the single-valuedness of $e^{i\zeta_n(R)}$ implies

$$e^{i\zeta_n(R(T))} = e^{i\zeta_n(R(0))}, \tag{9.33}$$

or equivalently $\zeta_n(R(T)) = \zeta_n(R(0)) + 2\pi\times$integer. Therefore using 9.29

$$\begin{aligned}\gamma_n(T) \to \gamma'_n(T) :&= \oint_C \mathbf{A}_i'^n(R) dR^i = \oint_C \mathbf{A}_i^n(R) dR^i - 2\pi \times \text{integer} \\ &= \gamma_n(T) - 2\pi \times \text{integer}.\end{aligned} \tag{9.34}$$

As it can be seen in this expression $\gamma_n(T)$ (defined only modulo 2π) is invariant under gauge transformations and cannot be removed. Thus for a closed path the extra phase phase factor cannot be transformed away, however this does not imply that $\gamma_n(C)$ can not be zero. In this cases the vector potential $\mathbf{A}^n(R)$ (and the connection one-form $A^n(R)$) need not to be zero but are "trivial", which means that for a well-defined function $\zeta(R)$, the vector potential (and the connection one-form) are given as

$$\mathbf{A}^n(R) = \nabla\zeta_(R) = -ie^{-i\zeta(R)}\nabla e^{i\zeta(R)}, \tag{9.35}$$
$$A^n(R) = d\zeta(R). \tag{9.36}$$

For such a $\zeta(R)$ the Berry phase angle can be transformed to zero by gauge transformation with phase factor $e^{-i\zeta(R)}$. Note that the curve C is still required to lie on a single patch of the parameter space. Otherwise 9.35 may only be satisfied on individual patches of the parameter space. If C lies not in one patch, the corresponding Berry phase may still be non trivial.

The Mead-Berry vector potential can be seen as an analogy to the vector potential of electromagnetism by noting that it satisfies the same gauge (phase) transformation rule (c.f. 9.27). Furthermore the set of phase factors $e^{i\zeta_n(R)}$ form the group $U(1)$ and thus this gives a gauge theory with gauge (symmetry) group $U(1)$ and gauge potential $\mathbf{A}^n(R)$.

Although $\mathbf{A}^n(R)$ is not an invariant quantity with respect to gauge transformations, the Berry phase is as shown above. However, this can also be seen by referring back to the analogy with electrodynamics. Indeed if the parameter space is three dimensional and hence the parameter R is a three-dimensional vector, there is a complete analogy. Nevertheless the physical interpretation of the quantities associated with the Berry phase is different: The gauge potential is defined in terms of the eigenvectors of the Hamiltonian and has nothing to do with electrodynamics. Considering an $\mathcal{M}$-dimensional parameter space, the Berry connection one-form together with the gauge transformations define a $U(1)$ gauge theory over an $\mathcal{M}$-dimensional parameter space.

To get a gauge invariant quantity, in analogy with electrodynamics, a gauge field strength tensor F^n may be defined. Its components are given by

$$F^n_{ij} := \frac{\partial}{\partial R^i}A^n_j - \frac{\partial}{\partial R^j}A^n_i, \quad i,j = 1,2,...,\mathcal{M}. \tag{9.37}$$

F^n defines an antisymmetric covariant tensor field of rank two, i.e., it is a differential two-form

$$F^n = \frac{1}{2}F^n_{ij}dR^i \wedge dR^j = \frac{\partial A^n_j}{\partial R^i}dR^i \wedge dR^j = dA^n. \tag{9.38}$$

Where the antisymmetry of the wedge product $\wedge$ has been used, and dA^n stands for the exterior derivative of the Mead-Berry connection one-form A^n. The two-form F^n associated to A^n is also called the *Mead-Berry curvature two-form* and given by

$$F^n = d(i\langle n;R|\, d\,|n;R\rangle) = i(d\langle n;R|) \wedge d\,|n;R\rangle\,, \tag{9.39}$$

using $d^2 = 0$. It is important to notice that the curvature two-form is indeed a gauge-invariant quantity. This follows directly from 9.28, 9.38 and again $d^2 = 0$,

$$F^n \to F'^n = dA'^n = dA^n - d^2\zeta = dA^n = F^n. \tag{9.40}$$

There are two important consequences of the gauge invariance of F^n:

1. F^n is a globally defined object over M.

2. F^n may be used to yield a direct formula for the Berry phase.

9.4.2 Derivation of a Globally Defined Formula for the Berry Phase

To get a globally defined formula, assume that the curve C bounds a surface $S \subset M$, and use Stoke's theorem to convert the loop integral into a surface integral over S (which can be arbitrarily chosen as long as it is bounded by the closed curve C

$$\gamma_n(C) = \oint_C A^n = \int_S dA^n = \int_S F^n \quad \mathrm{mod} 2\pi. \tag{9.41}$$

In the following the goal is to use this expression to investigate what happens when two energy levels become degenerate for some values of R. To achieve that rewrite F^n in terms of the eigenvalues $E_n(R)$ using the completeness of the basis $|m;R\rangle$ (i.e. $1 = \sum_m |m;R\rangle \langle m;R|$).

This gives for F^n

$$\begin{aligned} F^n &= d(i \langle n : R| \, d \, |n;R\rangle) = d(i \sum_m \langle n;R| \, |m;R\rangle \langle m;R| \, d \, |n;R\rangle) \\ &= i \sum_m [(d \langle n;R|) \, |m;R\rangle] \wedge [\langle m;R| \, d \, |n;R\rangle] = -i \sum_m [\langle n;R| \, d \, |m;R\rangle] \wedge [\langle m;R| \, d \, |n;R\rangle] \\ &= i \sum_{m \neq n} [\langle m;R| \, d \, |n;R\rangle] \wedge [\langle n;R| \, d \, |m;R\rangle], \end{aligned} \tag{9.42}$$

using the linearity of the exterior derivative in the third equality, orthonormality of the basis in the fourth (i.e. $\delta_{nm} = d(\langle n;R| \, |m;R\rangle = (d \langle n;R|) \, |m;R\rangle + \langle n;R| \, d \, |m;R\rangle)$, and the antisymmetry of the wedge product in the last. Substitute now 9.13 into the right hand side of this expression to show the dependence of F^n on the difference of eigenvalues,

$$F^n = i \sum_{m \neq n} \frac{\langle n;R| \, [\mathrm{d}H(R) \, |m;R\rangle \wedge \langle m;R| \, [\mathrm{d}H(R) \, |n;R\rangle}{[E_n(R) - E_m(R)]^2}. \tag{9.43}$$

The Berry phase is then given by this quantity via

$$\gamma_n(C) = \int_S F^n \quad \mathrm{mod} 2\pi. \tag{9.44}$$

The two expressions given above are the key results to keep in mind considering the approach which also Berry used in his original paper. Since the dependence on $d \, |n;R\rangle$ has been eliminated, the phase relations between eigenstates with different parameters are now immaterial, and it is therefore no longer necessary to choose single-valued basis vectors. Since by looking at expression 9.43 it can therefore be seen that it does not depend on the phase factor of the basis vectors it can be defined globally on M. This implies that the formula given above can be used to compute the Berry phase even for the cases where C does not lie in region where there exist globally smooth single-valued $|n;R\rangle$. Additionally the energy denominators in 9.43 show that if the curve C lies close to a point $\mathbf{R}^*$ in parameter space at which there is a degeneracy, $F^n(\mathbf{R})$ and hence $\gamma_n(C)$ is dominated by the terms n corresponding to the other states involved. Consider the most common situation, where the degeneracy involves only two states and expand the Hamiltonian $H(\mathbf{R})$ near $\mathbf{R}^*$ to first order in $\mathbf{R} - \mathbf{R}^*$[3]. Additionally the corresponding energy values and $\mathbf{R}^*$ may be set to zero without essential loss of generality. Then $H(\mathbf{R})$ can be represented by a 2×2 Hermitian matrix depending on three

parameters. The eigenvalues of this Matrix are then just given by $\pm\frac{1}{2}$ times the absolute value of $\mathbf{R}$. Therefore the degeneracy is an isolated point at which all three parameters vanish.

From the formulas derived above it can be seen that the Berry phase angle $\gamma_n(C)$ is independent of how the closed loop C is traversed if the condition for the validity of the adiabatic approximation is satisfied. Therefore the Berry phase does not depend on the details of the dynamics of the quantum system and is solely dependent on the path C. That is the reason why the Berry phase is sometimes also called the geometric phase.

9.5 Parallel Transport

The Berry phase can also be considered from a more geometrical point of view by noting that it is produced by the non-trivial geometry of the space of physical states. It is convenient to first obtain a law for the parallel transport of a vector over the surface of a sphere and express it in a form which is generalizable to quantum mechanics. The following section on parallel transport on a sphere and quantum parallel transport follow mainly [4] and [5].

9.5.1 Parallel Transport on a Sphere

Imagine a beetle moving a unit vector $\mathbf{v}$ along a closed path C on a sphere. The condition for parallel transport now imposes the constraint that $\mathbf{v}(t)$ must always lie in the local tangent plane, i.e., $\mathbf{v}\cdot\mathbf{e}_3 = 0$ where $\mathbf{e}_3$ is defined as the local normal vector (c.f. Fig. 9.1). Along the path parallel transport imposes the further restriction that the direction of $\mathbf{v}$ is perturbed minimally which means that it should never rotate about $\mathbf{e}_3$, i.e. any changes $d\mathbf{v}$ must be parallel to $\pm\mathbf{e}_3$, or equivalently

$$\mathbf{e}_3 \times d\mathbf{v} = 0. \tag{9.45}$$

Let C now be a circle on the sphere then the tangent planes are part of a cone and by flattening the cone, it can be seen that the term parallel transport does indeed make sense considering the no-rotation condition. In this "flattened" space, $\mathbf{v}$ is always fixed in direction. However going back to the view of the beetle, $\mathbf{v}$ does in general not return to its initial direction by completing the path. Instead, it makes a "geometric" path dependent angle $\alpha(C)$. This angle is sometimes also called holonomy.

Let $\mathbf{e}_1(t)$ and $\mathbf{e}_2(t)$ define a local coordinate frame, where t parametrizes C (on the sphere, these are usually the unit vectors along the latitude and longitude). This coordinate frame is needed to obtain an expression for α. Now expand $\mathbf{v}(t)$ at each point $\mathbf{R}(t)$

$$\mathbf{v}(t) = \cos\alpha(t)\mathbf{e}_1(t) + \sin\alpha(t)\mathbf{e}_2(t). \tag{9.46}$$

Moving along C, the triad $[\mathbf{v}, \mathbf{w}, \mathbf{e}_3]$ (where $\mathbf{w} = \mathbf{e}_3 \times \mathbf{v}$) rotates about the normal by $\alpha(t)$, relative to the local frame $[\mathbf{e}_1, \mathbf{e}_2, \mathbf{e}_3]$. Note that equation 9.45 implies that

$$\mathbf{e}_3 \times d\mathbf{w} = 0, \tag{9.47}$$

since $d(\mathbf{e}_3 \times \mathbf{v}) = d\mathbf{e}_3 \times \mathbf{v} + \mathbf{e}_3 \times d\mathbf{v}$. Using 9.46 in 9.45 with the normalization conditions $\mathbf{e}_1 \cdot d\mathbf{e}_1 = 0$, $\mathbf{e}_2 \cdot d\mathbf{e}_2 = 0$, and the fact that $\mathbf{v}(t)\cdot\mathbf{e}_1 = \sin\alpha$ (since $\mathbf{v}(t)$ and $\mathbf{e}_1(t)$ are unit vectors), the following expression may be obtained by multiplying by $\mathbf{e}_1(t)$

$$d\alpha = \mathbf{e}_1 \cdot d\mathbf{e}_2 \equiv \omega_{21} \tag{9.48}$$

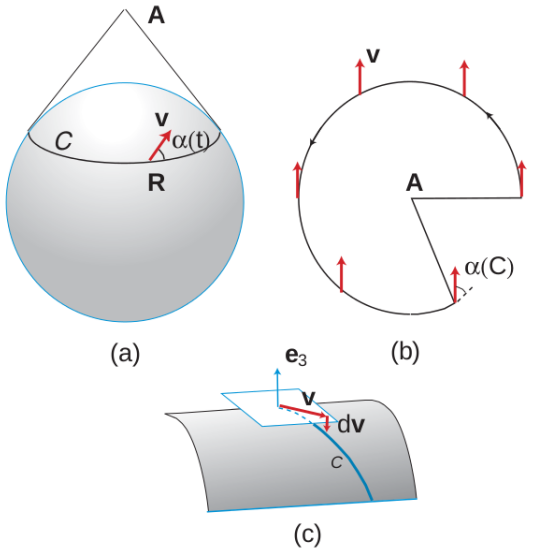

Figure 9.1: Figure (a) shows the transport of $\mathbf{v}$ along the curve C on a sphere. The tangent planes are given by the cone with apex A if C is a latitude circle. (b) shows that if the cone is flattened on a table, $\mathbf{v}$ remains parallel to its initial direction if it is prevented from rotating around the local normal vector $\mathbf{e}_3$ (parallel transport). Measured relative to the latitude, $\mathbf{v}$ makes an angle $\alpha(C)$ on returning to the starting point (holonomy). (c) Generally $\mathbf{v}$ is lying in the tangent plane to the curve C (white rectangle). The parallel transport condition imposes that the change $d\mathbf{v}$ must only have components perpendicular to the tangent plane, i.e. $\pm\mathbf{e}_3 || d\mathbf{v}$. (Taken from [4].)

The total angle $\alpha(C)$ is then given by the integral of the connection one-form ω_{21} which encodes the overlap between $d\mathbf{e}_2$ and $\mathbf{e}_1$.

This results may be written in a more compact form using complex vectors with the standard inner product on $\mathbb{C}$. Define $\hat{\mathbf{n}} = \frac{\mathbf{e}_1 + i\mathbf{e}_2}{\sqrt{2}}$ and $\hat{\psi} = \frac{\mathbf{v}+i\mathbf{w}}{\sqrt{2}}$. Equation 9.46 then becomes $\hat{\psi}(t) = \hat{\mathbf{n}}(t)e^{-i\alpha(t)}$, where the angle $\alpha(t)$ appears now as a phase. The parallel transport conditions (9.45, 9.47 and 9.48) are now given as

$$\hat{\mathbf{n}}^* \cdot d\hat{\psi} = 0, \quad d\alpha = -i\hat{\mathbf{n}}^* \cdot d\hat{\mathbf{n}}.. \tag{9.49}$$

9.5.2 Parallel Transport of Quantum States

The Berry-phase problem is characterized by a parameter which is slowly taken around a closed curve C, remaining according to the adiabatic assumption for all times in the same eigenstate $|n;\mathbf{R}\rangle$. This assumption is an analogous constraint to that on $\mathbf{v}$ in the case of parallel transport on a sphere.

The path C along which $\mathbf{R}$ varies lies on a surface in the parameter space. Now at each $\mathbf{R}$, the eigenstate $|n;\mathbf{R}\rangle$ may be seen as an analogous to $\hat{\mathbf{n}}(t)$ in the sense that it defines a local coordinate frame in the Hilbert space (in place of the tangent plane). The evolution of the ket $|\psi\rangle$ along C is then the parallel transport and therefore $|\psi\rangle$ acquires a phase angle relative to $|n;\mathbf{R}\rangle$, i.e. $|\psi\rangle = e^{-i\gamma_n}|n;\mathbf{R}\rangle$. The parallel condition is now given by $\langle n;\mathbf{R}|\,\mathrm{d}\,|\psi\rangle = 0$ (c.f. 9.49), and thus $\mathrm{d}\gamma = -i\,\langle n;\mathbf{R}|\,\mathrm{d}\,|n;\mathbf{R}\rangle$. The total Berry phase after completing the path C is then given by the line integral

$$\gamma_n(C) = -\oint_C i \langle n; \mathbf{R}| \, \mathrm{d} \, |n; \mathbf{R}\rangle \tag{9.50}$$

Which is the same result obtained in the previous section. Physically this statement can be interpreted by the fact that as $\mathbf{R}$ changes $|\psi\rangle$ stays "parallel" to its initial direction, while the local reference frame, defined by $|n; \mathbf{R}\rangle$ rotates relative to it. The Berry phase is then given by the angle between them.

9.5.3 Geometric Approach and Generalizations

In the following a it is briefly discussed how you can think about the Berry phase in a more abstract way and use this approach to get generalizations to the case discussed above. However, this can not be considered as being rigorous ore complete to get a more concise discussion please confer the sources which this lines are based on: [6], [7], [8] and [9].

As seen above the geometrical Berry phase is, in contrast to the dynamical phase, solely produced by the non-trivial geometry of the space of physical states. A "geometric phase" is then what mathematicians would call a $U(1)$ holonomy and therefore the concept of fiber bundles is the mathematically appropriate theory.

Consider the discussed case of a system which is described by two parameters, which shall be referred to as internal and external. The phase of the wavefunction may then be thought of as an internal parameter depending on $R(t)$ through the energies and the adiabatic phase. It is in this case not enough to say that the evolving wavefunction is, say, just a function of R, since its phase is a function of the whole previous history. A better approach is to think of it as living on a space that looks at least locally as $R \times U(1)$ which has its global topological properties encoded in the Potential $A^n(R)$. In the general case the underlying topology may be non trivial and thus this product may be "twisted" - which is the case when $A^n(R)$ has non removable singularities. The way to go in describing such twisted products, without talking about singularities, is to introduce the construction of fiber bundles.

A fiber bundle E with the fiber F can be thought of as a generalization of the product of two spaces $M \times F$. It looks locally, in a small neighbourhood U of any point in M, like the product space $U \times F$, but globally it may be topologically twisted. M is denoted as the base space, and the fibers of E may be thought of as residing vertically over the points of the base space M with one fiber above each point. Note that all fibers of E are homeomorphic to F.

A simple example of a fiber bundle is the Möbius strip. Its base space is given by a circle and the fiber is a line segment which may be taken to be the interval $[-1, 1]$. Every point on the circle has then a neighbourhood U over which the bundle is homeomorphic to $U \times [-1, 1]$, however globally the Möbius band is twisted. This can for example be seen by choosing a homeomorphism i between the fiber over a point x_0 and $[-1, 1]$. By extending i continuously around the circle and going one time around, it can be seen that once the initial point x_0 is reached again, its "direction" has been reversed. Topologically stated: transporting i around the circle results in $-i$. The additional minus sign is a simple example of a non-trivial holonomy.

In the case of the Berry phase, bundles which have a symmetry group G acting upon the fiber are of particular interest. They are also called principal bundles if the fiber F is the group G itself. One can think of the action of the group on the fiber as a change of coordinates of each fiber. An example for that is given by an n-dimensional vector space where it is necessary to choose a basis to label a vector. However there still remains an action of $U(n)$ representing the freedom to change bases.

Consider the Mead-Berry potential defined above, this potential gives in fact a rule for lifting a curve in the charged particle's position space to a curve in the $U(1)$ bundle of position wave-functions, as seen it is also an example of the notion of parallel transport defined by a connection.
Generally speaking, a connection provides a way to compare fibers at different points on the space M. Mathematically a connection is specified by defining a horizontal subspace H of the tangent space TE to the total space E. Complementary there is a vertical subspace V such that $TE = H \oplus V$. If you now consider a point u in E, the vertical subspace at u is defined to consist of the tangent vectors in TE which are tangent to the fiber passing trough u, i.e. their projections to the tangent space M are zero. Opposed to the definition of the vertical subspace by the fiber, the horizontal subspace (connection) can be chosen.
Another important concept which can be introduced once a connection is chosen is the notion of a horizontal lift. A horizontal lift defines how tangent vectors of a curve in M are lifted to tangent vectors of a curve in E by requiring that they are horizontal. Considering a closed curve as for the Berry phase the horizontal lift of such a curve is in general open. However generally starting at a given point in the fiber, the horizontal lift will return to the same fiber but may lie on a different point in that fiber. This is also what happens in the case of the Berry phase where $|\psi\rangle$ picks up the Berry phase. This difference within the fiber is again a holonomy. Therefore a horizontal lift with respect to a given connection defines a geometrical phase.
This interpretation of the Berry phase can also be used to define the phase without using the adiabatic assumption [10]). Non-abelian generalizations were first explicitly described by Wilczek and Zee [11].

9.6 Spinning Quantum System in an External Magnetic Field

9.6.1 Introduction

In the following a quantum particle with magnetic moment $\mathbf{m} = \mu_B g \mathbf{J}$ will be discussed. The particle is considered in an external magnetic field $\mathbf{B}(t) = B\hat{\mathbf{R}}(t)$ whose direction $\hat{\mathbf{R}}(t)$ is changing periodically. To simplify the calculations the case in which the direction of the magnetic field is precessing around the fixed 3-axis (of the laboratory coordinate frame) is considered. For a "slow" precession of the magnetic field the system may be described in the regime of the adiabatic approximation and the results obtained above using the adiabatic assumption may be used. This section mainly follows [2].

The Hamiltonian describing the system is given by

$$\begin{aligned} H &= H_0 - \mathbf{m}\cdot\mathbf{B} = H_0 - Bg(\frac{e}{2mc}\hat{\mathbf{R}}\cdot\mathbf{J}) \\ &= H_0 + b\hat{\mathbf{R}}\cdot\mathbf{J}. \end{aligned} \tag{9.51}$$

H_0 describes the part of the Hamiltonian which is independent of the magnetic field and will therefore be ignored in the following. $\hat{\mathbf{R}} = \frac{\mathbf{B}}{B}$ is the unit vector pointing along the direction of the magnetic field, $\mathbf{J}$ the angular momentum operator associated to the quantum physical system, and $b = -\frac{Bge}{2mc}$ is a constant. Additionally the relation between the magnetic dipole moment and the angular momentum has been used ($\mathbf{m} = \frac{e}{2mc}g\mathbf{J}$).

The parameter-dependent part of the Hamiltonian may in the case considered here be written as

$$h(\hat{\mathbf{R}}(t)) = -\frac{Bge}{2mc}\hat{\mathbf{R}}(t)\cdot\mathbf{J} = b\hat{\mathbf{R}}(t)\cdot\mathbf{J}, \tag{9.52}$$

where $\hat{\mathbf{R}}$ is again the parameter describing the changing environment.

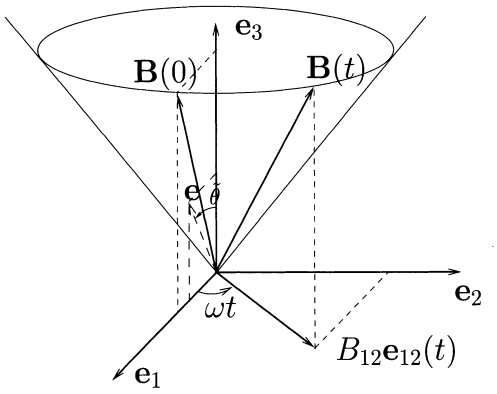

Figure 9.2: A quantum magnetic moment in an external magnetic field which precesses uniformly around a cone of semiangle θ with the rotation axis $\mathbf{e}_3$. The polar and azimuthal coordinates are given by (θ, ϕ), they define the rotation of the external magnetic field. The "polar and azimuthal angles" for the evolution of the state of the magnetic field are denoted by $(\tilde{\theta}, \phi)$.(Taken from [2].)

Furthermore the Bohr magneton is given by $\mu_B = \frac{e\hbar}{2mc}$, g is the Landé factor of the quantum particle and b can be interpreted as a frequency where $\omega_L \equiv \frac{b}{(-g)}$ is called the Larmor frequency.

9.6.2 Parametrization of Basis Vectors

The parameter space of the quantum system described by the Hamiltonian given above is the set of all unit vectors $\hat{\mathbf{R}}$ in the three-dimensional Euclidean space $\mathbb{R}^3$. Each of this unit vectors defines a point on the unit sphere, S^2, centered at the origin, and thus the parameter space may be identified with the unit sphere S^2 embedded in $\mathbb{R}^3$. The points of S^2 are parametrized by the polar and azimuthal angles (θ, ϕ) as follows

$$\hat{\mathbf{R}} = \hat{\mathbf{R}}(\theta, \phi) = \begin{pmatrix} \sin\theta\cos\phi \\ \sin\theta\sin\phi \\ \cos\theta \end{pmatrix}, \tag{9.53}$$

where the parameter ranges are given by $0 \leq \theta \leq \pi$, and $0 \leq \phi < 2\pi$.
The parametrization uniquely determines each unit vector $\hat{\mathbf{R}}$ by a pair (θ, ϕ) except for the vector

$$\mathbf{e}_3 := \begin{pmatrix} 0 \\ 0 \\ 1 \end{pmatrix} \tag{9.54}$$

which may be thought of as describing the north pole $\mathcal{N}$, whilst the unit vector $-\mathbf{e}_3$ describes the south pole $\mathcal{S}$. These vectors are given by $\theta = 0$ and $\theta = \pi$ respectively, for all values of ϕ in the range defined above. Therefore the value of ϕ is not uniquely determined for a given $\hat{\mathbf{R}} = \pm\mathbf{e}_3$.

The case of a magnetic field precessing uniformly about the 3-axis is described by

$$\mathbf{B}(t) = B(\sin\theta\cos\omega t, \sin\theta\sin\omega t, \cos\theta) = B\hat{\mathbf{R}}(\theta, \omega t) \tag{9.55}$$

where B, θ and $\omega = \frac{\phi}{t}$ are constants. The situation described is given in figure 9.2. Assume that for $t = 0$ the magnetic field lies in the 1-3 plane

$$\mathbf{B}(0) = B(\sin\theta, 0, \cos\theta) = (B_{12}, 0, B_3). \tag{9.56}$$

The component $B_{12} = B\sin\theta$ rotates in the 1-2 plane as time progresses

$$\mathbf{B}_{12} := B\sin\theta\mathbf{e}_{12} := B\sin\theta(\mathbf{e}_1\cos\omega t + \mathbf{e}_2\sin\omega t) \tag{9.57}$$

and thus the magnetic field precesses as

$$\begin{aligned}\mathbf{B}(t) &= B_{12}\mathbf{e}_{12}(t) + B_3\mathbf{e}_3 \\ &= B[\sin\theta(\mathbf{e}_1\cos\omega t + \mathbf{e}_2\sin\omega t) + \cos\theta\mathbf{e}_3] = \frac{b}{(-\frac{eg}{2mc})}\hat{\mathbf{R}}(\theta,\omega t).\end{aligned} \tag{9.58}$$

The Hamiltonian 9.52 is then given by

$$h(t) = b\hat{\mathbf{R}}(t)\cdot\mathbf{J} = b(\sin\theta\mathbf{e}_{12}(t) + \cos\theta\mathbf{e}_3)\cdot\mathbf{J} = b\cos\theta[J_3 + tan\theta\mathbf{e}_{12}\cdot\mathbf{J}] \tag{9.59}$$

The time-dependent part of this equation may be rewritten in the following form

$$\mathbf{e}_{12}(t)\cdot\mathbf{J} = J_1\cos\omega t + J_2\sin\omega t = e^{-i\omega tJ_3}J_1e^{i\omega tJ_3}. \tag{9.60}$$

Using that the Hamiltonian may be written as

$$h(t) = b\cos\theta J_3 + b\sin\theta e^{-i\omega tJ_3}J_1e^{i\omega tJ_3} = e^{-i\omega tJ_3}h_0e^{i\omega tJ_3}, \tag{9.61}$$

where $h_0 = b\hat{\mathbf{R}}(\theta,0)\cdot\mathbf{J} = be^{-i\theta J_2}J_3e^{i\theta J_2}$. As can be seen from the expression obtained the time-dependent Hamiltonian is periodic, $h(T) = h(0) = h_0$ with period $T = \frac{2\pi}{\omega}$. Furthermore an orthonormal base of eigenvectors $|k;R\rangle$ may be chosen, which are given by

$$h(R)\,|k;R\rangle = b\hat{\mathbf{R}}\cdot\mathbf{J}\,|k;R\rangle = bk\,|k;R\rangle\,. \tag{9.62}$$

These are eigenvectors of the operator $\hat{\mathbf{R}}(t)\cdot\mathbf{J}$, where the quantum number k is the quantum number for the component of angular momentum along the changing direction of the external magnetic field.

In this example the eigenvalues $E_k(R(t)) = bk$ of the time-dependent Hamiltonian $h(R(t))$ are constant opposed to the eigenvectors $|k;R(t)\rangle$ and eigenprojectors $|k;R\rangle\langle k;R|$ which are changing in time for $\omega \neq 0$. The eigenvalue k is a constant, nevertheless its physical interpretation changes in time; k is the eigenvalue of the observable $\hat{\mathbf{R}}\cdot\mathbf{J}$ which depends on $\hat{\mathbf{R}}(t)$ whose direction changes with respect to the laboratory frame.

In the case where the state vectors $|k;R\rangle$ are also eigenvectors of $\mathbf{J}^2$, the values k may take are $k = -j, -j+1, ..., j-1, j$ where $j \in \frac{\mathbb{Z}}{2}$. Therefore k can only take integer or half-integer values. Additionally $j(j+1)$ is the eigenvalue of $\mathbf{J}^2$. In the following it is assumed that j and any other additional quantum numbers, which may be connected with the eigenvalues of the rotationally invariant part H_0 of the total Hamiltonian $H^{total} = H_0 + h(\hat{\mathbf{R}})$, have fixed values and may therefore be suppressed throughout as labels of the state vectors $|k;R\rangle$.

The eigenvectors are parametrized by the unit vector $\hat{\mathbf{R}}$, or by the angles (θ,ϕ) and they can be obtained by applying (θ,ϕ)-dependent rotations to an eigenvector $|k;\hat{\mathbf{e}}_3\rangle$ of the component of

angular momentum in the direction of the north pole, $J_3 = \mathbf{e}_3 \cdot \mathbf{J}$. There exist different (θ, ϕ)-dependent rotations $\mathcal{R}(\theta, \phi) \in SO(3)$ which give the unit vector $\hat{\mathbf{R}}(\theta, \phi)$ when applied to $\mathbf{e}_3$. Here the following product of rotations is chosen

$$\begin{aligned}\mathcal{R}(\theta, \phi)\mathbf{e}_3 &= \mathcal{R}_3(\phi)\mathcal{R}_2(\theta)\mathcal{R}_3(-\phi)\mathbf{e}_3 \\ &= \mathcal{R}_3(\phi)\mathcal{R}_2(\theta)\mathbf{e}_3 \\ &= \mathcal{R}_3(\phi)\hat{\mathbf{R}}(\theta, 0) = \hat{\mathbf{R}}(\theta, \phi). \end{aligned} \tag{9.63}$$

The second equality follows since $\mathcal{R}_3(-\phi)$ does nothing to the unit vector $\mathbf{e}_3$, and the third since $\mathcal{R}_2(\theta)$ produces the unit vector $\hat{\mathbf{R}}(\theta, \phi)$ which lies in the 1-3 plane at an angle θ inclined to the $\mathbf{e}_3$-axis. The inclusion of the rotation $\mathcal{R}_3(-\phi)$ is to ensure that the rotation $\mathcal{R}(0, \phi)$ is independent of ϕ. Rotations are continuous transformations and are thus represented in the space of quantum physical states by unitary operators representing the group $SU(2)$. The unitary operators representing the rotations $\mathcal{R}_3$ and $\mathcal{R}_2$ are given by

$$U_3(\phi) = e^{-i\phi J_3} := I + \frac{\phi}{i} J_3 + \frac{1}{2!}\left(\frac{\phi}{i} J_3\right)^2 + ..., \tag{9.64}$$

$$U_2(\theta) = e^{-i\theta J_2}, \tag{9.65}$$

analogously for the rotations about the $\mathbf{e}_1$-axis. The representation of the product of two ore more rotations is given by the product of the corresponding operators and thus the rotation $\mathcal{R}(\theta, \phi)$ is represented by

$$U(\theta, \phi) = U_3(\phi)U_2(\theta)U_3(-\phi) = e^{-i\phi J_3} e^{-i\theta J_2} e^{i\phi J_3}. \tag{9.66}$$

Choosing a fixed normalized eigenvector $|k; \mathbf{e}_3\rangle$ of $J_3 = \mathbf{e}_3 \cdot \mathbf{J} = \hat{\mathbf{R}}(0, 0) \cdot \mathbf{J}$ and transforming it using the unitary operator $U(\theta, \phi)$ the following state vector may be obtained

$$|k; \theta, \phi\rangle := U(\theta, \phi)\,|k, \hat{\mathbf{e}}_3\rangle = e^{-i\phi J_3} e^{-i\theta J_2} e^{i\phi J_3}\,|k, \hat{\mathbf{e}}_3\rangle\,. \tag{9.67}$$

It is an eigenvector of the operator $\hat{\mathbf{R}}(\theta, \phi) \cdot \mathbf{J}$ with eigenvalue k, i.e.

$$\hat{\mathbf{R}}(\theta, \phi) \cdot \mathbf{J}\,|k; \theta, \phi\rangle = k\,|k; \theta, \phi\rangle\,. \tag{9.68}$$

The prove of this identity requires the following transformation properties of the angular momentum operators J_i, which follow form their commutation relations using the Baker-Campbell-Hausdorff formula

$$e^{-i\theta J_2} J_3 e^{i\theta J_2} = J_3 \cos\theta + J_1 \sin\theta, \tag{9.69}$$

$$e^{-i\phi J_3} J_1 e^{i\phi J_3} = J_1 \cos\phi + J_1 \sin\phi, \tag{9.70}$$

$$e^{-i\phi J_3} J_2 e^{i\phi J_3} = J_1(-\sin\phi) + J_2 \cos\phi. \tag{9.71}$$

The state vector 9.67 is a smooth vector-valued function of (θ, ϕ). It gives rise to a unique state vector for all $\hat{\mathbf{R}}$ except for $\mathcal{S}$, $\hat{\mathbf{R}} = -\mathbf{e}_3$, where $\theta = \pi$ and 9.69 becomes

$$e^{-i\pi J_2} J_3 e^{i\pi J_2} = -J_3. \tag{9.72}$$

This equation implies that $e^{-i\pi J_2}e^{-i\phi J_3}e^{i\pi J_2} = e^{i\phi J_3}$, and therefore for the state vector follows

$$\begin{aligned}|k;\pi,\phi\rangle &= e^{-i\phi J_3}e^{-i\pi J_2}e^{i\phi J_3}\,|k;\hat{\mathbf{e}}_3\rangle \\ &= e^{-i\pi J_2}e^{2i\phi J_3}\,|k,\hat{\mathbf{e}}_3\rangle \\ &= e^{-i\pi J_2}e^{2ik\phi}\,|k,\hat{\mathbf{e}}_3\rangle\,. \end{aligned} \tag{9.73}$$

From this expression one can see that at the south pole different normalized state vectors are obtained as ϕ varies in the range $0 \leq \phi < 2\pi$. However, $|k;\theta,\phi\rangle$ is single-valued at the north pole, although ϕ may vary there in the same range. This is due to the fact that the rotation $\mathcal{R}_3(-\phi)$ has been included and thus $|k;0,\phi\rangle$ does not depend on ϕ. Therefore 9.67 is a smooth single-valued vector function everywhere on S^2 except at the south pole.

Using a gauge transformation a smooth vector-valued function well defined at the south pole but not at the north pole may be obtained. This phase transformation is defined using the phase factor $e^{i\zeta(\theta,\phi)} = e^{-i2k\phi}$:

$$|k,\theta,\phi\rangle' = e^{-i2k\phi}\,|k,\theta,\phi\rangle = e^{-i\phi J_3}e^{-i\theta J_2}e^{-i\phi J_3}\,|k,0,0\rangle\,. \tag{9.74}$$

Then at the south pole $|k,\pi,\phi\rangle' = e^{-i\pi J_2}\,|k;\hat{\mathbf{e}}_3\rangle$ is uniquely determined but at the north pole it evaluates to many vectors $|k,0,\phi\rangle' = e^{-2ik\phi}\,|k;\hat{\mathbf{e}}_3\rangle$. Therefore $|k,\theta,\phi\rangle'$ may be used everywhere on S^2 except on the north pole. In the overlap region $O_1 \cap O_2$ ($O_1 := S^2 - \mathcal{S}$, $O_2 := S^2 - \mathcal{N}$) either of the vectors 9.67 or 9.74 may be used.

9.6.3 Calculation of the Mead-Berry Connection and Berry Phase

To calculate the Mead-Berry connection one-form A^k for the adiabatic evolution of the Hamiltonian recall that

$$A^k(R) = A^k_i dR^i = i\,\langle k;R|\,\frac{\partial}{\partial R^i}\,|k;R\rangle\,dR^i, \tag{9.75}$$

where $i = 1,2$ correspond to the coordinates θ and ϕ of either of the two patches O_1 or O_2 of the sphere S^2. In the following, the one-forms

$$A^{k',k}(R) = A^{k',k}_i dR^i = i\,\langle k';R|\,\frac{\partial}{\partial R^i}\,|k;R\rangle\,dR^i \tag{9.76}$$

are computed where the Mead-Berry connection one-form A^k is just given by the diagonal elements, A^{kk}, of the matrix of one-forms $(A^{k'k})$. On the patch O_1 where the state vectors are given by 9.67 the matrix elements are

$$A^{k',k}_\theta = i\,\langle k';\theta,\phi|\,\frac{\partial}{\partial\theta}\,|k;\theta,\phi\rangle = \langle k';\hat{\mathbf{e}}_3|\,iU^\dagger(\theta,\phi)\frac{\partial}{\partial\theta}U(\theta,\phi)\,|k;\hat{\mathbf{e}}_3\rangle \tag{9.77}$$

$$A^{k',k}_\phi = i\,\langle k';\theta,\phi|\,\frac{\partial}{\partial\phi}\,|k;\theta,\phi\rangle = \langle k';\hat{\mathbf{e}}_3|\,iU^\dagger(\theta,\phi)\frac{\partial}{\partial\phi}U(\theta,\phi)\,|k;\hat{\mathbf{e}}_3\rangle \tag{9.78}$$

Compute the terms within the brackets

$$iU^\dagger(\theta,\phi)\frac{\partial U(\theta,\phi)}{\partial\theta} = ie^{-i\phi J_3}e^{i\theta J_2}e^{i\phi J_3}\frac{\partial}{\partial\theta}e^{-i\phi J_3}e^{-i\theta J_2}e^{i\phi J_3} = e^{-i\phi J_3}J_2e^{i\phi J_3}$$
$$= (J_2\cos\phi - J_1\sin\phi), \tag{9.79}$$
$$iU^\dagger(\theta,\phi)\frac{\partial U(\theta,\phi)}{\partial\phi} = U^\dagger(\theta,\phi)J_3U(\theta,\phi) - U^\dagger(\theta,\phi)U(\theta,\phi)J_3$$
$$= -(J_1\cos\phi + J_2\sin\phi)\sin\theta + J_3(\cos\theta - 1). \tag{9.80}$$

Substituting these two expressions the following may be obtained

$$A_\theta^{k',k} = \langle k';\hat{\mathbf{e}}_3|\left(J_2\cos\phi - J_1\sin\phi\right)|k;\hat{\mathbf{e}}_3\rangle \tag{9.81}$$
$$A_\phi^{k',k} = \langle k';\hat{\mathbf{e}}_3|\left[-(J_1\cos\phi + J_2\sin\phi)\sin\theta + J_3(\cos\theta - 1)\right]|k;\hat{\mathbf{e}}_3\rangle\,. \tag{9.82}$$

J_1 and J_2 do not contribute to the diagonal matrix elements and therefore they may be written as

$$A_\theta^k(\theta,\phi) = 0 \tag{9.83}$$
$$A_\phi^k(\theta,\phi) = \langle k;\hat{\mathbf{e}}_3|\,J_3(\cos\theta - 1)\,|k;\hat{\mathbf{e}}_3\rangle = -k(1-\cos\theta), \quad \theta\neq\pi. \tag{9.84}$$

Repeating the same calculation for the coordinate patch O_2 in which the state vectors are given by 9.74 leads to

$$A_\theta'^{k',k} = e^{2i(k'-k)\phi}\,\langle k'\hat{\mathbf{e}}_3|\left(J_2\cos\phi - J_1\sin\phi\right)|k,\hat{\mathbf{e}}_3\rangle \tag{9.85}$$
$$A_\phi'^{k',k} = e^{2i(k'-k)\phi}\,\langle k'\hat{\mathbf{e}}_3|\left[-(J_1\cos\phi + J_2\sin\phi)\sin\theta + J_3(\cos\theta - 1) + 2k\right]|k,\hat{\mathbf{e}}_3\rangle\,. \tag{9.86}$$

The diagonal matrix elements can be calculated to

$$A_\theta'^k(\theta,\phi) = 0 \tag{9.87}$$
$$A_\phi'^k(\theta,\phi) = \langle k;\hat{\mathbf{e}}_3|\left[J_3(\cos\theta - 1) + 2k\right]|k;\hat{\mathbf{e}}_3\rangle = k(1+\cos\theta), \quad \theta\neq 0. \tag{9.88}$$

According to the gauge theory described one would expect from the transformation behavior of the Mead-Berry potential (c.f. 9.27) and $\zeta = -2k\phi$,

$$A'^k - A^k = -d\zeta(\theta,\phi) = d(2k\phi) = 2kd\phi. \tag{9.89}$$

Which is consistent with the terms computed above since indeed $A_\phi'^k - A_\phi^k = 2k$.

To compute the curvature two-form recall that this is according to 9.38 given by

$$F^k = dA^k = \frac{\partial A_\theta^k}{\partial\phi}d\phi\wedge d\theta + \frac{\partial A_\phi^k}{\partial\theta}d\theta\wedge d\phi. \tag{9.90}$$

Using the values obtained above the following may be obtained

$$F^k = F_{\theta\phi}^k d\theta\wedge d\phi = -k\sin\theta d\theta\wedge d\phi. \tag{9.91}$$

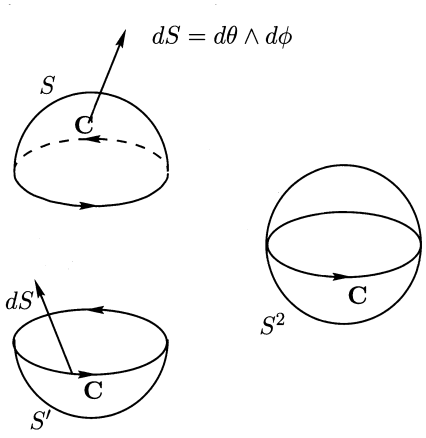

Figure 9.3: Using Stokes's theorem, the difference of the line integrals of A and A' can be transformed into an integral over the closed 2-surface $S \cup S'$. (Taken from [2].)

The Berry phase for a closed path C is thus given by

$$\gamma_k(C) = \int_S F^k = -k \int_S \sin\theta d\theta \wedge d\phi = -k \int_S d\Omega \mod 2\pi, \tag{9.92}$$

where it is integrated over a surface S which has the closed curve C as its boundary ($C = \partial S$). $d\omega$ is defined as the element of solid angle (area element of the unit sphere). The direction in which C is traversed is taken along the fingers and the direction normal to S i.e. the direction of $d\theta \wedge d\phi$ along the thumb of the right hand (Fig. 9.3).

The Berry phase angle can also be written as

$$\gamma_k(C) = -k\Omega(C) \mod 2\pi, \tag{9.93}$$

by defining $\Omega(C)$ as the solid angle subtended by C, i.e.

$$\Omega(C) := \int_S \sin\theta d\theta \wedge d\phi. \tag{9.94}$$

As explained before the curvature two-form F^k is unlike the single-valued basis vectors $|k;\theta,\phi\rangle$ and the connection one-form A^k independent of the choice of local coordinates. This implies that a surface $S \subset O_1$ or $S' \subset O_2$ can be chosen in the calculation of the Berry phase and as long as both surfaces S and S' have C as their boundaries, i.e. $\partial S = C = \partial S'$ the calculation does not depend on the choice. This property of the curvature two-form has some noticeable consequences. To see them compute the Berry phase angle using S'

$$\gamma_k(C) = \int_{S'} F^k = -k \int_{S'} \sin\theta d\theta \wedge d\phi = k \int_{S^2 \setminus S} \sin\theta d\theta \wedge d\phi, \tag{9.95}$$

where the direction of the normal S' and the direction in which C is traversed are given by the right-hand rule. This implies that the normal of S' is pointing into the sphere and the normal of S out of the sphere. Furthermore, $S^2 \setminus S$ denotes the surface with the same area as S' but with normal pointing out of the sphere S^2. This expression may be rewritten in the form

$$\gamma_k(C) = k \left(\int_{S^2} \sin\theta d\theta \wedge d\phi - \int_S \sin\theta d\theta \wedge d\phi \right). \tag{9.96}$$

Using that the integral of the unit solid angle $d\Omega$ over the whole unit sphere is 4π, and the integral over the surface S is given by 9.94 the berry phase is given by

$$\gamma_k(C) = +k(4\pi - \Omega(C)) \qquad \mod 2\pi. \tag{9.97}$$

Comparing this equation with 9.93 it follows that

$$-k\Omega(C) = 4\pi k - k\Omega(C) \qquad \mod 2\pi. \tag{9.98}$$

However, this can only be satisfied if $k = 0, \pm\frac{1}{2}, \pm 1, \pm\frac{3}{2}, \pm 2, ...$, and therefore k must be an integer or a half-integer. This result is new if the basis vectors are not eigenvectors of $\mathbf{J}^2$, which may be of importance considering molecules.

Up until now, there are no restrictions on the curve C as long as it is closed and on the unit sphere. Considering a special path $C_1 : [0, T] \to S^2$ given by 9.55, and shown in figure 9.2, namely

$$C_1(t) := R(\theta(t), \phi(t)) = R(\theta = const., \phi = \omega t), \tag{9.99}$$

the Berry phase may be written as

$$\gamma_k(C_1) = -k \int_0^{2\pi} \int_0^{\theta} \sin\theta' d\theta' d\phi = -2\pi k(1 - \cos\theta), \tag{9.100}$$

with θ being the constant angle shown in figure 9.2.

9.7 Geometric Quantum Computing

The Berry phase is, as it follows from the considerations made above, a purely geometrical effect of an evolving quantum system. The phase depends only on the area covered by the curve the system follows, and is independent of the details of traversal such as the speed, or minor fluctuations around the path which may cancel each other. That are reasons why the Berry phase finds applications in quantum computing, in which it is tried to implement fault tolerant quantum logic gates. The following section is mainly based on [12], [13], [14], [15] and [16].

9.7.1 Notation

A *qubit* is the quantum mechanical analog of a classical bit. It is realized by a quantum system in which the boolean states 0 and 1 are represented by a pair of mutually orthogonal quantum states labeled as $|0\rangle, |1\rangle$. In contrast to a simple boolean variable, a qubit can exist in an arbitrary superposition $\alpha|0\rangle + \beta|1\rangle$, where $|\alpha|^2 + |\beta|^2 = 1$. This is one of the reasons for quantum computers to be more powerful for certain computations than classical computers. Qubits can for example be implemented by microscopic systems such as an atom, a nuclear spin, or a polarized photon. Essential for quantum computing is to be able to implement *quantum logic gates* which are devices performing unitary operations on selected qubits in a fixed period of time.

$$input \to \boxed{\text{quantum logic gate}} \to output$$

A *quantum circuit* is then defined as a device consisting of quantum logic ates whose computational steps are synchronized in time. The *size* of the network is the number of gates it contains.

Since quantum mechanics is linear and norm-preserving, a quantum computation on n qubits is a $2^n \times 2^n$ unitary matrix and therefore the gates may be represented by such matrices. Since it is usually not a particularly sensible approach to directly implement any desired quantum gate it is more convenient to focus on a *universal set of quantum gates* and then obtain the other gates by joining these basic gates together to form quantum circuits.

Usually, one roughly distinguishes between single- and two-qubit gates. The single qubit gates are most often described by two gates: the Hadamard gate H and the phase shift gate Φ. For the case of a spin as a qubit, which is considered here, these gates correspond to rotations of a spin about some axis, and as will later be further explained, they may be implemented using nuclear magnetic resonance (NMR) by applying resonant radio frequency (RF) pulses to the spins. In the two-qubit case the gate which is of importance in this paper, is the controlled phase shift gate $B(\phi)$. An important result in the theory of quantum computation states, that the Hadamard gate and all $B(\phi)$ phase shift gates form a universal set. In fact any n-qubit unitary operation can be simulated exactly using these gates with less than $C4^n n$ such gates, for some constant C [12].

The *phase shift gate* Φ acts on one qubit in the following way

$$\begin{aligned} \Phi : |0\rangle &\rightarrow |0\rangle \\ |1\rangle &\rightarrow e^{i\phi} |1\rangle , \end{aligned} \tag{9.101}$$

which using the basis $\left\{ |0\rangle = \begin{pmatrix} 1 \\ 0 \end{pmatrix}, |1\rangle = \begin{pmatrix} 0 \\ 1 \end{pmatrix} \right\}$, can be written in matrix form

$$\Phi = \begin{pmatrix} 1 & 0 \\ 0 & e^{i\phi} \end{pmatrix}. \tag{9.102}$$

The *Hadamard gate* H performs the following unitary transformation on one qubit

$$\begin{aligned} H : |0\rangle &\rightarrow \frac{1}{\sqrt{2}}(|0\rangle + |1\rangle) \\ |1\rangle &\rightarrow \frac{1}{\sqrt{2}}(|0\rangle - |1\rangle), \end{aligned} \tag{9.103}$$

written in matrix form

$$H = \frac{1}{\sqrt{2}} \begin{pmatrix} 1 & 1 \\ 1 & -1 \end{pmatrix}. \tag{9.104}$$

The *controlled phase shift gate* $B(\phi)$ is defined in such a way that the outcoming state gets, as its name suggests, a complex phase only if the control and the target bit are in the state $|1\rangle$. In matrix form this is given in the tensor product basis $\{|00\rangle, |01\rangle, |10\rangle, |11\rangle\}$ as

$$B(\phi) = \begin{pmatrix} 1 & 0 & 0 & 0 \\ 0 & 1 & 0 & 0 \\ 0 & 0 & 1 & 0 \\ 0 & 0 & 0 & e^{i\phi} \end{pmatrix}. \tag{9.105}$$

9.7.2 Nuclear Magnetic Resonance

The study of direct transitions between Zeeman levels of an atomic nucleus in a magnetic field is also called Nuclear Magnetic Resonance (NMR). Most of the atomic nuclei possess a spin and have therefore also a magnetic moment. If the nucleus is now placed in a magnetic field the spin will be quantized along the direction of the field. In most cases the relevant nuclei for quantum computing have spin one half and have therefore two spin states separated by the Zeeman splitting

$$\Delta E = \hbar g B, \tag{9.106}$$

where g is the gyromagnetic ratio which is a constant depending on the nuclear species and B is the modulus of the magnetic field.

Transition between these Zeeman levels will then occur when electromagnetic radiation of the correct frequency is applied. Involved in this process is the absorption of a photon with energy $E = h\nu_0$, where ν_0 is the resonance radio frequency (RF) which has to match the Larmor precession frequency ($\nu_L = \frac{gB}{2\pi}$) of the nuclear magnetic moment in the constant magnetic field. Therefore a magnetic resonance absorption will occur when $\nu_0 = \nu_L$.

In fact NMR is, as of today, representing the most mature technology for the implementation of quantum computing [15]. The logic bits are given by the nuclear spins of the atoms in custom designed molecules. By applying (RF) fields on resonance, spin flips may be achieved. The initialization process is implemented via a cooling of the system to the ground state or a known low-entropy state, which is also working at room temperature [15]. The measurement is then carried out by measuring the magnetic induction signal which is generated by the precessing spin on the receiver coil.

Single Qubit Gates

As already mentioned above single qubit gates correspond to rotations of a spin about an axis. One of the simplest example of such a rotation is that about an axis in the xy-plane, which can be implemented using resonant RF pulses. The angle through which the spin is rotated, depends on the length and the power of the applied RF pulse, while the phase angle (and thus the azimuthal angle made by the rotation axis in the xy-plane) may be controlled by choosing the initial phase angle of the RF. It is possible to implement all single qubit gates out of rotations in the xy-plane. Using a composition of such rotations any desired single qubit gate can be built and thus also the Hadamard gate.

Two Qubit Gates

In the following a derivation of a possible implementation of the controlled phase shift gate $B(\phi)$ will be given, which is based on the concept of the Berry phase.

To achieve this implementation of a two-qubit gate, consider a system consisting of two non-interacting spin-half particles a and b in magnetic fields $\mathbf{B}_a$ and $\mathbf{B}_b$ along the z-axis. The Hamiltonian describing this system is then given by

$$H_0 = \frac{\hbar}{2}(\omega_a \sigma_{az} \otimes \mathbf{1}_b + \omega_b \mathbf{1}_a \otimes \sigma_{bz}), \tag{9.107}$$

where the frequencies $\frac{\omega_a}{2\pi}$ and $\frac{\omega_b}{2\pi}$ are the transition frequencies of the two spins and $\sigma_{az} = \sigma_{bz} = \sigma_z = \begin{pmatrix} 1 & 0 \\ 0 & -1 \end{pmatrix}$ are the Pauli operators. Written in the basis of eigenstates (which are quantized along the z-axis) $\{|\sigma_{az}, \sigma_{bz}\rangle_{\sigma_{az},\sigma_{bz}} = |\uparrow\uparrow\rangle, |\uparrow\downarrow\rangle, |\downarrow\uparrow\rangle, |\downarrow\downarrow\rangle\}$ the Hamiltonian is given in matrix form

$$H_0 = \frac{\hbar}{2}\begin{pmatrix} \omega_a + \omega_b & 0 & 0 & 0 \\ 0 & \omega_a - \omega_b & 0 & 0 \\ 0 & 0 & -\omega_a + \omega_b & 0 \\ 0 & 0 & 0 & -\omega_a - \omega_b \end{pmatrix}, \tag{9.108}$$

assuming that $\omega_a \neq \omega_b$ and $\omega_a > \omega_b$.

If the two particles are sufficiently close to each other, the interactions can not be ignored which creates additional splittings between the energy levels. In the case of two spin-half particles, the direct or indirect influence of the magnetic field of one spin will affect the energy levels of the other spin resulting in an energy increase of the system if the spins are aligned and a decrease if they are anti-aligned. The Hamiltonian of the total system including the interactions is then given by

$$H = H_0 + \frac{\hbar}{2} J\sigma_{az} \otimes \sigma_{bz} = \frac{\hbar}{2}(\omega_a \sigma_{az} \otimes \mathbf{1} + \omega_b \mathbf{1} \otimes \sigma_{bz} + J\sigma_{az} \otimes \sigma_{bz}), \tag{9.109}$$

or in the previously chosen basis,

$$H_0 = \frac{\hbar}{2}\begin{pmatrix} \omega_a + \omega_b + J & 0 & 0 & 0 \\ 0 & \omega_a - \omega_b - J & 0 & 0 \\ 0 & 0 & -\omega_a + \omega_b - J & 0 \\ 0 & 0 & 0 & -\omega_a - \omega_b + J \end{pmatrix}. \tag{9.110}$$

Add a circularly polarized magnetic field $\mathbf{B}_x(t)$ in the xy-plane with the characteristic frequency $\omega_x = \mu|\mathbf{B}_x|$ - which represents a RF-pulse. The Hamiltonian H'_a of spin a (trace out spin b) is then given as

$$H'_a = \frac{\hbar}{2}(\omega_a \pm J)\sigma_{az} + \frac{\hbar}{2}\omega_x \sigma_x(t), \tag{9.111}$$

where the $\pm$ sign in front of J depends on the specific state (up or down) of the spin b and $\sigma_x = \begin{pmatrix} 0 & e^{-i\omega t} \\ e^{i\omega t} & 0 \end{pmatrix}$, with the angular frequency ω of the field $B_x(t)$. Transform this Hamiltonian now into the rotational frame for spin a which is rotating at speed ω

$$\begin{aligned} H_a &= RHR^{-1} + i(\frac{\partial}{\partial t}R)R^{-1} \\ &= \frac{\hbar}{2}(\omega_a - \omega \pm J)\sigma_z + \frac{\hbar}{2}\omega_x(t) = \frac{\hbar}{2}(\omega_\pm - \omega)\sigma_z + \frac{\hbar}{2}\omega_x(t), \end{aligned} \tag{9.112}$$

where $\omega_\pm = \omega_a \pm J$ and the rotational matrix is given by

$$R(t) = e^{i\omega\frac{\sigma_z}{2}t}. \tag{9.113}$$

This expression indicates that for $|\omega_x| \ll |\omega_\pm - \omega|$ the direction of the Hamiltonian lies close to the z-axis and for $|\omega_x| \gg |\omega_\pm - \omega|$ it lies close to the x-axis. Therefore the system is quantized along

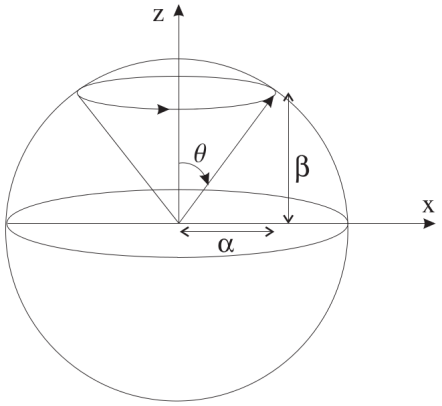

Figure 9.4: Spin half particle in a magnetic field: the frequencies $\alpha = \omega_x$ and $\beta = \omega_\pm - \omega$ are drawn in at the respective axes.

the z-axis if the RF-pulse with frequency ω is applied far away from the resonance frequency $\omega_\pm$. Close to the resonance frequency, $\omega \approx \omega_\pm$ it is quantized along the x-axis. Therefore it is possible to continuously sweep between these two cases. Additionally, if the variations are executed adiabatically the spin of the system will follow the Hamiltonian. A Berry phase has by definition to be acquired by a circular motion, which can be imposed by adiabatically varying the phase of the RF-pulse. In the case that the RF-pulse is not swept all the way to resonance, but only to some final value ω_f cones with arbitrary opening angles θ may be implemented (c.f. fig 9.4).

The opening angle is then given by

$$\cos\theta_\pm = \frac{\omega_x}{\sqrt{(\omega_\pm - \omega)^2 + \omega_x^2}}, \tag{9.114}$$

which implies for the Berry phase

$$\gamma_\pm = -\pi(1 - \cos\theta_\pm). \tag{9.115}$$

As can be seen the Berry phase of spin a depends on the respective state of spin b and therefore this implements a conditional Berry phase. It is now crucial to find a way to remove the dynamical phase in order to implement this principle as a conditional quantum gate. One approach is to use a refocusing technique known as spin-echo. The basic idea behind this technique is to apply the cyclic evolution twice for each spin, with the second application surrounded by a pair of fast π transformations (they simply swap the basis states $|\uparrow\rangle$ and $|\downarrow\rangle$). The resulting effect of this compound transformation would be to cancel *all* the acquired phases except that the second cycle evolution is performed by retracing the first in the opposite direction such that the dynamical phases cancel out and the geometric add up instead. After applying this procedure the net transformation of the system, up to global phases, is given by

$$|\psi_f\rangle = \begin{pmatrix} e^{2i\Delta\gamma} & 0 & 0 & 0 \\ 0 & e^{-2i\Delta\gamma} & 0 & 0 \\ 0 & 0 & e^{-2i\Delta\gamma} & 0 \\ 0 & 0 & 0 & e^{2i\Delta\gamma} \end{pmatrix} |\psi_a\rangle \otimes |\psi_b\rangle\,, \tag{9.116}$$

where $\Delta\gamma = \gamma_+ - \gamma_-$. Therefore this implements a conditional evolution, since the state of the qubit given as spin a influences the phase acquired by the second qubit given as spin b. This gate essentially introduces a phase of $e^{2i\Delta\gamma}$ if the spins are aligned and $e^{-2i\Delta\gamma}$ if they are anti-aligned. It is equivalent to the controlled phase shift gate $B(\phi)$ introduced above.

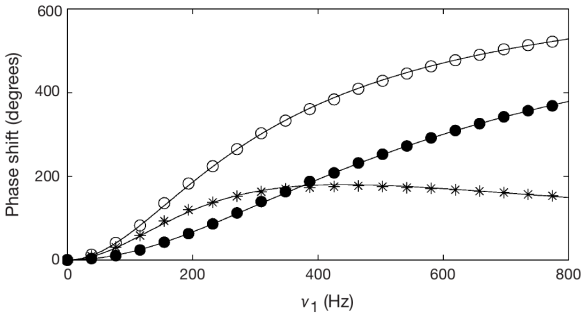

Figure 9.5: Experimental values for the Berry phases γ_-, γ_+, and the controlled Berry phase difference, $\Delta\gamma$, as a function of the maximum radio frequency field strength ν_1. The filled circles show the results for γ_-, the open for γ_+ and the stars $\Delta\gamma$. The theoretical values are shown as smooth curves. (Taken from [17].)

Experimental Verification

The theory explained above has been verified experimentally by Jones, Vedral, Ekert and Castagnoli [17]. The sample consisted of 100 mg of 99% ^{13}C-labeled $CHCL_3$ dissolved in 0.2 ml of 99.96% $CDCL_3$ laced in a Shigemi microtube. A single 1^H nucleus has been used as spin a and the 13-nucleus as spin b. The interaction frequency for this system was given by $J = 209.2Hz$. The experiments were performed with RF-pulses set at the frequency $\omega_x = 221.3$ Hz whilst ω was varied between 0 and 774 Hz. The geometric phase was measured for both 1^H resonances. The obtained results are shown in figure 9.5. It can be clearly seen that the measured phases lie close to the theoretically predicted values and that there is a splitting of the geometric phases due to the respective spin state. The controlled Berry phase is rising smoothly up to a broad maximum at 180°, and then falling slowly back down towards zero. Additionally the effects of a breakdown of the adiabatic criterion were examined. They concluded experimentally that below a sweep time of 50 μs the loss of adiabaticity is severe and major distortions were observed.

9.8 Conclusion

The adiabatic assumption assures that a system which is slowly transported around a closed circuit will return to its original state. During that evolution the system will not surprisingly pick up a dynamical phase factor. "The remarkable and rather mysterious result", as Berry called it [3], is the additional phase factor which is of geometric nature. The additional property of gauge invariance then provided a way to define a direct and globally defined formula for the Berry phase. However, the adiabatic limit is not the most general regime in which Berry's phase may be described and as stated above there exist generalizations to non-adiabatic evolutions.

The application of the derived formulas to a spinning quantum system in an external magnetic field essentially showed that the Berry phase is in this special case given by the unit solid angle on the sphere which is subtended by the path traced out in parameter space. This result could then be used to describe how a controlled phase shift gate based on the technique of nuclear magnetic resonance can be implemented, where the theoretical values are in high agreement with the experimentally obtained data.

Bibliography

[1] M. Born and V. Fock, "Beweis des adiabatensatzes," *Zeitschrift für Physik*, vol. 51, no. 3-4, pp. 165–180, 1928.

[2] A. Bohm, A. Mostafazadeh, H. Koizumi, Q. Niu, and J. Zwanziger in *The Geometric Phase in Quantum Systems*, Texts and Monographs in Physics, Springer Berlin Heidelberg, 2003.

[3] M. V. Berry, "Quantal phase factors accompanying adiabatic changes," *Proceedings of the Royal Society of London. A. Mathematical and Physical Sciences*, vol. 392, no. 1802, pp. 45–57, 1984.

[4] N. P. Ong and W.-L. Lee, "Geometry and the Anomalous Hall Effect in Ferromagnets," in *Foundations of Quantum Mechanics in the Light of New Technology ISQM-Tokyo '05* (S. Ishioka and K. Fujikawa, eds.), pp. 121–126, June 2006.

[5] M. Berry, "The quantum phase, five years after," *Geometric phases in physics*, vol. 7, 1989.

[6] D. Chruscinski and A. Jamiolkowski, *Geometric phases in classical and quantum mechanics*, vol. 36. Springer, 2004.

[7] Y. Ben-Aryeh, "Berry and pancharatnam topological phases of atomic and optical systems," *arXiv preprint quant-ph/0402003*, 2004.

[8] R. W. Batterman, "Falling cats, parallel parking, and polarized light," *Studies in History and Philosophy of Science Part B: Studies in History and Philosophy of Modern Physics*, vol. 34, no. 4, pp. 527–557, 2003.

[9] R. A. Bertlmann, *Anomalies in quantum field theory*, vol. 91. Oxford University Press, 2000.

[10] A. Bohm, L. J. Boya, and B. Kendrick, "Derivation of the geometrical berry phase," in *Group Theoretical Methods in Physics*, pp. 346–350, Springer, 1991.

[11] F. Wilczek and A. Zee, "Appearance of gauge structure in simple dynamical systems," *Phys. Rev. Lett.*, vol. 52, pp. 2111–2114, Jun 1984.

[12] A. Ekert, M. Ericsson, P. Hayden, H. Inamori, J. A. Jones, D. K. Oi, and V. Vedral, "Geometric quantum computation," *Journal of modern optics*, vol. 47, no. 14-15, pp. 2501–2513, 2000.

[13] J. Jones, "Nuclear magnetic resonance quantum computation," *Quantum Entanglement and Information Processing, Ecole dEte de Physique des Houches, 79th, Les Houches, France*, p. 357, 2003.

[14] K. Durstberger, *Geometric phases in quantum theory*. PhD thesis, Master thesis, University of Vienna, 2002.

[15] Z. Zhang, G. Chen, Z. Diao, and P. R. Hemmer, "Nmr quantum computing," in *Advances in Applied Mathematics and Global Optimization*, pp. 465–520, Springer, 2009.

[16] E. Sjöqvist, "A new phase in quantum computation," *Physics*, vol. 1, no. 35, 2008.

[17] J. A. Jones, V. Vedral, A. Ekert, and G. Castagnoli, "Geometric quantum computation using nuclear magnetic resonance," *Nature*, vol. 403, no. 6772, pp. 869–871, 2000.

Chapter 10

Graphene and Emergent Spin

Author: Nilas Falster Klitgaard
Supervisor: Philippe de Forcrand

In this report, I will discuss the quantization of graphene and some of its physical consequences. I will describe graphene through a model of spin 0 fermions. Expanding around the Fermi energy it will become clear that the spectrum can be understood as describing massless spin 1/2 particles. As a test of this formalism, I will calculate the Berry phase of graphene. Next, I will look at another model sharing this emergence of spin. The model of the square lattice in a magnetic field. I will when go on to describe the quantum Hall effect and show how our understanding of graphene leads to predictions of Landau levels and the quantum Hall resistance. Finally, I will give a qualitative description of bilayer graphene showing differences and similarities with monolayer graphene.

10.1 Structure and Quantization of Graphene

In this section, I will derive and diagonalize a Hamiltonian describing graphene in the tight binding approximation. The formalism of spinless fermions will leads to spinor like quantity around the Brillion zone describing massless fermions. Finally, I will do a calculation of the Berry phase finding that it takes the value expected for spin 1/2 particles. The discussion is based on [2], the calculation of Berry phase is found in [3], a more detailed calculation taking into account the overlap of neighboring sites can be found in [1].

Graphene is characterized by a two dimensional hexagonal structure. At each site in the lattice, there will be a carbon atom. Since I have a hexagonal structure my basis will have two atoms a and b I choose my basis such that basis vectors x_1 is in upward right direction and x_2 in upward left see fig. 10.1. I will now look at a model of spinless fermions on my lattice. This seemingly contradicts the spin statistics theorem stating that bosons must have integer spin and fermions half integer spin. However the proof of the spin statistics theorem relies on Lorentz invariance, since I am on a lattice I will only consider transformations that leave my lattice invariant that is finite rotations and translations. Hence, my model will explicitly break Lorentz invariance and the spin statistics theorem does not apply. Note that disregarding spin-spin interaction among the different fermions, the energy of a state in grapene does not depend on spin, so taking spin into account just leads to a double degeneracy of states.

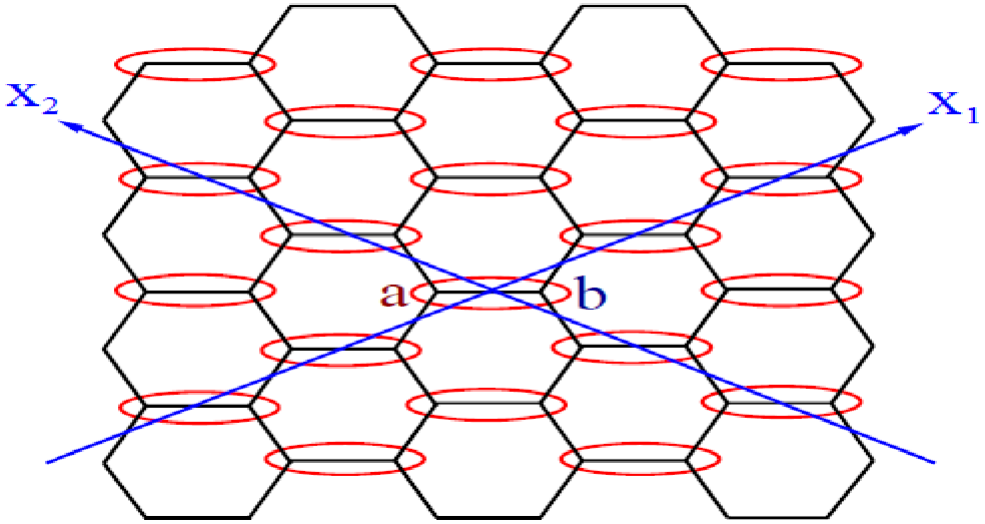

Figure 10.1: Lattice of graphene, a and b are the atoms of the basis x_1 and x_2 describes basis vectors

Note that a carbon have 6 electrons in total. 2 of these atoms are in the s-1 orbital and are so tightly bound that they can be ignored when discussing dynamics of graphene. 3 of the electrons will take part in the binding of the grapene lattice. Each will be part of a sp-2 pair binding together neighboring sites. This leaves graphene with one dynamical electron pr. atom. I can with great successes apply the tight binding approximation. In this approximation I see the electron as localized in a p-2 orbital around an atom. This orbital corresponds to orbits transverse to the graphene plane. I can now find a Hamiltonian for this system. Describing my system through a nearest neighbor interaction with electrons able to jump to neighboring sites.

$$H = K \sum_{x_1,x_2} \left(a^\dagger_{x_1,x_2} b_{x_1,x_2} + b^\dagger_{x_1,x_2} a_{x_1,x_2} + a^\dagger_{x_1+1,x_2} b_{x_1,x_2} + b^\dagger_{x_1,x_2} a_{x_1+1,x_2} + a^\dagger_{x_1,x_2} b_{x_1,x_2+1} + b^\dagger_{x_1,x_2+1} a_{x_1,x_2} \right) \tag{10.1}$$

The constant K in eq. (10.1) is known as the hopping parameter and describes how tightly bound the electrons are. This is the fundamental energy scale of graphene. The different terms consist of fermionic creation and annihilation operators for sites a and b. Each term are moving an electron from one site to the neighboring site. I have divided them into three groups of two terms horizontal, right leaning and left leaning terms. See fig. 10.1

I will now proceed to diagonalize my Hamiltonian. To do this I will employ the standard tricks of Fourier transform to go to momentum space.

$$\tilde{a}_{p_1,p_2} = \sum_{x_1,x_2} \left(e^{-ix_1 p_1} e^{-ix_2 p_2} a_{x_1,x_2} \right) \tag{10.2}$$

Since I am on a discrete lattice, my momenta are quantized and limited to a finite interval. The way to see this is to realize that the wave function describing my electron can't have a smaller wavelength than the lattice spacing. In particular, with the above convention of the Fourier transform p_1 and p_2 are restricted to some interval of length 2π. I chose $-\pi < p_1, p_2 \leq \pi$. In the limit of macroscopic, the different discrete levels of momenta come so close that I approximate them as continues. Now using eq. (10.2) it is easy to see that eq. (10.1) is equivalent to the following expression

$$H = K \int \frac{dp_1}{2\pi} \frac{dp_2}{2\pi} \begin{pmatrix} \tilde{a}^\dagger_{p_1,p_2} & \tilde{b}^\dagger_{p_1,p_2} \end{pmatrix} \begin{pmatrix} 0 & z \\ z^* & 0 \end{pmatrix} \begin{pmatrix} \tilde{a}_{p_1,p_2} \\ \tilde{b}_{p_1,p_2} \end{pmatrix}. \tag{10.3}$$

[1] I am choosing x and p to be unitless in order to get physical quantities one must use xa and $\frac{p}{a}$ where a is the lattice spacing of graphene

The z in eq. (10.3) is a complex number depending on the momenta. It is given by $z = 1+e^{-ip_1}+e^{ip_2}$. Looking at eq. (10.1) and fig. 10.1 one sees that the individual terms of z correspond precisely the horizontal, right leaning and left leaning terms of eq. (10.1).It now proves advantageous to consider states that are in the momentum basis as well. That is

$$\Psi = \begin{pmatrix} p_1 \\ p_2 \end{pmatrix} \tag{10.4}$$

Using the states from eq. (10.4) the integrals of eq. (10.3) become integrals over delta functions and the creation and annihilation operators act trivially hence eq. (10.3) reduce to the matrix equation

$$H = K \begin{pmatrix} 0 & z \\ z* & 0 \end{pmatrix}. \tag{10.5}$$

Diagonalizing H is now trivial and I get eigenstates

$$\Psi = \frac{1}{\sqrt{|2z|}} \begin{pmatrix} \sqrt{z} \\ \pm\sqrt{z^*} \end{pmatrix} \tag{10.6}$$

and eigenvalues

$$\pm K\,|z| \tag{10.7}$$

Using state counting arguments from solid state physics I know that theory that the filled states of undoped graphene corresponds to all the state with negative energy in eq. (10.7). Hence the Fermi level will be at $|z| = 0$. Moreover, the physical relevant behavior is the one seen around these points. Using the definition of z I see that in order for the imaginary part to cancel I must have $p_1 = p_2$. In order for the real part to cancel they must each contribute -1/2 this leads to $p_1 = p_2 = \pm\frac{2}{3}\pi$. Hence, I get two different expansion points so my states are double degenerate. Looking at the eigenstates (10.6) I see that the behavior of these two different zero points has the same structure as a spin up and a spin down state for a spin 1/2 particle. Another interesting thing is to look at the dispersion relation close to the zero points. Taylor expanding the exponential in z I see that eq. (10.7) is given by

$$E = \pm K\sqrt{\frac{1}{2}\left((p_1+p_2)^2 + p_1^2 + p_2^2\right)}. \tag{10.8}$$

Looking at eq. (10.8) I see that the behavior of my particles is the same as a massless relativistic particle.[2] Note however that the "speed of light" for this particle is given by my lattice properties as $c = Ka$. The fact that my particle is massless is due to the potential of the graphene lattice and since free electrons are massive, the effective massless ones should not move at the true speed of light. Starting out with a non-relativistic theory in the limit around physical particles, I found a dispersion relation corresponding to a relativistic particle. It now makes sense that these excitations fulfill spin statistics and therefore describes spin 1/2 particles as seen above. This feature of a model quantized using spin 0 particles leading to particles of spin 1/2 is known as emergence of spin. Note that this is only possible since I considered a model explicitly breaking Lorentz invariance. (Looking at (10.1) the Hamilitonian is nonlocal). Because the theory was not Lorentz invariant particles are no longer required to transform in a particular representation of the Lorentz algebra characterized by their spin. This makes phenomena like the emergence of spin is possible.

One non-trivial test I can do in order to show that my particles really behave like spin 1/2 particles is to find the Berry phase. The Berry phase characterizes the phase change in the wavefunction as the state move along a close curve in parameter space. Using the spin algebra one can show that a free spin s particle will have Berry phase $2\pi s$. The following equation gives the Berry phase

$$\theta = \oint_C \langle\psi(t)|\,\frac{d}{dt}\,|\psi(t)\rangle \tag{10.9}$$

[2]The unusual form of eq. (10.8) is due to x_1 and x_2 not being orthogonal

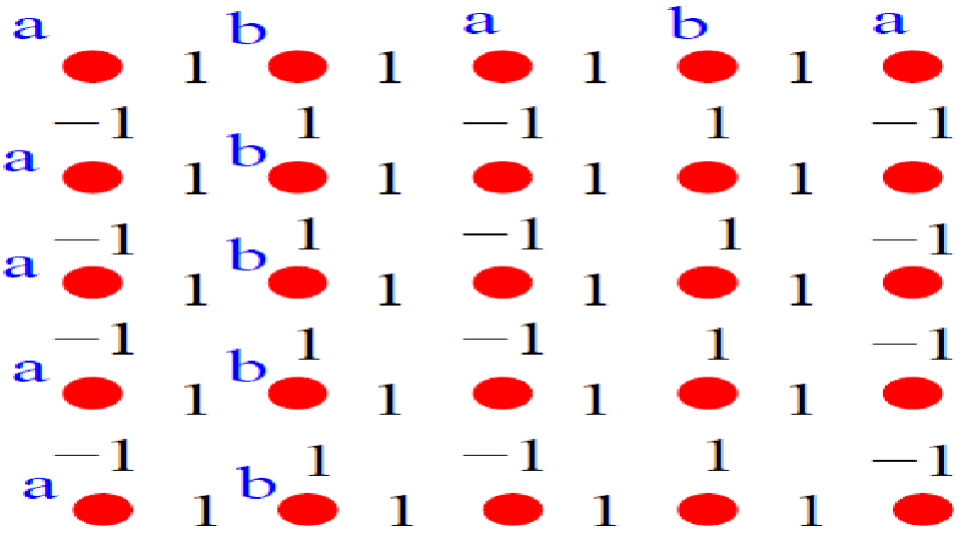

Figure 10.2: The square lattice: a and b are the atoms of the basis and the numbers are phase factors along a given link.

Looking at (10.6) I see that the nontrivial part of this integral is due to the complex square root. Complex analysis tells me that the square root has a branch cut corresponding to picking up a factor of -1 under a rotation. This can be seen by noting that $\sqrt{e^{i2\pi}} = e^{i\pi}$. This shows that Graphene has a Berry phase of π. Comparing with the theoretical $s2\pi$ I see that the interpretation of the excitations as massless spin 1/2 particles is consistent.

10.2 The Square Latice

The emergence of spin is not a unique effect for graphene, but a more general effect for a class of lattice models. I will now consider another model also having emergence of spin the model of a square lattice in a magnetic field. This section is based on [2] which also have a more general discussion of higher dimensional square lattice models and their connection to lattice q.c.d.

Like in the case of graphene it will prove prudent to start out with a discussion of the basis and structure of our lattice. I will consider a 2-d square lattice with a constant magnetic field transverse too the lattice. I consider a tight binding approximation with spin less fermions able to hop among the different sites of my lattice. Physics now depend on the fundamental flux around a primitive loop in my lattice $\frac{p}{q}$. Hofstadter solved the model for general magnetic field showing chaotic behavior at general values of the magnetic field. In this report I will however only consider the case $\frac{p}{q} = \frac{1}{2}$. When moving around a closed loop my wave function will pick up a phase factor $e^{i2\pi\frac{p}{q}} = -1$. Gauge freedom allows me to choose the phase along a given link at will as long as the phase around a closed loop remains invariant. I will make a gauge choice such that all horizontal links have phase factor 1 every second vertical line has phase factors 1 and every second phase factors -1. See fig. 10.2 for a depiction of lattice and phase factors. Since the columns have, different phase factors I now need to move two spaces in the x-direction in order to get to an equivalent site. This means my basis consist of two atoms that are horizontal neighbors. I denote the atom at -1 by a and the one at 1 by b see fig. 10.2.

I now proceed to diagonalize the Hamiltonian. Like the case of graphene this is best done by going to a momentum basis. Note however that I must move two sites in the x-direction to get to an equivalent site and only one in the y direction. Hence, my momentum in the x-direction can only be half the maximum size of the one in the y-direction. I choose unitless momenta defined like the ones for grapheen I have $0 \leq p_y < 2\pi$ and $0 \leq p_y < \pi$. The Hamiltonian can now be found by applying

the laws of electromagnetism and in a momentum basis $\psi = \begin{pmatrix} p_x \\ p_x \end{pmatrix}$ the Hamiltonian becomes

$$H = K \begin{pmatrix} 2cos(p_y) & 1 + e^{2ip_x} \\ 1 + e^{-2ip_x} & 2cos(p_y) \end{pmatrix}. \tag{10.10}$$

Diagonalizing the Hamiltonian is now trivial and I find eigenvalues

$$E = \pm 2K\sqrt{cos^2(p_x) + cos^2(p_y)}. \tag{10.11}$$

Looking at eq. (10.11) I see that like in the case of grapene this model characterized by two energy bands. The physical relevant region will be around the Fermi level at $E = 0$ there the energy bands meet. Looking at eq. (10.11) I see that this implies $cos(p_x) = cos(p_y) = 0$ with the above restrictions on the range of the momenta this equation has two solutions $p_x = \frac{\pi}{2}, p_y = \frac{\pi}{2}$ and $p_x = \frac{\pi}{2}, p_y = \frac{3\pi}{2}$. Just like in the case of graphene the energy bands meet at two different values of momenta. I interpret the states expanded around these points as spin up and spin down states and the model hence leads to the emergence of spin. Taylor expanding eq. (10.11) allows me to find the dispersion relation I get $E = \pm 2K\,|p|$ describing massless relativistic particles. So this is another case of a model of nonrelativistic spin zero fermions predicting relativistic, massless spin 1/2 fermions around the Fermi level.

10.3 Quantum Hall Effect

One of the interesting consequences of our above model is that it allows us to understand the Landau levels of graphene and hence it' s quantum Hall effect. In this section, I will start out by describing the classical Hall effect. I will when proceed by explaining and derivin the quantum Hall effect, finally using the above model for graphene I will look at how the, quantum Hall effect, manifests itself in the case of graphene. This section is based on [4]. This paper includes correct quantum mechanical derivation of all the results and discuss fractional quantum Hall effect. The semi classical derivation of the Landau levels is based on [3].

In order to explain the quantum Hall effect I first need to explain the classical Hall effect. Consider a two dimensional conducting system with a current in the x-direction. Apply a magnetic field in the z direction transverse to the system, see fig. 10.3. Due to the Lorentz force the electrons carrying the current will be bend in the y direction. This leads to a buildup of opposite charges on the two sides of the conductor. Until a steady state is reached where the electric force due to the buildup of charge precisely cancels the Lorentz force due to the magnetic field. The electric potential in the y direction can now be measured and I define the Hall resistance as $\rho_H = E_y/J_x$. ρ_H will in general be proportional to the magnetic field and in the case of a metal I get

$$\rho_H = -\frac{B}{ne}.^3 \tag{10.12}$$

I will now make a derivation of eq. (10.12). I am interested in the steady state solution $\frac{dp}{dt} = 0$. The effects that leads to a change in my particles trajectories are the electric force and scattering on the impurities of the material. Hence, I can express the change in momenta as

$$\frac{dp}{dt} = -e(E + \frac{p}{m} \times B) - \frac{p}{\tau} \tag{10.13}$$

The τ in eq. (10.13) is the average time between two scatterings. I introduce new constants $\sigma_0 = \frac{ne^2\tau}{m}$ and $\omega_c = \frac{eB}{m}$. σ_0 is known as the drude conductivity and describes the conductivity of a metal, ω_c is

[3]There is a sign choice in this this equation depending on the choice of coordinate system. I have here chosen the sign convention coincident with fig. 10.3 but opposite of [4]. In the sections where I discuss the quantum Hall effect I will use the opposite sign convention instead.

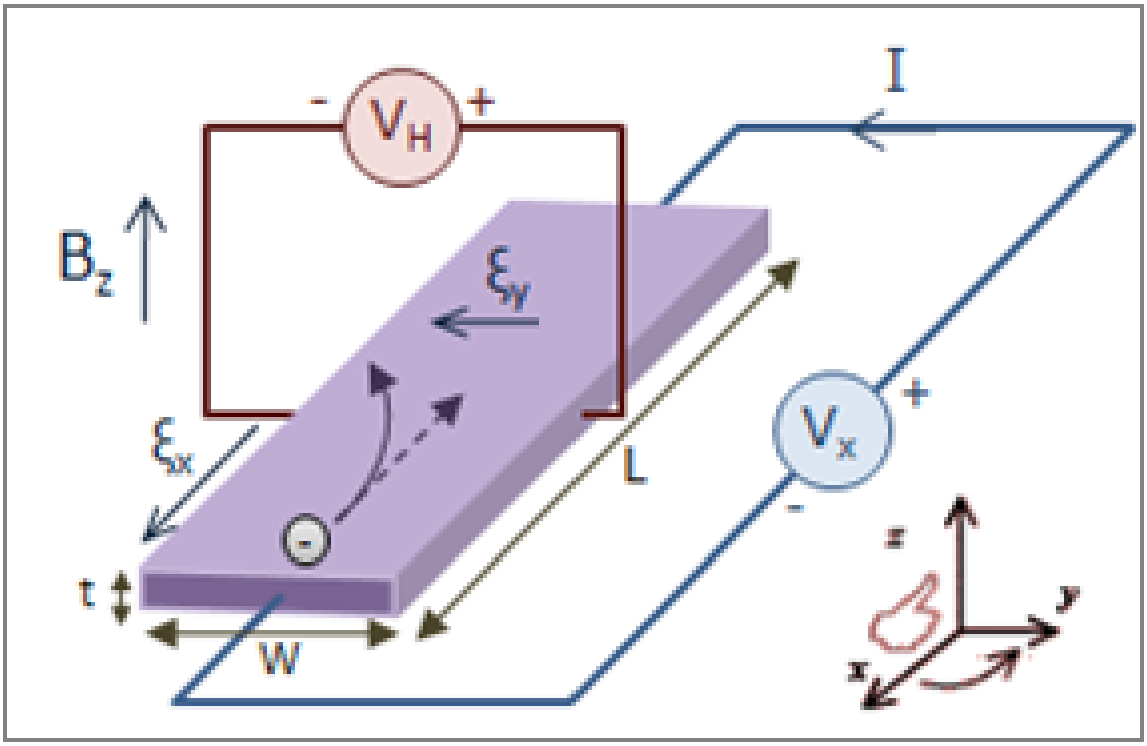

Figure 10.3: The classical Hall effect: Applying a magnetic field in the z direction for a system with a current in the x direction leads to an buildup of charge and hence electric potential in the y direction.

the cyclotron frequency and describes the angular frequency in the cyclic orbit predicted by classical electromagnetism for charged particles in a constant and uniform magnetic field. Since the velocity of a particle is $\frac{p}{m}$ and the charge density is $-en$ I can express the current as $J = -\frac{enp}{m}$. Isolating E in (10.13) and using amperes law $E = \rho j$ I get a matrix equation for ρ. Picking the right component gives me a formula for ρ_H.

$$E = \rho j = \frac{1}{\sigma_0}\begin{pmatrix} 1 & \omega_c\tau \\ -\omega_c\tau & 1 \end{pmatrix} J \Rightarrow \rho_H = -\frac{\omega_c\tau}{\sigma_0} = -\frac{B}{ne} \tag{10.14}$$

In the last section I showed that classical physics predicts a linear dependence between the Hall resistance and the applied magnetic field. However measuring at low enough temperatures and strong enough magnetic fields, this behavior is no longer observed see fig. 10.4. The observed behavior is instead rapid change followed by plateaus of constant resistance. Looking at the Hall conductance at a given plateau it always takes the value $n\frac{e^2}{\hbar}$ for integer n so conductance is quantized in quanta $\frac{e^2}{\hbar}$. This is a very precise result independent of geometry, material composition and impurities. This result is in fact that it is used as the operational standard for resistance.

In order to understand the above messurments I need 3 results. First I need to show that in a constant and uniform magnetic field free electrons will be divided into different energy levels known as Landau levels with energy

$$E_n = \hbar\omega_c(n + \frac{1}{2}). \tag{10.15}$$

Next I need the conductance of a full Landau level which is given as

$$G_n = \frac{e^2}{\hbar}. \tag{10.16}$$

Finally, I will need that the number of states in a Landau level increases with B. In particular one can show

$$N = \frac{Be}{h}A. \tag{10.17}$$

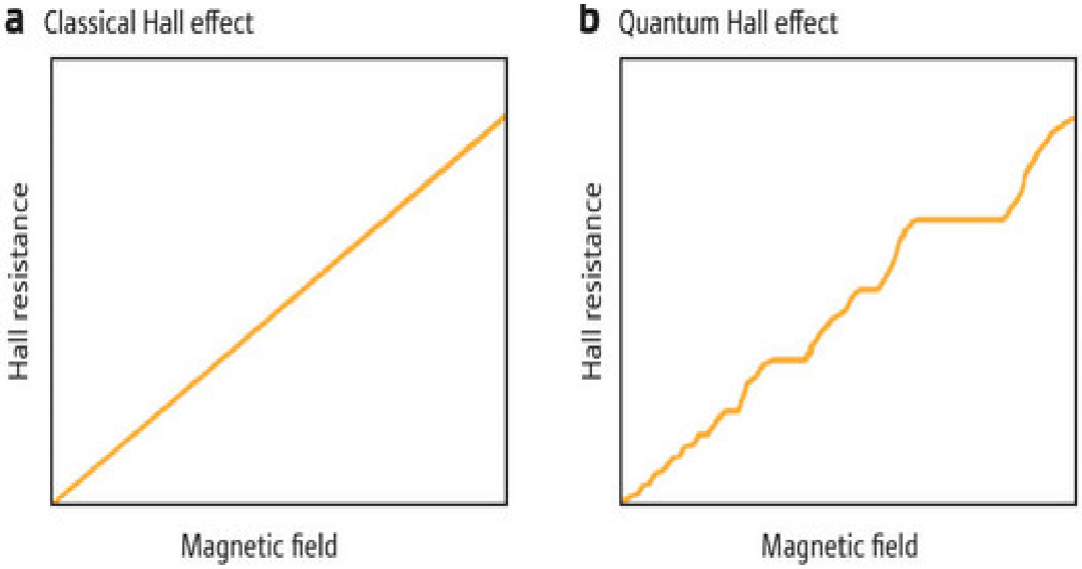

Figure 10.4: Comparing measured quantum Hall and predicted classical Hall effect. x-axis has magnetic field strength and y axis Hall resistance.

I will now give a semi classical argument for each of these results for a more thorough quantum mechanical derivation see [4].

I will start out by deriving eq. (10.15). In order to do this I will assume that the flux through a closed loop is quantized that is

$$\Phi = \frac{nh}{e}. \tag{10.18}$$

This formula can be derived starting from single valueness of the semi classical wave describing the electron $\oint dr\frac{p}{\hbar} = 2\pi n$. Splitting the covariant momenta up into regular momenta and magnetic vector potential and doing the integrals I end up with eq. (10.18) see [3] for more details. The classical motion is cyclic orbits at constant velocity. The flux is hence given by

$$\Phi = \pi r^2 B. \tag{10.19}$$

Since I have a cyclic orbit at constant velocity I can now find a formula for the momenta and using eq. (10.18) and eq. (10.19) I can remove the r dependence. Expressing everything in terms of the magnetic field B I get

$$p^2 = (\omega_c r m)^2 = \frac{\omega_c^2 nhm^2}{eB\pi} = \frac{eBnh}{\pi}. \tag{10.20}$$

Now I assume that my particle is a nonrelativistic massive particle and using the corresponding dispersion relation, I get an expression for the energy of the Landau levels.

$$E = \frac{p^2}{2m} = \frac{eBnh}{2\pi m} = n\hbar\omega_c \tag{10.21}$$

This is precisely the result stated in (10.15) up to the zero point energy. It is however to be expected that a semi classical approach will fail to consider this. Since the zero point energy is a purely quantum mechanical effect with no classical analogue. I will now do a trick that will allows me to predict the zero point energy not only for the free electron gas but amazingly also for graphene. Despite the two systems having different zero point energy. The trick is to go back to the original condition leading to quantization of flux and add π to the right hand side. This have the effect of substituting n for $n + \frac{1}{2}$ and hence gives the correct zero point energy.

I proceed to derive the conductance of a full Landau level eq. (10.16). Introducing states $|n, k\rangle$. Where n referes to the landau level and k is the wave vector. I can now express the total current

due to this Landau level as

$$I_n = -\frac{e}{L}\sum_k \langle n,k|\, v\, |n,k\rangle \tag{10.22}$$

Looking at a single term and calculating it' s contribution. I get

$$\langle n,k|\, v\, |n,k\rangle = \frac{1}{\hbar}\frac{\partial \epsilon_{n,k}}{\partial k} = \frac{L}{2\pi\hbar}\frac{\Delta\varepsilon_{n,m}}{\Delta m} = \frac{L}{h}\left(\varepsilon_{n,m+1} - \varepsilon_{n,m}\right). \tag{10.23}$$

In the first equality, I used the dispersion relation to calculate the velocity of my propagating wave. The second equality swap my wave number for a discreet index m describing the y position of my wave introducing the relevant normalization. The finale equality absorbs the 2π into $\hbar$ and write out the differences. Now I insert eq. (10.23) into eq. (10.22) allowing me to finish the calculation of I_n.

$$I_n = -\frac{e}{h}\sum_m \left(\varepsilon_{n,m+1} - \varepsilon_{n,m}\right) = -\frac{e}{h}\left(\mu_{max} - \mu_{min}\right) = \frac{e^2}{h}V \tag{10.24}$$

In the second equality I used the fact that the sum was telescoping reducing it to two terms. I then used that I am in a steady state situation so the energy of my particles are precisely the free energies. The finale equality used that the energy difference between different points is due to my electric potential. This means that for a steady state solution the difference in free energy will be the difference in potential energy, that is the electric potential times the charge. Using the result for the current it is now trivial to find the conductance and I get

$$G_n = \frac{I_n}{V} = \frac{e^2}{h}. \tag{10.25}$$

I will now argue for the finale result. Note that the radius of an orbit decreases as I increase the magnetic field strength. This can be seen either by studying the classical equation of motion or by looking at the quantization of flux. Hence, my orbit takes up less space and it makes sense that I can fit more of the same type of orbit into my constant area. That is the number of states in a landau level is proportional to the total area over the area of one orbit and hence increase linearly with B. Since the area of an orbit is inversely proportional to B.

Having "derived" the three results I can go on to explain how these results leads to the observed quantum Hall effect. If the temperature is low enough it will be the case that $K_B T << \hbar\omega_c$. This means that thermal fluctuation will be unable to excite higher Landau levels. The electrons will fill up the landau levels from the bottom leaving empty spots only in the top Landau level. Looking at eq. (10.17), I note that increasing the magnetic field strength leads to the number of states in the lower lying Landau levels increasing. This means electrons will jump from the highest Landau level to lower levels until this level is completely empty and the next level starts emptying. Since the contribution to conductivity from a full Landau level is always the same by eq. (10.16). The conductivity will decrease with the number of levels leading to an increasing Hall resistance. In order to understand fig. 10.4 I also need to explain the behavior of rapid changes followed by plateaus and the value of a plateau. Note that the electrons will not be a perfect free electron gas. Instead the impurities and lattice atoms of the material leads to small minima and maxima in the potential. Most of the electrons in a Landau level will orbit such minima hence they will be locale restricted to the position of the minimum. Since such electrons can't contribute to the macroscopic movement leading to a current, I can ignore them when looking at the conductivity. Only a tiny fraction of the electrons is actually able to contribute to the conductivity calculated in result 2. It is now possible understand the experimental results increasing the magnetic field leads to electrons jumping from the highest Landau level. First, the mobile electrons are removed leading to a rapid change in conductivity. When these are removed, only the locale electrons are left these do not contribute to the conductivity so the contribution corresponds to that of n filled Landau levels there n is the number of lower lying levels. By eq. (10.16) this is a constant $G = \frac{ne^2}{h}$ so the conductivity does not change leading to a plateau at conductivity $G = \frac{ne^2}{h}$ for some integer n.

Having consider the quantum Hall effect in general I will now look at the case of graphene. Going over the derivation of the Landau levels eq. (10.15), I note two differences for graphene. The first difference is the Berry phase this gives an extra π precisely canceling the one introduced to get a zero point energy. Hence, I make the prediction that graphene has no zero point energy. The second difference is the dispersion relation. Graphene's dispersion relation is linear instead of quadric. This leads me to predict a different n dependence using eq. (10.20) I predict the Landau levels

$$E = vp = \pm v\sqrt{2ne\hbar B} \tag{10.26}$$

The factor v is the constant factor in the dispersion relation. It can be interpreted as the velocity of my massless particle and depend on the lattice properties. This factor leads to the Landau levels having larger energy and hence the possibility for quantum Hall all the way up to room temperature. Another difference is that graphene being a semiconductor have both holes and electrons. Depending on the experimental setup, we can measure quantum Hall for electrons or for holes. Because the holes are positively charged their quantum Hall effect will have the opposite sign. Finally, I note that the Landau levels are four times degenerate two times due to the spin of the electron and two times due to the two expansion points. Hence my jumps in conductivity between different Landau levels will be $\frac{4e^2}{\hbar}$ instead of $\frac{e^2}{\hbar}$. Note that the ground state will have equal number of holes and electrons. Since the contribution from electrons and positrons cancel each other this level can at most contribute with half the normal level and I hence get the following formula for the conductivity at a plateau.

$$G_n = \frac{e^2}{h}\left(4n + 2\right). \tag{10.27}$$

Where n is an integer.

10.4 Bilayer Graphene

In this section, I will give a qualitative discussion of bilayer graphene. As the name suggest bilayer graphene has two graphene layers. I will look at how the formalism for monolayer graphene generalizes considering emergence of spin, Berry phase and quantum Hall effect. This section is based on [1]

Just like any other solid-state model, I need to understand the lattice structure of bilayer grapene in order to quantize it. Bilayer grapheen consist of two layers of Graphene stacked on top of each other. The properties depend on how this stacking is preformed. I introduce basis points in the top layer A_1, B_1 and in the bottom layer $A-2$ and $B-2$ defined as the basis for monolayer graphene in each layer. The stacking I consider is the AB stacking this means that the A basis atoms in the top layer is precisely over the B atoms in the bottom layer. While the top layer B atom and bottom layer A atom is displaced with respect to each other. See fig. 10.5

Now I can start quantizing my system I again consider spinless fermions with a nearest neighbor interaction. Since I have, four atoms in the basis I need a four by four matrix to describe the system. I go to a momentum basis and the quantitation for the two layers proceed just like the case of monolayer graphene. However, the system now have an interaction between the two layers. This is characterized by an exchange between the top A atom and bottom B atom. Note I ignore other exchanges between the layers since the other atoms are further apart and their contribution is therefore only a small correction. This leads to Hamiltonian

$$H = \begin{pmatrix} 0 & K_1 z & 0 & 0 \\ K_1 z^* & 0 & K_2 & 0 \\ 0 & K_2 & 0 & K_1 z \\ 0 & 0 & K_1 z^* & 0 \end{pmatrix}. \tag{10.28}$$

The introduced K_1 describes the interaction strength between atoms in a layer and K_2 the interaction strength between the layers. It is now simple to diagonalize the Hamiltonian and I find eigenvalues

$$E_{\pm}^{\alpha} = \pm\frac{K_2}{2}\left(\sqrt{1 + \frac{4K_1^2|z|^2}{K_2^2}} + \alpha\right) \tag{10.29}$$

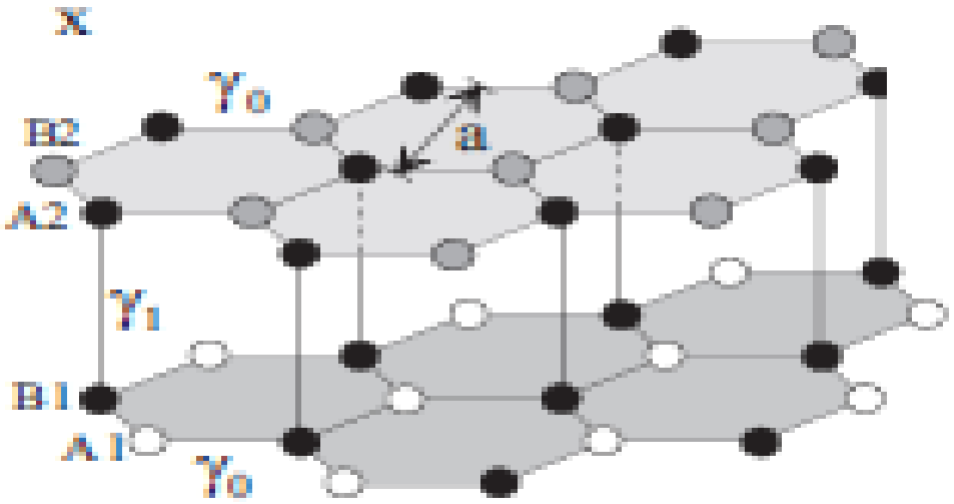

Figure 10.5: Bilayer graphene in the AB staking note the difference between A and B atoms in the top layer. A atoms have an atom directly below them this is not the case for B atoms.

The α introduced in the above equation is either 1 or -1 and describe the splitting in energy levels due to the perturbativ bilayer interaction. I see that the solution has four energy bands and since I now have four free electrons the lower two bands corresponding to negative energy will be full and the positive energy bands will be empty at T=0. In order to better understand eq. (10.29) I will now look at two limiting cases. First, consider the case $K_1^2|z|^2 >> K_2^2$. In this case, the interaction in the layers dominate the bilayer interaction and the bilayer interaction is viewed as a small perturbation. I can ignoring the 1 in the square root in this limit and find energies

$$E_{\pm}^{\alpha} \approx \pm \left(K_1|z| + \frac{K_2}{2}(\alpha + 1) \right). \tag{10.30}$$

I hence see a linear dispersion relation just like the one observed for monolayer graphene. The effect of the interaction is to split up my degenerate states with splitting K_2. This is exactly the behavior expected from perturbation theory. Now consider the case $K_1^2|z|^2 >> K_2^2$ here I can expand z and make the physical interpretation $K_1^2|z|^2 \approx v^2p^2$. Note that this case corresponds to the limit there the energy is close to zero and it is therefore the physically relevant regime. I again have expansion around $|z| = 0$ leading too two separate expansion points. Therefore, this model leads to the emergence of spin just like the monolayer model. Tayler expanding eq. (10.29) I find the energy

$$E_{\pm}^{\alpha} \approx \pm \left(\frac{v^2p^2}{K_2} + \frac{K_2}{2}(1 + \alpha) \right) \tag{10.31}$$

I am now going to discuss the Berry phase of bilayer graphene. Using calculations similar to the ones for monlayer graphene it is possible to show that bilayer graphene has Berry phase 0. One ad hock argument for this is to note that bilayer graphene consist of two layers of monolayer graphene. Ignoring the interaction between the layers the Berry phase is given as the sum of Berry phases that is $\theta = \pi + \pi = 2\pi = 0$ since the Berry phase is only defined mod 2π. Another adhock argument is to note that the excitations of graphene consist of two spin 1/2 particles. Hence the total spin is 0 or 1 and using the connection between spin and Berry phase I predict $\theta = 0$.

Finally, I am going to discuss the Landau levels of bilayer graphene. Since my excitation are now massive I expect an expression similar to the one found in eq. (10.15). This is the case for large n as the general n depends is

$$E_n = c\sqrt{n(n-1)}. \tag{10.32}$$

The n in the above equation is a non-negative integer and the c is a constant depending on the interaction strength. Note that $E_0 = E_1 = 0$ so the ground state is double degenerate. The

groundstate therefore have double the conductance of the one in monolayer graphene. This leads to the following formula for the conductance

$$G_n = \frac{e^2}{h} 4n \tag{10.33}$$

. The n is a non zero integer describing the relevant level.

10.5 Conclusion

In this report, I made an investigation of graphene's properties. Using the tight binding approximation, I considered a model of spinless fermions with nearest neighbor interaction. Expanding the spectrum around the Fermi energy, I found two solutions. This was interpreted as spin of a spin half particle. Looking at the dispersion relation, I saw that the excitation behaved like relativistic massless particles. The phenomena that a spin 0 lattice model led to spin 1/2 excitation in the physical limit was called emergence of spin. As a nontrivial test of this formalism I calculated the Berry phase finding the π expected for a free spin 1/2 particle. I when went on to consider a model sharing this emergence of spin. The model of a square lattice in a magnetic field. The same qualitative structure was found. Having done this I considered the quantum Hall effect. First I derived the classical Hall effect for a metal. I when showed how three simple results leads to the behavior observed in the quantum Hall effect giving semi classical derivations of each result. Finally, I considered graphene showing how the above model allowed me to predict Landau levels and the conductance at a plateau. I when considered bilayer graphene showing that this lattice model also had emergence of spin. But the bilayer interaction gave the electrons a mass and let to a band gap in the spectrum. I also stated the Berry phase given as 0. Finally, I considered the Landau levels noting that the groundstate was double degenerate leading to a slightly different conductance at each plateau. Continuing this work one could consider other staking schemes and the possibility of tuning the band gap. This naturally leads to a discussion of the many suggested applications of graphene. This direction is somewhat explored in [1]. Another direction is to consider the emergence of spin in more detail showing how this connect to the doubling of fermions in lattice models and discuss how the 3-d generalization of the square lattice leads to staggered fermions. This is discussed in [2], and is a topic of great interest in lattice qcd.

Bibliography

[1] Edward McCann *Electronic properties of monolayer and bilayer graphene* http://arxiv.org/pdf/1205.4849v1.pdf

[2] Michael Creutz *Emergent spin* http://arxiv.org/pdf/1308.3672v2.pdf

[3] Jiamin Xue *Berry phase and the unconventional quantum Hall effect in graphene* /n http://arxiv-web3.library.cornell.edu/pdf/1309.6714v1.pdf

[4] Mark O. Goerbig *Quantum Hall Effects* http://arxiv.org/pdf/0909.1998v2.pdf

Chapter 11

Skyrmions

Author: Urs Hähner
Supervisor: Jens Langelage

We review the Skyrme model which describes baryons as solitons of an effective meson theory. We start with a detailed discussion of the original two flavor Skyrme model where we derive expressions for the nucleon and delta masses which depend only on a single free parameter. We next discuss chiral symmetry in the context of QCD. Based on these considerations we construct the three flavor Skyrme model of pseudoscalars only. We then compute the mass spectrum of the low-lying $\frac{1}{2}^+$ and $\frac{3}{2}^+$ baryons which is within 10% of the experimental values. We also briefly discuss the inclusion of vector mesons and compare the three Skyrme model with pseudoscalars only and vector mesons included with experimental results using the example of the magnetic moment. The soliton description of baryons does not give highly accurate results but a good qualitative insight into the physics.

11.1 Introduction

The Skyrme model was proposed by Tony Hilton Royle Skyrme in 1961 [1] at a time when quarks did not yet "exist" and the theory of quantum chromodynamics (QCD) still had to be developed. In his approach to describe baryons, Skyrme provided a model based on just the pion fields. Baryons then emerge as solitons in this effective meson theory.
Solitons are solutions to the classical field equations with localized energy density and finite total energy. The finite total energy is regarded as the mass of these "particle-like" objects. However, the real characteristic property of solitons is that they have a topological structure which differs from the vacuum. These classical field configurations posses a non-vanishing, integral *topological charge* or *winding number*.
In the Skyrme model the solitons are called *Skyrmions* and the conserved topological charge is interpreted as the baryon number.

Today, QCD is well established as the fundamental theory of strong interaction, but there is still the need of exploiting models in order to describe the low-energy properties of baryons. The gauge coupling constant in QCD (figure 11.1) increases at the low energy scales which are relevant when one studies nucleons or other hadrons. Consequently, the application of perturbation theory, as e.g. in QED, is not possible at low energies. One must then either use lattice calculations or revert to models which are deduced or at least motivated from QCD.

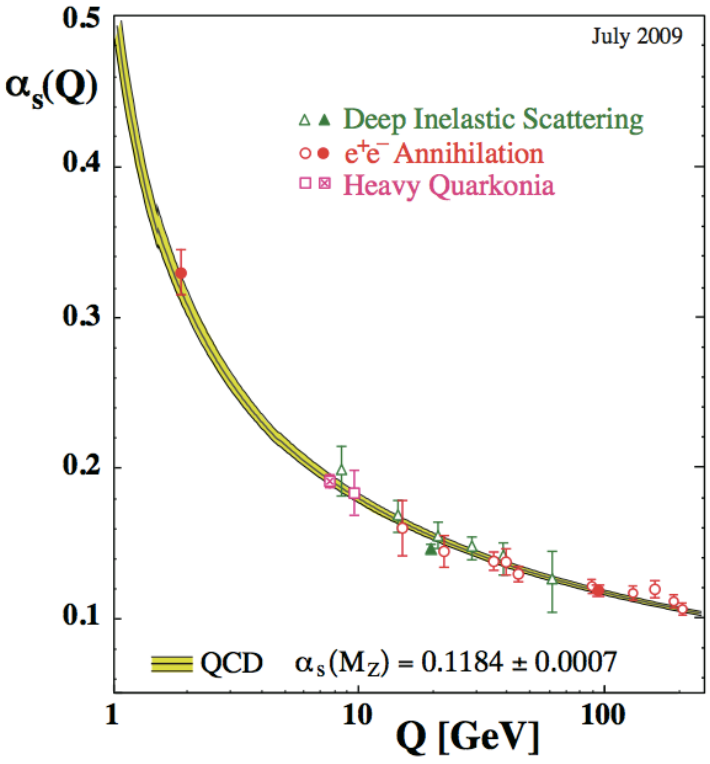

Figure 11.1: Summary of measurements of α_s as a function of the respective energy scale Q [8]. The coupling constant of QCD g is related to α_s via $\alpha_s = \frac{g^2}{4\pi}$.

When one models QCD one should certainly embed the correct symmetries of QCD. We will derive in section 11.3 that these consist of a $SU_{\mathrm{L}}(N_f) \times SU_{\mathrm{R}}(N_f)$ flavor symmetry and its spontaneous breakdown to $SU_{\mathrm{V}}(N_f)$, where N_f is the number of flavors. In addition, on should of course impose Lorentz invariance on the effective Lagrangian.
Interestingly, the Lagrangian chosen by Skyrme incorporates this though he was lead by three completely different motivations [2]: i) the idea of combining bosons (pions) and fermions (baryons) in a common model, ii) the feeling that point particles are inconsistent since their quantum field theory formulation introduces singularities which are only "swept under the rug" by the renormalization procedure and iii) the wish to eliminate fermions from a fundamental formulation since they have no simple classical analog.
Having Skyrme's motivations in mind we will introduce the original Skyrme model for two flavors in the next section and show how baryons emerge as solitons of this effective meson theory of pion fields only. In particular we will present rather detailed how one solves this model and ends up with the nucleon and delta masses. Thereafter in section 11.3, we will need to go through some theory of chiral symmetry and its breaking in QCD. Based on these symmetry considerations we will construct the Skyrme model for three flavors following the current justifications of the model. We will only briefly sketch the steps to solve the three flavor model but show some comparison of its predictions with experimental data. Section 11.5 gives a short summary of this report and adds some discussion.

11.2 The Skyrme model for two flavors

We start with the non-linear sigma model Lagrangian

$$\mathcal{L}_{\mathrm{nl}\sigma} = \frac{f_\pi^2}{4} \operatorname{tr}(\partial_\mu U \, \partial^\mu U^\dagger), \tag{11.1}$$

where $f_\pi = 93$ MeV is the pion decay constant. The "chiral field" $U(\mathbf{x},t) : \mathbb{R}^3 \times \mathbb{R} \to SU(2)$ is a matrix field and has the form

$$U(\mathbf{x},t) = \exp\left\{\frac{\sqrt{2}i}{f_\pi}\Phi(\mathbf{x},t)\right\}. \tag{11.2}$$

$\Phi(\mathbf{x},t)$ again is a 2×2 matrix containing the pion degrees of freedom and is given by

$$\Phi = \sum_{k=1}^{3}\phi_k\tau_k = \begin{pmatrix} \frac{1}{\sqrt{2}}\pi_0 & \pi^+ \\ \pi^- & -\frac{1}{\sqrt{2}}\pi_0 \end{pmatrix}, \tag{11.3}$$

where the τ_k's are the Pauli matrices. In particular, this implies that $i\Phi \in \mathfrak{su}(2)$ and therefore $U \in SU(2)$. We will later show that U transforms under the chiral group $SU_{\mathrm{L}}(2)\times SU_{\mathrm{R}}(2)$ according to

$$U \longrightarrow LUR^\dagger, \quad L,R \in SU(2). \tag{11.4}$$

Substituting (11.4) in $\mathcal{L}_{\mathrm{nl}\sigma}$, (11.1), one can easily check by using the cyclicity of the trace that the Lagrangian is indeed invariant under $SU_{\mathrm{L}}(2)\times SU_{\mathrm{R}}(2)$ flavor symmetry. As being a Lorentz scalar the non-linear sigma model Lagrangian, (11.1), is of course also Lorentz invariant.

In order to obtain a localized energy density the pion matrix Φ must vanish at spatial infinity. By definition this implies that U then needs to approach a constant value, which we can set to unity, i.e.,

$$U(\mathbf{x},t) \underset{|\mathbf{x}|\to\infty}{\longrightarrow} \mathbb{1}. \tag{11.5}$$

We can therefore regard our coordinate space $\mathbb{R}^3$ to be compactified to the three-sphere $\mathbb{S}^3$. In the case of only two flavors, the target space, $SU(2)$, is isomorphic to $\mathbb{S}^3$ and for fixed time we consider mappings $U(\mathbf{x}) : \mathbb{S}^3 \to \mathbb{S}^3$. These mappings fall into distinct equivalence classes of the third homotopy group $\pi_3(\mathbb{S}^3) \cong \mathbb{Z}$ [3]. The equivalence classes are therefore characterized by an integer which is referred to as the *winding number* or *topological charge* Q of the mapping $U(\mathbf{x})$. This number counts the coverings of the target space and for mappings $U(\mathbf{x}) : \mathbb{S}^3 \to \mathbb{S}^3$ is given by [4]

$$Q = \frac{1}{24\pi^2}\epsilon_{\nu\rho\sigma}\int_{\mathbb{R}^3}\mathrm{d}^3x\,\mathrm{tr}\left[\left(U^\dagger\partial^\nu U\right)\left(U^\dagger\partial^\rho U\right)\left(U^\dagger\partial^\sigma U\right)\right]. \tag{11.6}$$

The winding numbers are conserved by definition since they are integers which can not change under continuous time evolution. We identify them with the baryon number of the static field configuration $U(\mathbf{x})$.

The Euler Lagrange equations of motion for the chiral field $U(\mathbf{x})$ are highly non-linear partial differential equations. To simplify these equations Skyrme used the hedgehog *ansatz*

$$U(\mathbf{x}) = U_0(\mathbf{x}) \equiv \exp\left\{i\boldsymbol{\tau}\cdot\hat{\mathbf{x}}F(r)\right\}, \quad r = |\mathbf{x}|, \tag{11.7}$$

where $\boldsymbol{\tau}$ is a 3-vector whose entries are the Pauli matrices and the radial function $F(r)$ is called the "chiral angle". Due to the scalar product of $\boldsymbol{\tau}$ with the direction vector $\hat{\mathbf{x}}$ the hedgehog *ansatz* mixes rotations in coordinate and flavor space. Note that this will become a problem later when we want to quantize the hedgehog.
For this *ansatz* the Lagrangian, (11.1), yields the energy functional, $E = -\int \mathrm{d}^3x\,\mathcal{L}$,

$$E_{\mathrm{nl}\sigma}[F] = 2\pi f_\pi^2\int_0^\infty \mathrm{d}r\,\left(r^2F'^2 + 2\sin^2 F\right), \tag{11.8}$$

where a prime denotes the derivative with respect to the radial coordinate, r. One can easily show by a simple substitution of variables in (11.8) that

$$E_{\mathrm{nl}\sigma}[F(\lambda r)] = \frac{1}{\lambda}E_{\mathrm{nl}\sigma}[F(r)]. \tag{11.9}$$

This scaling behavior implies that $\mathcal{L}_{nl\sigma}$ can not give rise to any static, stable classical solutions, which can be seen by the following argument. Let us assume that $F_0(r)$ minimizes $E_{\mathrm{nl}\sigma}$. Then by substituting this solution into equation (11.9) and setting $\lambda = 2$ we obtain

$$E_{\mathrm{nl}\sigma}[F_0(2r)] = \frac{1}{2}E_{\mathrm{nl}\sigma}[F_0(r)] < E_{\mathrm{nl}\sigma}[F_0(r)], \tag{11.10}$$

which obviously contradicts the assumption that $F_0(r)$ minimizes $E_{\mathrm{nl}\sigma}$.
In order to obtain stable solitons Skyrme suggested the four derivate term,

$$\mathcal{L}_{\mathrm{Sk}} = \frac{1}{32e^2}\mathrm{tr}\left(\left[U^\dagger\partial_\mu U, U^\dagger\partial_\nu U\right]\left[U^\dagger\partial^\mu U, U^\dagger\partial^\nu U\right]\right), \tag{11.11}$$

which is only quadratic in the time derivatives. In (11.11) e is a free parameter, the dimensionless "Skyrme constant". In analogy to the non-linear sigma model Lagrangian one can compute the energy functional of the Skyrme term, E_{Sk}, and prove that it obeys

$$E_{\mathrm{Sk}}[F(\lambda r)] = \lambda E_{\mathrm{Sk}}[F(r)]. \tag{11.12}$$

Therefore, the total classical energy functional $E_{\mathrm{cl}}[F] = E_{\mathrm{nl}\sigma}[F] + E_{\mathrm{Sk}}[F]$ scales as

$$E_{\mathrm{cl}}[F(\lambda r)] = \frac{1}{\lambda}E_{\mathrm{nl}\sigma}[F(r)] + \lambda E_{\mathrm{Sk}}[F(r)]. \tag{11.13}$$

$E_{\mathrm{cl}}[F(\lambda r)]$ now can have a minimum at $\lambda = 1$ provided that $F(r)$ satisfies $E_{\mathrm{nl}\sigma}[F(r)] = E_{\mathrm{Sk}}[F(r)]$. Introducing the dimensionless coordinate $x = eF_\pi r$ we can write the classical energy functional as

$$E_{\mathrm{cl}}[F] = \frac{2\pi f_\pi}{e}\int_0^\infty \mathrm{d}x\,\left[\left(x^2F'^2 + 2\sin^2 F\right) + \sin^2 F\left(2F'^2 + \frac{\sin^2 F}{x^2}\right)\right], \tag{11.14}$$

where the prime now denotes the derivative with respect to x. As we require a finite energy density we necessarily need $F(\infty) = 0$. Plugging the hedgehog *ansatz*, (11.7), into equation (11.6) leads to

$$Q = \frac{F(0) - F(\infty)}{\pi} = \frac{F(0)}{\pi}. \tag{11.15}$$

Thus, in order for our Skyrmions to describe single baryons we need to satisfy the second boundary condition: $F(0) = \pi$. The chiral angle $F(r)$ restricted to these two boundary conditions, i.e. finite energy and unit baryon number, that minimizes the energy functional, (11.14), is obtained numerically. The result is shown in figure 11.2.

Since we want to describe baryons, which have spin and isospin, we have to assign good spin and flavor quantum numbers to the Skyrmion. In order to do so, we need to quantize its rotational degrees of freedom in coordinate and flavor space. However, as mentioned above, the hedgehog configuration, (11.7), mixes rotations in coordinate and flavor space and is invariant only under a combined spatial and flavor rotation but not with respect to either of them separately. This means that the Skyrmion *spontaneously* breaks the symmetries of the theory. To "restore" the symmetries we will use collective coordinates that transform the chosen ground state configuration, the hedgehog *ansatz*, (11.7), along the symmetries of the model. Since rotations in flavor and coordinate space are not broken completely but related via the hedgehog structure, we only need collective coordinates for one of the two symmetries. Our *ansatz* is to introduce a time-dependent $SU(2)$ matrix $A(t)$ which describes the spin and flavor orientation of the hedgehog. A time-dependent configuration is then approximated by

$$U(\mathbf{x}, t) = A(t)U_0(\mathbf{x})A^\dagger(t), \tag{11.16}$$

where $U_0(\mathbf{x})$ is the hedgehog *ansatz*, (11.7). This procedure will allow us to write down a Hamiltonian which we will diagonalize. The eigenstates with proper spin and isospin will then correspond to the

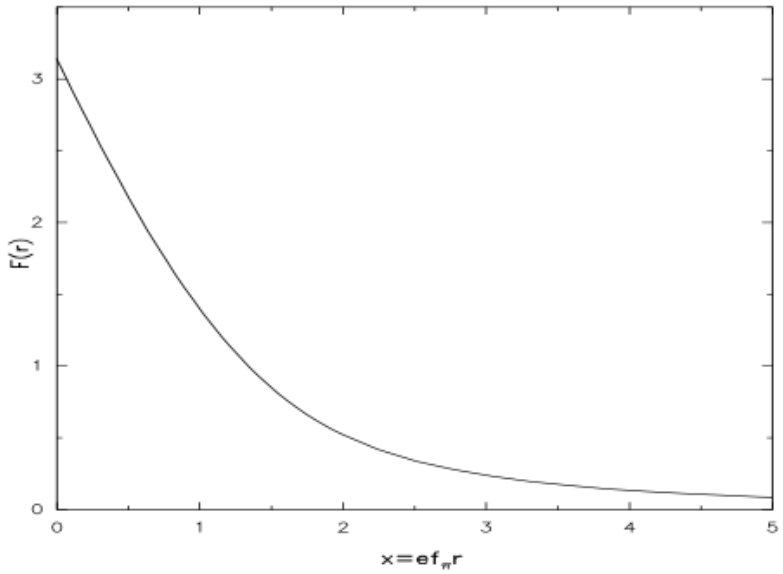

Figure 11.2: Numerical solution for the chiral angle $F(r)$ that minimizes equation (11.14) and fulfills the boundary conditions $F(0) = \pi$ and $F(\infty) = 0$ [4].

nucleon and the delta. Substitution of the time-dependent *ansatz*, (11.16), into the Skyrme model Lagrangian, $\mathcal{L}_{\mathrm{nl}\sigma} + \mathcal{L}_{\mathrm{Sk}}$, (11.1) and (11.11), integration over coordinate space and some algebra yields the Lagrange Function

$$L = -E_{\mathrm{cl}}[F] + \lambda[F] \operatorname{tr}\left(\frac{\partial}{\partial t} A(t) \frac{\partial}{\partial t} A^{\dagger}(t)\right), \tag{11.17}$$

where

$$\lambda[F] = \frac{8\pi}{3e^3 f_\pi} \int_0^\infty \mathrm{d}x\, x^2 \sin^2 F \left(1 + F'^2 + \frac{\sin^2 F}{x^2}\right). \tag{11.18}$$

The first term is just the negative of the classical energy functional. The second term is due to the collective coordinates and will be quantized. The $SU(2)$ matrix $A(t)$ can be parameterized as

$$A(t) = a_0(t)\mathbb{1}_2 + i \sum_{k=1}^{3} a_k(t)\tau_k, \tag{11.19}$$

with time-dependent, real coefficients $a_k(t)$ which obey the constraint $\sum_{k=0}^{3} a_k^2(t) = 1$. Plugging the parameterization (11.19) into equation (11.17) we find

$$\begin{aligned} L &= -E_{\mathrm{cl}} + \lambda \operatorname{tr}\left(\sum_{k=0}^{3} \dot{a}_k^2\, \mathbb{1}_2\right) \\ &= -E_{\mathrm{cl}} + 2\lambda \sum_{k=0}^{3} \dot{a}_k^2. \end{aligned} \tag{11.20}$$

By introducing the canonical momenta $\pi_k \equiv \frac{\partial L}{\partial \dot{a}_k} = 4\lambda \dot{a}_k$ we obtain the Hamiltonian

$$\begin{aligned} H &= \sum_{k=0}^{3} \pi_k \dot{a}_k - L \\ &= E_{\mathrm{cl}} + \frac{1}{8\lambda} \sum_{k=0}^{3} \pi_k^2, \end{aligned} \tag{11.21}$$

which still contains the classical energy functional. We can now apply the usual canonical quantization procedure ($\hbar \equiv 1$)

$$\pi_k \longrightarrow -i\frac{\partial}{\partial a_k} \tag{11.22}$$

and get

$$H = E_{\text{cl}} + \frac{1}{8\lambda}\sum_{k=0}^{3}\left(-\frac{\partial^2}{\partial a_k^2}\right). \tag{11.23}$$

Because of the constraint $\sum_{k=0}^{3} a_k^2(t) = 1$, the operator $\sum_{k=0}^{3}\left(\frac{\partial^2}{\partial a_k^2}\right)$ is to be interpreted as the Laplace operator ∇^2 on the three-sphere. In analogy to the Laplace operator on $\mathbb{S}_2$ its eigenfunctions are generalized spherical harmonics, i.e. traceless, symmetric polynomials in the a_k's. They are of the form $\Psi = (a_0 + ia_1)^s, s \in \mathbb{N}$, [3] and fulfill the eigenvalue equation

$$-\nabla^2\Psi = s(s+2)\Psi. \tag{11.24}$$

Using the spin and isospin operators [3]

$$\begin{aligned} I_k &= \frac{1}{2}i\left(a_0\frac{\partial}{\partial a_k} - a_k\frac{\partial}{\partial a_0} - \varepsilon_{klm}a_l\frac{\partial}{\partial a_m}\right), \\ J_k &= \frac{1}{2}i\left(a_k\frac{\partial}{\partial a_0} - a_0\frac{\partial}{\partial a_k} - \varepsilon_{klm}a_l\frac{\partial}{\partial a_m}\right), \end{aligned} \tag{11.25}$$

one can further prove that such an eigenfunction has spin and isospin $\frac{1}{2}s$.
Per construction of $U = AU_0A^\dagger$, A and $-A$ correspond to the same chiral field U. This fact might make one think that one should require $\Psi(-A) = \Psi(A)$. However, it turns out that there are two consistent ways to quantize the soliton [6]. Requiring $\Psi(-A) = \Psi(A)$ corresponds to quantizing the soliton as a boson, requiring $\Psi(-A) = -\Psi(A)$ leads to fermions. Since we want to describe baryons our wave functions must be polynomials of *odd* degree in the a_k's. Therefore, the nucleons ($I = J = \frac{1}{2}$) correspond to linear wave functions in a_k ($s = 1$), while the deltas ($I = J = \frac{3}{2}$) correspond to cubic wave functions in a_k ($s = 3$). For example the properly normalized wave functions for proton and neutron with spin up or spin down along the z-axis are given by [7]

$$\begin{aligned} |p\uparrow\rangle &= \frac{1}{\pi}(a_1 + ia_2), & |p\downarrow\rangle &= -\frac{i}{\pi}(a_0 - ia_3), \\ |n\uparrow\rangle &= \frac{i}{\pi}(a_0 + ia_3), & |n\downarrow\rangle &= -\frac{1}{\pi}(a_1 - ia_2). \end{aligned}$$

Going back to the Hamiltonian, (11.23), its eigenvalues are now given by

$$E = E_{\text{cl}} + \frac{1}{8\lambda}s(s+2), \tag{11.26}$$

where $s = 2J$. Thus, the nucleon ($J = \frac{1}{2}$) and delta ($J = \frac{3}{2}$) masses are given by

$$M_N = E_{\text{cl}} + \frac{1}{2\lambda}\frac{3}{4}, \quad M_\Delta = E_{\text{cl}} + \frac{1}{2\lambda}\frac{15}{4}. \tag{11.27}$$

Of course we still need to assign a value to our free parameter e, which hides not only in E_{cl} but is also part of λ. One usually adjusts e to fit the physical value of the pion decay constant, $F_\pi = 93$ MeV, and the empirical delta-nucleon mass difference, $M_\Delta - M_N \approx 293$ MeV, which according to equation (11.27) is predicted in the two flavor Skyrme model as $\frac{3}{2\lambda}$. The result is $e \approx 4.75$.
Having fixed e one can now compute a variety of baryon properties, e.g. the magnetic moment of the proton μ_p. However, the results are not very convincing. This is no surprise since our model is

still very simple containing only pseudoscalar mesons and two flavors. We can certainly improve the predictions of the model by including all three light flavors, i.e. up, down and strange. Until now we also neglected the effects of finite quark masses. In order to extend the Skyrme model to three flavors, we need to introduce some basic concepts of chiral symmetry in QCD. We can then start from scratch following the basic idea of contracting a model of meson fields which "mocks up" as many symmetries and properties of the QCD Lagrangian as possible and end up with the three flavor pseudoscalar Skyrme model. On our way we will also derive $\mathcal{L}_{nl\sigma}$ using this modern approach. Later we will also briefly discuss the inclusion of vector mesons which certainly improves the predictions of the model in the meson sector.

11.3 Chiral symmetry (breaking)

We start with the matter part of the QCD Lagrangian

$$\mathcal{L}_{\mathrm{QCD}}^{\mathrm{matter}} = \sum_{f=1}^{N_f} \left[\bar{q}_{f,\mathrm{L}} \left(i\partial\!\!\!/ + gA\!\!\!/ \right) q_{f,\mathrm{L}} + \bar{q}_{f,\mathrm{R}} \left(i\partial\!\!\!/ + gA\!\!\!/ \right) q_{f,\mathrm{R}} - m_f \left(\bar{q}_{f,\mathrm{L}} q_{f,\mathrm{R}} + \bar{q}_{f,\mathrm{R}} q_{f,\mathrm{L}} \right) \right]. \tag{11.28}$$

In equation (11.28) we have used the slash-notation, i.e. $A\!\!\!/ \equiv \gamma^\mu A_\mu$ and $\partial\!\!\!/ \equiv \gamma^\mu \partial_\mu$. In addition, $q_{\mathrm{L,R}} = \frac{1}{2}(1 \mp \gamma_5) q$ are the left-handed and right-handed projection of the the quark fields, A_μ is the matrix representation of the gluon fields and g is the coupling constant.
There are $N_f = 6$ flavors of quarks in nature, named up (u), down (d), strange (s), charm (c), bottom (b), and top (t), with masses $m_u \approx 5$ MeV, $m_d \approx 9$ MeV, $m_s \approx 120 - 170$ MeV, $m_c \approx 1.5$ GeV, $m_b \approx 4.5$ GeV, $m_t \approx 175$ GeV. In the low energy region up to about 1 GeV it is not possible to produce particles containing c, b or t quarks and we can therefore, in good approximation, drop them from our model. Furthermore, we neglect the u, d and s masses in a first approximation and include their effects later as a perturbation. The Lagrangian restricted to these approximations is then given by

$$\mathcal{L}_{\mathrm{QCD}}^{\mathrm{approx}} = \sum_{f=1}^{3} \left[\bar{q}_{f,\mathrm{L}} \left(i\partial\!\!\!/ + gA\!\!\!/ \right) q_{f,\mathrm{L}} + \bar{q}_{f,\mathrm{R}} \left(i\partial\!\!\!/ + gA\!\!\!/ \right) q_{f,\mathrm{R}} \right]. \tag{11.29}$$

It has the global chiral symmetry $U_{\mathrm{L}}(3) \times U_{\mathrm{R}}(3)$:

$$\begin{aligned} & q_{\mathrm{L}} \longrightarrow L\, q_{\mathrm{L}}, \quad q_{\mathrm{R}} \longrightarrow R\, q_{\mathrm{R}} \\ & \text{with} \quad q_{\mathrm{L,R}} = \begin{pmatrix} q_u \\ q_d \\ q_s \end{pmatrix}_{\mathrm{L,R}} \quad \text{and} \quad L, R \in U(3). \end{aligned} \tag{11.30}$$

Since this symmetry has $9+9 = 18$ generators, applying Noether's theorem yields eighteen conserved vector and axial vector currents

$$j_{ij}^\mu = \bar{q}_j \gamma^\mu q_i, \quad j_{ij,5}^\mu = \bar{q}_j \gamma^\mu \gamma_5 q_i \quad (i, j \in \{u, d, s\}). \tag{11.31}$$

However, not all Noether currents are necessarily conserved at the quantum level (anomaly) and indeed that is the case for the so called axial singlet current. Therefore, the true global symmetry of massless three flavor QCD is not $U_{\mathrm{L}}(3) \times U_{\mathrm{R}}(3)$ but $U_{\mathrm{V}}(1) \times SU_{\mathrm{L}}(3) \times SU_{\mathrm{R}}(3)$. The conserved charge corresponding to the $U_{\mathrm{V}}(1)$ symmetry,

$$q_{\mathrm{L,R}} \longrightarrow e^{-i\theta_{\mathrm{V}}} q_{\mathrm{L,R}}, \tag{11.32}$$

is the baryon number.
The symmetry of the physical states is further reduced by the "*spontaneous* breakdown" mechanism. The massless QCD vacuum forms a non-vanishing quark "condensate"

$$\langle \Omega | \bar{q}_u q_u + \bar{q}_d q_d + \bar{q}_s q_s | \Omega \rangle \neq 0. \tag{11.33}$$

Here $|\Omega\rangle$ denotes the QCD vacuum state. Under an infinitesimal chiral transformation

$$L = 1 + \frac{i}{2}\sum_{a=1}^{8}\epsilon_{\rm L}^a\lambda^a, \quad R = 1 + \frac{i}{2}\sum_{a=1}^{8}\epsilon_{\rm R}^a\lambda^a, \tag{11.34}$$

where the λ^a's are the Gell-Mann matrices (generators of $SU(3)$), the variation of the quark condensate, (11.33), is given by

$$\delta(\bar{q}q) = \sum_{a=1}^{8}(\epsilon_{\rm L}^a - \epsilon_{\rm R}^a)\,\bar{q}\lambda^a\frac{i}{2}\gamma_5 q. \tag{11.35}$$

Equation (11.35) shows that the condensate is invariant only under the vector type transformation $SU_{\rm V}(3)$ for which $L = R$ holds.
The $SU_{\rm V}(3)$ symmetry of massless QCD is further *explicitly* broken when we take into account the non-zero quark masses. The effect of the quark masses is included by adding to the Lagrangian the mass term

$$\mathcal{L}_{\rm QCD}^{\rm mass} = -\begin{pmatrix}\bar{q}_u & \bar{q}_d & \bar{q}_s\end{pmatrix}\begin{pmatrix}m_u & 0 & 0\\ 0 & m_d & 0\\ 0 & 0 & m_s\end{pmatrix}\begin{pmatrix}q_u\\ q_d\\ q_s\end{pmatrix} \tag{11.36}$$

$$= -\frac{m_u + m_d}{2}\bar{q}\mathcal{M}q \tag{11.37}$$

$$\text{with} \quad \mathcal{M} = \frac{2+x}{3}\mathbb{1} + y\lambda_3 + \frac{1-x}{\sqrt{3}}\lambda_8,$$

$$\text{where} \quad x = \frac{2m_s}{m_u + m_d}, \quad y = \frac{m_u - m_d}{m_u + m_d}.$$

Note that $\mathcal{L}_{\rm QCD}^{\rm mass}$ would be invariant under $SU_{\rm V}(3)$ if the quark masses were the same since in this case the mass matrix in equation (11.36) would commute with a rotation matrix in flavor space. The matrix $\mathcal{M}$ in equation (11.37) was introduced simply because it will show up in the next section.

To summarize our findings, low energy massless QCD is invariant under $SU_{\rm L}(3)\times SU_{\rm R}(3)\times U_{\rm V}(1)$ which is spontaneously broken to $SU_{\rm V}(3)\times U_{\rm V}(1)$. The $SU_{\rm V}(3)$ invariance is further explicitly broken by including the effects of the non-zero quark masses. Our goal now is to construct a model of meson fields which "mocks up" these properties of low energy QCD. Since we have already shown that conservation of the baryon number will also be incorporated by the topological structure of the Skyrmions, we can put this symmetry aside.

11.4 The Skyrme model for three flavors

We start with a general 3×3 matrix field M_{ij} and require that it transforms under $SU_{\rm L}(3)\times SU_{\rm R}(3)$ as the quark combination $q_{{\rm L},i}\bar{q}_{{\rm R},j}$, i.e.,

$$\begin{aligned} q_{{\rm L},i}\,\bar{q}_{{\rm R},j} &\longrightarrow (Lq_{\rm L})_i\,(\bar{q}_{\rm R}R^\dagger)_j = L_{im}q_{{\rm L},m}\,\bar{q}_{{\rm R}n}R^\dagger_{nj}\\ \Longrightarrow\ M_{ij} &\longrightarrow L_{im}M_{mn}R^\dagger_{nj}\\ \Leftrightarrow\ M &\longrightarrow LMR^\dagger. \end{aligned} \tag{11.38}$$

A chirally invariant Lagrangian is then given by

$$\mathcal{L} = \frac{1}{2}{\rm tr}(\partial_\mu M\partial^\mu M^\dagger) - V(M, M^\dagger), \tag{11.39}$$

where the potential V is a function of chirally invariant expressions like ${\rm tr}(MM^\dagger)$ or ${\rm tr}(MM^\dagger MM^\dagger)$. Spontaneous breakdown to $SU_{\rm V}(3)$ is implemented by choosing V to have a minimum such that $\langle M\rangle = const.\times\mathbb{1}$. Thus, the vacuum expectation value of M, $\langle M\rangle$, transforms as

$$\langle M\rangle = const.\times\mathbb{1} \longrightarrow const.\times LR^\dagger, \tag{11.40}$$

and is only invariant under the vector type transformation $SU_V(3)$ in agreement with equation (11.35). We now expand M around the vacuum solution by using the polar decomposition of M into a product of an hermitian and an unitary matrix $M = HU$ and setting $H = const. \times \mathbb{1}$ [4]. The first term of the Lagrangian, (11.39), then becomes

$$\frac{1}{2}\mathrm{tr}(\partial_\mu M\, \partial^\mu M^\dagger) \longrightarrow \frac{1}{2}\mathrm{tr}(\partial_\mu U\, \partial^\mu U^\dagger) = const. \times \mathcal{L}_{\mathrm{nl}\sigma}. \tag{11.41}$$

By definition, U transforms in the same way as M under $SU_\mathrm{L}(3) \times SU_\mathrm{R}(3)$:

$$U \longrightarrow LUR^\dagger. \tag{11.42}$$

It is now straightforward to show that also the Skyrme term $\mathcal{L}_\mathrm{Sk}$, (11.11), is invariant under (11.30). Being an unitary matrix, the chiral field U can be written as $U = phase \times \exp(i\Phi)$. Since we want U to describe pseudoscalar fields, Φ, we have to check the transformation under parity. We require

$$\Phi \xrightarrow{P} -\Phi, \tag{11.43}$$

which implies

$$U \xrightarrow{P} \exp(-i\Phi) = U^\dagger. \tag{11.44}$$

However, the Skyrme model Lagrangian, $\mathcal{L}_{\mathrm{nl}\sigma} + \mathcal{L}_\mathrm{Sk}$, (11.1) and (11.11), is invariant under (11.44) and $\mathbf{x} \longrightarrow -\mathbf{x}$ *separately*. To break this unwanted extra symmetry one needs to include at the level of the action the so called Wess-Zumino term [4]

$$\Gamma_\mathrm{WZ} = -\frac{iN_C}{240\pi^2}\int_{M_5} \mathrm{d}^5x\, \epsilon^{\mu\nu\rho\sigma\tau}\mathrm{tr}[\alpha_\mu\alpha_\nu\alpha_\rho\alpha_\sigma\alpha_\tau]. \tag{11.45}$$

Here N_C is the number of colors, $\alpha_\mu = (\partial_\mu U)U^\dagger$ and M_5 is chosen such that $\partial M_5 = M_4$, Minkowski space.
Finally, we must also incorporate the effects of the non-zero quark mass terms, (11.37). The minimal symmetry breaking part of the effective Lagrangian is given by [4]

$$\mathcal{L}_\mathrm{SB} = \mathrm{tr}\left\{\mathcal{M}\,\left[-\beta'\left(\partial_\mu U\, \partial^\mu U^\dagger\, U + U^\dagger\, \partial_\mu U\, \partial^\mu U^\dagger\right) + \delta'\left(U + U^\dagger - 2\right)\right]\right\}, \tag{11.46}$$

where the matrix $\mathcal{M}$ was introduced in equation (11.37) and β' and δ' are numerical parameters. In particular, the δ' term splits the pseudoscalar meson masses.
To summarize, we constructed the Skyrme model for three flavors by exploiting the symmetries of low energy QCD. The Lagrangian containing only pseudoscalar degrees of freedom is given by the sum of the non-linear sigma model Lagrangian, (11.1), the Skyrme term, (11.11), and the symmetry breaking mass term, (11.46). In addition, we have to add the Wess-Zumino term, (11.45), to the action.

In the three flavor case the chiral field U is a $U(1) \otimes SU(3)$ matrix and contains the degrees of freedom of the pseudoscalar meson nonet (figure 11.3). More precisely, it is given by

$$U(x) = \exp\left(i\frac{1}{\sqrt{3}F_\pi}\eta_0\right)\exp\left(i\Phi\right). \tag{11.47}$$

While the η_0 meson ($SU(3)$ singlet) is separated, the matrix field Φ now not only contains the three pion degrees of freedom but also the other five mesons of the $SU(3)$ octet, the four kaons and the η_8 meson. It is given by

$$\Phi = \sum_{a=1}^{8}\frac{1}{F_\pi}\phi^a\lambda^a = \begin{pmatrix} \frac{1}{\sqrt{2}}\pi^0 + \frac{1}{\sqrt{6}}\eta_8 & \pi^+ & K^+ \\ \pi^- & -\frac{1}{\sqrt{2}}\pi^0 + \frac{1}{\sqrt{6}}\eta_8 & K^0 \\ K^- & \bar{K}^0 & -\frac{2}{\sqrt{6}}\eta_8 \end{pmatrix}, \tag{11.48}$$

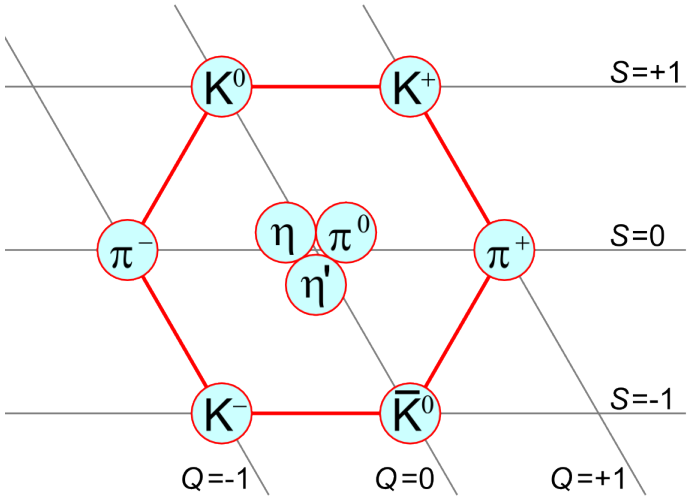

Figure 11.3: Pseudoscalar meson nonet [9]. η and η' are the observed particles which are linear combinations of the $SU(3)$ singlet state η_0 and the $SU(3)$ octet state η_8.

where the λ^a's are the Gell-Mann matrices.
In order to solve the three flavor Skyrme model one has to generalize the hedgehog *ansatz*, (11.7). It turns out that the correct generalization is simply given by the embedding of the $SU(2)$ hedgehog in the $SU(3)$ matrix [4],

$$U_0(\mathbf{x}) = \left(\begin{array}{cc|c} & & 0 \\ \exp(i\boldsymbol{\tau}\cdot\hat{\mathbf{x}}F(r)) & & 0 \\ \hline 0 & 0 & 1 \end{array}\right) . \tag{11.49}$$

In a similar manner as in the two flavor model one then introduces collective coordinates and quantizes the system. Instead of going into detail we will directly move on to the results which we can compare to empirical data.

As in the two flavor model there is a single parameter to fit, the Skyrme constant e. Adjusting it to

Baryons	Model	Experiment
$\Lambda - N$	154	177
$\Sigma - N$	242	254
$\Xi - N$	366	379
$\Delta - N$	278	293
$\Sigma^* - N$	410	446
$\Xi^* - N$	544	591
$\Omega - N$	677	733

Table 11.1: Mass differences of the $\frac{1}{2}^+$ and $\frac{3}{2}^+$ baryons in the three flavor pseudoscalar Skyrme model for $e = 4.0$ and the experimental values [4]. All values in MeV.

the mass differences of the low-lying $\frac{1}{2}^+$ and $\frac{3}{2}^+$ baryons yields $e \approx 4$. The resulting baryon spectrum is shown in table 11.4. We observe a 10% or better agreement with the experimental values which we characterize as good.
For a consistent overall picture the Skyrme model as an effective *meson* theory should not only give accurate predictions in the baryon sector but also in the meson sector. Certainly, the predictions within the mesonic sector are improved by including the vector mesons, at least with masses up to about 1 GeV. Of course the inclusion of vector mesons makes the model a lot more complicated. In particular, an additional parameter appears that can not be determined from meson properties but has to be guessed.

As mentioned above the Skyrme model not only predicts the baryon masses but also their static

B	μ (Sk)	μ (VM)	μ_{exp}	μ/μ_p (Sk)	μ/μ_p (VM)	$(\mu/\mu_p)_{\text{exp}}$
p	2.03	2.36	2.79	1	1	1
n	-1.58	-1.87	-1.91	-0.78	-0.79	-0.68
Λ	-0.71	-0.60	-0.61	-0.35	-0.25	-0.22
Σ^+	1.99	2.41	2.42	0.98	1.02	0.87
Σ^-	-0.79	-1.10	-1.16	-0.39	-0.47	-0.42
Ξ^0	-1.55	-1.96	-1.25	-0.76	–0.83	-0.45
Ξ^-	-0.64	-0.84	-0.69	-0.32	-0.36	-0.25

Table 11.2: Predictions of the three flavor Skyrme model of pseudoscalars only (Sk) [10] and including vector mesons (VM) [11] for the magnetic moments of the spin-$\frac{1}{2}$ baryons compared to the experimental values. Absolute values are in units of μ_N.

properties. These can be computed as matrix elements of the Noether currents. The way is straightforward but involves some lengthy and complicated computations. Again we do not want to go into detail. Instead we want to compare the predictions of the three flavor Skyrme model and the vector meson model with experimental data using the example of the magnetic moment μ. In table 11.2 we summarize the results for various baryons. We observe that the inclusion of vector mesons does not always improve the predictions. Neither of the two models gives highly accurate predictions. However, the magnitude and more importantly the sign of the predicted values is always correct.

11.5 Summary

It is worthwhile to stress that the Skyrme model is a model for describing baryons with only one free parameter, two when we include the vector mesons. Having fixed those, one can compute in principle any baryon property in the low energy regime. Aside from the baryon spectrum the soliton description allows us to study static properties of baryons, nucleon resonances, deep inelastic scattering and many more. Usually one does not end up with very accurate results, but gets a good qualitative insight into the physics of baryons in the low energy region. Even though the Skyrme model is more than 50 years old its soliton picture of baryons might still improve our understanding of the structure and dynamics of baryons.

Bibliography

[1] T.H.R. Skyrme, Proc. Roy. Soc. **A260** (1961) 127.

[2] T.H.R. Skyrme, Int. J. Mod. Phys. **A3** (1988) 2745.

[3] I. Zahed and G.E. Brown, Physics Reports **142** (1986) 1.

[4] J. Schechter and H. Weigel, arXiv:hep-ph/9907554.

[5] H. Weigel, *Chiral Soliton Models for Baryons*, Springer-Verlag Berlin Heidelberg, 2008.

[6] D. Finkelstein and J. Rubinstein, J. Math. Phys. **9** (1968) 1762.

[7] G.S. Adkins, C.R. Nappi, E. Witten, Nucl. Phys. **B228** (1983) 552.

[8] S. Bethke, arXiv:0908.1135 [hep-ph].

[9] Wikipedia, *Pseudoscalar meson* [Online] 19 April 2014, `http://en.wikipedia.org/wiki/Pseudoscalar_meson`.

[10] N.W. Park, J. Schechter and H. Weigel, Phys. Rev. **D43** (1991) 869.

[11] N.W. Park and H. Weigel, Nucl. Phys. **A541** (1992) 453.

Chapter 12

$U(1)$ Monopoles

Author: Alice Chau
Supervisor: Johannes Broedel

Although magnetic monopoles have not been observed in Nature so far, their hypothetical existence could lead to the quantization of the electric charge. We will discuss here Dirac's assumption and result which he obtained by slightly modifying Maxwell equations and satisfying physical consistency. We will show that in this context, the vector potential can not be globally and uniquely defined but needs at least two functions. We will explicitly construct it and express it using the language of the fibre bundle, essentially following the work of Wu-Yang. In both approaches, Dirac quantization will show up naturally, from the continuity of the gauge transformation and uniqueness of the transition function respectively. We will conclude by a few remarks on the properties of the Dirac monopole.

12.1 Dirac Monopole

12.1.1 Maxwell equations

In the 19^{th} century, Maxwell achieved to unify the description of electricity and magnetism in a concise way. We briefly recall his celebrated four equations:

$$\vec{\nabla}\cdot\vec{E}=\rho, \qquad \vec{\nabla}\cdot\vec{B}=0,$$
$$\vec{\nabla}\times\vec{E}+\frac{\partial}{\partial t}\vec{B}=0, \qquad \vec{\nabla}\times\vec{B}-\frac{\partial}{\partial t}\vec{E}=\vec{j}.$$

In those equations, however, the electric and magnetic fields are not treated symmetrically: the latter is free of divergences and thus does not admit any monopoles, but only dipoles. In order to restore the symmetry between both fields, Dirac assumed in 1932 that the magnetic field behaves in the same way as the electric one by considering the existence of magnetic monopoles which requires to take the divergence of the magnetic field to be different from zero.

12.1.2 Basics about a magnetic monopole

Consider a point-like magnetic monopole of strength g conveniently located at the origin. Its magnetic field is written by analogy with the electric field of a point electric charge. Thus:

$$\vec{B} = \frac{g}{r^3}\vec{r} \tag{12.1}$$

$$= \frac{g}{r^2}\mathbf{e_r}, \tag{12.2}$$

where $\vec{r}$ is the distance vector and $\mathbf{e_r}$ the radial unit vector.
By taking the divergence of $\vec{B}$ and using $\vec{\nabla}^2\left(\frac{1}{r}\right) = -4\pi\delta^3(r)$, we immediately verify that the divergence is different from zero and corresponds to the magnetic charge density of a point particle:

$$\vec{\nabla}\cdot\vec{B} = \vec{\nabla}\cdot\left((-g)\vec{\nabla}\left(\frac{1}{\vec{r}}\right)\right) \tag{12.3}$$

$$= 4\pi g\delta^3(\vec{r}). \tag{12.4}$$

As the magnetic monopole is assumed to be a point object, it therefore has a spherical symmetry. In order to study the magnetic flux around the monopole and take care of this symmetry, we consider a sphere of radius r.

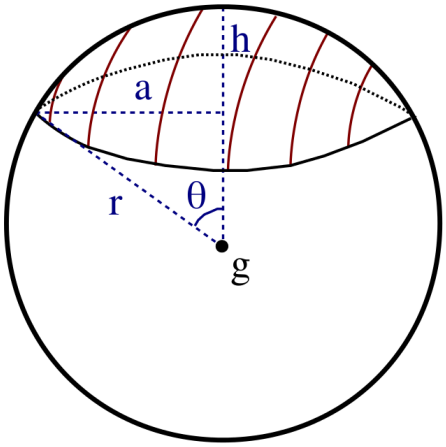

Figure 12.1: The cap is parametrized by a and h, or equivalently r and θ

Let us take the surface of a cap of it: $\pi(a^2+h^2)$ where a is the radius of the cap and h its height (see figure 12.1). The magnetic flux induced by the monopole through the cap reads:

$$\Phi(r,\theta) = \int \vec{B}\,d\vec{s} \tag{12.5}$$

$$= \frac{g}{r^2}\pi(a^2+h^2). \tag{12.6}$$

We have not yet expressed the surface in terms of the spherical coordinates but we will do so later when constructing the vector potential $\vec{A}$. Let us also write the relation between the latter and the flux:

$$\Phi = \int \vec{B}\,d\vec{s} \tag{12.7}$$

$$= \int \vec{\nabla}\times\vec{A}\,d\vec{s} \tag{12.8}$$

$$= \oint \vec{A}\,d\vec{l}, \tag{12.9}$$

where we expressed $\vec{B}$ as the curl of its vector potential $\vec{A}$ in the second line and applied Stokes theorem in the last equation.
Let us go back to the sphere and place ourselves on top of it: the surface of the cap is a point and the magnetic flux is equal to 0. If θ is increased, the cap encloses more and more surface and so more and more flux. When we reach the South Pole, i.e. $\theta = \pi$, we have englobed the whole sphere and expect $\Phi = 4\pi r^2 B = 4\pi g$. But by looking at the loop, we note that it has shrunk to a point again. Thus, from (12.9), $\vec{A}$ has to be singular at $\theta = \pi$ because of the requirement that the flux is finite. As we took a sphere of arbitrary radius, this holds for every radius. As a consequence, $\vec{A}$ is singular along the whole negative z-axis, which is the so-called Dirac string. Is this a physical singularity? Rotate the shell and the Dirac string will look different depending on the choice of coordinates. By the same argument, it does not need to be straight. The Dirac string is therefore a *coordinate* singularity. However one point does never change up to rotation: the origin. Only at this point, there exists a real and physical singularity.

12.1.3 Wavefunction and Dirac quantization

Let us recall the wavefunction of a free particle:

$$\Psi_{free} = |\Psi|\, e^{\frac{i}{\hbar}(\vec{p}\vec{r} - Et)}. \tag{12.10}$$

For a particle with charge e in a magnetic field, the momentum changes as $\vec{p} \to \vec{p} - \frac{e}{c}\vec{A}$. Indeed, under this prescription the corresponding Lagrangian reads $L = \frac{1}{2}m\dot{\vec{r}}^2 + \frac{e}{c}\vec{A}\dot{\vec{r}}$ and the corresponding equation of motion describes particles submitted to a Lorentz force.
Thus, the wavefunction of the charged particle in the field of the monopole is given by:

$$\begin{aligned} \Psi &= |\Psi| \exp\Big(\frac{i}{\hbar}(\vec{p}\,\vec{r} - \frac{e}{c}\vec{A}\,\vec{r} - Et)\Big) && (12.11)\\ &= |\Psi|_{free} \exp\Big(-i\frac{e}{\hbar c}\vec{A}\,\vec{r}\Big). && (12.12) \end{aligned}$$

Equivalently, the phase of the wavefunction changes as $\alpha \to \alpha - \frac{e}{\hbar c}\vec{A}\vec{r}$.
Consider a charged particle moving on the sphere along a circular path. At fixed r and θ and for $\varphi \in [0, 2\pi)$, the phase changes as

$$\begin{aligned} \Delta\alpha &= \frac{e}{\hbar c}\oint \vec{A}\, d\vec{l} && (12.13)\\ &= \frac{e}{\hbar c}\Phi(r,\theta), && (12.14) \end{aligned}$$

where we used the same steps as for the result (12.9).
Each time the particle crosses the circle, the wavefunction appears to be multivalued since it acquires an extra phase. However, physical consistency requires it to be single-valued everywhere. Thus, the phase change of the wavefunction must be an integer multiple of 2π. Note also that if the path encircled the Dirac string, the latter could be detected. The requirement for the string to be unobservable yields the same condition for the phase change:

$$\Delta\alpha = 2\pi n. \tag{12.15}$$

We use (12.14) at $\theta = \pi$:

$$\frac{e}{\hbar c}4\pi g = 2\pi n, \tag{12.16}$$

and rewrite it in the following form:

$$e = \frac{n\hbar c}{2g}. \tag{12.17}$$

This is the Dirac quantization condition. The appearance of $\hbar$ in this expression makes the electric charge explicitly depend on the quantum theory. This is the most important consequence of the existence of magnetic monopoles. Note that a single monopole is sufficient to guarantee this condition. Was there a magnetic monopole anywhere in the Universe, the electric charge would be quantized.

Dirac veto

The coordinate singularity in the vector potential at $\theta = \pi$ also gives rise to an undetermined phase of the wavefunction at this point. But we have to guarantee that a charged particle can not be found along the negative (positive respectively) z-axis, where we have this singularity. (The pictorial analogy would be to avoid the particle to hit the solenoid attached to the monopole at the origin, see the Wu-Yang construction). Thus, we require a zero probability of finding the particle at the Southern (Nothern respectively) pole and therefore we *impose* the vanishing of the wavefunction at this point. This is the so-called Dirac veto.

12.2 Wu-Yang Monopole

To get rid of the coordinate singularity in the vector potential $\vec{A}$, we have to give up the idea of a unique and global description of it. Instead, we define two vector potentials covering a different domain of the sphere, each regular on its region, and adjust them on the overlap region. In this section we explicitly construct $\vec{A}$ and show how the Dirac quantization appears in this context. We also briefly explain how this can be formalized in terms of fiber bundles.

12.2.1 Construction of the vector potential

We divide the sphere surrounding the monopole in two domains: the Northern and the Southern hemispheres with the equator as the overlap region. We call them R^+ and R^- respectively and the corresponding vector potentials A^+ and A^-, that we naturally express in spherical coordinates.
Let us begin with A^+. As the magnetic field is radial, see (12.2), only the radial component of the curl of $\vec{A}$ is of interest:

$$(\vec{\nabla} \times \vec{A})_r = \frac{1}{r \sin\theta} \left(\frac{\partial}{\partial\theta}(\sin\theta\, A_\varphi) - \frac{\partial}{\partial\varphi} A_\theta \right), \tag{12.18}$$

but by symmetry, the potential can not depend on φ. We deduce that it only can have the form: $\vec{A} = A_\varphi(r,\theta)\mathbf{e}_\varphi$, where $\mathbf{e}_\varphi$ is the unit vector in the φ-direction.
Ultimately, we want to use the same steps as for the result (12.9), i.e. the relation

$$\int \vec{B}\, d\vec{s} = \oint \vec{A}\, d\vec{l} \tag{12.19}$$

to derive the vector potential. Let us then find the form of the magnetic field. Take a magnetic dipole and place one extremity at the origin and the other one at the negative infinity. The latter is far away enough to not influence what happens at the origin. This construction makes sense with respect to the domain of definition of the vector potential: since $\vec{\nabla} \cdot \vec{B} \neq 0$, $\vec{A}$ cannot be defined on the whole space $\mathbb{R}^3$ and we have just excluded the Dirac string by defining $\vec{B}$ on it. Let us write this magnetic field as the one of a magnetic monopole to which we attach an infinitely long solenoid along the negative z-axis:

$$\vec{B} = \frac{g}{r^2}\mathbf{e}_r + g\Theta(-z)\delta(x)\delta(y)\mathbf{e_z}, \tag{12.20}$$

where Θ is the Heavyside function.
We express the surface of the cap in spherical coordinates is: $\pi(a^2 + h^2) = \pi(2r^2 - 2r^2\cos\theta)$ (see figure 12.1). Let us rewrite (12.19) in terms of all the known quantities:

$$\frac{g}{r^2}\pi(2r^2 - 2r^2\cos\theta) = 2\pi r \sin\theta A_\varphi. \tag{12.21}$$

We finally obtain

$$A_\varphi = \frac{g}{r}\frac{1-\cos\theta}{\sin\theta}. \tag{12.22}$$

For A^-, the same steps are repeated with a dipole that is stretched between the positive infinity and the origin and the coordinate transformation $\theta \to \pi - \theta$.

Let us summarize our results: $\vec{A}$ is given by:

$$A_\varphi^+ = \frac{g}{r}\frac{1-\cos\theta}{\sin\theta} \qquad \text{in the domain } R^+ \tag{12.23}$$

$$A_\varphi^- = -\frac{g}{r}\frac{1+\cos\theta}{\sin\theta} \qquad \text{in the domain } R^-. \tag{12.24}$$

Singularities do not show up in this constructions as both functions are finite on their own domain. Still, we need to study them on the equator, the overlap region. Their difference can be expressed as a gauge transformation because of the $U(1)$ gauge freedom of the electrodynamics. Indeed the vector potential $\vec{A}$ and the scalar potential ϕ are non-physical degrees of freedom whereas $\vec{B}$ and $\vec{E}$ are physical ones. A transformation $\begin{cases} \vec{A} \to \vec{A} + S\vec{\nabla}S^{-1} \\ \phi \to \phi - S\frac{\partial}{\partial t}S^{-1} \end{cases}$ can be performed since it leaves the fields $\vec{B}$ and $\vec{E}$ invariant. S is a scalar function.
The two functions of the vector potential of the monopole are related via:

$$A_\varphi^- = A_\varphi^+ - \frac{2g}{\sin\theta} \tag{12.25}$$

$$= A_\varphi^+ - \frac{i}{e}S\vec{\nabla}_\varphi S^{-1}, \tag{12.26}$$

with $S = e^{2ige\varphi}$ and $\hbar = c = 1$. We have to ensure the continuity of the gauge transformation. Otherwise we would let a fitting function have a jump, which we do not want. This means that the function S has to be single-valued when $\varphi \to \varphi + 2\pi$. This requirement is equivalent to the Dirac quantization condition. Indeed:

$$e^{2ige(\varphi+2\pi)} \stackrel{!}{=} e^{2ige\varphi} \qquad \Rightarrow \qquad 2ge\,2\pi = 2\pi n. \tag{12.27}$$

In other words, this condition arises with the non-triviality of the gauge transformation.

12.2.2 Construction of the fibre bundle

A brief definition of a fibre bundle is provided here. For further details, readers are invited to consult the 9th and 10th chapters of ref. [2].

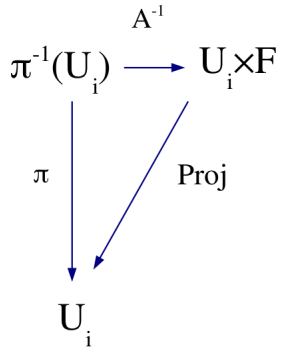

Figure 12.2: Definition domains of a fibre bundle

Conceptually, a fibre bundle is the construction suited for topological spaces that look *locally* like the direct product of two spaces. Take a **total space** E that we wish to write as the direct product

of a **base space** M and a **fibre space** F. E, M and F are manifolds, i.e. topological spaces that look *locally* like flat. They can be deformed continuously, and locally, to $\mathbb{R}^n$; they are said to be homeomorphic to $\mathbb{R}^n$ locally. Since M is generally not homeomorphic to $\mathbb{R}^n$ globally, it needs a set of covering $\{U_i\}$ to be described entirely. Thus, more precisely, we wish to express a subspace of E as the direct product of a covering U_i and F. This is achieved in the following way: there exists a natural projection from $U_i \times F$ to U_i (see figure 12.2). We define a **projection** π from E to U_i such its inverse image $\pi(U_i)$ is diffeomorphic to the direct product $U_i \times F$, diffeomorphic meaning that the space can be deformed to the other smoothly.
Let us study more carefully what happens at each point of the fibre bundle. π projects a element u of E into a point p of M. The inverse image $\pi^{-1}(p) \equiv F_p$ is called the fibre at p. We define a diffeomorphism $A_i : U_i \times F \to \pi^{-1}(U_i)$, called the **local trivialisation** and associated to the covering U_i. A_i is the key function since its inverse takes an element u and express it onto the direct product of an element p and a fibre f, thus $A_i^{-1}(u) = (p, f)$.
Take a point p of M that is described by two coverings U_i and U_j, i.e. $U_i \cap U_j \neq \emptyset$. We write the associated local trivialisations $A_i(p, f) = A_{i,p}^{-1}$. We need transition functions t_{ij} to describe how the fibre element behaves when we pass from a covering to the other one. We require that t_{ij} belongs to the **structure group** G, the Lie group which acts on F on the left. Therefore:

$$t_{ij}(p) = A_{i,p}^{-1} A_{j,p}. \tag{12.28}$$

Let us now study the magnetic monopole as a fibre bundle. The base space M is the sphere S^2 on which we define the vector potential. At each point of S^2, we attach a circle, $U(1) = S^1$ due to the local gauge invariance of $\vec{A}$. In our case, the fibre $U(1)$ is already a Lie group and it naturally acts on itself. Therefore the fibre is identical to the structure group, $F = G = U(1)$.
A sphere has at least two coverings. Indeed, take a point on the sphere and join it to the North Pole. Continue in a straight line and intersect the equatorial plane. The point has been projected from the North Pole onto this plane. This is possible for all points except the North Pole. Therefore we need at least a second projection from the South Pole to cover the whole sphere. It is the so-called stereographic projection. Let us take again the conventional choice of the Northern and the Southern hemispheres, R^+ and R^-, on which A^+ and A^- are defined.
In the context of the fibre bundle, we identify the vector potential to be the local trivialisation. Indeed its functions need to be adjusted on an overlap region. A^+ and A^- are functions of a point p of the sphere and a phase, an element f of the fibre attached at p:

$$A_+ = A_+(p, f) = A_+((\theta, \varphi), e^{i\alpha_+}) \tag{12.29}$$
$$A_- = A_-(p, f) = A_-((\theta, \varphi), e^{i\alpha_-}). \tag{12.30}$$

On the equator, we explicitly construct the transition functions from the relation (12.28):

$$t_{+-} = A_+^{-1} A_- \tag{12.31}$$
$$= e^{-i\alpha_+} e^{i\alpha_-}. \tag{12.32}$$

Let us take a transition function t_{+-} of the form $e^{in\varphi}$, where n must be an integer so that the function is uniquely defined. Explicitly, there is a correspondence between $\varphi = 0$ and $\varphi = 2\pi$:

$$\varphi = 0 : \quad e^{i\alpha_-} = e^{i\alpha_+} \tag{12.33}$$
$$\varphi = 2\pi : \quad e^{i\alpha_-} e^{i\Delta\alpha} = e^{i2\pi n} e^{i\alpha_+}. \tag{12.34}$$

This holds if $\Delta\alpha = 2\pi n$, which is the Dirac quantization. In the context of homotopy theory, one can show that n, which characterizes the monopole charge, is a winding number too. The latter counts how many times the image of S^1 winds the space $U(1)$. Therefore it tells us how the transition function twists the local pieces of the bundle when glued together. If $n = 0$, the fibre bundle is

trivial, i.e. the direct product $M \times F$ globally. A trivial topology corresponds to the case where there is no magnetic monopole, consequently $n = 0$ is excluded in our case. It is remarkable that the topological structure of the fibre bundle of the monopole is characterised by an integer that is directly related to its strength $2g$.

12.3 Searches for Dirac Monopoles

Current researches are conducted in cosmology, particle physics and geophysics. To date there exist no confirmed observations of magnetic monopoles. In 1975, Price *et al.* announced the detection of a moving magnetic monopole through a cosmic ray track etched in a plastic detector but Alvarez refuted the interpretation a few months later. The other well-known discovery claim was made in 1982 by Cabrera, who reported a single event in a induction loop. Nevertheless no one has been able to duplicate the result which makes it spurious.
For known particles, precision measurements were performed on magnetic charges they might possess. For the electron it has been found $g_e < 10^{-24} g_D$, where g_e is the magnetic charge of the electron and g_D the one of a particle with a Dirac charge. This result was obtained with the induction method: moving magnetic charges which pass through a superconducting ring induce a tiny permanent current, which is measured. The detection was performed using the Superconducting Quantum Interference Devices (SQUID) technology. Another technique, mainly employed in colliders and cosmic rays searches, uses scintillators, gas chambers and nuclear track detectors to measure the energy loss of Dirac particles, which is estimated to be thousand times larger than particles with electric charge.

Colliders searches

In colliders, searches are either direct or indirect. For the latter, multi-photon final states are looked after since there has been proposed that virtual monopoles processes can occur. But difficulties arise when calculating theoretical uncertainties. In direct searches, tracks of magnetic charged particles are sought. Results are usually expressed for the upper limits on a production cross section and/or mass. However they are model-dependent since calculations can only be made with ansatzes to model the kinematics of monopole-antimonopole pair production. Indeed, due to the strong coupling of the magnetic charge, perturbation theory cannot be trusted. Obtaining reliable production cross-sections is thus still an open question. A quite recent (2011) review has been made by Milstead and Weinberg [8], which compares the results obtained in collider experiments. One can cite the E882 and CDF experiments at the Tevatron, which are sensitive to monopoles with masses up to 900 Gev and charges between g_D and $6g_D$. Their upper cross-section limits are about 0.5 pb and 0.2 pb.
In 2012, De Roeck *et al.* reported about the sensitivity of the LHC to exotic particles [9]. There are hopes to investigate trapped monopoles in the central beam pipes of the CMS and ATLAS detectors, which have been removed during the current shutdown of the LHC. The induction method applied to these detectors would be sensitive to very high magnetic charges, $|g| > 4.5 g_D$. To probe moderate high magnetic charges ($3g_D < |g| < 4.5g_D$), the MoEDAL or ALICE detectors would be needed. The MoEDAL detector has been specially designed to detect highly ionising particle, and particularly, it is sensitive to cross sections lower by more than two orders of magnitude.

Cosmological and astrophysical searches

We do not discuss experiments in cosmology, which are mainly more relevant to the 't Hooft-Polyakov monopole searches, but we mention that early cosmic ray searches observed monopoles candidates but couldn't confirm them. More recent experiments use large-scale detectors. [8] gives a short overview on the topic as well.

Bulk Materials searches

There have been searches for monopoles bound in matter, mainly in bulk materials. They are assumed to have absorbed incident cosmic ray monopoles over millions of years. Examples of materials are moon rock, manganese modules, meteorites, and deeply buried rocks in sea water. Searches on the two latter obtained an upper limit on the ratio of the monopoles per nucleon of 10^{-29}. Bendtz *et al.* recently (2013) analysed 24.6 kg of polar volcanic rocks [10]. They found no monopoles and set a limit on the monopole density of $9.8 \cdot 10^{-5}$/gram at 90% confidence level. Using a simple model, they concluded to a limit of $1.6 \cdot 10^{-5}$/gram in the matter averaged over the whole Earth.

Synthetic Dirac monopole

In 2014, Ray *et al.* created Dirac monopoles in the synthetic magnetic field produced by a spinor Bose-Einstein condensate [12]. Monopoles are identified at the termini of vortex lines within the condensate, matching with numerical simulations. Although this experiment opens further investigations, such as condensate spin textures that correspond to other exotic electromagnetic fields and possibly those of the non-Abelian monopole, it exploits a very particular material, indeed ferromagnetic one. Plus, the creation and manipulation of the monopole are performed in a controlled environment and are not directly related to free magnetic monopoles.

12.4 Concluding Remarks

As stated in the introduction, we worked out the consequences of a *hypothetical* magnetic monopole as introduced by Dirac. We postulate it to be point-like and to have an arbitrary mass. The main prediction is that the product of the charges of the electric and magnetic monopoles are modulo some natural constants an integer. With so few properties, Dirac monopoles can be generalized and included in other theories as in grand unified theories where massive and extended monopoles arise (see the *'t Hooft-Polyakov Monopole* chapter). They also do not enter in conflict with well-known results such as the constants of the standard model: quarks have a fractional charge but if the magnetic charge is a multiple of its inverse, their product will satisfy the Dirac condition.
From the experimental side, the existence of such magnetic monopoles in Nature is open. Research has been mainly conducted in cosmology and particle physics where some limits have been calculated. Still, this is far away from observing a free magnetic monopole anywhere in the Universe.

Bibliography

[1] L. H. Ryder, *Quantum Field Theory*, Cambridge University Press, 1996.

[2] M. Nakahara, *Geometry, topology, and physics*, Adam Hilger, Bristol and New York, 1990.

[3] P. A. M. Dirac, *Quantised Singularities in the Electromagnetic Field*, Proc. R. Soc A133, 60 (1931)

[4] T. T. Wu and C. N. Yang, *Concept of nonintegrable phase factors and global formulations of gauge fields*, Phys. Rev. D12 (1975), 3845

[5] P. Goddard and D. I. Olive, *Magnetic monopoles in gauge field theories*, Rep. Prog. Phys., Vol. 41 (1978), 1357

[6] J. A. Harvey, *Magnetic Monopoles, Duality, and Supersymmetry*, arXiv:hep-th/9603086, 1996

[7] K. A. Milton, arXiv:hep-ex/0602040, 1995

[8] J. Beringer *et al.* (Particle Data Group), Phys. Rev. D86, 010001 (2012), listing on *Searches for Magnetic Monopoles*

[9] A. De Roeck *et al*., arXiv:1112.2999, 2012

[10] K. Bendtz *et al*., arXiv:1301.6530v2, 2013

[11] M. W. Ray *et al*.,, arXiv:1301.6530v2, 2013

[12] M. W. Ray *et al*., Nature 505, 657-660, 2014

Chapter 13

't Hooft-Polyakov and BPS Monopoles

Author: Chrysoula Markou
Supervisor: Dr. Florian Goertz

"In this review we consider the 't Hooft-Polyakov monopole, a type of magnetic monopole that arises naturally as a solution of the equations of motion for the Georgi-Glashow model. We will study its properties and topology and conclude that its existence is a profound topological consequence of a suitable configuration of the fields of the model. Moreover, we will discuss general topological concepts related to Homotopy Theory for a gauge theory with an arbitrary gauge group G, which will enable us to decide in which gauge theories topological monopoles can appear. In addition, we will derive a lower bound on the mass of the monopole in the Georgi-Glashow model, the so-called Bogomol'nyi bound, and we will study its saturation, which corresponds to the so-called BPS monopoles. Finally, we will discuss the Witten effect as well as a generalization of electromagnetic duality for BPS monopoles, known as $SL(2,\mathbb{Z})$ duality."

13.1 Magnetic Monopoles

Magnetic monopoles have not been observed in nature so far; this fact is consistent with one of the Maxwell's equations, that is Gauss's law for magnetism: $\vec{\nabla} \cdot \vec{B} = 0$. However, as we have seen in the review of the Dirac monopoles, the concept of duality is what triggers theoretical interest in the matter and what may have prompted Dirac to postulate the existence of magnetic monopoles - we also saw how this claim inevitably leads to the celebrated Dirac quantization condition

$$qg = 2\pi\hbar n \tag{13.1}$$

where q and g are any electric and any magnetic charge (of the theory) and n is an integer, see for example [1]. As for the latter, we note that the quantization of electric charge is considered to be a fundamental experimental fact, which is certainly a strong argument in favour of Dirac's Ansatz.

Since the Dirac monopole is a *postulated* point-like particle, we would like to explore the possibility of having extended *solutions*. In what follows, we will discuss a gauge theory in which the magnetic monopole arises naturally as a finite energy solution of the theory, which is very interesting topologically and has internal structure and computable mass. In general, gauge theories are particularly important because they can allow the unification of the weak and electromagnetic interactions

and can thus serve as models of describing nature (although that's not the case for the one we are going to discuss - we will see why we nevertheless discuss this model later). We note that cosmic inflation is the mechanism considered responsible for the abscence of monopoles, that these theories predict, in experimental data up to date [2].

13.2 The Georgi-Glashow model

The gauge theory that is going to concern us for most of this review is the so-called Georgi-Glashow model, which describes the interaction of a Higgs field ϕ^a with a gauge field W^a_μ. The corresponding Lagrangian density is

$$\mathscr{L} = -\frac{1}{4}G^a_{\mu\nu}G^{a\mu\nu} + \frac{1}{2}(D^\mu\phi)^a(D_\mu\phi)^a - V(\phi) \tag{13.2}$$

The first term of equation (13.2), the so-called Yang-Mills term, is the kinetic term for the field W^a, where $G^a_{\mu\nu}$ is the respective field strenth given by

$$G^a_{\mu\nu} = \partial_\mu W^a_\nu - \partial_\nu W^a_\mu - e\varepsilon_{abc}W^b_\mu W^c_\nu, \tag{13.3}$$

where ε_{abc} is the Levi-Civita symbol. The second term of (13.2) is the kinetic term for the Higgs field ϕ^a, with the covariant derivative $(D_\mu\phi)^a$ of ϕ^a given by

$$(D_\mu\phi)^a = \partial_\mu\phi^a - e\varepsilon_{abc}W^b_\mu\phi^c, \tag{13.4}$$

where it is precisely the second term that corresponds to the coupling of the Higgs field to the gauge one, with e being the corresponding coupling constant. The last term of (13.2) is the Higgs potential

$$V(\phi) = \frac{1}{4}\lambda(\phi^2 - a^2)^2 \tag{13.5}$$

where λ, a are non-negative parameters and $\phi^2 = \phi_a\phi^a$.

The Lagrangian (13.2) is constructed so as to be invariant under the following $SO(3)$ gauge transformations of the fields:

$$\begin{aligned} \phi \mapsto \phi' &= g(x)\phi g(x)^{-1} \\ W_\mu \mapsto W'_\mu &= g(x)W_\mu g(x)^{-1} + \frac{1}{e}(\partial_\mu g(x))g(x)^{-1}, \end{aligned} \tag{13.6}$$

where $g(x)$ is an element of the group $SO(3)$ and x is the position parameter. In the above we write the fields in the basis of the hermitian generators T^a of $SO(3)$ in the adjoint representation:

$$W^\mu = W_a{}^\mu T^a \tag{13.7}$$

and

$$\phi = \phi_a T^a. \tag{13.8}$$

In the adjoint representation the generators T^a are the structure constants of the group, which can be thought of as the Levi-Civita symbols in three dimensions (recall that $SO(3)$ is isomorphic to $SU(2)$). Consequently, W^μ and ϕ are 3×3 matrices (in representation space); this means that $W_a{}^\mu$ and ϕ_a are 3×1 vectors and we can, thus, denote:

$$\begin{aligned} \vec{\phi} &= \phi^a \\ \vec{W}_\mu &= W^a_\mu, \end{aligned} \tag{13.9}$$

where $a = 1, 2, 3$. Moreoever, the structure constants in the adjoint representation are of course also Levi-Civita symbols. This is why the latter appear in 13.3 and 13.4: they arise from the commutator of the generators.

Making use of the alternative vector notation, it is instructive to write equations (13.3) and (13.4) in the following form:

$$\vec{G}_{\mu\nu} = \partial_\mu \vec{W}_\nu - \partial_\nu \vec{W}_\mu - e\vec{W}_\mu \times \vec{W}_\nu, \tag{13.10}$$

$$D_\mu \vec{\phi} = \partial_\mu \vec{\phi} - e\vec{W}_\mu \times \vec{\phi} \tag{13.11}$$

By substituting the form of $\mathscr{L}$ from (13.2) in the Euler - Lagrange equations, it is straightforward to obtain the following equations of motion for the fields:

$$\begin{aligned} D_\nu \vec{G}^{\mu\nu} &= -e\vec{\phi} \times D^\mu \vec{\phi} \\ D^\mu D_\mu \vec{\phi} &= -\lambda(\phi^2 - a^2)\vec{\phi}. \end{aligned} \tag{13.12}$$

We also note that starting from the Jacobi identity for the covariant derivative, with the latter acting on ϕ, one can easily prove a useful identity [1], the so-called Bianchi identity:

$$D_\mu * G^{\mu\nu} = 0, \tag{13.13}$$

where $*G^{\mu\nu}$ is the dual field strength tensor, given by

$$*G^{\mu\nu} = \frac{1}{2}\varepsilon^{\mu\nu\lambda\rho} G_{\lambda\rho}. \tag{13.14}$$

At this point it is important to question ourselves why it is the Georgi-Glashow model that we will investigate in regard to magnetic monopoles. This is firstly because, as we will see in section 1.8, the Georgi-Glashow model fulfills the requirements necessary for magnetic monopoles to appear. However, the Georgi-Glashow model is just a toy model, since there is strong experimental evidence that the Standard Model of Particle Physics ("SM") is what might be realized in nature. Perhaps unfortunately, the latter, with $SU(3) \times SU(2) \times U(1)$ as its gauge group, does not allow the existence of magnetic monopoles. At first sight, this appears very discouraging for our search for the latter; yet they might do appear if we consider theories with gauge groups larger than that of the SM (with the larger gauge group expected to spontaneously break down to the gauge group of the SM), such as $SU(5)$ (see for example [4], [10]), or in the context of Supersymmetry and String Theory [5], [6]. We should note that there are many arguments that make these cases good candidates for describing nature and that the derivation of the existence of monopoles in such cases bares similarities with the corresponding one for the Georgi-Glashow model, which is why we consider the latter in this review.

13.3 The spectrum of the model

We can now calculate the hamiltonian density, i.e. the energy density, for the Georgi-Glashow model. For that we define the conjugate momenta of the fields by

$$\begin{aligned} \vec{\mathscr{E}}^i &= -\vec{G}^{0i} \\ \vec{\Pi} &= D_0 \vec{\phi}. \end{aligned} \tag{13.15}$$

We also define

$$\vec{G}_{ij} = -\varepsilon_{ijk} \vec{\mathscr{B}}^k. \tag{13.16}$$

To justify the definitions of $\vec{\mathscr{E}}^i$ and $\vec{\mathscr{B}}^i$, we remark that they are made in the same spirit as in the case of classical electromagnetism. Now, making a Legendre transformation of the Lagrangian, or by computing the $00-$ component of the conserved Noether current corresponding to $SO(3)$ symmetry transformations, we can easily arrive at the following expression for the energy density:

$$\mathscr{H} = \frac{1}{2}[\vec{\mathscr{E}}_i \cdot \vec{\mathscr{E}}^i + \vec{\Pi} \cdot \vec{\Pi} + \vec{\mathscr{B}}_i \cdot \vec{\mathscr{B}}^i + D_i \vec{\phi} \cdot D^i \vec{\phi}] + V(\phi), \tag{13.17}$$

which is manifestly positive definite.

Field	Mass	Charge
A_μ	0	0
φ	$\mu = a\hbar\sqrt{2\lambda}$	0
W_μ	$M = ae\hbar$	$\pm e\hbar$

Table 13.1: The Particle Spectrum

We can now specify the vacuum of the model: we define the vacuum configuration to be the field configuration for which $\mathscr{H} = 0$ everywhere, i.e. if (and only if) all the three equations

$$\vec{G}^{\mu\nu} = 0 \tag{13.18}$$

$$D^\mu \vec{\phi} = 0 \tag{13.19}$$

$$V(\phi) = 0 \tag{13.20}$$

hold everywhere, we have a vacuum configuration. Moreover, we can as usual define the Higgs vacuum as the field configuration for which of course equations (13.19) and (13.20) hold, but not necessarily (13.18).

In addition, we can derive the particle spectrum of the model. In the Higgs vacuum, equation (13.20) tells us that $\phi^2 = a^2$, or $\phi \in \mathscr{M}_0$, where $\mathscr{M}_0$ is a sphere of radius a in the three-dimensional (representation) space in which ϕ is defined. The rotational invariance of the sphere implies that all points of the sphere, i.e. all possible Higgs vacuum states, are equivalent. However, to be able to read off masses from the Lagrangian density, we have to choose a specific vacuum state for the Higgs field to perturb around, such as $\vec{\phi} = a\hat{z}$, where $\hat{z}$ is a unit vector of an orthonormal basis of the three-dimensional representation space. As is well known, by doing so the whole $SO(3)$ symmetry breaks down to $U(1)$ symmetry: this is the famous mechanism of spontaneous symmetry breaking; consequently we can say that in the Higgs vacuum we have classical Maxwell electromagnetism.

If we indeed substitute $\vec{\phi} = \vec{a} + \vec{\varphi}$ (choice of vacuum state), where for example $\vec{a} = a\hat{z}$, and expand in terms of $\vec{\varphi}$ in the Lagrangian density, the coefficients of the terms quadratic in the fields will give the respective masses squared of the fields, modulo a factor $\frac{1}{2\hbar^2}$, and the final particle content will be accounted for by the Higgs mechanism. In particular, the model will have a massive scalar field φ, which is identified with the Higgs particle, a massless vector boson

$$A^\mu = \frac{1}{a}\vec{a} \cdot \vec{W}^\mu \tag{13.21}$$

identified with the photon and two massive vector bosons, whose masses are given in table 13.1. Apart from the masses, we can also specify the charges, which can be simply read off by comparing the covariant derivative $\partial^\mu + ieW_a^\mu T_a$ of the Georgi-Glashow model with the electromagnetic covariant derivative $\partial^\mu + \frac{i}{\hbar}QA^\mu$, where T_a (in the adjoint representation) and Q are the $SO(3)$ and $U(1)$ generators respectively. We conclude that

$$Q = \frac{e\hbar}{a}\vec{a} \cdot \vec{T} \tag{13.22}$$

with which we compute the charges also given in table 13.1.

13.4 The 't Hooft-Polyakov Ansatz

We would now like to find a solution to the equations of motion (13.12) that may correspond to a magnetic monopole. We will approach the matter indirectly, that is we will first try to construct finite energy solutions and then we will compute the gauge field strength tensor, hoping that we will

arrive at a magnetic field that is that of a monopole. For that, we observe that finite energy E means that the intergral

$$E = \int d^3\vec{r}\mathscr{H} \tag{13.23}$$

exists. This, in turn, means that at spatial infinity the fields must be asymptotically in a vacuum configuration and, more specifically, that at spatial infinity the Higgs field must be in the Higgs vacuum asymptotically.

Moreoever, since we are looking for particle-like solutions, we expect them to be localised. As such, these solutions cannot be invariant under translations, which, however, is not the case for the equations of motion. In addition, the solutions cannot be invariant under P (parity) and Z (Z's action is similar to the one of parity but it may only change the sign of the fields and not the sign of the position parameter) seperately (again this is not the case for the equations of motion), because both P and Z reverse the sign of $\vec{\nabla}\cdot\vec{B}$ and, thus, that of the magnetic charge. However, PZ does not reverse this sign and, consequently, we can assume that the solutions are invariant under PZ.

What about rotational symmetry? If the solution is invariant under $SO(3)$ rotations in representation space, then the Higgs field is forced to vanish everywhere, so $V(\phi) \neq 0$ everywhere, which means that we cannot have a vacuum configuration asymptotically. If the solution is invariant under $SO(3)$ rotations in real space, then asymptotically the Higgs field is forced to be a constant function in real space and, consequently, a constant vector field in representation space. However, the topology of the Higgs field should be more interesting than the topology of a constant configuration, because, since we are looking for a particle-like solution, we expect to find a "lump" of energy around the origin, which may correspond to a particle. As we will later see explicitly, this lump can only be created if the Higgs field far away from the origin is in the Higgs vacuum in a non-trivial way: rather than being a constant vector, its direction should change from point to point, i.e. "twists" of the Higgs field far away from the origin are necessary for particle-like solutions.

We conclude that the solutions cannot be invariant under rotations in real (spatial) and representation (isotopic) space seperately; however, they are invariant under simultaneous and equal rotations in real and representation space; the latter correspond to the diagonal subgroup of $SO(3)\times SO(3)$ that has generators $-i\vec{r}\times\vec{\nabla}+\vec{T}$ (i.e. linear combinations of the generators $-i\vec{r}\times\vec{\nabla}$ of spatial rotations and the generators $\vec{T}$ of rotations in isospin space).

An Ansatz for a finite energy solution that respects the above symmetries, proposed independently by 't Hooft [7] and Polyakov [8], is the following:

$$\begin{aligned} \phi^a &= \frac{r^a}{er^2}H(aer) \\ W_a^i &= -\varepsilon_{aij}\frac{r^j}{er^2}[1-K(aer)] \\ W_a^0 &= \frac{r^a}{er^2}J(aer), \end{aligned} \tag{13.24}$$

where H, K, J are arbitrary functions of $aer \equiv \xi$. We emphasize that the symmetries of this Ansatz form a subgroup of the symmetries of the equations of motion. This Ansatz has the highest spherical symmetry possible, it is time-independent and we will now further restrict ourselves to the cases in which $J = 0$.

Now, if we substitute equations (13.24) into (13.23), we get

$$E = \frac{4\pi a}{e}\int_0^\infty \frac{d\xi}{\xi^2}[\xi^2(\frac{dK}{d\xi})^2 + \frac{1}{2}(\xi\frac{dH}{d\xi}-H)^2 + \frac{1}{2}(K^2-1)^2 + K^2H^2 + \frac{\lambda}{4e^2}(H^2-\xi^2)^2], \tag{13.25}$$

and if we require that this integral gives finite energy we have to impose the following boundary conditions for K, H

$$\xi\to 0 : H\to 0 \sim H \leq O(\xi), K\to 1 \sim K-1 \leq O(\xi) \tag{13.26}$$

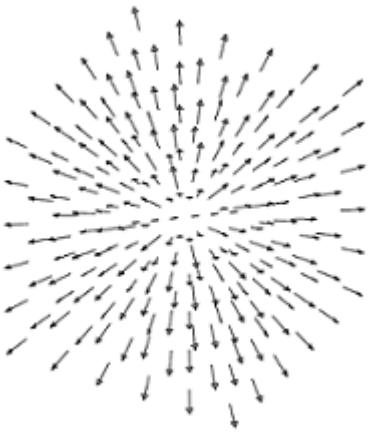

Figure 13.1: *The hedgehog configuration of the Higgs field at spatial infinity, taken from* [9].

$$\xi \to \infty : H/\xi \to 1, K \to 0. \tag{13.27}$$

The asymptotic condition $H/\xi \to 1$ of (13.27), if substituted in the Ansatz (13.24) for the Higgs field, gives

$$\phi^a = a\frac{r^a}{r}. \tag{13.28}$$

This means that the index a can take values both in real and in representation space and that the position vector (in real space) is aligned to the Higgs field vector (in representation space) at spatial infinity. Consequently, the Higgs field at spatial infinity has a radial configuration in representation space. This is the so-called hedgehog configuration of the Higgs field [10], given in figure 13.1 at spatial infinity, where the "twists" of the Higgs field are explicitly shown. In fact, equation (13.28) also tells us that, at spatial infinity, as the position vector winds around the sphere S^2 in real space once, also the Higgs field winds around the sphere $\mathscr{M}_0$ in representation space precisely once.

Could the 't Hooft-Polyakov Ansatz, together with the boundary conditions for K, H, correspond to a magnetic monopole? To answer this question let us compute the gauge field strength tensor at very large distances. We have that $G_a^{0i} = 0$ and at leading order:

$$\begin{aligned} G_a^{ij} &\sim -e\varepsilon_{abc}W_b^i W_c^j \\ &\sim -e\varepsilon_{abc}\varepsilon_{bik}\varepsilon_{cjl}\frac{r^k}{er^2}\frac{r^l}{er^2} \\ &\sim \frac{1}{er^4}[\delta_{ai}\delta_{ck} - \delta_{ak}\delta_{ci}]\varepsilon_{cjl}r^k r^l \\ &\sim -\frac{1}{er^4}\varepsilon_{ijl}r^a r^l \\ &\sim -\frac{1}{aer^4}\varepsilon_{ijl}r^l a\hat{r}^a r \\ &\sim -\frac{1}{aer^3}\varepsilon_{ijl}r^l\phi_a, \end{aligned} \tag{13.29}$$

where we notice that in the third equivalence the first term vanishes since the Levi-Civita symbol is contracted with a symmetric tensor. To compute the electromagnetic field, we recall from the analysis of the particle spectrum that the photon field is identified with $A_\mu = \frac{1}{a}\phi^a W_\mu^a$ for the Higgs field being in the Higgs vacuum; we can, thus, argue that the electromagnetic field strength tensor $F_{\mu\nu}$ is given by

$$F_{\mu\nu} = \frac{1}{a}\phi^a G_{\mu\nu}^a, \tag{13.30}$$

where the Higgs field is in the Higgs vacuum. Therefore, $F_{0i} = 0$, which means that the Ansatz has

no electric field, and

$$\begin{aligned} F_{ij} &= -\frac{1}{a}\phi^a \frac{1}{aer^3}\varepsilon_{ijl} r^l \phi_a \\ &= -\frac{1}{er^3}\varepsilon_{ijl} r^l, \end{aligned} \tag{13.31}$$

since $\phi^a \phi_a = a^2$ in the Higgs vacuum, i.e. far away from the origin. Comparing (13.31) with $F_{ij} = -\varepsilon_{ijk} B^k$ we conclude that the Ansatz has a magnetic field B^i given by

$$B^i = \frac{1}{er^3} r^i, \tag{13.32}$$

which is of course the magnetic field of a magnetic monopole.

- **Charge**

  Equation (13.32) tells us that indeed the 't Hooft-Polyakov Ansatz corresponds to a magnetic monopole with magnetic charge $g = \frac{4\pi}{e}$, or

  $$ge = 4\pi, \tag{13.33}$$

  or, setting $q = e\hbar$:

  $$gq = 4\pi\hbar. \tag{13.34}$$

  We would like to compare equation (13.34) to the Dirac quantization condition $qg = 2\pi\hbar n$ for the minimum electric charge. For that the Dirac quantization condition is

  $$gq_0 = 2\pi\hbar n. \tag{13.35}$$

  By comparing (13.34) and (13.35), we get that $n = 2$ for the 't Hooft-Polyakov monopole. However, this is not the case, because q in equation (13.34) is not in fact the minimum electric charge. Rather, it corresponds to the coupling constant of the interaction between the gauge field and the Higgs field, which, as we saw, is accounted for by the second term of equation (13.4). So what is the minimum electric charge in the Georgi-Glashow model? Equation (13.22) tells us that, due to the symmetry breaking, the electric charge is the eigenvalue of the isospin generator (in the adjoint representation) and, thus, the minimum electric charge is $q_o = \frac{1}{2}q$. Consequently the Dirac and the 't Hooft -Polyakov monopole yield the same quantization condition and the latter indeed carries one unit of Dirac magnetic charge.

- **Existence**

  To check that the proposed Ansatz is indeed a solution to the equations of motion (13.12), we need to check that its equations of motion have a solution, or, equivalently, that the equations of motion for H, K have a solution. By substituting the Ansatz into (13.12), we derive the following equations of motion for the functions H and K:

  $$\begin{aligned} \xi^2 \frac{d^2K}{d\xi^2} &= KH^2 + K(K^2 - 1) \\ \xi^2 \frac{d^2H}{d\xi^2} &= 2K^2 H + \frac{\lambda}{e^2} H(H^2 - \xi^2). \end{aligned} \tag{13.36}$$

  Now, it has been shown that solutions to this system of equations, together with the boundary conditions (13.26), exist: this was shown at first with the use of numerical calculations and was later rigorously proven [11].

- **Size**

  To determine the size of the 't Hooft-Polyakov monopole, we would like to check what happens to the functions H, K as ξ approaches infinity. In this limit equations (13.36) become

$$\begin{aligned} \frac{d^2K}{d\xi^2} &= K \\ \frac{d^2h}{d\xi^2} &= \frac{2\lambda}{e^2}h, \end{aligned} \tag{13.37}$$

  where we have set $H = h + \xi$. These equations have the following solutions compatible with the boundary equations:

$$\begin{aligned} K &\sim e^{-\xi} = e^{-\frac{Mr}{\hbar}} \\ H - \xi = h &\sim e^{-\frac{\mu r}{\hbar}}. \end{aligned} \tag{13.38}$$

  So H and K approach their asymptotic form as the distance from the (center of the) 't Hooft-Polyakov monopole approaches the Compton wavelength $\frac{\hbar}{\mu}$ of the Higgs field and the Compton wavelength $\frac{\hbar}{M}$ of the massive gauge particle of the spectrum respectively.

  Moreover, far away from the monopole the Higgs field is in the Higgs vacuum and, as we will see in the next section, all (massive) gauge fields vanish while only electromagnetism survives. As a result, the 't Hooft-Polyakov monopole has a finite size determined by the largest of the above Compton wavelengths, whereas outside the monopole we expect the field configuration to decay to the Higgs vacuum exponentially.

- **Stability**

  As we saw, at spatial infinity the Higgs field must be in the Higgs vacuum in order to have a finite energy solution. This defines a map from the sphere S^2 at spatial infinity (in real space) to the sphere $\mathscr{M}_0$ (in the representation space where ϕ is defined). The number N of times ϕ covers $\mathscr{M}_0$ as $\vec{r}$ covers S^2 is the so-called Brouwer degree of the map and is of course an integer. This is a topological number that characterizes the finite energy configuration and has the remarkable property that, as an integer, it is invariant under any continuous deformation. This means that a finite energy configuration with $N \neq 0$ will never dissipate to the trivial state with $N = 0$; we conclude that such a finite energy configuration, and, thus, the 't Hooft-Polyakov monopole, will be stable. We will now see how this topological number N is related to the magnetic charge of the monopole.

13.5 The topology of the monopole field configuration

Bearing in mind our remarks concerning the size and stability of the 't Hooft-Polyakov monopole, we can make the following reasonable assumption: any finite energy (that is not necessarily time-independent) solution reduces to the Higgs vacuum everywhere, except from a finite number of (well seperated and compact) regions with finite size, which are identified with monopoles. In the space outside the monopoles, that is, in the Higgs vacuum, we can argue that (generally)

$$\vec{W}^\mu = \frac{1}{a^2 e}\vec{\phi} \times \partial^\mu \vec{\phi} + \frac{1}{a}\vec{\phi} A^\mu, \tag{13.39}$$

where A^μ is arbitrary, since it corresponds to the component of $\vec{W}^\mu$ in the $\vec{\phi}$ direction (the other components are determined by equation (13.19) which holds in the Higgs vacuum and gives the first term of (13.39). Using (13.39) it can be shown that

$$\vec{G}^{\mu\nu} = \frac{1}{a}\vec{\phi} F^{\mu\nu}, \tag{13.40}$$

where

$$F^{\mu\nu} = -\frac{1}{a^3 e}\vec{\phi}\cdot(\partial^\mu\vec{\phi}\times\partial^\nu\vec{\phi}) + \partial^\mu A^\nu - \partial^\nu A^\mu. \tag{13.41}$$

We should note that it can be easily shown that both $F^{\mu\nu}$ and its dual satisfy the Maxwell equations, so outside the monopoles the theory reduces to classical electromagnetism as we remarked when discussing the size of the 't Hooft-Polyakov monopole [1].

Now let us compute the magnetic flux g_Σ through a closed surface Σ in the Higgs vacuum whose respective volume contains at least one monopole (otherwise the flux is zero):

$$\begin{aligned} g_\Sigma &= \int_\Sigma \vec{B}\cdot d\vec{S} \\ &= \int_\Sigma (-\frac{1}{2}\varepsilon_{ijk}F^{jk})dS^i \\ &= \frac{1}{2a^3 e}\int_\Sigma \varepsilon_{ijk}\vec{\phi}\cdot(\partial^j\vec{\phi}\times\partial^k\vec{\phi})dS^i - \frac{1}{2}\int_\Sigma \varepsilon_{ijk}(\partial^j A^k - \partial^k A^j)dS^i \end{aligned} \tag{13.42}$$

where the second term vanishes due to Stoke's theorem. In addition, the first term gives a non-zero contribution only when $j,k \neq i$, which means that only the derivatives of $\vec{\phi}$ that are tangential to Σ contribute. We, thus, deduce that the magnetic charge enclosed by a surface depends only on the values the Higgs field takes on the surface. We note that the radius of the volume that corresponds to Σ should be much larger than the radii of the monopoles it encloses, since equation (13.39) was derived for the Higgs vacuum.

Moreover, it is straightforward to see that small variations $\delta\vec{\phi}$ of the Higgs field (for which $\vec{\phi}\cdot\delta\vec{\phi} = 0$ so that we still have that $\phi^2 = a^2$) result in zero variation of $\vec{\phi}\cdot(\partial^j\vec{\phi}\times\partial^k\vec{\phi})$ [1]; hence any such small variation of the Higgs field does not affect the magnetic flux. This fundamental result can be generalized to any changes of the Higgs field which are made of infinitesimal deformations, the so-called homotopies. Such examples of changes of the Higgs field are time development, gauge transformations and also changes that appear as a result of continuous deformations of Σ within the Higgs vacuum. We conclude that g_Σ is time-independent, gauge invariant and remains constant under continuous deformations of Σ.

It has been shown in [12] that the topological quantum number N which we introduced in the previous section can be identified with

$$N = \frac{1}{4\pi}\frac{1}{2a^3}\int_\Sigma \varepsilon_{ijk}\vec{\phi}\cdot(\partial^j\vec{\phi}\times\partial^k\vec{\phi})dS^i \tag{13.43}$$

so that we have

$$g_\Sigma = \frac{4\pi}{e}N, \tag{13.44}$$

which means that g_Σ is quantized: we have arrived at the Dirac's quantization condition using purely topological arguments. For the 't Hooft-Polyakov monopole we have already seen that, as the position vector covers S^2 once, the Higgs field also covers $\mathscr{M}_0$ once, so $N = 1$ in this case, which confirms equation (13.33).

Moreover, g_Σ is additive. To see this, let us consider two monopoles, 1 and 2, enclosed in a surface Σ, through which the magnetic flux is g_Σ. Σ can be continuously deformed into two surfaces Σ_1 and Σ_2 that enclose monopoles 1 and 2 respectively. Yet, as we explained before, g_Σ is unchanged under this deformation and must consequently be equal to g_Σ after the deformation, which is merely $g_{\Sigma_1} + g_{\Sigma_2}$.

13.5.1 A generalization

Given that the Georgi-Glashow model is not realised in nature, we will consider a more general case in which the Lagrangian still has the form (13.2) but is now invariant under gauge transformations

(of the fields) that belong to a general gauge group G, assumed to be compact and connected. We also assume that there is a vacuum degeneracy which causes G to spontaneously break down to H, a subgroup of G that is assumed to be compact. $\mathscr{M}_0$ is again the manifold on which the ϕ that are in the Higgs vacuum (which is still identified with equations (13.19), (13.20)) lie, i.e.

$$\mathscr{M}_0 = \{\phi : V(\phi) = 0\}. \tag{13.45}$$

In the Georgi-Glashow model G and H correspond to $SO(3)$ and $U(1)$ respectively and $\mathscr{M}_0$ is S^2. We note that the internal structure of the monopole is largely determined by the gauge group G, whereas the importance of G is, in a sense, suppressed when it comes to the macroscopic properties of the monopole (i.e. the properties of the monopole far away from its core), such as the structure of $\mathscr{M}_0$, which are largely determined by H. We will see this in more detail in section 1.8. More advanced tools from group theory and homotopy theory will help us gain further insight into the structure of $\mathscr{M}_0$.

Elements of Group Theory and the structure of $\mathscr{M}_0$

- **Orbit**

  Two points ϕ_1, ϕ_2 are said to be on the same orbit if there exists an element $g \in G$ such that

  $$\phi_1 = R(g)\phi_2, \tag{13.46}$$

  where R is a representation of the group G.

- **Transitivity**

  We say that G acts trasitively on $\mathscr{M}_0$ if for every $\phi_1, \phi_2 \in \mathscr{M}_0$ there exists a $g_{12} \in G$ such that

  $$\phi_1 = R(g_{12})\phi_2. \tag{13.47}$$

We will indeed assume that G acts trasitively on $\mathscr{M}_0$, i.e. that $\mathscr{M}_0$ consists of a single orbit of the group G. This should be expected since all Higgs vacuum states are equivalent; this degeneracy is accounted for by the invariance of the theory under gauge transformations that belong to G. In the Georgi-Glashow model the action of $SO(3)$ on S^2 is transitive due to the rotational invariance of the sphere S^2 in the three-dimensional representation space.

- **Little Group**

  The little group H_ϕ of a point $\phi \in \mathscr{M}_0$ consists of those elements $h \in G$ for which $R(h)\phi = \phi$:

  $$H_\phi = \{h \in G : R(h)\phi = \phi\}. \tag{13.48}$$

  For two points ϕ_1, ϕ_2 in the same orbit (and both belonging to $\mathscr{M}_0$), if G acts transitively on $\mathscr{M}_0$, we have that

  $$H_{\phi_1} = g_{12}^{-1} H_{\phi_2} g_{12}. \tag{13.49}$$

  Thus, the structure of H_ϕ is independent of ϕ and can in fact be identified with the unbroken symmetry group H we mentioned at the beginning of this section, so we have $H = H_\phi$. H is physically very important for the theory: its dimension (i.e. the number of unbroken generators of G) corresponds to the number of massless gauge particles and the eigenvalues of its generators determine the values of the physical charges.

It can been shown as in [1] that G and H determine $\mathscr{M}_0$ completely in a very specific way:

$$\mathscr{M}_0 = G/H, \tag{13.50}$$

i.e. $\mathscr{M}_0$ is the space of right cosets of H in G. We can think of a coset as a "shifted subgroup"; in our case this means that we can think of $\mathscr{M}_0$ as a shifted H. This helps us understand equation (13.50): $\mathscr{M}_0$ cannot be just H since we also have to take into account the gauge symmetry: if we "shift" the fields (that is if we make a gauge transformation) we get all fields that belong to $\mathscr{M}_0$ due to transitivity.

For example, in the case of the 't Hooft-Polyakov monopole, we have that $\mathscr{M}_0 = SO(3)/U(1)$. Every vacuum state is symmetric under $U(1)$ gauge transformations; however, different vacuum states are related by $SO(3)$ gauge transformations, i.e. "shifts". This fixes completely the manifold of degenerate vacua, which is $\mathscr{M}_0$. Consequently, we could say that for a general gauge theory the macroscopic properties of the monopole are largely determined by H: the structure of $\mathscr{M}_0$ depends on G/H and not on the details of the Higgs field.

Now that we have investigated the structure of $\mathscr{M}_0$, we would like to see what happens to the gauge fields W_μ in the Higgs vacuum. For our general theory we can consider a set $\{T^a\}$ of hermitian generators of G and write the gauge fields in this basis:

$$W^\mu = W^\mu_a T^a. \tag{13.51}$$

The covariant derivative can then be written as:

$$D^\mu \phi = \partial^\mu \phi + ieR(W^\mu)\phi, \tag{13.52}$$

where R is again a representation of G. We remark that the gauge field has been introduced in the above expression in order to have D^μ transform covariantly under gauge transformations.

Using the above one can easily show that in general

$$[D^\mu, D^\nu]\phi = ieR(G^{\mu\nu})\phi, \tag{13.53}$$

where $G^{\mu\nu} = G^{\mu\nu}_a T^a$ [1]. But in the Higgs vacuum the left hand side of (13.53) is zero due to equation (13.19), so we have:

$$R(G^{\mu\nu})\phi = 0. \tag{13.54}$$

This tells us that all components of $G^{\mu\nu}$ vanish except from those that correspond to the generators of H. We conclude that in the Higgs vacuum, and, thus, outside the monopole, only these components of $G^{\mu\nu}$ survive: in the case of the 't Hooft-Polyakov monopole these correspond to the electromagnetic field. Consequently, equation (13.54) can be viewed as a generalization of equation (13.40).

Elements of Homotopy Theory and topological quantum numbers

- **Homotopy, Absolute Homotopy Class**

  Two maps f_1, f_2: $X \to Y$, where X, Y are topological spaces, are called homotopic if there exists a continuous map F: $X \times [0,1] \to Y$, called a homotopy, for which

  $$\begin{aligned} F(x,0) &= f_1(x) \\ F(x,1) &= f_2(x). \end{aligned} \tag{13.55}$$

  In other words, F is the continuous deformation of f_1 into f_2. Homotopy enables us to categorize maps in equivalence classes: two maps are said to belong to the same absolute homotopy class if and only if they are homotopic.

How can homotopy be of interest in regard to magnetic monopoles? Let us consider again the "gas" of monopoles surrounded by the Higgs vacuum. Moreover, let us consider a closed surface Σ in the Higgs vacuum that encloses one monopole once. As we saw in the special case of the 't Hooft-Polyakov monopole, the Higgs field ($\vec{r} \to \phi(\vec{r}, t)$) defines a map from Σ to $\mathscr{M}_0$. As time evolves, imagine that the monopoles move and change shape. Then, supposing that the monopoles do not

intersect, the Higgs field varies continuously so that the map $\Sigma \to \mathscr{M}_0$ varies continuously; this continuous change is precisely a homotopy, that is, the deformation (in time) of $\phi(\vec{r}, t_1)$ into $\phi(\vec{r}, t_2)$.

Moreover, we can regard the surface Σ and the sphere S^2 as homeomorphic, i.e. equivalent for homotopy theory. We denote by $\widetilde{\Pi_2}(\mathscr{M}_0)$ the absolute homotopy class for the maps $\Sigma \to \mathscr{M}_0$ or equivalently for the maps $S^2 \to \mathscr{M}_0$. The 2 in $\widetilde{\Pi_2}(\mathscr{M}_0)$ corresponds to the dimension of the sphere S^2. $\widetilde{\Pi_2}(\mathscr{M}_0)$ gives a classification of the magnetic monopoles which is independent of time and of the choice of Σ and has also been shown to be gauge-invariant, see for example [1]. Consequently, $\widetilde{\Pi_2}(\mathscr{M}_0)$ gives rise to a topological "quantum number" analogue for our classical theory. In the case of the 't Hooft-Polyakov monopole, we saw that the homotopy was a mapping between spheres S^2 and the homotopy classes were labeled by the winding number N (the Brouwer degree) of the map.

- **Relative Homotopy Class, Homotopy Group**

  As the 't Hooft-Polyakov case suggests, it is reasonable to consider homotopic maps $S^n \to Y$, where S^n is the n-dimensional sphere. We denote by $\widetilde{\Pi_n}(Y)$ the absolute homotopy classes. Then, the relative homotopy classes $\Pi_n(Y)$ are homotopy classes that correspond only to maps in which the image of one particular point of S^n is kept fixed at a certain point in Y. However, one can show that if Y is connected (which is the case for $\mathscr{M}_0$ because G is assumed to be connected and acts transitively on $\mathscr{M}_0$) then $\Pi_n(Y)$ does not depend on the fixed image of the particular point.

  Now, one can define a product operation in $\Pi_n(Y)$ with which $\Pi_n(Y)$ becomes a group, the so-called n^{th} homotopy group of Y. It has been shown that for a simply connected Y the absolute and relative homotopy classes are equivalent [1]. These concepts will help us later to understand the connection between the Dirac and the 't Hooft-Polyakov monopole. They will also be very important in establishing a criterion concerning the type of gauge theories in which monopoles can appear.

13.6 The Bogomol'nyi bound

We will now show that there is a lower limit on the mass of monopoles in the Georgi-Glashow model. This is easy to see in the center of mass frame, where the entire energy of the monopole equals its mass. Starting from equation (13.17), and observing that the terms $\vec{\Pi} \cdot \vec{\Pi}$ and $V(\phi)$ are non-negative, we have:

$$\begin{aligned} M &\geq \frac{1}{2} \int_{\mathbb{R}^3} d^3\vec{r} [\vec{\mathscr{E}}_i \cdot \vec{\mathscr{E}}^i + \vec{\mathscr{B}}_i \cdot \vec{\mathscr{B}}^i + D_i\vec{\phi} \cdot D^i\vec{\phi}] \\ &= \frac{1}{2} \int_{\mathbb{R}^3} d^3\vec{r} [||\vec{\mathscr{E}}_i - D_i\vec{\phi}\sin\theta||^2 + ||\vec{\mathscr{B}}_i - D_i\vec{\phi}\cos\theta||^2] + \sin\theta \int_{\mathbb{R}^3} d^3\vec{r} D_i\vec{\phi} \cdot \vec{\mathscr{E}}^i + \cos\theta \int_{\mathbb{R}^3} d^3\vec{r} D_i\vec{\phi} \cdot \vec{\mathscr{B}}^i \\ &\geq \sin\theta \int_{\mathbb{R}^3} d^3\vec{r} D_i\vec{\phi} \cdot \vec{\mathscr{E}}^i + \cos\theta \int_{\mathbb{R}^3} d^3\vec{r} D_i\vec{\phi} \cdot \vec{\mathscr{B}}^i, \end{aligned} \tag{13.56}$$

where we have introduced an arbitrary angular parameter θ that will help us arrive to the desired result. Now we can compute:

$$\begin{aligned}
\int_{\mathbb{R}^3} d^3\vec{r} D_i\vec{\phi}\cdot\vec{\mathscr{B}}^i &= \int_{\mathbb{R}^3} d^3\vec{r}(D_i\phi)_a\mathscr{B}^i_a \\
&= \int_{\mathbb{R}^3} d^3\vec{r}[\partial_i\phi_a - e\varepsilon_{abc}W_{ib}\phi_c]\mathscr{B}^i_a \\
&= \int_{\mathbb{R}^3} d^3\vec{r}\partial_i(\phi_a\mathscr{B}^i_a) - \int_{\mathbb{R}^3} d^3\vec{r}[\phi_a\partial_i\mathscr{B}^i_a + e\varepsilon_{abc}W_{ib}\phi_c\mathscr{B}^i_a] \\
&= \int_{\Sigma_\infty} \vec{\phi}\cdot\vec{\mathscr{B}}_i dS_i - \int_{\mathbb{R}^3} d^3\vec{r}[\phi_a\partial_i\mathscr{B}^i_a + e\varepsilon_{cba}W_{ib}\phi_a\mathscr{B}^i_c] \\
&= a\int_{\Sigma_\infty} \vec{B}\cdot d\vec{S} - \int_{\mathbb{R}^3} d^3\vec{r}\phi_a[\partial_i\mathscr{B}^i_a - e\varepsilon_{abc}W_{ib}\mathscr{B}^i_c] \\
&= ag - \int_{\mathbb{R}^3} d^3\vec{r}\phi_a D_i\mathscr{B}^i_a \\
&= ag.
\end{aligned} \tag{13.57}$$

In the above calculation, we performed integration by parts in going from the second to the third line. In going from the third to the fourth line, we use Gauss' theorem for the first term with Σ_∞ being the sphere at spatial infinity and in going from the fourth to the fifth line, we deduce from equation (13.30) (which is valid since we will integrate over Σ_∞ which means that $F_{\mu\nu}$ is evaluated at very large distances) that

$$B_i = \frac{1}{a}\vec{\phi}\cdot\vec{\mathscr{B}}_i. \tag{13.58}$$

In the last step we use the Bianchi identity to show that $D_i\varepsilon^{0ijk}\vec{G}_{jk} = 0$ and thus $D_i\vec{\mathscr{B}}_i = 0$.

In a similar manner (this time using the equations of motion instead of the Bianchi identity) we see that

$$\int_{\mathbb{R}^3} d^3\vec{r} D_i\vec{\phi}\cdot\vec{\mathscr{E}}^i = aq. \tag{13.59}$$

We note that the q and g are respectively the electric and magnetic charges of a monopole-like solution in the Georgi-Glashow model. We conclude that

$$\begin{aligned}
M &\geq aq\sin\theta + ag\cos\theta \\
&\geq ag\cos\theta[1 + \frac{q}{g}\tan\theta].
\end{aligned} \tag{13.60}$$

We now observe that the right hand side reaches a maximum for $\tan\theta = q/g$, so:

$$M \geq ag\cos\theta[1 + \frac{q^2}{g^2}] \tag{13.61}$$

but

$$\begin{aligned} ag\cos\theta[1+\frac{q^2}{g^2}] &= \frac{a}{g}\cos\theta[q^2+g^2]\frac{\sqrt{q^2+g^2}}{\sqrt{q^2+g^2}} \\ &= a\cos\theta[q^2+g^2]\frac{\sqrt{(q/g)^2+1}}{\sqrt{q^2+g^2}} \\ &= a\cos\theta[q^2+g^2]\frac{\sqrt{(\tan\theta)^2+1}}{\sqrt{q^2+g^2}} \\ &= a[q^2+g^2]\frac{1}{\sqrt{q^2+g^2}} \\ &= a\sqrt{q^2+g^2}, \end{aligned} \tag{13.62}$$

so

$$M \geq a\sqrt{q^2+g^2}, \tag{13.63}$$

which is the so-called Bogomol'nyi bound for the mass of a monopole-like solution.

With this bound we can calculate the mass of the lightest 't Hooft-Polyakov monopole. The latter has no electric charge, so in natural units:

$$\begin{aligned} M_{min} = a|g| &= \frac{4\pi a}{e} \\ &= \frac{4\pi M_W}{e^2} \\ &= \frac{M_W}{\alpha} \sim 11TeV, \end{aligned} \tag{13.64}$$

where we assume $M_W \sim 80$GeV for the mass of the vector bosons of the model and $\alpha = \frac{1}{137}$ the fine structure constant.

This would be the right point to mention detection methods of magnetic monopoles. To begin with, one can look for monopoles produced in accelerator experiments; the MoEDAL experiment at CERN is designed for this purpose. However, bearing in mind equation (13.64), we expect the mass of a magnetic monopole to be proportional to the mass of the gauge bosons also for more realistic gauge theories, such as $SU(5)$, than the Georgi-Glashow model, that also predict magnetic monopoles. But for such theories the relevant new gauge bosons are expected to be heavier than the massive gauge bosons of the Georgi-Glashow model. This means that the corresponding magnetic monopoles would be heavier than 11TeV, which puts them beyond the current experimental energy scale.

Moreover, one can also look for already existing monopoles in cosmic rays and in astrophysical data; examples are the IceCube and the RICE experiment. Given that inflation predicts that magnetic monopoles are extremely scarce (for example in [13] a density $\leq 10^{-19}cm^{-3}$ is predicted), such experiments are conducted with a view of determining the upper bound of the flux of the monopoles. Currently this bound is estimated (under some assumptions) to be of the order of $10^{-16} - 10^{-18}cm^{-2}s^{-1}sr^{-1}$ [14], [15], [17].

13.7 BPS monopoles

The Bogomol'nyi-Prasad-Sommerfeld monopoles, known as BPS monopoles, are those monopole solutions that saturate the Bogomol'nyi bound (13.63). As should be obvious from the previous section, for the BPS monopoles the non-negative terms that we ingore in deriving the Bogomol'nyi bound must be set to zero. We thus have

$$D_0\vec{\phi} = 0, \tag{13.65}$$

$$V(\phi) = 0 \tag{13.66}$$

and

$$\vec{\mathscr{E}}_i - D_i\vec{\phi}\sin\theta = 0 \tag{13.67}$$

$$\vec{\mathscr{B}}_i - D_i\vec{\phi}\cos\theta = 0. \tag{13.68}$$

If we further assume that $\vec{\mathscr{E}}_i = 0$ for the BPS monopoles, we conclude that $\sin\theta = 0$ but $\cos\theta \neq 0$ (so that the bound is not satisfied trivially). Consequently

$$\vec{\mathscr{B}}_i = \pm D_i\vec{\phi}. \tag{13.69}$$

We should note that equation (13.66) should be realised by taking the limit $\lambda \to 0$ and not by requiring that the Higgs field is in the Higgs vacuum everywhere. To see that this is indeed the case, we observe that if we did require $\phi^2 = a^2$ everywhere, we would get that $\vec{\phi}\cdot D_i\vec{\phi} = 0$ and thus, using equation (13.69), we would have $\vec{\phi}\cdot\vec{\mathscr{B}}_i = 0$ everywhere, which means that the magnetic monopole has no magnetic charge, which of course cannot be true. However, we do impose that the Higgs field satisfies $\phi^2 = a^2$ at spatial infinity as we did before in the case of the 't Hoof-Polyakov monopole.

It is straightforward to show that the BPS monopole satisfies the same equations of motion as the 't Hoof-Polyakov monopole but with $\lambda = 0$ [1]. Moreover, if we substitute the 't Hooft-Polyakov Ansatz into the restriction (13.69) from the BPS monopoles, we get the following system of differential equations:

$$\begin{aligned} \xi\frac{dK}{d\xi} &= -KH \\ \xi\frac{dH}{d\xi} &= H - (K^2 - 1), \end{aligned} \tag{13.70}$$

which is just a special case of the system (13.36). Equations (13.70) admit the following solution at the limit $\xi \to \infty$:

$$\begin{aligned} H &= \xi\coth\xi - 1 \\ K &= \frac{\xi}{\sinh\xi}. \end{aligned} \tag{13.71}$$

13.8 Dirac, 't Hooft-Polyakov and BPS monopoles: A Comparison

Let us begin by summarizing what we know so far. The Dirac monopole arises if we simply postulate the existence of a point-like magnetic monopole which has, therefore, an arbitrary mass. Moreover, it necessitates the existence of *different* vector potentials $\vec{A}$ for different regions of spacetime which are singular on *different* string-like regions, the so-called Dirac strings; this is important in order to keep $\vec{\nabla}\cdot\vec{B} = 0$ valid everywhere (except from the origin), which is necessary if we intend to write the magnetic field as $\vec{B} = \vec{\nabla}\times\vec{A}$. However, this last equation would unavoidably hold for different $\vec{A}$'s throughout space, since we would like to avoid having singularities in the physical domain [5], [6]. The existence of different $\vec{A}$'s, which are put in by hand, is precisely what gives rise to the magnetic charge of the monopole.

On the other hand, the 't Hooft-Polyakov monopole arises as a finite-energy solution in the context of the Georgi-Glashow model; it is everywhere regular and has a calculable mass. Its magnetic charge is a consequence of the behaviour of the Higgs field far away from the core of the monopole, as equation (13.42) demonstrates, and it is conserved and gauge-invariant purely due to topological reasons. Moreover, it is an extended object with an internal structure and from far away it looks like the point-like Dirac monopole. In fact, the electromagnetic field strenth tensor of the 't Hooft-Polyakov monopole (in the Higgs vacuum) is related to that of the Dirac monopole via a gauge transformation [1].

property/monopole type	**Dirac**	**'t Hooft-Polyakov**
appearance	postulated	solution of the E.o.M.
mass	arbitrary	calculable
size	point-like	extended
magnetic charge	"put in by hand"	topological
singularities	yes	no

Table 13.2: Differences between the Dirac and the 't Hooft-Polyakov monopoles.

In addition, both the Dirac and the 't Hooft-Polyakov monopole result in the Dirac quantization condition. Instead of being a mere coincidence, this is a profound topological result: it can be shown that the homotopy groups (considered far away from the monopoles) for these two types of monopoles are equivalent. To begin with, it can be shown that [1]:

$$\Pi_2(G/H) \simeq \Pi_1(H)_G, \tag{13.72}$$

where $\Pi_2(G/H)$ is the second homotopy group of $\mathscr{M}_0$ which classifies the configurations of the Higgs field at infinity (i.e. it may classify different monopoles), while $\Pi_1(H)$ classifies the configurations of the $U(1)$ gauge fields at infinity in the case of the Dirac monopole. $\Pi_1(H)_G$ is the subgroup of closed paths in $\Pi_1(H)$ which may contracted to a point in G.

In the Georgi-Glashow model, we can consider the isomorphic group to the model's gauge group $SO(3)$; this is $SU(2)$ and it is simply connected. In other words, the Georgi-Glashow model has a simply connected universal covering group, namely $SU(2)$. Consequently, $G \simeq SU(2)$ is simply connected, so $\Pi_1(H)_G \simeq \Pi_1(H)$ and thus

$$\Pi_2(G/H) \simeq \Pi_1(H). \tag{13.73}$$

Moreover, for $H = U(1)$ it is easy to see that $\Pi_1(H) = \mathbb{Z}$ which is not trivial, so equation (13.73) tells us that $\Pi_2(G/H)$ is not trivial. Thus, in this model topological monopoles can exist, classified by $\Pi_2(G/H) = \mathbb{Z}$. We have already seen the specific example of the 't Hooft-Polyakov monopole. Equation (13.73) tells us that far away from the 't Hooft-Polyakov monopole, we can in a sense ignore the non-abelian fields and instead consider only the $U(1)$ fields that give rise to the Dirac monopole. We conclude that, in a way, the 't Hooft-Polyakov and the Dirac monopole are equivalent descriptions of the same monopole from far away. Intuitively, in the case of the 't Hooft-Polyakov monopole the Dirac string is "smoothed out" into all other directions via $SO(3)$ gauge transformations, which gives the stable hedgehog configuration we have discussed.

We will now argue that this does not happen in the Standard Model for which $G = SU(3) \times SU(2)_L \times U(1)_Y$. In this model the generator Q that corresponds to the electric charge is a linear combination of generators of $SU(2)_L$ and $U(1)_Y$. However, Q is also the generator of $H = U(1)_{EM}$ of electromagnetism. So $U(1)_{EM}$ is a subgroup of G, but the latter is not simply connected. This means that not any closed path in H can be deformed to a point in G, so $\Pi_1(H)_G = 0$. Equation (13.72) tells us that $\Pi_1(G/H) = 0$, so we conclude that the Standard Model does not predict the existence of topological monopoles. An extension of this model to a model with a larger gauge group which is simply connected and has $U(1)_{EM}$ as a subgroup could admit monopole solutions with masses much higher than that of the 't Hooft-Polyakov monopole.

Now let us turn to the BPS monopole. If we take the limit $\xi \to \infty$ (i.e. spatial infinity) of the differential equation (13.70) for H, we find that the solution approaches its asymptotic form as

$$H - \xi = 1 + O(e^{-\xi}). \tag{13.74}$$

This approach is slower than the corresponding one in the case of the generic 't Hooft-Polyakov monopole; the latter is just $e^{-\frac{\mu r}{\hbar}}$ as given by equation (13.38). This should be expected because for the BPS monopole we have that $\lambda \to 0$, which means that $\mu \to 0$: the Higgs field is now massless as the photon and, therefore, long range. Consequently, the BPS monopole, in contrast to the generic 't Hooft-Polyakov monopole, could be distinguished from a Dirac monopole even from far away.

- A remark on the force between BPS monopoles

Apart from the magnetic one, two BPS monopoles also experience another force which is accounted for by the massless Higgs field and which can be shown to be always attractive. Moreover, for static monopoles this force depends on the distance between the two monopoles in the same way as the magnetic one; it is namely proportional to $1/r^2$. Using the above it can be shown that, although two Dirac monopoles of equal magnetic charge repel each other, two static BPS monopoles feel no net force since the magnetic force is canceled by the one accounted for by the Higgs field [16].

13.9 The Witten effect

Let us consider a general finite energy (monopole-like) solution for the Georgi-Glashow model with electric and magnetic charge being q and g respectively, as in the derivation of the Bogomol'nyi bound. Moreoever, let us consider the following gauge transformation (infinitesimally)

$$\begin{aligned} \delta\vec{\phi} &= 0 \\ \delta\vec{W}_\mu &= \frac{1}{ea} D_\mu \vec{\phi}. \end{aligned} \tag{13.75}$$

This means that we have considered a generalization of $U(1)$ gauge transformations about the axis $\vec{\phi}$ (see for example [5]). Since $U(1)$ is a subgroup of $SO(3)$, and given that ϕ belongs to the adjoint representation of $SO(3)$, a rotation of 2π around the ϕ axis yields the same field configuration, so it corresponds to an identity trasnformation, i.e.

$$e^{2\pi i N} = 1, \tag{13.76}$$

where N is the generator of these transformations and $e^{2\pi i N}$ is the corresponding group element. Equation (13.76) tells us that N is an integer; we will use this information later. We should note that in the Higgs vacuum we have $D_\mu\vec{\phi} = 0$, so the transformations (13.75) do not affect the fields at spatial infinity.

N is also the charge that corresponds to this transformation and now we would like to compute it using Noether's theorem. If J^μ is the corresponding conserved current, we have that (assuming again $\vec{W}_0 = 0$ as for the 't Hooft-Polyakov monopole)

$$\begin{aligned} N &= \int d^3\vec{r} J^0 \\ &= \int d^3\vec{r} \frac{\partial \mathscr{L}}{\partial(\partial_0 \vec{W}_i)} \delta\vec{W}_i \\ &= -\frac{1}{ea} \int d^3\vec{r} (\vec{G}^{0i}) D_i \vec{\phi} \\ &= \frac{1}{ea} \int d^3\vec{r} \vec{\mathscr{E}}^i \cdot D_i \vec{\phi}. \end{aligned} \tag{13.77}$$

If we use equation (13.59), we have that

$$N = \frac{q}{e}, \tag{13.78}$$

which is a quantization condition since N is an integer.

Now let us see what happens to equation (13.78) when we add a specific term in the Lagrangian, the so-called θ-term:

$$\mathscr{L}_\theta = -\frac{e^2\theta}{32\pi^2} * \vec{G^{\mu\nu}} \cdot \vec{G_{\mu\nu}}, \tag{13.79}$$

where θ is a parameter. In fact, as we will see in the review of Instantons that follows, θ has the properties of an angular parameter that parametrizes inequivalent vacuum states. The θ-term is

Particle	Mass	Charge
Photon	0	0
Higgs	0	0
$W_\pm$ boson	aq	$(\pm q, 0)$
$M_\pm$ monopole	ag	$(0, \pm g)$

Table 13.3: The Particle Spectrum with BPS monopoles at $\lambda = 0$, $\theta = 0$.

a total derivative so it can be added to the Lagrangian without affecting the equations of motion; however, the conserved charge changes: it becomes N', given by

$$N' = N + \delta N, \tag{13.80}$$

where we compute

$$\begin{aligned} \delta N &= \int d^3\vec{r} \frac{\partial \mathscr{L}_\theta}{\partial(\partial_0 \vec{W}_i)} \delta \vec{W}_i \\ &= -\frac{1}{ea}\frac{e^2\theta}{32\pi^2}\int d^3\vec{r}(2\varepsilon^{0ijk}\vec{G}_{jk})D_i\vec{\phi} \\ &= -\frac{e\theta}{16\pi^2 a}\int d^3\vec{r}\varepsilon^{ijk}\vec{G}_{jk}D_i\vec{\phi} \\ &= \frac{e\theta}{16\pi^2 a}\int d^3\vec{r} 2\vec{\mathscr{B}}^i \cdot D_i\vec{\phi}, \end{aligned} \tag{13.81}$$

and if we use equation (13.57), we conclude that

$$N' = \frac{q}{e} + \frac{eg\theta}{8\pi^2}. \tag{13.82}$$

We now see that the allowed values of the electric charge of the solution, which before adding the θ-term were

$$q = Ne, \tag{13.83}$$

are shifted by a term proportional to the parameter θ, after we add the the θ-term:

$$\begin{aligned} q &= N'e - \frac{e\theta}{2\pi}\frac{eg}{4\pi} \\ &= n_e e - n_m \frac{e\theta}{2\pi}, \end{aligned} \tag{13.84}$$

where we have set $N' = n_e$ and we have used the Dirac quantization condition (as derived for the 't Hooft-Polyakov monopole) $eg = 4\pi n_m$. This shift corresponds to the so-called Witten effect: a magnetic monopole with no magnetic charge can aquire one due to the θ-term in the Lagrangian.

13.10 The Montonen-Olive conjecture and $SL(2,\mathbb{Z})$ duality

In this section we will, at first, try to establish an electromagnetic duality for the Georgi-Glashow model; we will then try to promote this to $SL(2,\mathbb{Z})$ duality in the BPS limit with the addition of the θ-term to the Lagrangian. Let us begin by considering the spectrum, given in table 13.3, of the model with BPS monopoles (the latter have no electric charge since we have assumed $\vec{\mathscr{E}}_i = 0$), i.e. $\lambda = 0$, assuming for the moment that $\theta = 0$. We have also set $q = e\hbar$. We notice that the masses M of all particles of table 13.3 satisfy the Bogomol'nyi bound $M \geq a\sqrt{{Q_e}^2 + {Q_m}^2}$, where

$$Q_e = n_e e, Q_m = n_m \frac{4\pi}{e}. \tag{13.85}$$

Moreover, we observe that the spectrum is invariant under the electromagnetic duality:

$$\begin{aligned}(\vec{E},\vec{B}) &\mapsto (\vec{B},-\vec{E})\\ (q,g) &\mapsto (g,-q).\end{aligned} \tag{13.86}$$

This has lead to the famous Montonen-Olive conjecture: the duality transformation of the Georgi-Glashow model gives a dual theory in which the gauge bosons have become BPS monopoles. We should note that if the coupling e of the Georgi-Glashow model is small, then, since $g \sim 1/e$, the coupling g of its dual theory is very large. This means that the duality relates two different theories: for the one with the small coupling perturbation theory can be applied, although this is not the case for the other. We also note that this conjecture comes with several drawbacks, some of which can be eliminated in the context of supersymmetry [5], [6].

But what happens to the conjecture if we introduce the θ-term (13.79) in the Lagrangian of the Georgi-Glashow model (still for $\lambda = 0$)? Is is straightforward to see that with this term we can rerwrite the Lagrangian as (after relabeling $\vec{W}_\mu \mapsto e\vec{W}_\mu$)

$$\begin{aligned}\mathscr{L} &= -\frac{1}{32\pi} Im\{(\frac{\theta}{2\pi} + i\frac{4\pi}{e^2})(\vec{G}^{\mu\nu} + i*\vec{G}^{\mu\nu})(\vec{G}_{\mu\nu} + i*\vec{G}_{\mu\nu})\} + \frac{1}{2}D^\mu\vec{\phi}\cdot D_\mu\vec{\phi}\\ &= -\frac{1}{32\pi} Im(\tau\vec{\mathscr{G}^{\mu\nu}}\cdot\vec{\mathscr{G}_{\mu\nu}}) + \frac{1}{2}D^\mu\vec{\phi}\cdot D_\mu\vec{\phi},\end{aligned} \tag{13.87}$$

where we have set

$$\vec{\mathscr{G}^{\mu\nu}} = \vec{G}^{\mu\nu} + i*\vec{G}^{\mu\nu} \tag{13.88}$$

and

$$\tau = \frac{\theta}{2\pi} + i\frac{4\pi}{e^2}, \tag{13.89}$$

which means that we combine e and θ into a single complex parameter τ.

Now, since θ is an angular variable, it is periodic with period 2π. Consequently, the Lagrangian is invariant under the transformation

$$\tau \mapsto \tau + 1. \tag{13.90}$$

Moreover, the electromagnetic duality (13.86) corresponds to the transformation (for $\theta = 0$)

$$\tau \mapsto -\frac{1}{\tau}. \tag{13.91}$$

It has been established that (13.90) and (13.91) together generate the group $SL(2,\mathbb{Z})$. This group has as elements all 2×2 matrices with integer components a, b, c, d and unit determinant (i.e. $ad - bc = 1$) that act on complex parameters as linear fractional operators. This means that $SL(2,\mathbb{Z})$ determines the transformations

$$\tau \mapsto \frac{a\tau + b}{c\tau + d}. \tag{13.92}$$

We now suspect that $SL(2,\mathbb{Z})$ transformations are symmetry transformations of the Georgi-Glashow model for arbitrary θ. In fact, one can show that $SL(2,\mathbb{Z})$ transformations indeed relabel particle states, i.e. the quantum numbers of the states, which are the electric and magnetic charges in this case [5]; this relabeling is of course more complex than the simple $(q,g) \mapsto (g,-q)$ of the Montonen-Olive conjecture. Moreover, one can show that the mass formula for BPS monopoles is indeed invariant under $SL(2,\mathbb{Z})$ transformations. We conclude that $SL(2,\mathbb{Z})$ duality is a symmetry of the Georgi-Glashow model that includes the θ-term and appears to be more promising in terms of testability than the Montonen-Olive conjecture [5].

Bibliography

[1] P. Goddard, D. I. Olive. *Magnetic monopoles in gauge field theories*. Rep. Prog. Phys. Vol. 41 (1974)

[2] A. H. Guth, S. -H. H. Tye. *Phase Transitions and Magnetic Monopole Production in the Very Early Universe*. Phys. Rev. Lett. 44, 631 (1980)

[3] M. Gabella. *Non-Abelian Gauge Theories with Spontaneous Symmetry Breaking: Higgs Mechanism*. Talk at EPFL (2006)

[4] H. Liu, T. Vachaspati. *SU(5) Monopoles and the Dual Standard Model*. arXiv:hep-th/9604138 (1996)

[5] J. Harvey. *Magnetic Monopoles, Duality, and Supersymmetry*. arXiv:hep-th/9603086 (1996)

[6] J. M. Figueroa-O' Farrill. *Electromagnetic Duality for Children*. Lecture Notes (1998)

[7] G. 't Hooft. *Magnetic monopoles in unified gauge theories*. Nuclear Physics B79, 276-284 (1974)

[8] A. M. Polyakov. JETP Lett. 20 194-5 (1974)

[9] A. Rajantie. *Introduction to Magnetic Monopoles*. arXiv:1204.3077v1 [hep-th] (2012)

[10] J. Preskill. *Magnetic monopoles*. Ann. Rev. Nucl. Part. Sci. 34:461-530 (1984)

[11] A. S. Schwarz. Nucl. Phys. B 112 358-64 (1976)

[12] J. Arafune, P. G. O. Freund, C.J. Goebel. J. Math. Phys. 16 433-7 (1975)

[13] Ya.B. Zeldovich, M.Yu. Khlopov. *On the concentration of relic magnetic monopoles in the universe*. Phys. Lett. B Vol. 79, Issue 3: 239-241 (1978)

[14] IceCube Collaboration. *Search for non-relativistic Magnetic Monopoles with IceCube*. arXiv:1402.3460 [astro-ph.CO] (2014)

[15] D. Hogan, D. Besson, J. Ralston, I. Kravchenko, D. Seckel. *Relativistic Magnetic Monopole Flux Constraints from RICE*. Phys.Rev. D78 (2008), p. 075031.

[16] N. S. Manton. *The Force Between 't Hooft-Polyakov Monopoles*. Nucl. Phys. B 126 (1977) 525.

[17] S. Eidelman et al. (Particle Data Group). *Magnetic monopole searches*. Phys. Lett. B 592, 1 (2004)

[18] J. Preskill. *Cosmological production of superheavy magnetic monopoles*. Phys. Rev. Lett., Vol. 43, Nr. 19 (1979)

Instantons

Student: Jacob Shapiro
Supervisor: Dr. Philippe de Forcrand

May 29, 2014

Abstract

This document encompasses a report corresponding to a presentation given in ETHZ in the spring semester of 2014 as part of a proseminar on topological objects in physics, directed by Dr. Philippe de Forcrand. Its purpose is to make precise that which was shown in the presentation.

After reviewing some "toy" models in quantum mechanics which allow us to exhibit the important concepts of instantons in a familiar environment– essentially a tunneling description between distinct vacua–a discussion of instantons in non-Abelian gauge field theory follows. Finally a brief chapter on the consequences of instantons in QCD concludes the report.

Note that this document exists in two versions: an unabridged version which contains all proofs with full detail and is not meant to be printed, and an abridged version which contains *no proofs*. You are now reading the abridged version. The unabridged version can be found at
http://www.phys.ethz.ch/∼jshapiro/PDFs/Instantons_report_unabridged.pdf.

Contents

Part I

Instantons in Quantum Mechanics

Chapter 1

The Cumbersome Harmonic Oscillator

In this chapter we shall derive the ground state energy eigenvalue for the harmonic oscillator in a cumbersome way, following very closely the presentation of [9]. This way shall prove very useful for quantum field theory.

1.1 Path-Integral Formulation of Quantum Mechanics

A point particle of mass $m \equiv 1$ (in properly chosen units) moves in two spacetime dimensions. Its position, varying with time, is described by a function $x \in \mathbb{R}^{\mathbb{R}}$, and we further assume that the particle is under the influence of some potential $V[x](t)$. The Lagrangian for this system is given by $L[x](t) \equiv \frac{1}{2}(\dot{x}(t))^2 - V[x](t)$. Let $\{x_i, x_f, t_i, t_f\} \subset \mathbb{R}$.

1.1.0.1 Fact

According to Feynman's path-integral formulation of quantum mechanics [6], if the particle was initially at x_i at time t_i, the *transition amplitude* of the particle to be found finally at x_f at time t_f–conventionally denoted by $\langle x_f, t_f \,|\, x_i, t_i\rangle$–is given by:

$$\boxed{\langle x_f, t_f \,|\, x_i, t_i\rangle = \mathcal{N} \int_{\{x \in \mathbb{R}^{\mathbb{R}}:\, x(t_f)=x_f \wedge x(t_i)=x_i\}} \mathcal{D}x \exp\left\{ i \frac{\int_{t_i}^{t_f} dt L[x](t)}{\hbar} \right\}} \tag{1.1}$$

1.1.0.2 Remarks

1. $\mathcal{N}$ is a normalization factor which will be determined later.
2. This formulation gives a natural scale for the action, $\hbar$. Now we can answer what is a "large" action, whereas in classical mechanics that notion had no meaning. From here on we shall choose our units such that $\hbar \stackrel{!}{=} 1$, in order to simplify the formulas.

3. Usually in quantum mechanics the transition amplitude $\langle x_f,\, t_f \,|\, x_i,\, t_i\rangle$ is in fact denoted by $\left\langle x_f \left| \exp\left\{i\hat{H}\left(t_f - t_i\right)\right\} \right| x_i \right\rangle$ where $\hat{H}$ is the time-evolution operator on the Hilbert space of states of the particle (and the various $|x\rangle$'s are vectors in this space). However, the path-integral formulation was conceived exactly in order to blur the distinction between space and time (which is impossible in the Hamiltonian formulation of mechanics and only possible in the Lagrangian formulation of mechanics) and so we may operate agnostically to the existence of $\hat{H}$ and proceed dealing only with the functional L, which is now the fundamental object of the theory.

1.2 Imaginary Time

An invaluable tool in path integral computations is the Euclidean path integral, which is a formal analytic continuation of the path integral to complex-valued time $\langle x_f,\, -it_f \,|\, x_i,\, -it_i\rangle$.

1.2.1 Ground State and Energy for Large Times

1.2.1.1 Claim

$\lim_{T\to\infty} \left\langle x_f,\, -i\frac{T}{2} \,\middle|\, x_i,\, i\frac{T}{2}\right\rangle = \lim_{T\to\infty} e^{-E_0 T}\psi_0\left(x_f\right)\psi_0^*\left(x_i\right)$ where $\psi_0\left(x\right)$ is the wave function corresponding to the lowest lying energy eigenstate.
This is half of why it is useful to work in imaginary time.

1.2.2 Euclidean Time Path Integral

1.2.2.1 Claim

$\left\langle x_f,\, -i\frac{T}{2} \,\middle|\, x_i,\, i\frac{T}{2}\right\rangle = \mathcal{N}\int_{\left\{x\in\mathbb{R}^{\mathbb{R}}:\, x\left(\frac{T}{2}\right)=x_f \wedge x\left(-\frac{T}{2}\right)=x_i\right\}} \mathcal{D}x \exp\left\{-\int_{-\frac{T}{2}}^{\frac{T}{2}} dt \left[\frac{1}{2}\left(\dot{x}\left(t\right)\right)^2 + V\left[x\right]\left(t\right)\right]\right\}$ for any $T \in \mathbb{R}$.

1.2.2.2 Remarks

The effect of Euclidean time on the path integral is two fold:

1. The exponent in the path integral is now real. If we assume that $\min\left(\left\{V\left[x\right] \,|\, x\right\}\right) = 0$ (and we may do that without loss of generality by choosing the energy scale appropriately) , then the exponent is always negative, which means we may be more optimistic about the convergence of the path integral.

2. It turns out that to calculate path-integrals it is worthwhile to investigate the classical paths of the action first (as we shall see soon). In classical mechanics, what we have achieved by the complex-valued time is equivalently an inverted potential: $V\left[x\right] \mapsto -V\left[x\right]$. This identification will help us "read off" classical paths using preexisting intutition in classical mechanics (although now we shall employ it on inverted potentials).

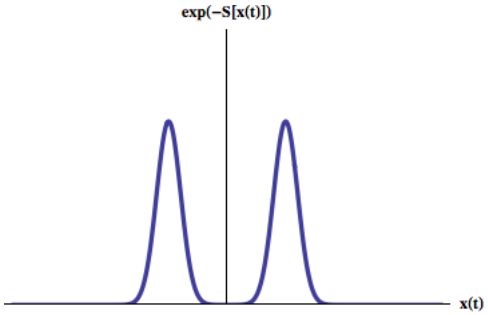

Figure 1.1: The volume under the curve can be approximated as the sum of two separate Gaussian integrals.

1.3 Approximating the Path Integral

In a crude way, assume that for our problem at hand $\int_{-\frac{T}{2}}^{\frac{T}{2}} dt \left\{ \frac{1}{2} \left(\dot{x} \left(t \right) \right)^2 + V \left[x \right] \left(t \right) \right] \Big\} \gg 1$ $\forall$ paths to be integrated on. This corresponds to the semiclassical approximation where we assume $\hbar$ is very small compared to the action. Then it is clear that most of the contribution to the path integral will come from those paths which minimize the Euclidean action. This is exactly the definition of the classical paths with potential $(-V \left[x \right])$. If there is only *one* such extremum path for the action, which we denote by $x_{cl} \left(t \right)$ (that is, we assume that $\ddot{x}_{cl} \left(t \right) = V' \left[x \right]$), then we can estimate $\mathcal{N} \int_{\left\{ x \in \mathbb{R}^{\mathbb{R}} : x\left(\frac{T}{2} \right) = x_f \wedge x\left(-\frac{T}{2} \right) = x_i \right\}} \mathcal{D}x \exp \left\{ -S \left[x \right] \right\} \sim \exp \left\{ -S \left[x_{cl} \right] \right\}$ (by using the symbol S we really mean S_E–this will be true till the end of this text).

If $\exists$ more than one such extremal path, then we would make a reasonable approximation by *summing* over the contribution from each path, assuming these extremum points are well separated in function space.

An analogy can be made to integrating over two Gaussians which are well separated (see Figure 1.1).

For our $V \left[x \right]$, the inverted harmonic oscillator, we know that there exists only one solution to the equation of motion which has finite action (infinite action doesn't interest us because its contribution would be zero anyway): $x_{cl} \left(t \right) = 0$, with boundary conditions $x_{cl} \left(\pm \frac{T}{2} \right) = 0$.

1.3.1 Taylor Expanding the Action

Pick some $\varepsilon \in (0,\, 1)$. Define $\eta \left(t \right) := \frac{1}{\varepsilon} \left[x \left(t \right) - x_{cl} \left(t \right) \right]$, where $x \left(t \right) \in \left\{ x \in \mathbb{R}^{\mathbb{R}} : \, x \left(\frac{T}{2} \right) = x_f \wedge x \left(-\frac{T}{2} \right) = x_i \right\}$ is the set of paths we would be integrating over. Because $x_{cl} \left(t \right)$ is a solution to the classical equation of motion with the same boundary conditions, we have that $\eta \left(\pm \frac{T}{2} \right) = 0$.

1.3.1.1 Claim

The action can be approximated as $S \left[x_{cl} + \varepsilon \eta \right] \approx S \left[x_{cl} \right] + \frac{1}{2} \sum_{n \in \mathbb{N}} c_n^2 \left(\left(\frac{\pi n}{T} \right)^2 + \frac{\partial^2 V[x_{cl},\, \dot{x}_{cl}]}{\partial x^2} \right) + \mathcal{O} \left(\varepsilon^3 \right)$ where c_n are expansion coefficients of $\varepsilon \eta$ in a complete set of eigenfunctions of the differential operator $-\frac{d^2}{dt^2} + \frac{\partial^2 V[x_{cl},\, \dot{x}_{cl}]}{\partial x^2}$.

1.3.2 Path-Integral Approximation

1.3.2.1 Claim

$\left\langle 0,\, i\frac{T}{2} \,\middle|\, 0,\, -i\frac{T}{2} \right\rangle \approx \sqrt{\frac{1}{2\pi}\frac{\omega}{sinh(\omega T)}}$ for the simple harmonic oscillator.

1.3.3 Ground State Energy for the Harmonic Oscillator

To get an actual expression for the energy eigenvalues, we take the limit $T \to \infty$:

$$\begin{aligned}
\lim_{T\to\infty} \left\langle 0,\, i\frac{T}{2} \,\middle|\, 0,\, -i\frac{T}{2} \right\rangle &\approx \lim_{T\to\infty} \sqrt{\frac{1}{2\pi}\frac{\omega}{sinh\left(\omega T\right)}} = \\
&= \lim_{T\to\infty} \sqrt{\frac{\omega}{\pi}\frac{e^{-\omega T}}{1-e^{-2\omega T}}} \\
&\approx \sqrt{\frac{\omega}{\pi}} \lim_{T\to\infty} e^{-\frac{\omega}{2}T}\left(1+\frac{1}{2}\mathcal{O}\left(e^{-2\omega T}\right)\right)
\end{aligned}$$

- Comparing this result with the expression from usual quantum mechanics we find: $\boxed{\lim_{T\to\infty} e^{-E_0 T}\left|\psi_0\left(0\right)\right|^2 \approx \sqrt{\frac{\omega}{\pi}} \lim_{T\to\infty} e^{-\frac{\omega}{2}T}}$
  The sense in which this is an approximation is that higher order terms on the left hand side will give us contributions from higher states of the system (only $n \in 2\mathbb{N}$ though because for $n \in 2\mathbb{N}+1$, $\psi_n\left(0\right)=0$).

- Thus we deduce that $\boxed{E_0 = \frac{\omega}{2}}$ and $\boxed{\left|\psi_0\left(0\right)\right|^2 = \sqrt{\frac{\omega}{\pi}}}$, which thankfully agrees with the usual canonical quantization computation, as in [7].

1.4 Conclusion

In conclusion, to find the ground state energy of a system and the ground state wave function evaluated at $x=0$, we have found the formula: $\lim_{T\to\infty} e^{-E_0 T}\left|\psi_0\left(0\right)\right|^2 \approx e^{-S[x_{cl}]}\sqrt{\frac{\omega}{\pi}}\lim_{T\to\infty} e^{-\frac{\omega}{2}T}$ where $\omega \equiv \sqrt{\frac{\partial^2 V[x_{cl},\dot{x}_{cl}]}{\partial x^2}}$.

Chapter 2

The Double-Well Potential

Our setup is the same as before, however now our potential is given by $V[x] = \frac{\omega^2}{8a^2}\left(x^2 - a^2\right)^2$ where $\{a, \omega\} \subset (0, \infty)$.

In order to simplify the expressions to come, define $\lambda := \frac{\omega^2}{8a^2}$ so that $V[x] = \lambda\left(x^2 - a^2\right)^2$.

This is the quartic double well potential, which we study as an archetype for tunneling phenomena in quantum mechanics. It is a prominent example for a system where employment of perturbation theory (for example, expansion in λ) will not reveal tunneling, and we must use another approach to see the effect.

2.1 Computation With Usual QM Methods

The Schroedinger equation reads (if we assume $m = 1$ and define $\hbar \equiv 1$):

$$\left[\frac{d^2}{dx^2} - 2\lambda\left(x^2 - a^2\right)^2 + 2E\right]\psi(x) = 0 \tag{2.1}$$

2.1.0.1 Claim

The two lowest energy eigenvalues of this differential equation are given by:

$$\begin{cases} E_0 = \frac{\omega}{2}\left[1 - \sqrt{\frac{2\omega^3}{\pi\lambda}}\exp\left(-\frac{\omega^3}{12\lambda}\right)\right] \\ E_1 = \frac{\omega}{2}\left[1 + \sqrt{\frac{2\omega^3}{\pi\lambda}}\exp\left(-\frac{\omega^3}{12\lambda}\right)\right] \end{cases}$$

Note: $E_0 - E_1 \sim \exp\left(-\frac{\omega^3}{12\lambda}\right)$, which cannot be expanded in perturbation series for small λ.

2.2 Computation With Euclidean Path Integral

Our strategy for the double-well is the same as the quantum harmonic oscillator: find the classical paths (which minimize the action), and expand the action around them. Finally plug this expansion into the path-integral. This means that classical paths whose action is infinite will have no contribution to the path integral. We shall now try to compute $\left\langle -a \middle| e^{-T\hat{H}} \middle| a \right\rangle$ (from here on referred to

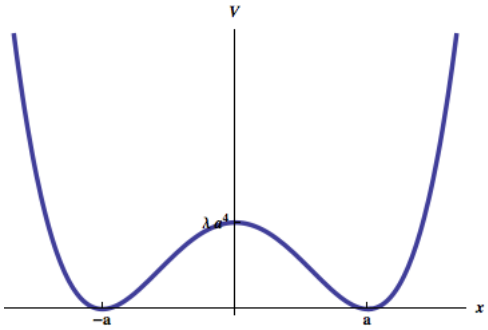

Figure 2.1: The double well.

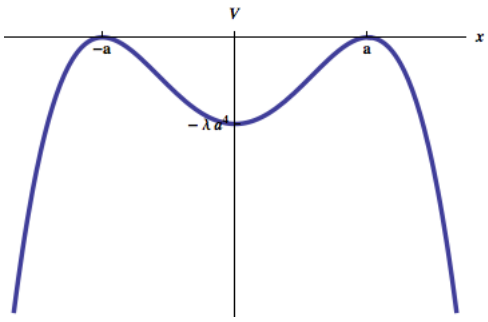

Figure 2.2: In Euclidean spacetime the potential is inverted.

as $BC1$) and $\left\langle a \left| e^{-T\hat{H}} \right| -a \right\rangle$ (from here on referred to as $BC2$), two transitions which we associate with quantum tunneling.

2.2.1 The Classical Euclidean Paths of Finite Action

Because we are working in Euclidean spacetime, our potential is inverted and we are looking for solutions for the following equation of motion:

$$\boxed{\ddot{x}_{cl}(t) = 4\lambda \left[x_{cl}(t)^2 - a^2 \right] x_{cl}(t)} \tag{2.2}$$

2.2.1.1 Claim

The *only* solutions to this equation are $\boxed{a \cdot \tanh\left(\pm\frac{\omega}{2}(t-\mathcal{T})\right)}$ for all $\mathcal{T} \in \mathbb{R}$, where the $+$ variant corresponds to $BC1$ and the $-$ variant corresponds to $BC2$.

2.2.1.2 Remarks

- These solutions' boundary conditions are:
  - For $+$ version, $x_{cl}(-\infty) = -a$ and $x_{cl}(\infty) = a$. This solution is called an *instanton* at time $\mathcal{T}$ and shall be denoted from here until the end of this chapter as $I_{\mathcal{T}}(t)$.

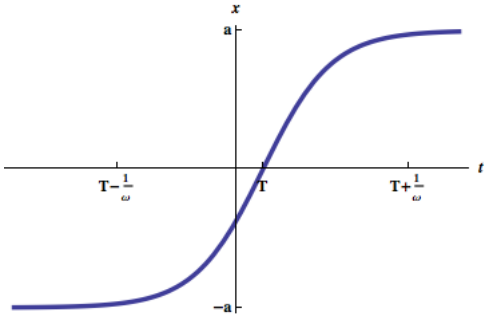

Figure 2.3: An instanton at $\mathcal{T}$.

- For the $-$ version $x_{cl}(-\infty) = a$ and $x_{cl}(\infty) = -a$. This solution is called an *anti-instanton* at time $\mathcal{T}$ and shall be denoted $A_{\mathcal{T}}(t)$.

- Thus they are only *approximate* solutions if our boundary conditions are $x_{cl}\left(\pm\frac{T}{2}\right) = \pm a$, and become precise solutions only when $T \to \infty$.

- These solutions, which correspond to tunneling are only made possible by the fact we are working in the Euclidean spacetime framework. In Minkowski spacetime $\nexists$ such solutions, because classically $\nexists$ tunneling!

- Observe that $\lim_{t\to\infty}(I_{\mathcal{T}}(t) - a) = \lim_{t\to\infty} -2ae^{-\omega(t-\mathcal{T})}$ and so we can imagine the "width" of an (anti) instanton in time is proportional $\propto \frac{1}{\omega}$. In other words, it happens within a time window of width about $\frac{1}{\omega}$ centered at $\mathcal{T}$, where before and after nothing happens.

2.2.1.3 Claim

Let $n \in 2\mathbb{N}+1$. Let $\mathcal{T}_1 \in \left(-\frac{T}{2}, \frac{T}{2}\right)$, $\mathcal{T}_2 \in \left(\mathcal{T}_1, \frac{T}{2}\right)$, $\ldots$, $\mathcal{T}_n \in \left(\mathcal{T}_{n-1}, \frac{T}{2}\right)$. Then $\boxed{a\prod_{j=1}^{n}\tanh\left[\pm\frac{1}{2}\omega(t-\mathcal{T}_j)\right]}$ are *approximate* solutions to the equation of motion.
The $+$ $(-)$ variant corresponding to $BC1$ $(BC2)$.
We call the solution with the plus "n instantons", denoted by $I^n_{\mathcal{T}_1,\ldots,\mathcal{T}_n}(t)$. Observe that it obeys exactly the same boundary conditions as the single instanton. The solution with the minus is called "n anti-instantons", denoted by $A^n_{\mathcal{T}_1,\ldots,\mathcal{T}_n}(t)$, and obeys the same boundary conditions as the single anti-instanton.

2.2.2 Features of Instanton Solutions

2.2.2.1 Claim

$E[I_{\mathcal{T}}] \equiv \frac{1}{2}\dot{I_{\mathcal{T}}}(t)^2 - V[I_{\mathcal{T}}] = 0$ and the same for $A_{\mathcal{T}}$. Thus we would see that the instantons and anti-instantons have zero total (Euclidean) energy.

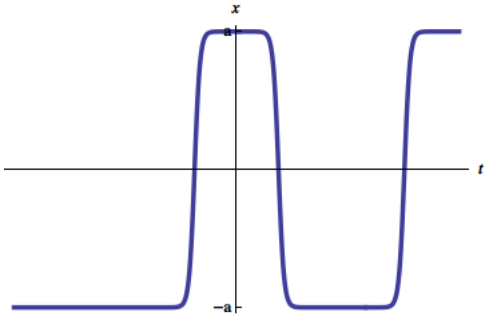

Figure 2.4: A 3-instanton.

2.2.2.2 Claim

$S[I_{\mathcal{T}}] = S[A_{\mathcal{T}}] = \frac{\omega^3}{12\lambda}$ (in particular, the action of instantons and anti-instantons is independent of their parameter $\mathcal{T}$!)

Define $\boxed{S_0 := \frac{\omega^3}{12\lambda}}$.

2.2.2.3 Claim

$S\left[I^n_{\mathcal{T}_1,\ldots,\mathcal{T}_n}(t)\right] = S\left[A^n_{\mathcal{T}_1,\ldots,\mathcal{T}_n}(t)\right] = n\,S_0$

2.2.3 Structure of Transition Amplitude Approximation

We find that the most general classical *approximate* solution to the equation of motion with either $BC1$ or $BC2$ is indexed by some *odd* integer n, together with n consecutive numbers in the interval $\left(-\frac{T}{2}, \frac{T}{2}\right) \subset \mathbb{R}$.

As we remarked in the first chapter, if we want to make an approximation for the path integral around stationary paths, and if $\exists$ more than one stationary path, then in general we could approximate the path integral as a sum of approximations around the various stationary paths.

Thus we expect

$$\left\langle -a \left| e^{-T\hat{H}} \right| a \right\rangle \tag{2.3}$$
$$\approx \sum_{n\in 2\mathbb{N}+1} \int_{-T/2}^{T/2} d\mathcal{T}_1 \ldots \int_{\mathcal{T}_{n-1}}^{T/2} d\mathcal{T}_n \left[\text{path integral approximation around } I^n_{\mathcal{T}_1,\ldots,\mathcal{T}_n}(t)\right]$$

and the anti-instanton approximation for $\left\langle a \left| e^{-T\hat{H}} \right| -a \right\rangle$.

Furthermore, by similar procedures it is clear that an even number of instantons or anti-instantons obey the boundary conditions of $x_{cl}\left(\pm\frac{T}{2}\right) = \pm a$ respectively, and thus, they form an *approximate* solution with these boundary conditions, and it is also clear that $\pm a$ (the constant map sitting always at either a or $-a$) is an *exact* solution to the classical equations of motion with zero action. We will use these solutions to compute $\left\langle a \left| e^{-\hat{H}T} \right| a \right\rangle$ or $\left\langle -a \left| e^{-\hat{H}T} \right| -a \right\rangle$ respectively.

2.3 Single Instanton Contributions

Our next step would be to compute the contribution of a *single* instanton (of some given $\mathcal{T}$) to $\left\langle -a \left| e^{-T\hat{H}} \right| a \right\rangle$ for which we expand the action around $I_{\mathcal{T}}$. (Or vice versa of an anti-instanton to $\left\langle a \left| e^{-T\hat{H}} \right| -a \right\rangle$). Using our experience with the harmonic oscillator, we can readily write down that contribution:

$$\begin{aligned}\left\langle -a \left| e^{-T\hat{H}} \right| a \right\rangle_{n=1} &\approx e^{-S[I_{\mathcal{T}}]}\mathcal{N}\prod\left\{\sqrt{2\pi}\varepsilon_n^{-\frac{1}{2}}\right\} \\ &= e^{-S_0}\mathcal{N}'\left\{\prod\varepsilon_n\right\}^{-\frac{1}{2}}\end{aligned}$$

where ε_n are the eigenvalues of the operator $-\frac{d^2}{dt^2}+\frac{\partial^2 V\left[I_{\mathcal{T}},\,\dot{I}_{\mathcal{T}}\right]}{\partial x^2}$.

Next, to make the following expressions shorter, define $\det(\text{operator}) := \prod(\text{eigenvalues of operator})$. This definition is not without sense, because as we've seen in the previous chapter, the product of the eigenvalues represents the contribution to the transition amplitude of quadratic quantum fluctuations around the classical path.

Then we can rewrite the contribution as:

$$\left\langle -a \left| e^{-T\hat{H}} \right| a \right\rangle_{n=1} = e^{-S_0}\mathcal{N}'\left\{\det\left(-\frac{d^2}{dt^2}+\frac{\partial^2 V\left[I_{\mathcal{T}},\,\dot{I}_{\mathcal{T}}\right]}{\partial x^2}\right)\right\}^{-\frac{1}{2}}$$

For convenience, we take the harmonic oscillator, $\left\{\det\left(-\frac{d^2}{dt^2}+\omega^2\right)\right\}^{-\frac{1}{2}}$, as a reference for our computations:

$$\begin{aligned}\left\langle -a \left| e^{-T\hat{H}} \right| a \right\rangle_{n=1} &= e^{-S_0}\mathcal{N}'\left\{\det\left(-\frac{d^2}{dt^2}+\omega^2\right)\right\}^{-\frac{1}{2}}\left\{\frac{\det\left(-\frac{d^2}{dt^2}+\frac{\partial^2 V\left[I_{\mathcal{T}},\,\dot{I}_{\mathcal{T}}\right]}{\partial x^2}\right)}{\det\left(-\frac{d^2}{dt^2}+\omega^2\right)}\right\}^{-\frac{1}{2}} \\ &= e^{-S_0}\sqrt{\frac{1}{2\pi}\frac{\omega}{sinh\left(\omega T\right)}}\left\{\frac{\det\left(-\frac{d^2}{dt^2}+\frac{\partial^2 V\left[I_{\mathcal{T}},\,\dot{I}_{\mathcal{T}}\right]}{\partial x^2}\right)}{\det\left(-\frac{d^2}{dt^2}+\omega^2\right)}\right\}^{-\frac{1}{2}}\end{aligned}$$

Next, a simple calculation shows that

$$\begin{aligned}\frac{\partial^2 V\left[I_{\mathcal{T}},\,\dot{I}_{\mathcal{T}}\right]}{\partial x^2} &= 4\lambda\left(3x^2-a^2\right)\Big|_{x=I_{\mathcal{T}}} \\ &= \omega^2-\frac{3}{2}\frac{\omega^2}{\left\{cosh\left[\frac{1}{2}\omega\left(t-\mathcal{T}\right)\right]\right\}^2}\end{aligned}$$

so we obtain finally:

$$\left\langle -a \left| e^{-T\hat{H}} \right| a \right\rangle_{n=1} = e^{-S_0} \sqrt{\frac{1}{2\pi} \frac{\omega}{sinh(\omega T)}} \left\{ \frac{\det\left(-\frac{d^2}{dt^2} + \omega^2 - \frac{3}{2} \frac{\omega^2}{\left\{cosh\left[\frac{1}{2}\omega(t-\mathcal{T})\right]\right\}^2}\right)}{\det\left(-\frac{d^2}{dt^2} + \omega^2\right)} \right\}^{-\frac{1}{2}}$$

where we have used our computation from the first chapter for the harmonic oscillator operator determinant, and "all" that is left for us is to compute $\frac{\det\left(-\frac{d^2}{dt^2}+\omega^2-\frac{3}{2}\frac{\omega^2}{\left\{cosh\left[\frac{1}{2}\omega(t-\mathcal{T})\right]\right\}^2}\right)}{\det\left(-\frac{d^2}{dt^2}+\omega^2\right)}$.

Thus the eigenvalue equation reads: $\boxed{\left(-\frac{d^2}{dt^2} + \omega^2 - \frac{3}{2}\frac{\omega^2}{\left\{cosh\left[\frac{1}{2}\omega\left(t-\mathcal{T}\right)\right]\right\}^2}\right) y_n(t) = \varepsilon_n y_n(t)}$.

It is clear that as $\omega^2 - \varepsilon_n > 0$ we will have a discrete set of eigenvalues and when $\omega^2 - \varepsilon_n < 0$ there will be a continuous spectrum. However, with our boundary conditions $y_n\left(\pm\frac{T}{2}\right) = 0$ the eigenvalues which are bigger than ω^2 will *also* be discrete, and only when taking the limit $T \to \infty$ they will "become" continuous.

2.3.0.1 Claim

$\left\{0, \frac{3}{4}\omega^2\right\} \subset \{\varepsilon_n\}_{n\in\mathbb{N}}$, where $\{\varepsilon_n\}_{n\in\mathbb{N}}$ are all the eigenvalues of $-\frac{d^2}{dt^2} + \omega^2 - \frac{3}{2}\frac{\omega^2}{\left\{cosh\left[\frac{1}{2}\omega(t-\mathcal{T})\right]\right\}^2}$. In particular, 0 is the lowest eigenvalue of $-\frac{d^2}{dt^2} + \omega^2 - \frac{3}{2}\frac{\omega^2}{\left\{cosh\left[\frac{1}{2}\omega(t-\mathcal{T})\right]\right\}^2}$.

2.3.1 Zero Modes–Collective Coordinates

We are in trouble, because the first eigenvalue is 0, and we have a term $(\varepsilon_0)^{-\frac{1}{2}} = \frac{1}{0}$ in our transition amplitude.

We identify the $y_0(t)$ eigenvector–the eigenvector corresponding to eigenvalue zero–as a "direction" in function space that leaves the action invariant. This is because $\left(-\frac{d^2}{dt^2} + \frac{\partial^2 V\left[I_\mathcal{T}, \dot{I}_\mathcal{T}\right]}{\partial x^2}\right)$ is actually $\frac{\delta^2 S}{\delta \eta^2}$ where η is a quantum variation around the classical path $I_\mathcal{T}$. But we know of such a "direction" already: varying $I_\mathcal{T} \mapsto I_{\mathcal{T}+\Delta\mathcal{T}}$ leaves the action invariant. Thus y_0 must correspond to this shift in $\mathcal{T}$. Thus if $I_\mathcal{T}(t) + \Delta\mathcal{T} y_0(t) \propto I_{\mathcal{T}+\Delta\mathcal{T}}(t)$ then $y_0(t) \propto \frac{I_{\mathcal{T}+\Delta\mathcal{T}}(t) - I_\mathcal{T}(t)}{\Delta\mathcal{T}} \overset{\Delta\mathcal{T}\to 0}{\to} -\frac{d}{d\mathcal{T}} I_\mathcal{T}(t) = \frac{d}{dt} I_\mathcal{T}(t)$. We must still normalize this vector to be able to use it: $\int_{-\infty}^{\infty} dt y_0(t)^2 \overset{!}{=} 1$, but this computation we have already made, and found $\int_{-\infty}^{\infty} dt \left(\frac{d}{dt} I_\mathcal{T}(t)\right)^2 = S_0$. Thus we find: $\boxed{y_0(t) = (S_0)^{-\frac{1}{2}} \frac{d}{dt} I_\mathcal{T}(t)}$.

So in the path integral which we separated in chapter one into an $|\mathbb{N}|$ dimensional integral over coefficients corresponding to eigenvectors, we must separate the zero mode, because it is in fact not Gaussian $\int_\mathbb{R} dc_0 e^0$. It is clear that c_0 actually corresponds to $\mathcal{T}$ and so we can swap this integral with an integral over $\mathcal{T}$. This is conventionally called the introduction of a *collective coordinate*. This fits well with our scheme as we already anticipated integration of the various $\mathcal{T}$ parameters.

2.3.1.1 Claim

$\int dc_0 = \sqrt{S_0} \int d\mathcal{T}$

2.3.2 The Remaining Eigenvalues

- Define $\det_0$ (operator) := $\prod$ (eigenvalues of operator except the zero one).

Going back to our product of eigenvalues, we thus omit the zero eigenvalue and replace it with "preparation" for integration over the zero mode:

$$\left\{ \frac{det\left(-\frac{d^2}{dt^2} + \frac{\partial^2 V\left[I_{\mathcal{T}}, \dot{I}_{\mathcal{T}}\right]}{\partial x^2}\right)}{\det\left(-\frac{d^2}{dt^2} + \omega^2\right)} \right\}^{-\frac{1}{2}} = \sqrt{\frac{S_0}{2\pi}} d\mathcal{T} \left\{ \frac{det_0\left(-\frac{d^2}{dt^2} + \frac{\partial^2 V\left[I_{\mathcal{T}}, \dot{I}_{\mathcal{T}}\right]}{\partial x^2}\right)}{\det\left(-\frac{d^2}{dt^2} + \omega^2\right)} \right\}^{-\frac{1}{2}}$$

For normalization purposes we must also multiply by $\frac{1}{\sqrt{2\pi}}$ which is what we would have obtained from the Gaussian integral of the zero mode. Recall from chapter one that the eigenvalues of $-\frac{d^2}{dt^2} + \omega^2$ were $\left(\frac{\pi n}{T}\right)^2 + \omega^2 \overset{T\to\infty}{\longrightarrow} \omega^2$. So for every term we don't include in the product we should "compensate" by dividing by ω^2 so that all together we have:

$$\sqrt{\frac{S_0}{2\pi}} \omega d\mathcal{T} \left\{ \frac{det_0\left(-\frac{d^2}{dt^2} + \frac{\partial^2 V\left[I_{\mathcal{T}}, \dot{I}_{\mathcal{T}}\right]}{\partial x^2}\right)}{\omega^{-2} \det\left(-\frac{d^2}{dt^2} + \omega^2\right)} \right\}^{-\frac{1}{2}}$$

2.3.2.1 Claim

$\frac{det_0\left(-\frac{d^2}{dt^2} + \frac{\partial^2 V\left[I_{\mathcal{T}}, \dot{I}_{\mathcal{T}}\right]}{\partial x^2}\right)}{\omega^{-2} \det\left(-\frac{d^2}{dt^2} + \omega^2\right)} = \frac{3}{4} \times \frac{1}{9}$

Notes So all together we have $\boxed{\lim_{T\to\infty} \left\langle -a \left| e^{-T\hat{H}} \right| a \right\rangle_{\text{one-instanton}} = \lim_{T\to\infty} \left(\sqrt{\frac{\omega}{\pi}} e^{-\frac{\omega}{2}T} \right) D\omega d\mathcal{T}}$

where we define $\boxed{D := \sqrt{\frac{6}{\pi}} \sqrt{S_0} e^{-S_0}}$ to make the expressions shorter.

2.4 Dilute Instanton Gas

2.4.1 Energy Eigenvalues

Because we know that a correction of one-instanton to the harmonic oscillator entails a factor of $D\omega d\mathcal{T}$ to the transition amplitude, we may readily generalize that the contribution of n instantons is $(D\omega d\mathcal{T})^n$.

2.4.1.1 Claim

The contribution of an n-instanton to the transition amplitude is $(D\omega)^n \, d\mathcal{T}_1 \ldots d\mathcal{T}_n$.

2.4.1.2 Conclusion

So we may finally write:

$$\begin{aligned}
\lim_{T\to\infty} \left\langle -a \left| e^{-T\hat{H}} \right| a \right\rangle_{n=1} &= \lim_{T\to\infty} \left(\sqrt{\frac{\omega}{\pi}} e^{-\frac{\omega}{2}T} \right) \sum_{n\in 2\mathbb{N}+1} \int_{-T/2}^{T/2} d\mathcal{T}_1 \ldots \int_{\mathcal{T}_{n-1}}^{T/2} d\mathcal{T}_n \left[D\omega \right]^n \\
&= \lim_{T\to\infty} \left(\sqrt{\frac{\omega}{\pi}} e^{-\frac{\omega}{2}T} \right) \sum_{n\in 2\mathbb{N}+1} (D\omega)^n \frac{T^n}{n!} \\
&= \lim_{T\to\infty} \left(\sqrt{\frac{\omega}{\pi}} e^{-\frac{\omega}{2}T} \right) sinh\left[D\omega T \right] \\
&= \lim_{T\to\infty} \left(\sqrt{\frac{\omega}{\pi}} e^{-\frac{\omega}{2}T} \right) \frac{1}{2} \left[e^{D\omega T} - e^{-D\omega T} \right] \\
&= \lim_{T\to\infty} \frac{1}{2} \sqrt{\frac{\omega}{\pi}} \left[e^{-\frac{\omega}{2}T + D\omega T} - e^{-\frac{\omega}{2}T - D\omega T} \right] \\
&= \lim_{T\to\infty} \frac{1}{2} \sqrt{\frac{\omega}{\pi}} \left[e^{-\frac{\omega}{2}(1-2D)T} - e^{-\frac{\omega}{2}(1+2D)T} \right] \\
&= \lim_{T\to\infty} \frac{1}{2} \sqrt{\frac{\omega}{\pi}} \left[e^{-\frac{\omega}{2}\left(1-\sqrt{\frac{2\omega^3}{\pi\lambda}} e^{-\frac{\omega^3}{12\lambda}}\right)T} - e^{-\frac{\omega}{2}\left(1+\sqrt{\frac{2\omega^3}{\pi\lambda}} e^{-\frac{\omega^3}{12\lambda}}\right)T} \right]
\end{aligned}$$

And so we find exactly the same two lowest energy eigenvalues as the ordinary quantum mechanics techniques.

2.4.2 Symmetry of Ground State

Using exactly the same procedure, we can evaluate $\left\langle a \left| e^{-\hat{H}T} \right| a \right\rangle$. Now we have one classical solution which is the solution $x(t) = a$. But as above, we also must take into account multi-instanton approximate solutions, which take us back and forth. However, in contrast to before, now we need an *even* numbered multi-instanton.

$$\begin{aligned}
\lim_{T\to\infty} \left\langle a \left| e^{-\hat{H}T} \right| a \right\rangle &\approx \lim_{T\to\infty} \left(\sqrt{\frac{\omega}{\pi}} e^{-\frac{\omega}{2}T} \right) \sum_{n\in 2\mathbb{N}} (D\omega)^n \frac{T^n}{n!} \\
&= \lim_{T\to\infty} \left(\sqrt{\frac{\omega}{\pi}} e^{-\frac{\omega}{2}T} \right) cosh\left[D\omega T \right] \\
&= \lim_{T\to\infty} \frac{1}{2} \sqrt{\frac{\omega}{\pi}} \left[e^{-\frac{\omega}{2}\left(1-\sqrt{\frac{2\omega^3}{\pi\lambda}} e^{-\frac{\omega^3}{12\lambda}}\right)T} + e^{-\frac{\omega}{2}\left(1+\sqrt{\frac{2\omega^3}{\pi\lambda}} e^{-\frac{\omega^3}{12\lambda}}\right)T} \right]
\end{aligned}$$

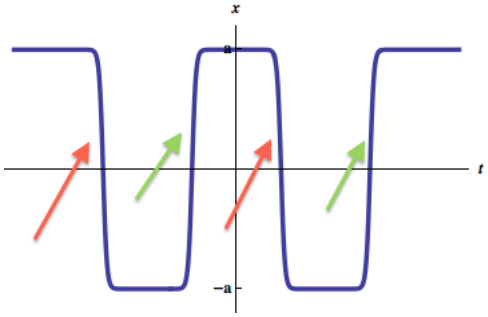

Figure 2.5: A 4-instanton. The green arrows point to instantons and red arrows point to anti-instantons in the sequence.

2.4.3 Wave Functions

From our analysis it is also possible to extract the energy eigenfunctions: $\psi_0(-a)\,\psi_0^*(a) = \psi_0(a)\,\psi_0^*(a) = \frac{1}{2}\sqrt{\frac{\omega}{\pi}} \Longrightarrow \boxed{\psi_0(a) = \psi_0(-a) = \left(\frac{\omega}{4\pi}\right)^{\frac{1}{4}}}$ and so it is appears that the wave function for the lowest state remains symmetric after all under the exchange of $\pm a$.

2.4.4 Validity of Dilute Instanton Approximation

Even though we are seemingly summing over an *arbitrarily large* number of instantons (and so the dilute gas approximation should break down at some point), in infinite sums of the form $\sum_{n\in\mathbb{N}} \frac{x^n}{n!}$, only the terms for which $n < x$ are non-negligible. That means for us only terms where $n < D\omega T$ are actually important in the infinite sum, where we recall $D \equiv \sqrt{\frac{6}{\pi}}\sqrt{S_0}e^{-S_0}$ from before.

For the dilute gas approximation to be valid, we have assumed that instantons don't "interact", that is, that one instanton event is finished well before another one starts: $|\mathcal{T}_i - \mathcal{T}_j| \gg \frac{1}{\omega}$. So we must make sure this condition holds, at least for all solutions with $n < D\omega T$. On average, we have $|\mathcal{T}_i - \mathcal{T}_j| = \frac{T}{n}$, and so, we only care about the "worst" case in which $|\mathcal{T}_i - \mathcal{T}_j| = \frac{T}{D\omega T} = \frac{1}{D} \times \frac{1}{\omega}$. So we find that in order for this approximation to hold we need $D \ll 1$, which means $\boxed{\sqrt{\frac{6}{\pi}}\sqrt{\frac{\omega^3}{12\lambda}}e^{-\frac{\omega^3}{12\lambda}} \ll 1}$. This will be true if $\lambda \ll 1$.

Chapter 3

The Periodic Well

Consider the same unit mass particle as before, but now under the influence of the potential $V[x] = \sum_{n\in\mathbb{Z}} v(x - na)$ where $v(x)$ is a single well inside $\left(-\frac{a}{2}, \frac{a}{2}\right)$ and zero outside that interval

A practical example for a system that has such a potential is the sine Gordon in QFT or just a simple pendulum in QM.

The x-values of the minima (maxima) of the potential are the set $a\mathbb{Z}$.

3.1 Kronig-Penny Type Model

Using Bloch's theorem we know that the eigenvalues of this system will be divided into energy bands, each of which a continuum (indexed by $k \in \left(-\frac{\pi}{a}, \frac{\pi}{a}\right)$) and that the energy eigenstates are also eigenstates of the translation operators by $a\mathbb{Z}$: $\hat{T}_{ma}\psi_k(x) \equiv \psi_k(x + ma) = e^{ikma}\psi_k(x)$. We shall try to obtain results using "instanton calculus" instead.

3.2 Generic Transition Amplitude

A single instanton $\frac{a}{2}\left[\tanh\left(\frac{\omega}{2}(t - \mathcal{T})\right) + 2j + 1\right]$ shifts site j to site $j+1$, anti-instantons $\frac{a}{2}\left[\tanh\left(-\frac{\omega}{2}(t - \mathcal{T})\right) + 2j + 1\right]$ shift from $j+1$ to j. Now an instanton is an event localized both in space *and* in time.

3.2.1 A sequence of single-instantons versus A single big instanton

If we want to move from j to $j + 5$ we could think of two options:

1. Stringing together 5 1-instantons, $j \to j+1$, $j+1 \to j+2$, ... Then the contribution is proportional to e^{-S_0} where $S_0 = 5\frac{2}{3}a^2\omega$ (as we computed in the double well).
2. Taking a single 5-instanton: $\frac{5a}{2}\left[\tanh\left(\frac{\omega}{2}(t - \mathcal{T})\right) + 2j + 1\right]$ contribution proportional to $e^{-S_0'}$ where $S_0' = \frac{2}{3}(5a)^2\omega$. Thus this is $\mathcal{O}\left(\left(e^{-S_0}\right)^5\right)$! We will only take into account stringing 1-instantons then.

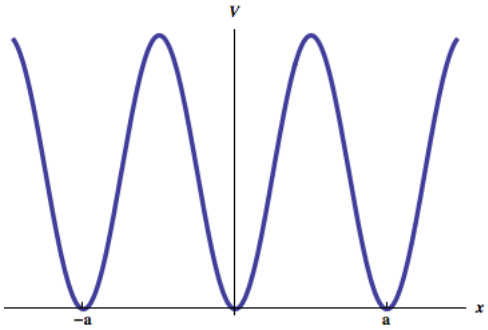

Figure 3.1: The periodic well.

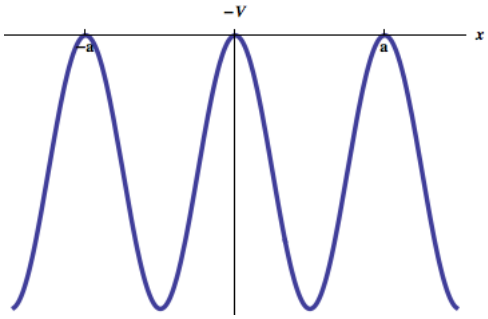

Figure 3.2: In Euclidean spacetime the potential is inverted.

So if we want to go from $j \to j'$ we assume any sequence of 1-instantons and anti 1-instantons are combined, just so that the number of instantons minus the number of anti-instantons is equal $j' - j$.

3.2.2 The Transition Amplitude

If we denote our minimum sites by j for $x = ja$ where $j \in \mathbb{Z}$, then we can write a transition amplitude as:

$$\lim_{T\to\infty} \left\langle j \left| e^{-\hat{H}T} \right| j' \right\rangle \approx \lim_{T\to\infty} \underbrace{\left(\sqrt{\frac{\omega}{\pi}} e^{-\frac{\omega}{2}T}\right)}_{\text{SHO}} \underbrace{\sum_{n\in\mathbb{N}} (D\omega)^n \frac{T^n}{n!}}_{n \text{ instantons}} \underbrace{\sum_{n'\in\mathbb{N}} (D\omega)^{n'} \frac{T^{n'}}{n'!}}_{n' \text{ anti-instantons}} \delta_{(j-j')-(n-n')}$$

What we have asserted with this statement is that we can have any number of instantons and anti-instantons (doesn't matter where) just as long as the total change in position $j - j'$ is equal to the total number of instantons n minus the total number of anti-instantons n'.

Next, write $\delta_{(j-j')-(n-n')} = \int_0^{2\pi} \frac{d\theta}{2\pi} e^{i\theta[(j-j')-(n-n')]}$ to get:

$$\begin{aligned}
\lim_{T\to\infty}\left\langle j\left|e^{-\hat{H}T}\right|j'\right\rangle &= \lim_{T\to\infty}\left(\sqrt{\frac{\omega}{\pi}}e^{-\frac{\omega}{2}T}\right)\sum_{n\in\mathbb{N}}\left[D\omega\right]^n\frac{T^n}{n!}\sum_{n'\in\mathbb{N}}\left[D\omega\right]^{n'}\frac{T^{n'}}{n'!}\int_0^{2\pi}\frac{d\theta}{2\pi}e^{i\theta\left[(j-j')-(n-n')\right]} \\
&= \lim_{T\to\infty}\left(\sqrt{\frac{\omega}{\pi}}e^{-\frac{\omega}{2}T}\right)\int_0^{2\pi}\frac{d\theta}{2\pi}e^{i\theta\left[(j-j')\right]}\sum_{n\in\mathbb{N}}\frac{1}{n!}\left[D\omega e^{-i\theta}T\right]^n\sum_{n'\in\mathbb{N}}\frac{1}{n'!}\left[D\omega e^{i\theta}T\right]^{n'} = \\
&= \lim_{T\to\infty}\left(\sqrt{\frac{\omega}{\pi}}e^{-\frac{\omega}{2}T}\right)\int_0^{2\pi}\frac{d\theta}{2\pi}e^{i\theta\left[(j-j')\right]}\exp\left[D\omega e^{-i\theta}T\right]\exp\left[D\omega e^{i\theta}T\right] \\
&= \lim_{T\to\infty}\left(\sqrt{\frac{\omega}{\pi}}e^{-\frac{\omega}{2}T}\right)\int_0^{2\pi}\frac{d\theta}{2\pi}e^{i\theta\left[(j-j')\right]}\exp\left[D\omega 2\cos\left(\theta\right)T\right] \\
&= \sqrt{\frac{\omega}{\pi}}\lim_{T\to\infty}\int_0^{2\pi}\frac{d\theta}{2\pi}e^{i\theta\left[(j-j')\right]}\exp\left[-\frac{\omega}{2}\left(1-4D\cos\left(\theta\right)\right)T\right]
\end{aligned}$$

3.2.3 The θ-Vacuum

We can read-off the energy eigenvalues from the previous expression readily:

$$E_\theta = \frac{\omega}{2} - D\omega 2\cos\left(\theta\right)$$

This is the same result we would obtain using Bloch's theorem. The barrier penetration coefficient enters in D via e^{-S_0}. This is already a "theta-vacuum" which will be important later in gauge theory: Even though we originally formulated a tunneling between $|j\rangle$ and $|j'\rangle$, it turns out that the actual vacua (by Bloch's theorem) have to be eigenstates of of the translation operator, and so, as we found, it is more natural to write $|\theta\rangle := \sum_n e^{-in\theta}|n\rangle$. Then

$$\begin{aligned}
\hat{T}_{ma}|\theta\rangle &= \sum_n e^{-ina\theta}\hat{T}_{ma}|n\rangle \\
&= \sum_n e^{-ina\theta}|n+m\rangle \\
&= e^{ima\theta}|\theta\rangle
\end{aligned}$$

Part II

Instantons in Quantum Field Theory

Chapter 4

Pure Yang-Mills Theory

In this chapter we finally get to field theory, in which the main goal will be to show that the vacuum has such a structure as to effectively add a CP-violating term to the Lagrangian. We follow the presentation in [3].

4.1 Gauge Theory

4.1.1 Gauge Groups and their Corresponding Lie Algebras

Let G be a compact Lie group, called *the gauge group*. Let $\{T^a\}_{a=1}^N$ be the generators of its corresponding Lie algebra $\mathfrak{g}$. Thus we have $\left[T^a, T^b\right] = f^{abc}T^c$ where f^{abc} are called *the structure constants* of $\mathfrak{g}$ and we employ the Einstein summation convention on the group indices (despite all group indices being superscript). For $SU(2)$ for example, $f^{abc} \equiv \varepsilon^{abc}$, the totally anti-symmetric tensor. If G is Abelian, for instance, for $U(1)$, the structure constants are $f^{abc} \equiv 0$.

We pick a representation of $\mathfrak{g}$ in which $tr\left(T^aT^b\right) \sim \delta^{ab}$. For example, for $SU(2)$, $T^a = -i\frac{\sigma^a}{2}$ where σ^a are the Pauli matrices. For $SU(3)$, $T^a = -i\frac{\lambda^a}{2}$ where λ^a are the Gell-Mann matrices.

4.1.1.1 Definition

Define the *Cartan inner product* between two generators so that we would have $\left(T^a, T^b\right) := \delta^{ab}$.

4.1.1.2 Claim

For $SU(2)$ in the representation of $\mathfrak{su}(2)$ specified above, $\left(T^a, T^b\right) = -2tr\left(T^aT^b\right)$.

4.1.2 Gauge Fields

Consider a field theory of N real vector fields, $\{A_\mu{}^a\}_{a=1}^N$, where N is the dimension of $\mathfrak{g}$ above. Because we are interested in instanton solutions, we will work exclusively in Euclidean spacetime. Thus all spacetime indices, still in Greek letters, will be subscript, yet Einstein summation convention is still in effect.

For convenience work instead with one *matrix-valued* vector field $A_\mu := gA_\mu{}^a T^a$ where $g \in \mathbb{R}$ is a *coupling constant*. So A_μ takes values in $\mathfrak{g}$. Define the field-strength tensor $\boxed{F_{\mu\nu} := \partial_{[\mu} A_{\nu]} + A_{[\mu} A_{\nu]}}$.

4.1.2.1 Note on Abelian Groups

If $G = U(1)$, this is the electromagnetic field-strength tensor because $U(1)$ is Abelian and for Abelian groups $[A_\mu, A_\nu] = 0$.

4.1.2.2 The Action

Assume that the (Euclidean) action for this theory is given by $S[A_\mu] = \frac{1}{4g^2} \int_{\mathbb{R}^4} d^4x \, (F_{\mu\nu}, F_{\mu\nu})$. This is a reasonable assumption (that is, this is the most generic term to put in the action) taking into consideration certain constraints:

- Lorentz invariance.
- Gauge invariance (to be verified later on).
- The need for renormalizability (that is, we need the mass dimension of this term to obey a certain constraint).
- Naively assuming CP invariance of the theory (this will turn out to be a misguided assumption, and as a result, we will *add* another term to the Lagrangian).

Note: because we are in Euclidean spacetime, there is no distinction between lower and upper spacetime indices.

4.1.3 Gauge Transformations

Define a *local gauge transformation* as the following map on A_μ: $\boxed{A_\mu \mapsto V A_\mu V^{-1} + V \partial_\mu V^{-1}}$ for any $V \in G^{\mathbb{R}^4}$ (here V is function of spacetime, and should really be written $V(x)$, but this is not explicit in the notation in order to keep the expressions in manageable size).

4.1.3.1 Claim

Under such a map, $F_{\mu\nu} \mapsto V F_{\mu\nu} V^{-1}$.

4.1.3.2 Claim

The action we defined above is gauge invariant

4.1.4 The Covariant Derivative

Define a *covariant derivative* for $F_{\mu\nu}$ by $D_\lambda F_{\mu\nu} := \partial_\lambda F_{\mu\nu} + [A_\lambda, F_{\mu\nu}]$.

4.1.4.1 Note

This reduces to the ordinary derivative when G is Abelian, because we have $[A_\lambda, F_{\mu\nu}] = 0$.

4.1.4.2 Claim

Then the equation of motion stemming from the action defined above is given by $\boxed{D_\mu F_{\mu\nu} = 0}$ (which is a generalized inhomogeneous source-free Maxwell's equation.)

4.1.4.3 Note about Abelian Groups

When G is Abelian, $[A_\nu, F_{\mu\nu}] = 0$ and the solution is $A_\mu = 0$. In the non-Abelian case, this equation is non-linear and non-trivial solutions may exist.

4.2 Finite Action

Just as for quantum mechanics, now for gauge field theory we are interested in the lowest energy eigenvalues. Thus we want to compute a path-integral. As we've seen in the case of quantum mechanics, it is thus worthwhile to know the classical solutions to the equations of motion and approximate the path-integral about those solutions.

Something that was implicit above should now be made clear: for this type of approximation (semi-classical approximation), classical solutions which have an infinite value for their corresponding action are not important, because their contribution to the path-integral is proportional to $e^{-S[sol.]}$ (however, in general, it is actually the solutions with *finite action* which form a set of measure zero in the space of all functions (and so should not contribute to the integral), and only gain significance in the context of the semi-classical approximation.)

4.2.0.4 Claim

In four spacetime dimensions if $S < \infty$ then $F_{\mu\nu}$ must decrease *more rapidly* than $\frac{1}{|x|^2}$.

4.2.1 Field Configurations of Finite Action

So we are interested in such field configurations so that in some series expansion of $\lim_{r\to\infty} F$ in powers of $\frac{1}{r}$, the first term in F is $\frac{1}{r^3}$. Naively, this means that in some series expansion of $\lim_{r\to\infty} A$ in powers of $\frac{1}{r}$, the first term in A is $\frac{1}{r^2}$, because $F \propto \partial_\mu A \propto \frac{1}{r^3}$.

4.2.1.1 Pure Gauge Configurations

However, it turns out that there is another possibility, which is more interesting. F could also be zero if A is some gauge transformation of zero (such a configuration is called a *pure gauge*). That is, $A_\mu = V\partial_\mu V^{-1}$ for some $V(x) \in G^{\mathbb{R}^4}$.

4.2.1.2 Claim

If A is a pure gauge then $F = 0$.

Conclusion Thus for finite action we need such fields configurations so that $\lim_{|x|\to\infty} A_\mu \overset{!}{=} V\partial_\mu V^{-1} + \mathcal{O}\left(\frac{1}{|x|^2}\right)$ for some $V(x) \in G^{\mathbb{R}^4}$. However, because in this expression V is only evaluated for $|x| \to \infty$, we can conveniently think of $V(x) \in G^{S^3}$ instead of $V(x) \in G^{\mathbb{R}^4}$, where S^3, mathematically the 4-dimensional sphere with radius *one*, is for us homeomorphic to the 4-dimensional sphere with radius infinity. So every finite action field configuration is associated with an element $V(x) \in G^{S^3}$. But if two pure gauge field configurations are in the same gauge orbit, their corresponding V is *not* the same. That is, V, which characterizes a field configuration, is *not* gauge invariant.

4.2.1.3 Claim

Gauge transforming a pure gauge field configuration $V\partial_\mu V^{-1}$ with $U \in G$ transforms V into UV.

Conclusion Thus effectively we have $V \mapsto UV$ instead of $V \mapsto V$, which is what we would expect from a gauge invariant object.

4.2.1.4 Claim

It is not possible, in general, to "gauge away" any pure gauge field configuration to zero by picking $U|_{r=\infty} = V^{-1}\big|_{r=\infty}$, thereby arranging that $A_\mu = \mathbb{1}\partial_\mu\mathbb{1}^{-1} = 0$.

Conclusion Even though we found $V \mapsto UV$ instead of $V \mapsto V$, U must be continously deformable to $\mathbb{1}$ and so: V and UV are continuously deformable into one another.

As a result, we find that the gauge-invariant object associated with $A_\mu = V\partial_\mu V^{-1}$ is not $V(x)$ per se but the class of all elements of G^{S^3} which are continuously deformable into $V(x)$.

4.3 Homotopy

Two maps that are continuously deformable into one another are *homotopic*. So to classify the gauge-invariant objects associated with finite-action field configurations, we need to find all homotopy classes in G^{S^3}. We also specialize to the case $G = SU(2)$ and so $\mathfrak{g} = \mathfrak{su}(2)$.

4.3.0.5 Claim

$SU(2) \simeq S^3$

Conclusion Using this homeomorphism we only need to think of homotopy classification of maps in $\left(S^3\right)^{S^3}$ instead of $SU(2)^{S^3}$, which is more convenient.

4.3.1 Third Homotopy Group of $SU(2)$ and the Winding Number

The classifications of all maps $S^3 \to S^3$ belongs in the field of algebraic topology [4]. For topologists, one main goal is to classify the spaces which constitute the *range* of these maps. Thus, in very crude terms, they decide if the topological spaces A and B are equivalent if the set of maps $S^n \to A$ is "equivalent" to the set of maps $S^n \to B$ for some $n \in \mathbb{N}$, where S^n is the n-sphere in $\mathbb{R}^n$. It turns out that these sets of maps (or rather equivalence classes of them–homotopy classes) form the mathematical structure of a group. This group is called *the n-th homotopy group of a space*. In order to decide if two groups are equivalent we have at our disposal the notion of *group isomorphism*. Algebraic topologists can then very clearly rule that A and B are *not* equivalent (homeomorphic, in topological jargon) if the corresponding n-th homotopy groups are not isomorphic (the converse is not in general true).

For our current purposes, the distinction between two topological spaces is not so important, but rather a "by product" of the hard work that algebraic topologists have made: the construction of the homotopy group. In order to give the n-th homotopy group the structure of a group, an equivalence relation is defined on the set of maps $S^n \to A$. Two maps $\{f, g\} \subset A^{S^n}$ are equivalent iff $\exists$ a point $x \in S^n$ and a *continuous* map $h \in A^{[0,1]\times S^n}$, called a homotopy between f and g, such that:

1. $h(0, -) = f(-)$
2. $h(1, -) = g(-)$
3. $h(-, x) = f(x) = g(x)$ for some $x \in S^n$.

That is, h can be thought of as a continuous deformation or interpolation between the "path" f to the "path" g, where all the deformations are based at $f(x) = g(x)$. The group of classes of maps in A^{S^n} which *have* a homotopy between them is denoted by $\pi_n(A)$. The law of composition on this group is defined in a natural way by concatenating two paths (and taking the equivalence class of that), the identity is the constant path at a point (or all paths equivalent to that), and inverses are paths that go in reverse direction. Thus it is clear that, for instance, if $\pi_1(A) \simeq \{0\}$, that is, the trivial group, then all paths are homotopic to the constant point. What that means is that all paths can be continuously contracted into one point (or rather, a path that just goes through one point for its range). This is not always possible, but when it is, the space is called *simply connected*.

Back to our matter at hand, we are interested in computing $\pi_3\left(S^3\right)$.

4.3.1.1 Claim

$\pi_3\left(S^3\right) \simeq \mathbb{Z}$.

Conclusion This integer in $\mathbb{Z}$ represents the number of times the 3-sphere wraps around itself (negative values for opposite orientation).

So the finite-action field configurations are "indexed" by $\mathbb{Z}$, in the sense that each A_μ obtains a label from $\mathbb{Z}$ and iff two finite-action field configurations have the same label they are homotopic.

This label is conventionally called *the winding number* of an element of $\left(S^3\right)^{S^3}$.

4.3.2 Standard Mappings of Integer Winding Numbers

Define the following reference maps which will serve us later:

1. $B\left(x\right)^{(0)} := \mathbb{1}$
2. $B\left(x\right)^{(1)} := \frac{1}{|x|}\left(x_4\mathbb{1} + i\vec{x}\cdot\vec{\sigma}\right)$ where $|x| \equiv \sqrt{\left(x_4\right)^2 + \left(x_1\right)^2 + \left(x_2\right)^2 + \left(x_3\right)^2}$. Observe how in this definition the group indices and the spacetime indices are mixed.
3. $B\left(x\right)^{(\nu)} := \left[B\left(x\right)^{(1)}\right]^{\nu}$ for any $\nu \in \mathbb{Z}$.

4.3.2.1 Claim

Using the homeomorphism we established between $SU\left(2\right) \simeq S^3$, $B\left(x\right)^{(1)}$ is actually the identity mapping between $S^3 \overset{B(x)^{(1)}}{\to} SU\left(2\right) \simeq S^3$.

4.3.2.2 Claim

$B\left(x\right)^{(\nu)} \in SU\left(2\right)^{S^3}$ for all $\nu \in \mathbb{Z}$.

Note With these standard mappings we can construct finite-action field configurations of arbitrary winding numbers.

4.3.3 Topological Charge

4.3.3.1 Definition

Define *the Cartan-Maurer Integral Invariant*,

$$\nu\left[V\left(x\right)\right] := \frac{1}{48\pi^2}\int_{S^3} d\theta_1 d\theta_2 d\theta_3 \sum_{i,j,k=1}^{3} \varepsilon_{ijk}\left(V\frac{\partial}{\partial\theta_i}V^{-1},\, V\left(\frac{\partial}{\partial\theta_j}V^{-1}\right)V\frac{\partial}{\partial\theta_k}V^{-1}\right)$$

$\forall\, V\left(x\right) \in SU\left(2\right)^{S^3}$ where θ_1, θ_2 and θ_3 are angles that parametrize S^3 and $(\,,\,)$ is the Cartan inner product.

4.3.3.2 Claim

The definition does not depend on a particular choice of parametrization

4.3.3.3 Example

In particular, for the representation we chose of $SU\left(2\right)$ we have:

$$\nu\left[V\left(x\right)\right] = -\frac{1}{24\pi^2}\int_0^{\pi} d\theta_1 \int_0^{\pi} d\theta_2 \int_0^{2\pi} d\theta_3 \varepsilon_{ijk} tr\left(V\left(\partial_i V^{-1}\right)V\left(\partial_j V^{-1}\right)V\partial_k V^{-1}\right)$$

4.3.3.4 Claim

$\nu\left[V\left(x\right)\right] = \nu\left[\tilde{V}\left(x\right)\right]$ if $V\left(x\right)$ is homotopic to $\tilde{V}\left(x\right)$.

4.3.3.5 Claim

$\nu\left[B\left(x\right)^{(1)}\right] = 1$

4.3.3.6 Claim

$\nu\left[U\left(x\right)V\left(x\right)\right] = \nu\left[U\left(x\right)\right] + \nu\left[V\left(x\right)\right]$ for any $\left\{U\left(x\right), V\left(x\right)\right\} \subset G^{S^3}$.

Conclusion Then we have $\nu\left[B\left(x\right)^{(n)}\right] = n \ \forall n \in \mathbb{Z}$. This follows from the fact that the winding number of a constant map is clearly zero, so $0 = \nu\left[\mathbb{1}\right] = \nu\left[\left(B^{(1)}\right)^{-1} B^{(1)}\right] \equiv \nu\left[B^{(-1)}B^{(1)}\right] = \nu\left[B^{(-1)}\right] + \nu\left[B^{(1)}\right]$ so $\nu\left[B^{(-1)}\right] = -1$. Then we can get all the other integers using the above formula.

4.3.3.7 Claim

$B\left(x\right)^{(n_1)}$ is homotopic to $B\left(x\right)^{(n_2)}$ iff $n_1 = n_2$.

4.3.3.8 Claim

$\forall\, V\left(x\right) \in SU\left(2\right)^{S^3}\ \exists\, n \in \mathbb{Z}$ such that $B\left(x\right)^{(n)}$ is homotopic to $V\left(x\right)$.

4.3.3.9 Claim

$\nu\left[V\left(x\right)\right] = \frac{1}{32\pi^2}\int_{\mathbb{R}^4} d^4x \left(F, \tilde{F}\right)$ where $\tilde{F}_{\mu\nu} \equiv \frac{1}{2}\varepsilon_{\mu\nu\lambda\sigma}F_{\lambda\sigma}$ is the Hodge dual of $F_{\mu\nu}$, and F is a field strength associated with some field configuration such that at $r \to \infty$, $A_\mu = V\partial_\mu V^{-1}$.

Note This formula is important because it gives us a way to compute the winding number of a *field configuration* rather than of a gauge group element which corresponds to a *pure gauge field configuration*. With this formula at hand, we can compute the winding number for *any* field configuration. For finite action field configurations, we are guaranteed the result would be some integer.

4.3.4 The Bogomol'nyi Bound and (anti-) Self Dual Field Strengths

4.3.4.1 Claim

$S\left[A_\mu\right] \geq \frac{8\pi^2}{g^2}\left|\nu\left[A_\mu\right]\right|$ and equality is obtained when $F_{\mu\nu} = \pm\tilde{F}_{\mu\nu}$.

4.3.4.2 Conclusion

We conclude that if we found such field configurations for which $\boxed{F_{\mu\nu} = \pm\tilde{F}_{\mu\nu}}$, they would actually *solve the equations of motion*, because such configurations indeed extremize the action. This is good because this equation is a first order differential equation compared with the second order EoM. We also know what is the value of the action when it is minimal: $\boxed{S_0 := \frac{8\pi^2}{g^2}}$ (for nontrivial solutions).

4.4 The BPST Instanton

In 1975 Belavin, Polyakov, Schwarz and Tyupkin suggested the following solution to the (anti-) self-dual field strength equation in [2].

4.4.0.3 Claim

The following family of field strengths, parametrized by $\rho \in \mathbb{R}$:

$$A_\mu = \frac{|x|^2}{|x|^2 + \rho^2} B(x)^{(1)} \partial_\mu \left\{ \left[B(x)^{(1)} \right]^{-1} \right\}$$

where$B(x)^{(1)} \in SU(2)^{\mathbb{R}^4}$ is as defined above, fulfill the anti-self-dual condition.

Notes

- This solution is called *the BPST instanton* (of winding number 1).
- Since [2] has been published, solutions of higher winding number to the self-dual equation have been found, but they are not so useful in finding the vacua structure as explained in the discussion of the periodic well detailing the difference between 5 single-instantons versus one 5-instanton. Further discussion can be found in [3].
- ρ is called the size of the instanton. The existence of solutions of arbitrary sizes is a necessary consequence of the scale invariance of the classical field theory.
- Anti-instanton is obtained by replacing $B(x)^{(1)}$ with $B(x)^{(-1)}$. The anti-instanton will fulfill the self-dual condition whereas the instanton fulfills the self-dual condition.
- Observe how in the limit $|x| \to \infty$, this solution is indeed a pure gauge, and as we computed already (using the formula for the winding number in terms of F (which is in turn given in terms of A)), its winding number is thus exactly 1.
- We shall denote these solutions as $A_{inst,\,\rho,\,\mu}(x)$.
- We can also define a shifted instanton as $A_{inst,\,\rho,\,x_0,\,\mu}(x) := A_{inst,\,\rho,\,\mu}(x - x_0)$ which we can think of as merely having a "center" in spacetime at x_0 instead of 0.

4.4.1 Collective Coordinates

In the double well, we had one "collective coordinate", $\mathcal{T}$, a parameter of the instanton solution which the action was invariant under. It was crucial to identify that coordinate in order to compute the path integral. In our case, *there are* 8 *different collective coordinates* for the instanton solutions we have just found.

4.4.1.1 Claim

$S[A_{inst,\,\rho_1,\,\mu}] = S[A_{inst,\,\rho_2,\,\mu}]$ (scale invariance). This gives us 1 collective coordinate.

Note The classical Yang-Mills Lagrangian is scale-invariant, as $\nexists$ a dimensionful parameter.

4.4.1.2 Claim

$S[A_{inst,\,\rho,\,x_0,\,\mu}] = S[A_{inst,\,\rho,\,\mu}]$ for all $x_0 \in \mathbb{R}^4$ (translation invariance). This gives us 4 collective coordinates.

4.4.1.3 Claim

The action is invariant a *global* $SU(2)$ gauge transformation on $A_{inst,\,\rho,\,x_0\,\mu}$. This gives us 3 collective coordinates (as many as there are generators of $SU(2)$).

4.4.1.4 Claim

$\nexists$ other invariants for the action (via an index theorem by Atiyah, Ward in [1] which determines the dimension of the modulo space of $SU(2)$ as exactly 8).

4.4.1.5 Conclusion

As before, we would need to integrate over these coordinates directly, when computing the contribution of these solutions to the path integral.

4.5 Finding the Vacuum

Following [3],we work in an axial gauge, in which $A_3 \stackrel{!}{=} 0$. (Then the path-integral formulation is equivalent to the canonical quantization, and there is no need for ghost fields or extra conditions on the space of states.)

We work in a spacetime box of spatial volume V from time $-\frac{T}{2}$ to time $\frac{T}{2}$. Eventually we will send $V \to \infty$ and $T \to \infty$. We employ boundary conditions on the three-dimensional boundary of the box at times $\pm\frac{T}{2}$ such that the tangential term (to the surface of the box) of A_μ is *constant*. Then the surface term of δS will be zero.

This constant, however, is not arbitrary. It must obey the following conditions to maintain consistency:

1. $A_3 \stackrel{!}{=} 0$ gauge must be respected.

2. At infinity we should have finite-action field configurations. Since only the tangential component of A_μ determines the winding number (...), this means that spacetime will be filled with field configurations of a definite winding number.

As $V \to \infty$, the definiteness of the winding number (which follows from the finiteness of the action) is the only specific feature that remains of the boundary conditions. So in the path-integral we can forget about the boundary conditions and simply add a delta function for field configurations that have a definite integer winding number. In this way we will clearly obtain only finite action field configurations:
$P(V, T, n) := \mathcal{N} \int \mathcal{D}A_1 \mathcal{D}A_2 \mathcal{D}A_4 e^{-S[A_\mu]} \delta(n - \nu[A_\mu])$ for some $n \in \mathbb{Z}$.

4.5.0.6 Claim

For large T_1 and T_2, $P(V, T_1 + T_2, n) = \sum_{n_1+n_2=n} P(V, T_1, n_1) P(V, T_2, n_2)$

4.5.1 The θ-Vacua

This composition law is not what we would expect from a transition matrix element that has a contribution from only a single energy eigenstate. In order to get the composition law we want, $e^{-E_i(T_1+T_2)}$, we make a Fourier transform of $P(V, T, n)$:

$$\begin{aligned} \tilde{P}(V, T, \theta) &:= \sum_{n\in\mathbb{Z}} e^{in\theta} P(V, T, n) \\ &= \mathcal{N} \int \mathcal{D}A_\mu e^{-S[A_\mu]} e^{i\nu[A_\mu]\theta} \end{aligned}$$

As a result of the previous composition law now we have $\tilde{P}(V, T_1 + T_2, \theta) = \tilde{P}(V, T_1, \theta) \tilde{P}(V, T_2, \theta)$. So $\tilde{P}$ must be proportional to $\left\langle e^{-\hat{H}T} \right\rangle$ in *some* energy eigenstate. We naturally label these eigenstates with θ and as before call them the θ-vacua:

$$\left\langle \theta \left| e^{-\hat{H}T} \right| \theta \right\rangle = \mathcal{N}' \int \mathcal{D}A_\mu e^{-S[A_\mu]} e^{i\nu[A_\mu]\theta} \tag{4.1}$$

The conclusion is that our theory is split into disconnected sectors labelled by θ, each with its own vacuum. Naively, we could have obtained the same result by merely postulating an extra term in the Lagrangian proportional to $\nu[A_\mu] \sim \int d^4x \left(F, \tilde{F}\right)$. This term was, in fact, only rejected to begin with because it violates CP ($\left(F, \tilde{F}\right) \sim \vec{E} \cdot \vec{B}$ and $\vec{B}$ doesn't change sign under P), but otherwise it is just as good as $\int d^4x (F, F)$. In addition, we found it is a total divergence, and so should have no effect on the EoMs. But there seems to be an effect to it none the less, which is not classical.

4.5.2 Dilute Instanton Gas

Just as in the periodic well, we build approximate solutions which consist of n instantons and n' anti-instantons, where their centers x_0 are integrated over. We then sum over all such possible configurations:

$$\begin{aligned}\left\langle \theta \left| e^{-\hat{H}T} \right| \theta \right\rangle &\propto \sum_{(n,\, n') \in \mathbb{N}^2} \frac{1}{n!} \left[\left(K e^{-S_0} \right) VT \right]^n \frac{1}{n'!} \left[\left(K e^{-S_0} \right) VT \right]^{n'} e^{i(n-n')\theta} \\ &= \exp\left\{ 2KVTe^{-S_0} \cos\left(\theta\right) \right\}\end{aligned}$$

where $S_0 = \frac{8\pi^2}{g^2}$, V is volume and K is some constant which can be computed by calculating the infinite product of eigenvalues of a corresponding differential operator (see [9]). In general K will contain an infrared "embarrassment"–a divergence–but fortunately it only diverges when we assume our approximation is not valid. From this we can read off the energy of $|\theta\rangle$:

$$\boxed{\frac{E\left(\theta\right)}{V} = -2Ke^{-S_0} \cos\left(\theta\right)}$$

Because the energy and also the vacuum expectation value depend non-trivially on θ we must conclude that all the θ states are in fact distinct!

4.5.3 Other Gauge Groups

4.5.3.1 Claim

Every simple Lie group contains a subgroup isomorphic to $SU\left(2\right)$.

- For example, $\begin{bmatrix} a & b & 0 \\ c & d & 0 \\ 0 & 0 & 1 \end{bmatrix}$ is a general element of such a subgroup of $SU\left(3\right)$ where $\begin{bmatrix} a & b \\ c & d \end{bmatrix} \in SU\left(2\right)$.

4.5.3.2 Notes

$\exists$ a theorem due to Raoul Bott saying that if G is any simple Lie group, $H \leq G$ such that $H \simeq SU\left(2\right)$, then any element of G^{S^3} is homotopic with some element of H^{S^3}. Then we can consider the same BPST solutions we have considered where $A_\mu = a \cdot A_\mu{}^{(H)} + b \cdot A_\mu{}^{(G \setminus H)}$ and we would take $b = 0$.

- For example, for $SU\left(3\right)$, which has 8 gauge fields, the following is an instanton solution: three of the fields are just as the $SU\left(2\right)$ instanton, and the remaining five are zero.
- This is the only instanton solution of $SU\left(3\right)$ with winding number 1.
- Then there would be 12, and not 8 collective coordinates (the action is invariant under a global $SU\left(3\right)$ transformation, so 8 coordinates instead of the 3 of $SU\left(2\right)$, but one of the generators commutes with $SU\left(2\right)$, so we are left with total of 7 collective coordinates from the global $SU\left(3\right)$ transformation)

Chapter 5

The Strong CP Probelm

As we have seen, the instanton solution effectively creates a θ term proportional to $\theta \int d^4x \left(F, \tilde{F}\right)$ in the Lagrangian, which, if $\theta \neq 0$, violates CP.

Using the CPT theorem we conclude that T is violated.

According to experimental measurements using the electric dipole moment of the neutron ($d_n \approx \theta e \frac{m_\pi^2}{m_n^2}$), the amount of T violation corresponds to $\theta < 10^{-5}$ ([10]) or even $\theta < 10^{-9}$. This raises a fine-tuning question, which is known as the *strong CP problem*. To explain this fine tuning we need to go beyond the standard model.

One couldn't just throw away the instanton concept, because it does solve the $U(1)$ problem: The non-observation in experiments of a $U(1)$ axial symmetry which is expected in QCD. It was thought to come from spontaneous symmetry breaking, but no corresponding Goldstone Boson was found. Finally it was explained by 't Hooft in [8] that this symmetry is anomalous and the instanton solution fits perfectly to explain how. So we definitely need the instantons.

5.1 Peccei–Quinn theory

Following [5], $\exists$ three approaches to explaining the value of θ:

1. Unconventional dynamics.
2. Spontaneously broken CP.
3. An additional chiral symmetry.

Peccei employs the third approach.

This chiral symmetry can arise from assuming $m_u = 0$ (up quark) which is inconsistent with experimental data. But if that were the case, we could perform a global chiral rotation $\psi_f \mapsto e^{i\alpha_f \gamma_5} \psi_f$. The change in the path integral measure introduces a term proportional to $\exp\left\{-\frac{ig^2}{16\pi^2}\alpha_f \int d^4x \left(F, \tilde{F}\right)\right\}$. So by picking α_f properly we could eliminate the θ term that comes from the instantons. However, as has been said, when we do this, we introduce a phase to the mass of the f Fermion, $m_f \mapsto e^{-i\alpha_f} m_f$. This could have only worked if we had one quark which is massless.

Alternatively the chiral symmetry can arise from an additional global $U(1)$ chiral symmetry, $U(1)_{PQ}$. This symmetry is then to be spontaneously broken. Its introduction into the theory replaces the static θ term in the effective Lagrangian with a dynamical CP conserving field which has come to be known as *the axion*–the Goldstone Boson of the broken $U(1)_{PQ}$ symmetry. This symmetry could not have been exact because the axion cannot be exactly massless.

Thus the θ-term in our Lagrangian becomes:

$$\mathcal{L} = \frac{\theta}{32\pi^2}\left(F,\,\tilde{F}\right) \mapsto \frac{1}{2}\left(\partial_\mu a\right)\left(\partial^\mu a\right) + \frac{\frac{a}{M}+\theta}{32\pi^2}\left(F,\,\tilde{F}\right)$$

where a is the dynamical axion field and M is the mass scale at which it appears. Then by an opportune shift in the axion field $a \mapsto a - \theta M$ we can get rid of the θ term. If the axion is very light ($\sim 1eV$), the cut-off scale at which it appears is very low.

We can also add interaction terms for the axion with the quarks, for instance, for the up quark, a term of the form $-i\frac{f_u}{M}\left(\partial_\mu a\right)\bar{u}\gamma_5\gamma^\mu u$ where f_u is the coupling constant for the interaction. Following the very same procedure of chiral perturbation theory we can construct an effective Lagrangian for the pion-axion interaction.

Bibliography

[1] M. F. Atiyah, N. J. Hitchin, and I. M. Singer. Self-duality in four-dimensional Riemannian geometry. *Proceedings of the Royal Society of London. A. Mathematical and Physical Sciences*, 362(1711):425–461, 1978.

[2] A. A. Belavin, A. Polyakov, A. S. M. Schwartz, and Yu. S. Tyupkin. Pseudoparticle solutions of the Yang-Mills equations. *Physics Letters B*, 59(1):85–87, 10 1975.

[3] Sidney Coleman. *Aspects of symmetry : selected Erice lectures of Sidney Coleman.* Cambridge University Press, Cambridge England New York, 1988.

[4] James Munkres. *Topology.* Pearson, 2 edition, January 2000.

[5] R.D. Peccei. The Strong CP problem and axions. *Lect.Notes Phys.*, 741:3–17, 2008.

[6] Michael E. Peskin and Dan V. Schroeder. *An Introduction To Quantum Field Theory (Frontiers in Physics)*, chapter 9. Functional Methods. Westview Press, 1995.

[7] Jun John Sakurai. *Modern Quantum Mechanics.* Addison-Wesley Publishing Company, Reading, MA, Revised edition, 1994.

[8] Gerard 't Hooft. How Instantons Solve the U(1) Problem. *Phys.Rept.*, 142:357–387, 1986.

[9] A.I. Vainshtein, Valentin I. Zakharov, V.A. Novikov, and Mikhail A. Shifman. ABC's of Instantons. *Sov.Phys.Usp.*, 25:195, 1982.

[10] F. Wilczek. Problem of strong P and T invariance in the presence of instantons. *Phys. Rev. Lett.*, 40:279–282, Jan 1978.

Chapter 15

The Higgs Mechanism

Author: Juanfernando Angel
Supervisor: Oscar Åkerlund

In this report the Higgs mechanism will be derived from a combination of spontaneous symmetry breaking and Yang-Mills theory as a formalism to give mass to massless vector gauge bosons. Several simple theories will be discussed and finally the mechanism will be applied to Electroweak Theory. This last step will focus on giving masses only to the weak vector bosons while keeping the photon massless.

15.1 Introduction and Tools

15.1.1 Introduction

A great achievement in particle physics was to introduce Yang-Mills as a framework to derive interacting theories out of symmetries. The interactions given by this method are mediated by massless vector bosons. Allthough Yang-Mills theory was very successful for quantum electrodynamics, it failed when applied to a description of weak interactions. A field mediated by massless bosons should have an infinite range, and observations of processes involving weak interaction clearly showed otherwise. Also the strength of the weak force, which is orders of magnitude lower than that of quantum electrodynamics, showed that something was wrong. Since force and range of a theory both depend on the masses of the mediating bosons it was a natural idea to try to give the weak bosons masses. This, however, is not a simple task since when done naively, for example by just adding mass terms to the Lagrangian, it destroys some fundamental features of the theory such as gauge invariance.

The problem was finally solved in the 1960's by the Higgs mechanism and, trying to stay as down-to-earth as possible, we will go through all the steps that were needed to finally do so and give masses to the weak gauge bosons.

15.1.2 Spontaneous Symmetry Breaking

Let $\mathfrak{L}$ be the Lagrangian of complex scalar field theory given by

$$\mathcal{L} := \frac{1}{2}|\partial_\mu \phi|^2 - V(\phi). \tag{15.1}$$

We can for first considerations just pick a standard ϕ^4 potential:

$$V(\phi) := m^2\phi^*\phi + \frac{\lambda}{2}(\phi^*\phi)^2, \quad m^2 > 0. \tag{15.2}$$

First of all it can be easily seen that the theory has a global $U(1)$-Symmetry given by $\phi \longmapsto e^{i\alpha}\phi$.

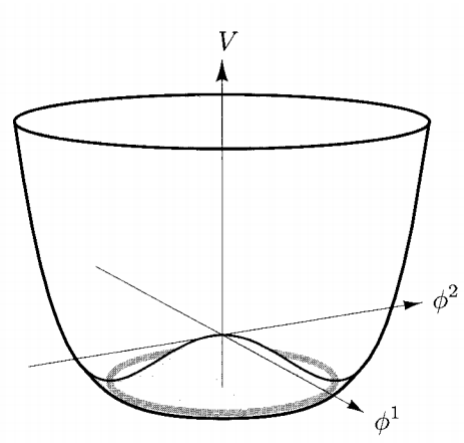

Figure 15.1: Symmetry breaking potential defined in eq. (1.3) [1].

If we further define the vacuum as the lowest energy state, i.e. the minimum of the potential, we see that the theory has a stable vacuum located at the trivial field configuration $\phi = 0$. The standard way of treating such an interacting theory involves applying perturbation theory around the vacuum and interpreting the different parts of the arising expansion in terms of Feynman diagrams. Since the vacuum being a global and stable minimum such an expansion at least seems to be a sensible idea.
In order to make the theory more interesting we can change the sign of the mass and consider the following potential:

$$V(\phi) := -\mu^2\phi^*\phi + \frac{\lambda}{2}(\phi^*\phi)^2, \quad \mu^2 > 0. \tag{15.3}$$

The first and most important thing that can be noted is that the former global minimum becomes a local maximum. This new potential now contains a continuous amount of global minima located on the circle defined by $|\phi| = \frac{\mu^2}{\lambda}$. Taking our definition of the vacuum we conclude that there is a continuous amount of equivalent vacua located at $\phi_0 = \sqrt{\frac{\mu^2}{\lambda}}$ and points related by $U(1)$-symmetry, i.e. by rotations of the complex plane. In other words: The new vacuum consists of a non-trivial field configuration.
The next observation we can make is that while with the former potential it made sense to apply perturbation theory around $\phi = 0$, this field configuration has now become unstable and a small perturbation will make it "fall" into one of the new vacua. Since all vacua are related by a simple coordinate transformation we can just assume that the vacuum the theory "falls" into points along the real axis. With this new choice of vacuum and the knowledge that it is stable under small perturbations along the radial direction and changes into equivalent vacua under small tangential perturbations we can expand ϕ around ϕ_0 and see where this leads us. We thus express ϕ as

$$\phi(x) := \phi_0 + \frac{1}{\sqrt{2}}(\phi_1(x) + i\phi_2(x)), \tag{15.4}$$

where ϕ_1 and ϕ_2 are both real fields. Plugging this into the potential (1.3) and simplifying we get

$$V(\phi) = \mu^2\phi_1^2 + \frac{\lambda}{8}\phi_1^4 + \frac{\lambda}{8}\phi_2^4 + \sqrt{\frac{\mu^2\lambda}{2}}\phi_1^3 + \sqrt{\frac{\mu^2\lambda}{2}}\phi_1\phi_2^2 \ \ (+\mathit{constant}\ ). \tag{15.5}$$

Before analyzing this expression let's recapitulate: We had an expression for V and naively thought looking at the resulting theory through perturbations around an empty ($\phi = 0$) vacuum would lead to sensible results. A quick analysis showed that the potential was unstable under small perturbations, so it wouldn't be wise to expect good results with this method. Noting this we found a continuous amount of non-trivial vacua that were stable and changed our point of view of the potential to be centered around one of this vacua.
From this point of view several aspects of the theory that were hidden become manifest. First we note that tere are also cubic interactions in addition to the quartic ones. Secondly it becomes apparent that the mass term is restricted to only one of the field components, while the other becomes massless. Lastly we see that in contrast to the first expression for the potential (1.3) the mass term appears with the right sign.
Now let's take a look at the symmetry. The theory in its original form (1.3) had a manifest global $U(1)$-symmetry. If we however take a look at (1.5) we see that, since a complex rotation has to mix the real and imaginary parts of the field, this is no longer the case: The symmetry has been broken.
We conclude this section by noting some general facts about spontaneous symmetry breaking that could be observed in the example previously discussed:

- Goldstone's Theorem states that for every broken symmetry in the theory there is a massless boson called the Goldstone boson. In this cased there was a broken (one dimensional) $U(1)$-symmetry, so we got one massless Goldstone boson: ϕ_2.
- By picking a suitable point of view of the potential several new interactions are unveiled that were formerly hidden. It is thus possible for the theory to become more intricate after symmetry breaking.

We can now continue to review the second ingredient needed to formulate the Higgs mechanism.

15.1.3 Yang-Mills Theory

The Idea of Yang-Mills theory can be quickly summarized as follows:
We will start with a free theory given by a Lagrangian that has a global symmetry. We will promote the global symmetry to a local one. In doing so we will encounter some trouble and will be forced to introduce new fields turning the former free theory into an interacting one. After introducing adequate kinetic terms for the newly added fields we will end up with a complete interacting theory invariant under a local symmetry group. Let's go through two examples.

Yang-Mills Theory for $SU(2)$

Let $\psi := \begin{pmatrix}\psi_1\\ \psi_2\end{pmatrix}$ be a two component Dirac-field. A free Lagrangian ϕ is given by

$$\mathcal{L} = \overline{\psi}\left(i\partial\!\!\!/ - m\right)\psi. \tag{15.6}$$

The two fields ψ_1 and ψ_2 can be transformed into each-other by $SU(2)$-transformations:

$$\psi \longmapsto \exp\left(i\alpha^i\tau^i\right)\psi, \tag{15.7}$$

where $\tau^k := \frac{\sigma^k}{2}$ and the σ^k are the Pauli-matrices. It can be easily shown that this transformations are a global symmetry of the theory. As mentioned before, we now want to turn this global symmetry into a local one. We can do this by demanding that the theory be invariant under the transformation given by

$$\psi(x) \longmapsto \exp\left(i\alpha^k(x)\tau^k\right)\psi(x). \tag{15.8}$$

Applying this transformation to the mass term in the Lagrangian $\overline{\psi}m\psi$ we see that it remains invariant under the new transformation. This can be attributed to the fact that the mass, as a constant commutes with the transformed field $\overline{\psi}\exp\left(-i\alpha^k(x)\tau^k\right)$, so the exponentials coming from ψ and $\overline{\psi}$ can cancel each-other out.
If we however take a look at the kinetic term $i\overline{\psi}\partial\!\!\!/\psi$ we get two problems. First of all the derivative does not commute with the exponential, meaning that no simple cancellation can take place as was the case for the mass term. Secondly, the standard derivative defined as

$$n^\mu\partial_\mu\psi = \lim_{\varepsilon\to 0}\frac{1}{\varepsilon}\left(\psi(x+\varepsilon n)-\psi(x)\right) \tag{15.9}$$

is ill-defined after the transformation, since $\psi(x+\varepsilon n)$ and $\psi(x)$ transform under multiplication by different factors. The solution to this problem is to redefine the derivative, so that it accounts for the "shift" in transformation behaviour encountered in its definition. In order account for this shift we need to define the comparator which depends on both points and includes both transformation behaviours. Writing the 2×2 transformation matrix as $V(x)=\exp\left(i\alpha^k(x)\tau^k\right)$ we thus see that the comparator should behave in the following way under symmetry transformations

$$U(y,x)\longmapsto V(y)U(y,x)V(x)^\dagger. \tag{15.10}$$

Setting $U(x,x)=\mathbb{1}$ we can define the covariant derivative as follows

$$n^\mu D_\mu\psi = \lim_{\varepsilon\to 0}\frac{1}{\varepsilon}\left(\psi(x+\varepsilon n)-U(x+\varepsilon n,x)\psi(x)\right) \tag{15.11}$$

and note that in the second term of the transformed version of the equation the $V(x)$ and the $V(x)^\dagger$ contributions of $\psi(x)$ and $U(x+\varepsilon n,x)$ multiply to one, leaving only a $V(x+\varepsilon n)$ contribution, i.e. the first and the second term in the definition transform equally, i.e. covariantly. Assuming that $U(y,x)$ is a continuous function we can expand it for small distances between x and y, s.t.

$$U(x+\varepsilon n,x)=\mathbb{1}+ig\varepsilon n^\mu A^i_\mu(x)\tau^i+\mathcal{O}(\varepsilon^2). \tag{15.12}$$

We introduced two new objects in this expression. The A^i_μ, called connections, are vector fields appearing as the coefficients in the limit $\partial_\mu U(x,x)=igA^i_\mu\tau^i$ as it would appear in the expansion, naturally there has to be one vector field for each generator of the group. The coupling constant g is a constant extracted for future convenience while defining the connections. Using this expansion and the definitions of the standard and covariant derivative we find the following expression:

$$D_\mu := \partial_\mu + igA^i_\mu\tau^i, \tag{15.13}$$

Plugging the expansion of $U(x+\varepsilon n,x)$ into the definition of the transformations behaviour of $U(y,x)$ we find that the transformation behaviour of the A^i is given by

$$A^i_\mu(x)\longmapsto V(x)\left(A^i_\mu(x)\tau^i+\frac{i}{g}\partial_\mu\right)V(x)^\dagger. \tag{15.14}$$

Plugging this new derivative into the kinetic term and using the right transformation behaviour for the connections, one finds that the Lagrangian becomes invariant under the local transformation.

Since we introduced new fields, we need to introduce kinetic terms for them. This can be done by analyzing what kind of gauge invariant terms can be constructed out of the A^i and its derivatives. The following suitable kinetic term can be found:

$$\mathcal{L}_{\text{kin}}=\frac{1}{4}(F^i_{\mu\nu})^2, \tag{15.15}$$

where we define $F^i_{\mu\nu}:=\partial_\mu A^i_\nu-\partial_\nu A^i_\mu+g\varepsilon^{ijk}A^j_\mu A^k_\nu$ (In general we have $F_{\mu\nu}=\frac{1}{ig}[D_\mu,D_\nu]$.). It is perhaps instructional to note how similar this looks to classical electrodynamics and just as in that

case the $F^i_{\mu\nu}$ are called the field strenghts, allthough now they are no longer gauge invariant.
We have now everything we need to put the whole Lagrangian of the interacting theory together:

$$\mathcal{L}_{\text{Yang-Mills}} = \overline{\psi}\left(i\not{D} - m\right)\psi + \frac{1}{4}(F^i_{\mu\nu})^2. \tag{15.16}$$

Since all its constituents were constructed to be invariant under the local symmetry transformation it is straight forward that the Lagrangian as a whole keeps this invariance. Note that there is at no point the necessity of introducing mass terms for the gauge fields, in fact doing so would ruin the gauge invariance of the theory. We thus conclude that the gauge fields must be massless. As stated at the beginning of the section we started from a free theory with a global symmetry and ended up with an interacting theory and a local symmetry, whose intractions are mediated by massless vector gauge bosons.

QED as a Yang-Mills Theory

Following the same steps as with $SU(2)$ quantum electrodynamics can be derived from a one component spinor field with global $U(1)$-symmetry. Just as before the procedure of promoting the global symmetry to a local symmetry leads to the following Lagrangian:

$$\mathcal{L}_{\text{QED}} = \overline{\psi}\left(i\not{D} - m\right)\psi + \frac{1}{4}(F_{\mu\nu})^2, \tag{15.17}$$

where $D_\mu := \partial_\mu + ieA_\mu$, $F_{\mu\nu} = \partial_\mu A_\nu - \partial_\nu A_\mu$, and the fields transform as

$$\psi \longmapsto \exp\left(i\alpha(x)\right)\psi \tag{15.18}$$

$$A_\mu \longmapsto A_\mu(x) + \frac{1}{e}\partial_\mu\alpha(x). \tag{15.19}$$

Note that while there were 3 different gauge boson fields A^i in $SU(2)$ Yang-Mills, there is only one gauge boson field A in QED, the photon field. The same goes for the field strength tensor.

Again we can conclude the section by listing the most important basic facts of Yang-Mills theory.

- The Yang-Mills formalism allows construction of interacting theories out of symmetries and free theories.
- The interactions are mediated by massless vector gauge bosons.
- There is one gauge boson for each generator of the local symmetry group, e.g. 1 for $U(1)$, 3 for $SU(2)$.

15.2 The Higgs Mechanism

Now that we have all necessary ingredients we can begin the analysis of how to give Yang-Mills gauge boson masses. Let's start with a simple example of the Higgs Mechanism.

15.2.1 An Abelian Example

Let's take the complex scalar field theory we discussed before in the context of symmetry breaking and couple it to the electromatnetic field. This can be simply done using the methods of Yang-Mills theory; we just have to exchange the derivative. As we saw before the mass term gives no problems and the kinetic term with a covariant derivative is constructed to be gauge invariant. Since the

covariant derivative includes the photon field as a connection the coupling happens automatically. We thus get the following Lagrangian:

$$\mathcal{L} := \frac{1}{2}|D_\mu\phi|^2 + \frac{1}{4}(F_{\mu\nu})^2 + \mu^2\phi^*\phi - \frac{\lambda}{2}(\phi^*\phi)^2. \tag{15.20}$$

Since we picked the potential that lead to symmetry breaking we again get a continuum of non-vanishing vacuum expectation values for ϕ. Like before make a particular choice of vacuum and expand ϕ around it. The potential changes in the exact same way as before, but what about the kinetic term? Plugging the expansion of ϕ and the definition of D_μ together we get

$$\begin{aligned}(D_\mu\phi)^*(D_\mu\phi) = \left((\partial_\mu + ieA_\mu)\left(\phi_0 + \frac{1}{\sqrt{2}}(\phi_1(x) + i\phi_2(x)\right)\right)^* \times \\ \times \left((\partial_\mu + ieA_\mu)\left(\phi_0 + \frac{1}{\sqrt{2}}(\phi_1(x) + i\phi_2(x)\right)\right),\end{aligned} \tag{15.21}$$

which after tedious calculations leads to

$$\begin{aligned}(D_\mu\phi)^*(D_\mu\phi) = \frac{1}{2}\left(\partial_\mu\phi_1\right)^2 + \frac{1}{2}\left(\partial_\mu\phi_2\right)^2 + e^2\phi_0^2(A_\mu)^2 + \sqrt{2}e^2\phi_0(A_\mu)^2\phi_1 + \\ + \frac{e^2}{2}(A_\mu)^2\phi_1^2 + \frac{e^2}{2}(A_\mu)^2\phi_2^2 + \sqrt{2}e\phi_0 A_\mu\partial_\mu\phi_2 + eA_\mu\phi_1\partial_\mu\phi_2 - eA_\mu\phi_2\partial_\mu\phi_1.\end{aligned} \tag{15.22}$$

Several things can be noted of this expression. We see that there are kinetic terms for each of the fields accompanied by cubic ($\sqrt{2}e^2\phi_0(A_\mu)^2\phi_1$, $eA_\mu\phi_1\partial_\mu\phi_2$, and $eA_\mu\phi_2\partial_\mu\phi_1$) and quartic ($\frac{e^2}{2}(A_\mu)^2\phi_2^2$, and $\frac{e^2}{2}(A_\mu)^2\phi_1^2$) interactions. The most interesting terms are however the two remaining ones. First of all we have the photon mass term we wanted:

$$\frac{1}{2}m_\gamma^2(A_\mu)^2 = e^2\phi_0^2(A_\mu)^2, \tag{15.23}$$

secondly we have the term $\sqrt{2}e\phi_0 A_\mu\partial_\mu\phi_2$, which represents some sort of transformation of ϕ_2 into A_μ. Now, a sensible field theory should not have non-trivial amplitudes for one particle to spontaneously change its type in a fundamental way, so at first sight it looks like something is wrong with the procedure we used. Let's try to reconcile this. From the way we constructed the theory we know that it is locally gauge invariant under $U(1)$ symmetry transformations. Until now we haven't chosen a gauge so we can start by demanding that ϕ be real at every point, i.e. we demand $\phi = \phi_0 + \frac{1}{\sqrt{2}}\phi_1$. This is a sensible thing to do, since we can simply rotate $\phi(x)$ at each point to point towards the real axis. With this gauge all terms containing the field ϕ_2 vanish, so we get rid of the awkward term and simplify the theory significantly. All in all we get the following Lagrangian:

$$\mathcal{L} = \frac{1}{2}(\partial_\mu\phi_1)^2 + \frac{1}{4}(F_{\mu\nu})^2 - \frac{1}{2}m_\phi^2\phi_1^2 + \frac{1}{2}m_\gamma^2(A_\mu)^2 + \mathcal{L}_{\text{Int}}, \tag{15.24}$$

where $m_\phi = \sqrt{2}\mu$, $m_\gamma = \sqrt{2}e\phi_o = \sqrt{\frac{2}{\lambda}}e\mu$, and $\mathcal{L}_{\text{Int}}$ contains all interaction terms.
It could be argued that we did something wrong, since the theory now looks as if we had gauged away one degree of freedom, but this can be understood the following way. As it is well known a massless vector particle such as the photon can only have two degrees of freedom, i.e. the two transverse polarizations. A massive vector field can however also be longitudinally polarized. So in the process of making A_μ a massive field, we also gave it a new degree of freedom, its longitudinal polarization. We can thus interpret the procedure in the following rather colloquial way: The photon field eats the Goldstone boson making it disappear from the theory. The degree of freedom associated with the scalar Goldstone boson remains in the theory as the longitudinal polarization of the now massive photon.

15.2.2 Systematics of the Higgs Mechanism

Now that we saw the Higgs mechanism in action we can try to analyze it in a more systematic way. Let $\phi = (\phi_1, \ldots, \phi_n)$ be a system of n real scalar fields that appear in a Lagrangian that is globally gauge invariant under a symmetry group G. The infinitesimal group transformations can be written as:

$$\phi_i \longmapsto (\mathbb{1} - \alpha^a T^a)_{ij} \phi_j, \tag{15.25}$$

where the T^a_{ij} are the generators of the group in a suitable (real) representation. The global gauge invariance can be made local by means of the covariant derivative defined as follows:

$$D_\mu \phi = (\partial_\mu \mathbb{1} + g A^a_\mu T^a)\phi. \tag{15.26}$$

We saw before that the gauge boson mass came from the kinetic term in the Lagrangian, as a next step we need to analyze it. Plugging the definition of the covariant derivative into the kinetic term it takes the following form:

$$\frac{1}{2}(D_\mu \phi_i)^2 = \frac{1}{2}(\partial_\mu \phi_i)^2 + g A^a_\mu (\partial_\mu \phi_i)(T^a_{ij}\phi_j) + \frac{1}{2} g^2 A^a_\mu A^{b\mu} (T^a \phi)_i (T^b \phi)_i, \tag{15.27}$$

where the implicit sums should not be forgotten.
We now want to assume that the Lagrangian of this theory has a potential that will induce spontaneous symmetry breaking. Under this assumption we can pick a vacuum ϕ_0 out of the possible minimum energy states of the potential and expand the field around it:

$$\phi = \phi_0 + \phi'. \tag{15.28}$$

If we plug this into expression (1.23) we see that from the last term we will get a contribution of the following form:

$$\frac{1}{2} g^2 (T_a \phi_0)_i (T^b \phi_0)_i A^a_\mu A^{b\mu}. \tag{15.29}$$

This expression, having the form of a mass term, motivates the definition of the mass matrix

$$m^2_{ab} = g^2 (T_a \phi_0)_i (T^b \phi_0)_i, \tag{15.30}$$

since then

$$\mathcal{L}_{\mathrm{M}} = \frac{1}{2} m^2_{ab} A^a_\mu A^{b\mu}. \tag{15.31}$$

Let's inspect the mass matrix a little further. It is rather easily seen that it is positive semi-definite. This follows from the fact that the diagonal elements $m^2_{aa} = g^2 (T_a \phi_0)^2 \geq 0$ are either positive or vanish in every basis, in particular in a diagonal basis. We can thus expect the A^i_μ to either become massive of remain massless. We should take a better look at these two cases.

Massless Gauge Bosons
In order for A^l to remain massless, the corresponding diagonal element of the mass matrix has to vanish, i.e.

$$m^2_{ll} = g^2 (T_l \phi_0)^2 = 0. \tag{15.32}$$

This is the case iff $T_l \phi_0 = 0$. This means that the vacuum is preserved by the symmetry transformation induced by T_l since:

$$\phi_0 \longmapsto (\mathbb{1} - \alpha^l T^l)\phi_0 = \mathbb{1}\phi_0 - \underbrace{\alpha^l T^l \phi_0}_{=0} = \phi_0. \tag{15.33}$$

We thus conclude that gauge bosons that remain massless correspond to unbroken symmetries of the vacuum.

Massive Gauge Bosons

In a very similar way as before we conclude that a necessary condition for the gauge boson A^k to become massive is given by

$$m_{kk}^2 = g^2(T_k\phi_0)^2 > 0. \tag{15.34}$$

Following the same path as before we notice that this is the case iff $T_k\phi_0 \neq 0$, and that this necessarily means that the vacuum is not preserved by the symmetry. We conclude that massive gauge bosons correspond to broken symmetries.

When we discussed the abelian example before, we came across an expression that "transformed" a scalar field into a vector gauge field. If we take a look at the second term of expression (1.23) we see that after insertion of the expanded field it gives rise to the following analogous term:

$$gA_\mu^k(\partial_\mu\phi)_i(T^k\phi_0)_i. \tag{15.35}$$

Where the sum runs over the T^k that break the symmetry. Since the T^k are unit-length tangent vectors on the group manifold, applying them to ϕ_0 creates vectors $T^k\phi_0$ pointing in the directions in which the symmetry of the vacuum is broke. Since this field directions are exactly the Goldstone boson components of ϕ. This means that the scalar product $(\partial_\mu\phi)_i(T^k\phi_0)_i$ simply projects $\partial_\mu\phi$ into the subspace spanned by the Goldstone bosons. To state it more bluntly: only Goldstone bosons appear in expression (1.31). This is of course what we wanted, since now we can pick a gauge where all Goldstone boson components of ϕ vanish. In this gauge, just as before, the theory is greatly symplified and all awkward factors vanish.

As for the degrees of freedom we can argue in the exact same way as before: The only gauge bosons that became massive corresponded to broken symmetries. As they became massive they gained the degree of freedom of longitudinal polarization. The chosen gauge eliminated an amount of fields exactly equal to the amount of broken symmetries, according to Goldstone's symmetries. We thus see, that the amount of degrees of freedom remained unchanged throughout the process, they just changed their form from Goldstone bosons to longitudinal polarization states of now massive vector gauge bosons.

15.2.3 Non-Abelian Examples

Spinor Representation of $SU(2)$

As a first a little more complex example we can take a look at a spinor representation of $SU(2)$. Using the methods of Yang-Mills theory we can determine the covariant derivative to be

$$D_\mu\phi = (\partial_\mu \mathbb{1}_{2\times 2} - igA_\mu^a\tau^a)\phi, \tag{15.36}$$

where ϕ is a two component scalar, and thus construct an interacting theory. In this theory ϕ interacts with three massless vector gauge boson fields, the A^a. Assuming that the Lagrangian of this theory leads to symmetry breaking we can pick the non-vanishing vacuum expectation value of ϕ to point in the 2-direction $\phi_0 = \frac{1}{\sqrt{2}}(0, v)$ and expand the scalar field around it to get the following contribution to the kinetic term of the Lagrangian:

$$|D_\mu\phi|^2 = \ldots + \frac{1}{2}g^2(0,v)\tau^a\tau^b\begin{pmatrix}0\\v\end{pmatrix}A_\mu^aA_\mu^b + \ldots . \tag{15.37}$$

Using that $\{\tau^a, \tau^b\} = \frac{1}{2}\delta^{ab}$ to simplify the expresion we get the following gauge boson mass contribution to the Lagrangian:

$$\mathcal{L}_M = \frac{g^2v^2}{8}A_\mu^aA_\mu^a = \frac{1}{2}m_A^2A_\mu^aA_\mu^a. \tag{15.38}$$

We see that all gauge bosons gain mass in this theory. This, as we saw before, is a consequence of the whole $SU(2)$ symmetry being broken. This means that it is not possible to find linear combinations of the generators of $SU(2)$, such that the vacuum remains unchanged by them.

Vector Representation of $SU(2)$

Let's change the situation a little and see what happens if we take ϕ to be a three component scalar field in the vector representation of $SU(2)$. The covariant derivative in the vector representation is given by:

$$(D_\mu \phi)_a = \partial_\mu \phi^a - g\varepsilon_{abc} A^b_\mu \phi^c. \tag{15.39}$$

Writing the vacuum expectation value as $\phi = (0, 0, v)$ we get the following gauge boson mass contribution to the Lagrangian:

$$\mathcal{L}_M = \frac{g^2 v^2}{2} \left((A^1_\mu)^2 + (A^2_\mu)^2 \right). \tag{15.40}$$

Two of the three gauge bosons acquire masses so we conclude that two of the three symmetries are broken. In the vector representation of $SU(2)$ this is actually pretty easy to understand. Given the correspondance $SU(2) \cong SO(3)$, we can just think of this representation as 3 dimensional rotations. All vacua lie on a sphere, which trivially has $SO(3)$ symmetry. If we however choose one specific vacuum, i.e. one radial direction, two of the symmetries are broken. The only symmetry that remains is a rotation around the axis given by the direction of the vacuum. Any other rotation will change the direction of the vacuum.

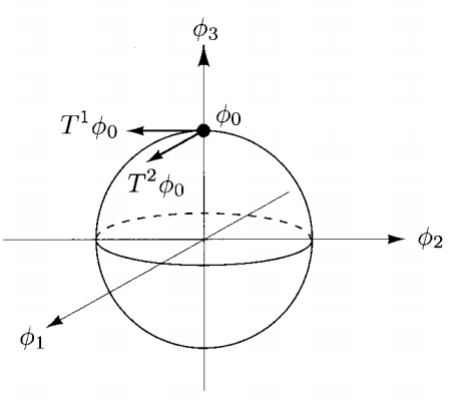

Figure 15.2: Symmetry breaking situation for the vector representation of $SU(2)$ [1].

15.3 Gauge Boson Masses in Electroweak Theory

15.3.1 Expectations

Up to now we have taken a look at the following theories:

- ***U*(1):** Higgs mechanism mediated by a complex scalar field with spontaneous symmetry breaking made the photon massive.
- ***SU*(2) Spinor:** Higgs mechanism mediated by a two component complex scalar field gave all three gauge bosons masses.
- ***SU*(2) Vector:** Higgs mechanism mediated by a three component real scalar field gave two gauge bosons masses while one remained massless.

For a theory of electroweak interactions we would like to have one massless gauge field corresponding to the photon of electromagnetism and three massive gauge fields corresponding to the $W^\pm$, and the Z^0 of the weak nuclear force. As can be seen above none of the groups and representations we have seen so far works by itself. We could try other groups of the same such as $SU(n)$ but even the next group, $SU(3)$, is too big for our purposes. A simpler Ansatz is to combine what we already have.

15.3.2 Glashow-Weinberg-Salam Theory

The idea of GWS-theory is to unite spinor representations of $SU(2)$ and $U(1)$. Since the spinor representation of $SU(2)$ gave rise to three massive gauge bosons and the representation of $U(1)$ gave rise to one massive gauge boson we can try to perhaps combine them, getting a theory with four gauge bosons as wanted, and hope that we can recombine its quantities to make one gauge boson massless. The two representations can be united by defining the following transformation behaviour of the two component scalar field ϕ:

$$\phi \longmapsto \underbrace{e^{i\frac{\beta}{2}}}_{U(1)} \underbrace{e^{i\alpha^a\tau^a}}_{SU(2)} \phi \tag{15.41}$$

It can be noted that since $\frac{\beta}{2}\mathbb{1}_{2\times 2} + \alpha^a\tau^a = H$ is just a general 2×2 hermitian matrix, $e^{iH} = U$ is just a general 2×2 unitary matrix. In other words: we are dealing with a representation of $U(2) = U(1)\times SU(2)$.
The next thing we can do is to let ϕ acquire the vacuum expectation value $\phi_0 = \frac{1}{\sqrt{2}}(0, v)$. We can now consider a gauge transformation with $\alpha^3 = \beta$, $\alpha^{1,2} = 0$:

$$\exp\left(i\frac{\beta}{2}\right)\exp\left[i\begin{pmatrix}\frac{\beta}{2} & 0\\ 0 & -\frac{\beta}{2}\end{pmatrix}\right]\frac{1}{\sqrt{2}}\begin{pmatrix}0\\ v\end{pmatrix} = \begin{pmatrix} e^{i\frac{\beta}{2}}e^{i\frac{\beta}{2}} & 0\\ 0 & e^{i\frac{\beta}{2}}e^{-i\frac{\beta}{2}}\end{pmatrix}\frac{1}{\sqrt{2}}\begin{pmatrix}0\\ v\end{pmatrix} = \frac{1}{\sqrt{2}}\begin{pmatrix}0\\ v\end{pmatrix}. \tag{15.42}$$

As can be seen from the above calculation such a transformation leaves the vacuum invariant. It can be shown that it is the only such transformation, so that we get one unbroken symmetry corresponding to the photon and three broken symmetries corresponding to the weak bosons.
We allready know the derivatives of the two theories by themselves, which makes constructing the covariant derivative of the joint theory pretty easy. A hand wavy way to understand how this is done, is that the product of the representations translates into its infinitesimal form, a sum, for the derivative. We thus just have to add the two connections of the theories and get:

$$D_\mu\phi = (\partial_\mu \cdot \mathbb{1}_{2\times 2} - i\frac{1}{2}g'B_\mu \cdot \mathbb{1}_{2\times 2} - igA^a_\mu\tau^a)\phi. \tag{15.43}$$

Having the covariant derivative the rest becomes just a matter of applying what we have seen until now. We are interested in the mass terms so we expand ϕ around ϕ_0 and pick them out of the kinetic term in the Lagrangian:

$$|D_\mu\phi|^2 = \ldots + \frac{1}{2}(0, v)(\frac{1}{2}g'B_\mu + gA^a_\mu\tau^a)(\frac{1}{2}g'B_\mu + gA^a_\mu\tau^a)\begin{pmatrix}0\\ v\end{pmatrix} + \ldots . \tag{15.44}$$

This expression can be greatly simplified to

$$|D_\mu\phi|^2 = \ldots + \frac{1}{2}\frac{v^2}{4}\left[g^2(A^1_\mu)^2 + g^2(A^2_\mu)^2 + (g'B_\mu - gA^3_\mu)^2\right] + \ldots . \tag{15.45}$$

As we saw before, the symmetry that remained unbroken was a combination of both symmetries involved. Taking this into account it would be naive to expect the gauge bosons of the symmetries not to mix. In expression (1.41) we see that B and A^3 mix to form one square term in the Lagrangian. Considering this we can define the following linear combinations:

$$W^\pm_\mu = (A^1_\mu \mp A^2_\mu) \tag{15.46}$$

$$Z^0_\mu = \frac{1}{\sqrt{g^2 + g'^2}}(g'A^3_\mu - gB_\mu) \tag{15.47}$$

$$A_\mu = \frac{1}{\sqrt{g^2 + g'^2}}(g'A^3_\mu + gB_\mu) \quad . \tag{15.48}$$

The definitions of Z^0 and $W^\pm$ follow directly from (1.41), the definition of the photon field A is just taken to be perpendicular to Z^0.

Putting everything together the gauge boson mass contribution to the Lagrangian takes the following form:

$$\mathcal{L}_M = \frac{1}{2}m_{W^+}^2(W_\mu^+)^2 + \frac{1}{2}m_{W^-}^2(W_\mu^-)^2 + \frac{1}{2}m_{Z^0}^2(Z_\mu^0)^2, \tag{15.49}$$

where the masses are naturally defined as:

$$m_W := m_{W^\pm} = g\frac{v}{2} \tag{15.50}$$

$$m_Z = \sqrt{g^2 + g'^2}\frac{v}{2} \tag{15.51}$$

$$m_A = 0. \tag{15.52}$$

All in all we see that a natural form for the bosonic mass term in an electroweak Lagrangian can be simply achieved by means of the Higgs mechanism.

15.4 Summary

The Higgs mechanism takes a gauge theory, couples it to a scalar field theory that supports symmetry breaking, and combining both mechanisms lets some of the gauge bosons become massive while keeping gauge invariance. The Goldstone bosons corresponding to the broken symmetries are eaten by the gauge bosons that become massive. During this process the degree of freedom that corresponds to the scalar Goldstone bosons goes into the vector gauge bosons as a newly gained longitudinal polarization.

If we had taken the previous considerations further it would have been possible to also account for the fermion masses by means of the Higgs mechanism. This makes it possible to account for all mass in the standard model by this system. In this context one should remember that the major mass contribution of to protons, neutrons and thus to atoms comes from the kinetic energy of the confined quarks, not from the intrinsic masses of its constituents. Electrons however seem to have no internal structure, meaning that their whole mass comes from the Higgs mechanism. Without this mass they could not be bound in finite orbits around the atom, and thus atoms would not exist.

15.5 Epilogue: The Higgs Boson

One of the scalar fields that appeared in GWS-theory was not gauged away. The question thus arises, if it is a physical object and if, as such, it can be observed in nature. This was for a long time a highly elusive question. It was known from theory that the quanta of the Higgs field, the Higgs bosons, interacted very weakly with other particles, making it very difficult to detect. Theoretical predictions also showed the Higgs bosons should have a very high mass, meaning that they could only be produced at very high energies in particle detectors and that they were very unstable particles.

The Higgs boson was finally observed at the LHC in Geneva in 2012 and confirmed in 2013 after tedious analysis of the huge amount of data. It is the first fundamental scalar particle to have been observed in nature.

Bibliography

[1] M.E. Peskin, D.V.Schroeder, An Introduction to Quantum Field Theory (Westview Press, 1995)

[2] "Broken Symmetries and the Masses of Gauge Bosons", Peter W. Higgs, Phys. Rev. Lett. 13, 508 (1964)

[3] "Broken Symmetry and the Mass of Gauge Vector Mesons", F. Englert and R. Brout, Phys. Rev. Lett. 13, 321 (1964)

The Higgs Mechanism for $T > 0$ - Baryogenesis

Author: Jakob Steinbauer
Supervisor: Florian Goertz

After giving a short overview over the evidences and requirements for a Baryon asymmetry in the universe, the main focus of this report will be on the mechanisms of baryogenesis, with special emphasis on the predictions of the Standard Model of particle physics. Because of its great importence for Standard Model baryogenesis, a big part of the discussion will deal with the electroweak phase transition, which will be investigated by means of perturbation theory. Towards the end, the results will be compared to those of non-perturbative lattice simulations. The results of the calculations (both perturbative and non-perturbative) will force us to consider models beyond the Standard Model with which the report will end.

1 Introduction - Evidences for a Baryon asymmety

Before dealing with the mechanisms that can lead to a Baryon-antiBaryon asymmetry it is necessary to check whether our most basic assumption - namely that there is more matter than antimatter in the universe - is justified.
On earth, there is almost no antimatter. The biggest amounts can be found in the antiproton accumulators at CERN and Fermilab.
The situation does not change when we are looking at our solar system: The fact that men traveled to the moon and returned savely is quite a strong indice that it is made out of matter. Most planets in our solar system have been visited by space probes - they survived. Particles from the sun tell us that our star is made of matter too and due to the absence of gamma ray flashes, it is also very unlikely that there are any other macroscopic objects made of antimatter in our solar system.
Regarding the whole universe we encounter a similar picture: There are no flashes of gamma rays from matter-antimatter annihilations and the composition of the cosmic radiation indicates an abundance matter over antimatter too.

How much more matter than antimatter is there in the universe? The ratio of antiprotons $n_{\bar{p}}$ to protons n_p in the cosmic radiation is [7]

$$\frac{n_{\bar{p}}}{n_p} \approx 3 * 10^{-4} \tag{15.1}$$

while the ratio of antihelium nuclei to helium nuclei is even smaller

$$\frac{n_{^4\bar{H}e}}{n_{^4He}} \approx 10^{-5}. \tag{15.2}$$

Both ratios can be explained by secondary production via collisions ($pp \to 3p + \bar{p}$). We can conclude that the asymmetry of Baryons to antiBaryons today is (almost) maximal - that means only Baryons and no net antiBaryons!

A very important quantity is the Baryon-to-entropy ratio (numerical values from [7])

$$\frac{n_B - n_{\bar{B}}}{s} \approx (6 \text{ to } 10) \times 10^{-11}$$

(where $n_B/n_{\bar{B}}$ is the number of Baryons/antiBaryons respectively)
that characterizes the asymmetry and which remains constant without B-number violating processes. It shall be remarked that, although the Baryon asymmetry is almost maximal today, at high temperature the relative difference of Baryons to antiBaryons was strongly reduced due to thermal quark-antiquark pairs! I.e. for $T \geq 1\text{GeV}$:

$$\frac{n_q - n_{\bar{q}}}{n_q} \approx 3 \times 10^{-8}.$$

2 Requirements for Baryon asymmetry

Now that we convinced ourselves that there is most likely a (huge) excess of Baryons over antiBaryons in the universe, it is justified to ask why this is the case.
One could of course claim that the situation we observe today merely reflects the initial conditions of the universe, that means that there has always been a Baryon asymmetry. This argument is of course not very satisfactory (and also quite delicate in regard of the subtleties of specific Baryon number changing processes).
Assuming an initially symmetric universe, *Andrei Sakharov* proposed in 1967 that there are 3 criteria which necessarily have to be fulfilled in order for a Baryon asymmetry to emerge.

- B-nonconserving interactions
- C and CP violation
- Departure from thermal equilibrium

These criteria shall be specified in more detail.

2.1 B violation

Let us consider a process

$$i \to f \tag{15.3}$$

If the Baryon numbers of the initial and the final states differ

$$B(i) \neq B(f) \tag{15.4}$$

then this process is said to violate Baryon number.
It is quite obvious that processes like these are needed in order for a Baryon asymmetry to occur. Otherwise, starting from an arbitrary ratio of Baryons to antiBaryons there would otherwise be nothing that could change the initial conditions.

2.2 C and CP violation

The second criterion in the list states that B-nonconserving process must not have equal probabilities for ΔB to positive and ΔB to be negative: Otherwise processes that increase the Baryon number would (in average) be compensated by processes that decrease it.
At first, let us define the different field transformations. Under *charge conjugation* C a fermion field ϕ transforms as

$$C: \ \psi_L \to \sigma_2 \psi_R^* = \psi_L^C, \ \psi_R \to -\sigma_2 \psi_L^* = \psi_R^C. \tag{15.5}$$

Under this transformation a particle is transformed into its antiparticle. (Note that the field changes its chirality too!)
Under the parity transformation P, the field changes its chirality:

$$P: \ \psi_L \to \psi_R, \ \psi_R \to \psi_L \tag{15.6}$$
$$\tag{15.7}$$

CP is just a combination of the two transformations:

$$CP: \ \psi_L \to \psi_R^C, \ \psi_R \to \psi_L^C \tag{15.8}$$
$$\tag{15.9}$$

If C or CP were concerved, then

$$[C, H] = [CP, H] = 0. \tag{15.10}$$

Starting from an initially CP symmetric universe $CP\,|\phi(t=0)\rangle = |\phi(t=0)\rangle$ (which is what we assume, since it leads to a Baryon symmetric initial state) CP conservation

$$\Rightarrow CP\,|\phi(t)\rangle = CPe^{i\hat{H}t}\,|\phi_0\rangle = e^{i\hat{H}t}(CP\,|\phi_0\rangle) = |\phi(t)\rangle\,, \ |\phi_0\rangle = |\phi(t=0)\rangle \tag{15.11}$$

would leave the universe CP symmetric (the same argument holds for C).
One might think that the violation of either C or CP would be enough to get a Baryon asymmetry, but it can be easily shown that the violation of both is needed. Consider for instance a process that violates C, but is CP conserving

$$\Gamma(X \to q_L q_L) \neq \Gamma(\bar{X} \to \bar{q_L}\bar{q_L}) \tag{15.12}$$
$$\Gamma(X \to q_L q_L) = \Gamma(\bar{X} \to \bar{q_R}\bar{q_R}) \tag{15.13}$$
$$\Gamma(X \to q_R q_R) = \Gamma(\bar{X} \to \bar{q_L}\bar{q_L}). \tag{15.14}$$

If we add up the amplitudes, we see that no net bayon number violation occurs (given that $n_X = n_{\bar{X}}$, which is true assuming a C-symmetric initial state):

$$\Gamma(X \to q_L q_L) + \Gamma(X \to q_R q_R) = \Gamma(\bar{X} \to \bar{q_R}\bar{q_R}) + \Gamma(\bar{X} \to \bar{q_L}\bar{q_L}) \tag{15.15}$$

There are some more subleties associated with this topic, but to keep the discussion short I refer to [13] .

2.3 Nonequilibrium

The last one of Sakharovs criteria (according to the list given above) is the requirement of nonequilibrium. Thermodynamical nonequilibrium gives a certain arrow of time - and therefore a direction in which processes tend to - which is necessary, since we need our processes to tend towards an excess of matter over antimatter.

A more quantitative argument was given in [11] and considers the expectation value of the Baryon-antiBaryon difference in thermal equilibrium.

$$\langle n_B - n_{\bar{B}} \rangle = \langle n_b \rangle = \mathrm{Tr}\left(e^{-H/(k_B T)} n_b\right) \tag{15.16}$$
$$= \mathrm{Tr}\left((CPT)(CPT)^{-1} e^{-H/(k_B T)} n_b\right) \tag{15.17}$$
$$= \mathrm{Tr}\left(e^{-H/(k_B T)} (CPT)^{-1} n_b (CPT)\right) \tag{15.18}$$

Note that here the chemical potentials of Baryons and antiBaryons is set to zero. In eq. 15.18 we used CPT-invariance.
The Baryon number n_b changes sign under C, but stays the same under P, T:

$$\Rightarrow \langle n_b \rangle = -\mathrm{Tr}\left(e^{-H/(k_B T)} n_b\right) \tag{15.19}$$
$$\Rightarrow \langle n_b \rangle = 0 \tag{15.20}$$

Therefore, the difference between Baryon- and antiBaryon number vanishes.

We shall now investigate whether the Sakharov criteria are fulfilled for specific theories - like the Standard Model (SM).

3 CP violation in the Standard Model

It is of course very interesting to start out asking, whether the Standard Model of particle physics meets the requirements necessary for baryogenesis. At first we shall investigate whether it fulfills the second of Sakharovs critera (according to this list) - C and CP violation.

3.1 The Cabbibo-Kobayashi-Maskawa matrix

In Glashow-Weinberg-Salam (GWS) theory, there are two kinds of interactions between fermions and gauge bosons: **Neutral Current** (NC) and **Charged Current** (CC) interactions.

For our purposes, we are interrested in the charged current interaction, since it mixes up- and down quarks (we will see why this is important for C/CP violation). The CC interaction of the GWS theory has the form:

$$\mathcal{L}_{CC} = \frac{g}{2\sqrt{2}} \left\{ W_\mu^+ \left[\sum_i \bar{u}_i' \gamma^\mu (1-\gamma_5) d_i' + \sum_i \bar{\nu}_i' \gamma^\mu (1-\gamma_5) l_i' \right] + h.c. \right\} \tag{15.21}$$

In this form, the lagrangian is written in terms of the interaction eigenstates. Changing to the mass eigenstates, the "quark vectors" u and d are transformed by unitary matrices s^u and s^d (which corresponds to a mixture of the different quark generatons).

$$u_i = s_{ij}^u u_j' \tag{15.22}$$

$$d_i = s_{ij}^d d_j' \tag{15.23}$$

Where s^u and s^d are unitary.

$$\Rightarrow \bar{u}_i' d_i' = \bar{u}_i \underbrace{s_{ik}^u (s^{d\dagger})_{kj}}_{=V_{ij}} d_j \tag{15.24}$$

Where V_{ij} is the so-called Cabbibo-Kobayashi-Maskawa (CKM) matrix. Now we can write the hadronic part in terms of mass-eigenstates:

$$\mathcal{L}_{CC(Hadronic)} = \frac{g}{2\sqrt{2}} \left\{ W_\mu^+ \sum_{i,j} \bar{u}_i \gamma^\mu (1-\gamma_5) V_{ij} d_j + h.c. \right\} \tag{15.25}$$

If the CKM matrix contains any complex phases, the lagrangian is not invariant under C and CP. To evaluate whether this is the case, we count the number of phases of a general unitary $N \times N$ matrix.

A unitary $N \times N$ matrix has N^2 degrees of freedom:

$$\text{N(N-1)/2 real numbers + N(N+1)/2 phases}$$

But redefining the fields like

$$u_i \to e^{i\phi_i} u_i \text{ and } d_j \to e^{i\theta_j} d_j \tag{15.26}$$

does not change physics! So $2N-1$ phases of the matrix can be absorbed by the fields, which leads to a shift

$$\Rightarrow V_{ij} \to V_{ij} e^{i(\theta_j - \phi_i)}. \tag{15.27}$$

We end up with a total number of $(N^2-3N)/2+1$ phases. For various numbers of generations, the corresponding number of complex phases is listed in table 15.1.

	Number of generations	Number of phases
	1	0
	2	0
$\Rightarrow$	**3**	**1**
	4	3

Table 15.1: Number of complex phases in the CKM matrix for different numbers of fermion generations.

3.2 Magnitude of CP violation

When looking at tabular 15.1, we see that there is exactly one complex phase given in the Standard Model - so it fulfills requirement of CP violation!

Still, there is the question whether this CP violation is strong enough to account for the Baryon-asymmetry that we observe today. To answer this question, one needs to quantify the maximal CP violation of the theory. This was for instance done by C. Jarlskog, (see [12]) who gave the basis independent quantity

$$J = \mathrm{Im}\{\det\,[m_u^2, m_d^2]\} \tag{15.28}$$

to account for the maximal CP violation. From this quantity, one can deduce a dimensionless constant (see [13], p. 29) that quantifies the magnitude of the CP violation to be about $\sim 10^{-20}$. This is too small to explain the Baryon asymmetry we observe today.

3.3 Additional CP violation by extending the SM

Since the Standard Model does not provide sufficient CP violation, one has to consider alternatives. One could be to extend the SM in some minimal fashion, and there are several ways to do this:

- **Higher dimensional Operators:** Here, the Standard Model is just seen as an effective theory, that is valid below some mass scale M. For high energies, one expects additional terms to become relevant - some of which are CP violating.
- **Two-Higgs Doublet Model:** In the 2HDM, an additional Higgs doublet is added to the theory, which can lead to large CP violation in bubble walls at the electro-weak phase transition.

The last one shall be scetched briefly, since we are going to use it afterwards.

2 Higgs Doublet Model (2HDM)

In the 2HDM (for discussions related to our topic, see [5] or [13]), the potential looks like

$$V = -\mu_1^2|H_1|^2 - \mu_2^2|H_2|^2 - (\mu_3^2 H_1^\dagger H_2 + h.c.) + \frac{1}{2}\lambda_1|H_1|^4 + \frac{1}{2}\lambda_2|H_2|^4 \tag{15.29}$$

$$+ \lambda_3|H_1|^2|H_2|^2 + \lambda_4|H_1^\dagger H_2|^2 + \frac{1}{2}\lambda_5\left[(H_1^\dagger H_2)^2 + h.c.\right] \tag{15.30}$$

In the third, as well as in the last term, complex phases can arises!
Making an ansatz for the profile of the Higgs field at the bubble wall

$$H_i(x) = \frac{1}{\sqrt{2}} h_i(x) e^{i\theta_i(x)} \tag{15.31}$$

$$h_i = \begin{pmatrix} cos\beta \\ sin\beta \end{pmatrix} h(x) \tag{15.32}$$

(where $h(x)$ is a real function) the potential turns into

$$V = -\frac{1}{2}(\mu_1^2 + \mu_2^2)h^2 - \mu_3^2 cos(\theta_2 - \theta_1)h^2 \tag{15.33}$$

$$+ \frac{1}{8}(\lambda_1 + \lambda_2 + 2\lambda_3 + 2\lambda_4)h^4 + \frac{1}{4}\lambda_5 cos(2(\theta_2 - \theta_1))h^4 \tag{15.34}$$

One can now see that the potental (and therefore the lagrangian) depends explicitly on the difference of the higgs-phases. This will be of great importance when discussing the electroweak phase transition!

4 Baryon number violation in the SM

We now want to investigate whether there are processes in the SM that allow Baryon number violation.

4.1 The Chiral Anomaly

Classically, Noether's theorem gives:

$$\partial_\mu j_B^\mu = \partial_\mu \frac{1}{3}\bar{Q}\gamma^\mu Q = 0 \tag{15.35}$$

Although classically the Baryon number (which is given by the spatial integral over the 0-component of j_B) is a conserved quantity, this classical conservation is spoiled by quantum effects! The evaluation of fermionic triangle loop (see fig. 15.1) yields:

$$\partial_\mu j_B^\mu = n_f \left(\frac{g^2}{32\pi^2} W_{\mu\nu}^a \widetilde{W}^{a\mu\nu} - \frac{g'^2}{32\pi^2} Y_{\mu\nu} \widetilde{Y}^{\mu\nu} \right) \tag{15.36}$$

With n_f being the number of flavors. Where

$$W_{\mu\nu}^a = \partial_\mu W_\nu^a - \partial_\nu W_\mu^a - ig\epsilon^{abc} W_\mu^b W_\nu^c \tag{15.37}$$

$$Y_{\mu\nu} = \partial_\mu Y_\nu - \partial_\nu Y_\mu \tag{15.38}$$

are the field-strength tensors of the non-abelian/abelian gauge fields (W_μ^a / Y_μ, respectively) of the theory, and

$$\widetilde{W}^{\mu\nu} = \frac{1}{2}\epsilon^{\mu\nu\alpha\beta} W_{\alpha\beta} \tag{15.39}$$

$$\widetilde{Y}^{\mu\nu} = \frac{1}{2}\epsilon^{\mu\nu\alpha\beta} Y_{\alpha\beta} \tag{15.40}$$

are the dual field-strength tensors.

To evaluate the Baryon number, it is customary to define four divergences $\partial_\mu k_W^\mu$ and $\partial_\mu k_Y^\mu$ so that

$$\partial_\mu j_B^\mu = n_f (\frac{g^2}{32\pi^2} \partial_\mu k_W^\mu - \frac{g'^2}{32\pi^2} \partial_\mu k_Y^\mu). \tag{15.41}$$

It can be easily shown, that they have the explicite form

$$k_Y^\mu = \epsilon^{\mu\nu\alpha\beta} Y_{\nu\alpha} Y_\beta \tag{15.42}$$

$$k_W^\mu = \epsilon^{\mu\nu\alpha\beta} (W_{\nu\alpha}^a W_\beta^a - \frac{g}{3}\epsilon_{abc} W_\nu^a W_\alpha^b W_\beta^c). \tag{15.43}$$

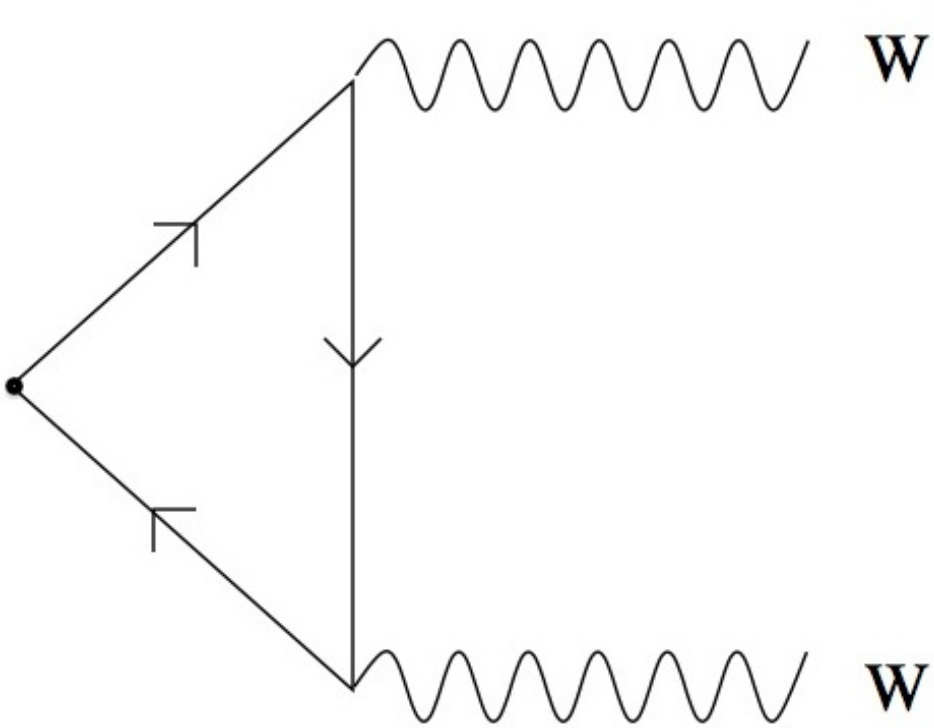

Figure 15.1: Triangle diagramm causing the anomaly

The integral over the zero component of $\frac{g^2}{32\pi^2}k_W^\mu + \frac{g'^2}{32\pi^2}k_Y^\mu$ gives:

Chern-Simons number (CS number)

$$N_{CS} = \frac{g^2}{32\pi^2}\int \mathrm{d}^3x\epsilon^{ijk}(W_{ij}^a W_k^a - \frac{g}{3}\epsilon_{abc}W_i^a W_j^b W_k^c) \tag{15.44}$$

(terms including the abelian field-strength tensor do not show up, since terms proportional to total derivatives vanish!)
This number is, up to an additive constant, proportional to the Baryon number (with proportionality factor n_f)!

4.2 Vacuum configurations

Since the Yang-Mills term in the lagrangian is positive semi-definite, we want it to vanish for vacuum field configurations:

$$\mathcal{L}_{YM} \propto W_{\mu\nu}^a W^{a\mu\nu} \stackrel{!}{=} 0 \tag{15.45}$$

This can be achieved by demanding W_μ to be pure gauge:

$$W_\mu = -\frac{i}{g}U(x)\partial_\mu U^{-1}(x) \tag{15.46}$$

$$\Rightarrow W_{\mu\nu} = 0 \tag{15.47}$$

Under gauge transformations

$$W'_\mu = V(x)W_\mu V^{-1}(x) - \frac{i}{g}V^{-1}(x)\partial_\mu V(x),\ V \in SU(2) \tag{15.48}$$

$$\Rightarrow W'_\mu = -\frac{i}{g}\underbrace{V(x)U(x)}_{=U'}\partial_\mu(U^{-1}V^{-1}) = -\frac{i}{g}U'\partial_\mu U'^{-1} \tag{15.49}$$

- the field-strength tensor $W'_{\mu\nu} = 0$ still vanishes!

- the CS-number may change (under "large transformation"), but $\Delta N_{CS} = N_{CS}(vacuum1) - N_{CS}(vacuum2)$ is invariant (can be easily checked by plugging in the definitions)!

It is also important to mention that there are no *continuous* field transformations that change the CS-number, but keep $W_{\mu\nu} = 0$!

Topological remarks

For pure gauge field configurations (like those showed before) and fixed time x^0, $U(x)$ defines a map $\mathbb{R}^3 \to SU(2)$. If we add a point at infinity there are bijective functions $f : \mathbb{R}^3 \cup \{\infty\} \to S^3$ that connect $\mathbb{R}^3$ to the 3-sphere. That means, if $U(x) \xrightarrow[x\to\infty]{} U_\infty$ is defined, at any fixed time x^0, $U(x)$ defines a map

$$U : \ S^3 \to SU(2) \tag{15.50}$$

and the Chern-Simons number is given by an integer winding number:

$$N_{CS} = \frac{1}{24\pi^2} \int \mathrm{d}^3x \epsilon^{ijk} \, \mathrm{Tr}(U\partial_i U^{-1} U\partial_j U^{-1} U\partial_k U^{-1}) \tag{15.51}$$

Each winding number N_{CS} corresponds to a homotopy class of maps $U : \ S^3 \to SU(2)$, the homotopy group is $\pi_3(S^3) = \mathbb{Z}$.

We end up with the following conclusions:

- Different vacua are defined by different Chern-Simmons number.

- Vacua with the same CS number belong to the same homotopy class.

- Vacua of different Baryonnumber are seperated by a potential barrier!

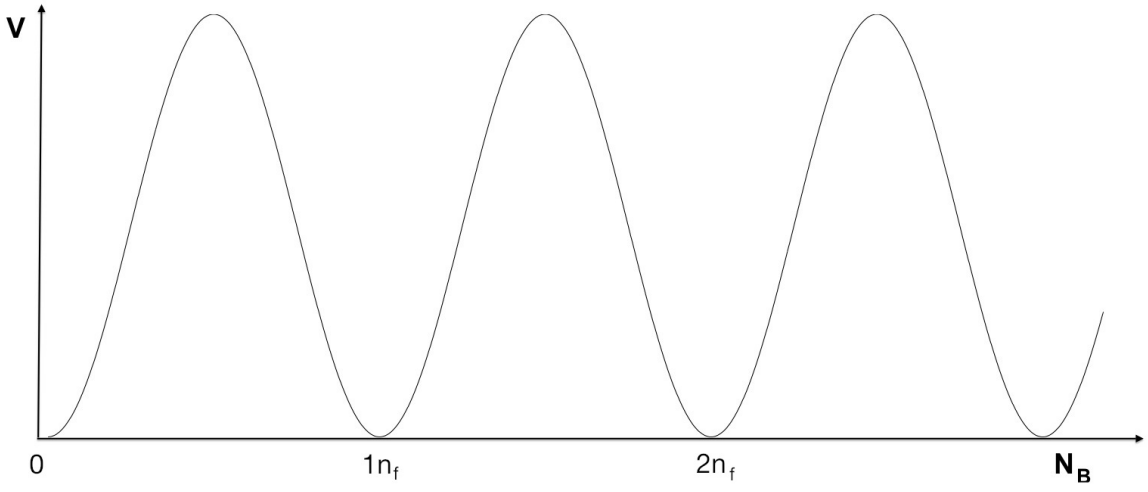

Figure 15.2: Potential as a function of the Baryon number.

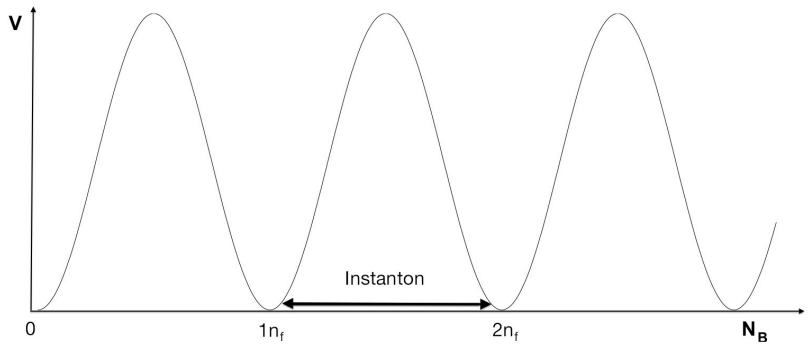

Figure 15.3: Illustration of an Instanton.

4.3 Instantons

Now that we know that there are different vacuum configurations associated with different Baryon numbers, we want to exploit different ways to get from one configuration to another.

One way is due to tunneling, like it is shown in fig. 15.3.
The trajectory in field space configuration that connects two vacua of different topological charge is called **Instanton**. Here, the eucledian action of the Instanton gives a semiclassical approximation for the transition probability (a more detailed calculation can be found in [11]).

$$\Gamma \sim |e^{-S_E}|^2 \sim e^{-(8\pi)^2/g^2} \sim 10^{-170} \tag{15.52}$$

This value is of course far too small to explain the Baryon asymmetry we encounter today.

4.4 Sphalerons

A different way to get from one vacuum configuration to another is given by so-called sphaleron processes. Here, the field does not tunnel "through" the potential barrier, but "jumps" over it - with energy from thermal fluctuations (which is quite promising in regard of the high temperatures in the early universe). The Sphaleron is the field configuration that maximizes the potential energy, it is a *static*, *unstable* solution of classical equations of motion.
To calculate the sphaleron, we make an ansatz (see [1]) for the gauge field W_μ (assuming zero Weinberg-angle)

$$W_0^a = 0 \tag{15.53}$$

$$W_i^a \sigma^a = -\frac{2i}{g} f(\xi) \partial_i U \, U^{-1} \tag{15.54}$$

and for the Higgs field $\mathbf{\Phi}$:

$$\mathbf{\Phi} = \frac{v}{\sqrt{2}} h(\xi) U \begin{pmatrix} 0 \\ 1 \end{pmatrix} \tag{15.55}$$

$$\text{with } U = \frac{1}{r} \begin{pmatrix} z & x+iy \\ -x+iy & z \end{pmatrix} \tag{15.56}$$

with $\xi = gvr$.

If we plug the ansatz into the equations of motion we get two coupled ordinary differential equations:

$$\frac{\mathrm{d}^2 f}{\mathrm{d}\xi^2} - \frac{2}{\xi^2} f(1-f)(1-2f) + \frac{1}{4} h^2 (1-f) = 0 \tag{15.57}$$

$$\frac{\mathrm{d}}{\mathrm{d}\xi} \left(\xi^2 \frac{\mathrm{d}h}{\mathrm{d}\xi} \right) - 2h(1-f)^2 - \frac{\lambda}{g^2} \xi^2 (h^2 - 1) h = 0 \tag{15.58}$$

Considering the boundary conditions $f(0) = h(0) = 0$ and $f(\infty) = h(\infty) = 1$ these can be solved numerically!
The solution can then be used to calculate the energy of the sphaleron:

$$E_{sph} = \frac{g \langle \phi(T) \rangle}{\alpha_W} B(\lambda/g^2) \tag{15.59}$$

Where $B(\lambda/g^2)$ is a polynomial fit, including numerically evaluated constants:

$$B(x) = 1.58 + 0.32x - 0.05x^2 \tag{15.60}$$

It is important to mention that although in our ansatz we neglected the effects of temperature, a temperature dependence is built into the sphaleron energy in an approximative manner by considering the Higgs expectation value being a function of temperature.

The preceding derivation revealed that the energy barrier between vacua of different Baryon number depends on the vacuum expectation value (VEV) of the Higgs field. Still, the question of the transition rate has not yet been solved.
Since the Sphaleron energy is proportional to the Higgs VEV, we assume that we have to distinguish two cases:

- $\langle \phi(T) \rangle = 0$ (symmetric phase before EW phase transition)
- $\langle \phi(T) \rangle \neq 0$ (broken phase after EW phase transition)

In the **symmetric phase**, i.e. for $T > T_c$, $\langle \phi(T > T_c) \rangle = 0$ - we can estimate B- violation rate on dimensional grounds:
Since we are looking for field configurations with $N_{CS} \sim 1$

$$\int \mathrm{d}^3x \; (g^2 FA \text{ or } g^3 A^3) \sim 1 \tag{15.61}$$

while the energy is determined by the temperature:

$$\int \mathrm{d}^3x \; F^2 \sim T \tag{15.62}$$

Combining the two expressions (with $\int \mathrm{d}^3x \sim R^3$), we can derive an approximation for the sphaleron rate in the symmetric phase

$$\frac{\Gamma}{V} \sim \frac{1}{R^4} \sim (g^2 T)^4 \tag{15.63}$$

One might doubt whether this argument is really robust - and it turns out that the actual sphaleron rate has a slightly different form (see for instance [13], p. 27).

In the **broken phase** the Higgs VEV is nonzero, so there is a potential barrier between the vacuum configurations. Here, the sphaleron rate is calculated by means of the Langer-Affleck theory [8]. The actual calculation includes a functional integration over the field configurations (scatched in [3]). A gaussian approximation around the sphaleron solution gives (see [9])

$$\frac{\Gamma}{V} \sim 2.8 \times 10^5 T^4 \left(\frac{\alpha_W}{4\pi} \right)^4 \kappa \frac{\zeta^7}{B^7} e^{-\zeta} \tag{15.64}$$

with $\alpha_W = g^2/4\pi$, $\zeta = E_{sph}(T)/T$, $B = B(\lambda/g^2)$.

Some words about eqn. 15.64 : We encounter a boltzmann factor directly form the sphaleron solution. The prefactors are due to the terms quadratic in the fields (since only those are retained in the gaussian approximation) and κ is functional determinant associated with changing from integrating over the fields to integrating over the fluctuations around the sphaleron. In [2], it has been estimated to be $10^{-4} \leq \kappa \leq 10^{-1}$.

4.5 Sphaleron rate vs. expansion of universe

Whether the sphalerons processes can reach equilibrium depends on the ratio of the sphaleron rate to expansion rate of the universe (which is quantified through Hubble rate). The Hubble rate H is defened as follows (see [9], for a more detailed discussion see [7])

$$H = \frac{\mathrm{d}a(t)}{\mathrm{d}t}\frac{1}{a(t)} \sim \sqrt{g_*}T^2/M_P \tag{15.65}$$

where $a(t)$ is the scale factor of universe (see [13]) and g_* is the number of relativistic degrees of freedom. Sphalerons can come to equilibrium when

$$\Gamma \geq H \Rightarrow 10^{-6}T \geq \sqrt{g_*}\frac{T^2}{M_P}. \tag{15.66}$$

After the EW phase transition the sphaleron rate is reduced, and when $H \geq \Gamma$ again, they become ineffective.
Why is this of relevance for our topic? When looking at fig. 15.4, one sees that just before the EW phase transition, the sphaleron processes are in equilibrium (process rate equal in both directions). Here, since sphalerons are as likely to increase the Baryon number as they are to decrease it, there is no Baryon asymmetry. The EW phase transition preceeds by the *nucleation of bubbles of true vacuum*[1] (with Higgs VEV not equal to zero) - here, CP-violating processes emerge (to be discussed in 4.6) and a Baryon asymmetry occurs inside the bubble. After the EW phase transition, sphalerons start to wash out this asymmetry to get to equilibrium again. In sec. 4.7, it will turn out that in order to preserve non-equilibrium the phase transition has to be of 1^{st} order.

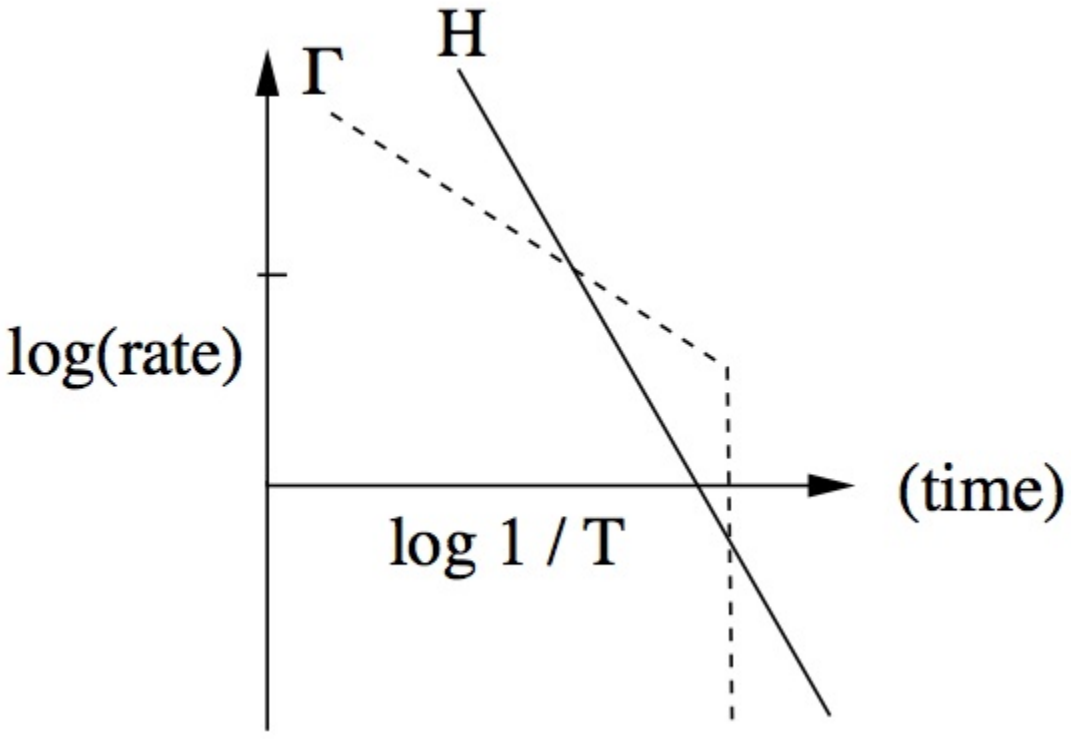

Figure 15.4: Sphaleron rate and Hubble rate vs. time. At the EWPT a drop in the sphaleron rate occurs.

[1]Here, "true vacuum" refers to the vacuum expectation value for which the effective potential (to be defined in sec. 5.1) has a global minimum.

4.6 Generation of Baryon asymmetry at bubble wall

We shall now sketch an particular example of how CP violation at the bubble wall could work to generate a Baryon asymmetry. Since this topic is quite extensive on its own, I just want to scetch the mechanisms briefly (for a more detailed discussion, see for instance [13], p. 46).

At the electroweak phase transition - one can approximate the shape of the Higgs field by solving the classical equations of motion.

Considering the 2HDM (like scetched in section 3.3), there is also a complex phase in the Higgs field that is a function of x (see e.g. [5] for a detailed calculation of the Higgs profile). For a profile like

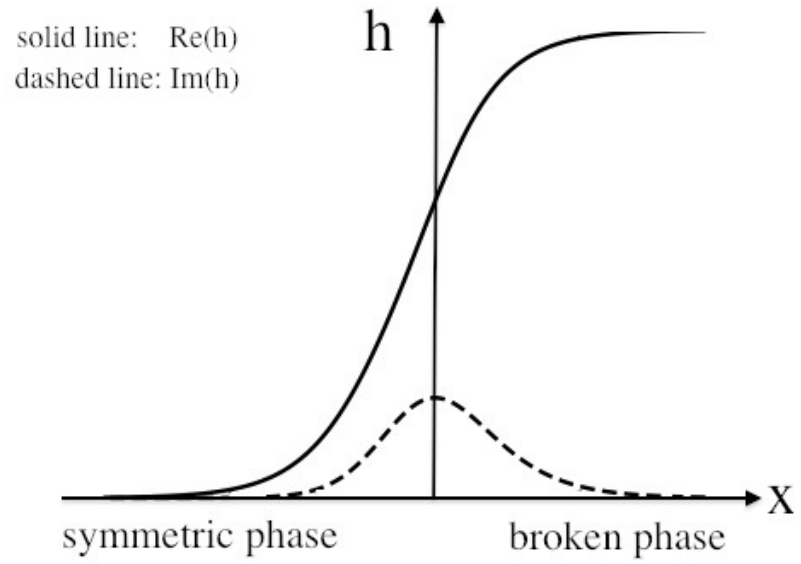

Figure 15.5: Schematical profile of the real and the imaginary part of the Higgs field at the bubblewall.

the one shown in fig. 15.5, the imaginary part of the Higgs field has its maximum at the bubble wall. This gives rise to a complex Yukawa coupling, resulting in a CP violation for scattering processes at the bubble wall. In that way, a local Baryon asymmetry emerges at both sides of the bubble wall (globally, we still have a bayon symmetry). The essential thing now is, that sphaleron processes outside of the bubbles are very effective and will wash out the Baryon asymmetry very quickly, while inside the bubble, sphalerons are supressed, according to eqn. 15.64. The idea is now, that If this supression inside the bubble is big enough (since the Higgs VEV is bigger than zero inside the bubbles), an asymmetry could survive!

4.7 Baryon asymmetry washout

After the EW phase transition, sphalerons try to washout B-asymmetry in broken phase again! We can quantify this effect by introducing a "washout factor", like

$$S(t) = \frac{n_b(t + t_{EW})}{n_b(t_{EW})}. \tag{15.67}$$

With the sphaleron rate, we can give a differential equation for this factor

$$\frac{\mathrm{d}S(t)}{\mathrm{d}t} = -kN_f \frac{\Gamma(t)}{T^3} S(t) \tag{15.68}$$

$$\Rightarrow S(t) = \exp\left\{ - \int_{t_{EW}}^{\infty} \mathrm{d}t \; kN_f \frac{\Gamma(t)}{T^3} \Delta t \right\} \tag{15.69}$$

where k is a constant, N_F number of flavors.
The Friedmann equations now yield a relation between time and temperature

$$t = \frac{1}{4\pi}\sqrt{\frac{45}{\pi g}}\frac{M_{Pl}}{T^2} \tag{15.70}$$

so we can substitute the time in eqn. 15.68 by temperature!
The Baryon density n_B in the observed universe gives a constraint for S (see [9]):

$$S \geq 10^{-5} \tag{15.71}$$

By plugging this into the expression for the washout, we get the requirement

$$E_{sph}(T_c)/T_c \geq 7\log(E_{sph}(T_c)/T_c) + 9\log 10 + \log\kappa \tag{15.72}$$

(with T_c being the critical temperature of the phase transition - defined in eq. 15.113) which, with $\kappa = 10^{-1}$ or 10^{-4} gives

$$\frac{E_{sph}(T_c)}{T_c} \geq 45 \text{ or } \geq 37. \tag{15.73}$$

If we now express the sphaleron energy through the Higgs VEV, we end up with a requirement for it at the EW phase transition

$$\frac{\langle\phi(T_c)\rangle}{T_c} \geq 1.3 \text{ or } \geq 1.0. \tag{15.74}$$

We conclude that the phase transition hast to be of 1^{st} order, since otherwise

$$\frac{\langle\phi(T_c)\rangle}{T_c} \simeq 0$$

.

4.8 Mechanisms of the phase transition

In order to have a 1^{st} order phase transition, the two degenerate minima $V_{eff}(\phi = 0) = V_{eff}(\phi \neq 0)$ at the critical temperature T_c have to be seperated through a potential barrier (like scetched in fig. 15.6)!

The "Tunnel probability" per unit volume to get from one minimum to the other is given (see [9]) by (analoge to eqn. 15.64)

$$\frac{\Gamma}{V} \sim A(T)e^{-S_3/T} \tag{15.75}$$

where $A(T) \sim \mathcal{O}(T^4)$ to have right scaling.
Here, S_3 is the 3-dimensional eucledian action

$$S_3 = \int \mathrm{d}^3x \left[\frac{1}{2}(\vec{\nabla}\phi)^2 + V_{eff}(\phi, T)\right] \tag{15.76}$$

corresponding to the energy of the field. Assuming spherical symmetry, we get

$$S_3 = 4\pi\int_0^\infty \mathrm{d}r\; r^2\left[\frac{1}{2}\left(\frac{\mathrm{d}\phi}{\mathrm{d}r}\right)^2 + V_{eff}(\phi, T)\right]. \tag{15.77}$$

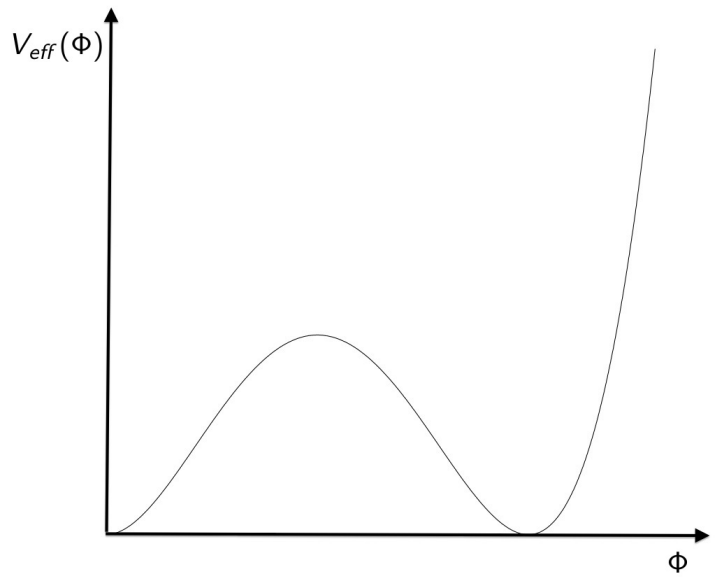

Figure 15.6: Effective Higgs potential at T_c, separating the two degenerate minima by a potential barrier

To investigate the mechanisms of the bubble nucleation, it is customary to split the eucledian action into a surface- and a volume term:

$$S_3 = 4\pi \underbrace{\int_0^\infty \mathrm{d}r\; r^2 \frac{1}{2}\left(\frac{\mathrm{d}\phi}{\mathrm{d}r}\right)^2}_{\sim 2\pi R^2 \left(\frac{\delta\phi}{\delta r}\right)^2 \delta r} + 4\pi \underbrace{\int_0^\infty \mathrm{d}r\; r^2 V_{eff}(\phi, T)}_{\sim \frac{4\pi}{3} R^3 \langle V(r<R)\rangle} \tag{15.78}$$

A bubble with radius R will grow when its expansion reduces its energy or, more explicitly if

$$\frac{\mathrm{d}S_3}{\mathrm{d}R} = 4\pi R \frac{\delta\phi}{\delta r}\delta r + 4\pi R^2 \langle V(r<R)\rangle \tag{15.79}$$

is smaller than 0.
In the last approximation, we set the potential outside the bubbles to be zero $\langle V(r>R)\rangle = 0$, which makes $\langle V(r<R)\rangle < 0$. Therefore - bubbles must be big in order to grow! According to eqn. 15.75 it is very unlikely that big bubbles are nucleated, but if the bubble production rate is bigger than the expansion rate of the universe - different bubbles can merge together!
If otherwise the Hubble rate is bigger than that of the bubble nucleation, the universe will be trapped in the false vacuum!

5 The Higgs Mechanism, $T > 0$ and the EW Phase Transition

The content of this section mainly leans on the lecture of M. Quiros [9].
It was already mentioned before that in order to get $\frac{\langle\phi(T_c)\rangle}{T_c} \geq 1.0$ we need to have a strongly 1^{st} order phase transition. In section 4.8 we also argumented that for such a phase transition, we need the degenerate minima of the effective Higgs potential at T_c to be separated by a potential barrier. Now the question arises of how to actually compute this effective Higgs potential - that shall be the topic of this section.

5.1 The effective action

The dynamics of the Higgs-expectation value are determined by the effective action:

$$\Gamma[\bar{\phi}] = W[j] - \int \mathrm{d}^4x \underbrace{\frac{\delta W[j]}{\delta j(x)}}_{\bar{\phi}} j(x) \tag{15.80}$$

This corresponds to a Legendre-transformation of the generating functional $W[j]$ (for connected n-point functions). It is worth looking at the variation of $\Gamma[\bar{\phi}]$ with respect to $\bar{\phi}$:

$$\frac{\delta\Gamma[\bar{\phi}]}{\delta\bar{\phi}} = \frac{\delta W[j]}{\delta j}\frac{\delta j}{\delta\bar{\phi}} - j - \bar{\phi}\frac{\delta j}{\delta\bar{\phi}} = -j(x) \tag{15.81}$$

$$\Rightarrow \left.\frac{\delta\Gamma[\bar{\phi}]}{\delta\bar{\phi}}\right|_{j=0} = 0 \tag{15.82}$$

The fact that the variation vanishes indicates that the expectation value $\bar{\phi}$ solves the classical eqs. of motion derived from the effective action.

The effective potential

Consider now a translationally invariant field expectation value

$$\bar{\phi}(x) = \phi_c. \tag{15.83}$$

For a constant field, the kinetic terms in lagrangian vanish.
We can then define the **effective potential** as follows:

$$\Gamma[\phi_c] = -\int \mathrm{d}^4x V_{eff}(\phi_c) \tag{15.84}$$

One can derive the explicit form (see [9])

$$V_{eff}(\phi_c) = -\sum_{n=0}^{\infty}\frac{1}{n!}\phi_c^n\Gamma^{(n)}(p_i = 0) \tag{15.85}$$

with $\Gamma^{(n)}(p_i = 0)$ being the one-particle irreducible Greens functions for zero momentum, like shown in fig. 15.7.

5.2 Finite temperature effects

Until now, we defined the Greens functions (for scalar fields) as

$$G(x_1, ..., x_n) = \langle T\phi(x_1)\cdots\phi(x_n)\rangle = \langle 0|\, T\phi(x_1)\cdots\phi(x_n)\,|0\rangle \tag{15.86}$$

which was true for temperature $T = 0$. Generally, the expectation value of an operator O is

$$\langle O\rangle = \mathrm{Tr}\,\{O\rho\} \tag{15.87}$$

where ρ is density operator.
We can use this now to derive a field theory that is valid for finite temperatures!
Since Greens functions are defined as expectation values, by knowing the density operator

$$\rho = \frac{\exp\{-\beta H\}}{Z}, \text{ with } \beta = \frac{1}{T} \tag{15.88}$$

$$Z = \mathrm{Tr}\,\{\exp\{-\beta H\}\} \tag{15.89}$$

(where we assumed 0 chemical potential) we can easily generalize them to finite temperatures

$$G(x_1, ..., x_n) = Z^{-1}\,\mathrm{Tr}\left\{e^{-\beta H}T\phi(x_1)\cdots\phi(x_n)\right\}. \tag{15.90}$$

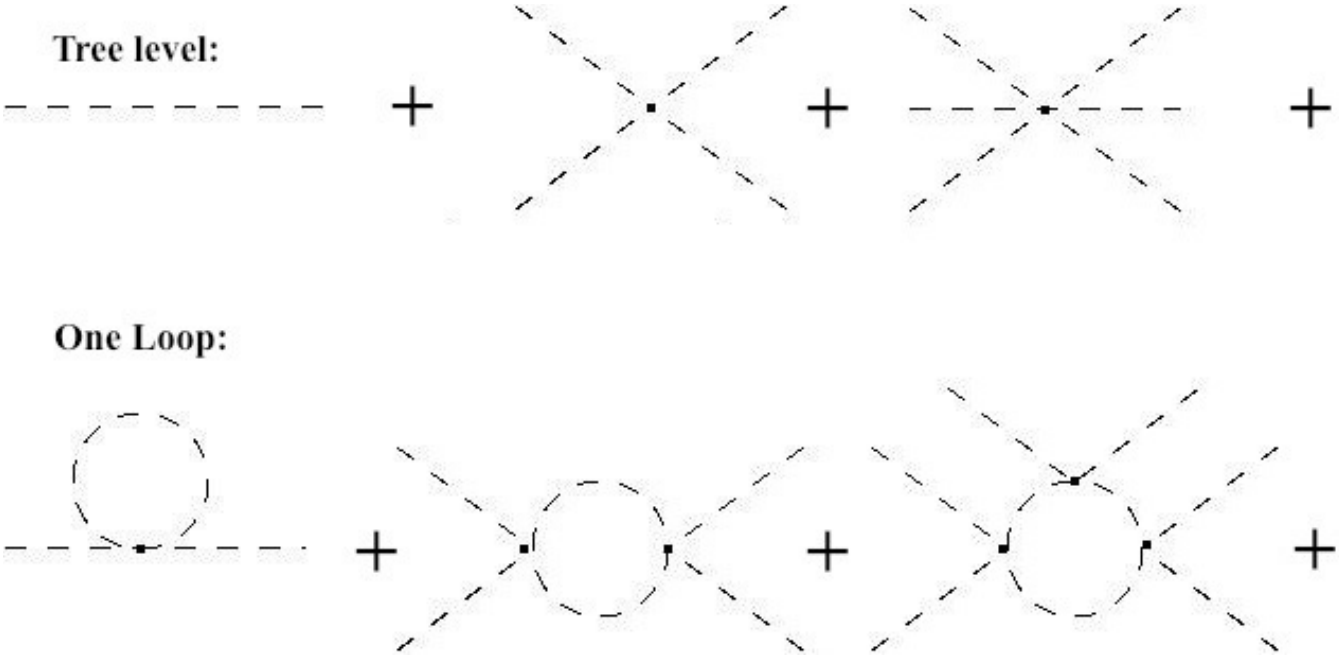

Figure 15.7: Tree-level and one-loop summands of the decomposition of the effective potential in 1PI greens functions.

Finite temperature feynman rules

Scalar fields.
With the definition of the scalar field operator

$$\phi(x) = \int \frac{\mathrm{d}^3 p}{(2\pi)^3 \sqrt{2\omega_p}} \left[a(p)e^{-ipx} + a^\dagger e^{ipx}\right] \tag{15.91}$$

$$\omega_p = \sqrt{\vec{p}^2 + m^2} \tag{15.92}$$

and

$$\left\langle a^\dagger(p)a(k)\right\rangle = n_B(\omega_p)\delta^{(3)}(\vec{p} - \vec{k}) \tag{15.93}$$

$$\left\langle a(p)a^\dagger(k)\right\rangle = [1 + n_B](\omega_p)\delta^{(3)}(\vec{p} - \vec{k}) \tag{15.94}$$

$$\tag{15.95}$$

(where $n_B(\omega) = \frac{1}{e^{\beta\omega}-1}$ is the bose distribution function)
we can calculate the two-point Green function

$$G(x-y) = \int \frac{\mathrm{d}^4 p}{(2\pi)^4} \rho(p) e^{-ip(x-y)} [\Theta(x^0 - y^0) + n_B(p^0)] \tag{15.96}$$

$$\text{with } \rho(p) = 2\pi[\Theta(p^0) - \Theta(-p^0)]\delta(p^2 - m^2). \tag{15.97}$$

Ferminic fields.
The fermion propagator $S_{\alpha\beta}(x-y)$ satisfies the dirac equation

$$(i\partial_\mu \gamma^\mu - m)_{\alpha\sigma} S_{\sigma\beta}(x-y) = i\delta(x-y)\delta_{\alpha\beta} \tag{15.98}$$

so the fermion propagator can be constructed from the Greens function $S(x-y)$

$$S_{\alpha\beta}(x-y) = (i\partial_\mu \gamma^\mu_{\alpha\beta} + m_{\alpha\beta}) S(x-y) \tag{15.99}$$

that satisfies the Klein-Gordon equation.
One arrives at an expression for $S(x-y)$, similar to $G(x-y)$

$$S(x-y) = \int \frac{\mathrm{d}^4p}{(2\pi)^4}\rho(p)e^{-ip(x-y)}[\Theta(x^0-y^0) - n_F(p^0)]. \tag{15.100}$$

Where $n_B(\omega) = \frac{1}{e^{\beta\omega}+1}$ is the fermi distribution function, which enters the equation in analogy to eq. 15.93 and eq. 15.94 . Evaluating the integrals for $G(x-y)$ and $S(x-y)$ (in imaginary time formalism), one can extract the finite temperature feynman rules:
Finite temperature feynman rules

$$\text{Boson propagator: } \frac{i}{p^2-m^2} \text{ ; } p^\mu = [2ni\pi\beta^{-1}, \vec{p}] \tag{15.101}$$

$$\text{Fermion propagator: } \frac{i(p_\mu\gamma^\mu + m)}{p^2-m^2} \text{ ; } p^\mu = [(2n+1)i\pi\beta^{-1}, \vec{p}] \tag{15.102}$$

$$\text{loop integral: } \frac{i}{\beta}\sum_{n=-\infty}^{\infty}\int\frac{\mathrm{d}^3p}{(2\pi)^3} \tag{15.103}$$

$$\text{vertex function: } -i\beta(2\pi)^3\delta_{\sum\omega_i,0}\delta^{(3)}(\sum_i \vec{p}_i) \tag{15.104}$$

In contrast to the zero-T feynman rules, a summation over the so-called Matsubara frequencies appears in the loop integral.

5.3 Effective Higgs potential for $T > 0$

Using the tools discussed before we can now calculate (for a detailed calculation, see [9]) the effective Higgs potential to be:

$$V_{eff}(\phi_c, T) = D(T^2 - T_0^2)\phi_c^2 - ET\phi_c^3 + \frac{\lambda(T)}{4}\phi_c^4 \tag{15.105}$$

with

$$D = \frac{2m_W^2 + m_Z^2 + 2m_t^2}{8v^2} \tag{15.106}$$

$$E = \frac{2m_W^3 + m_Z^3}{4\pi v^3} \tag{15.107}$$

$$T_0^2 = \frac{m_h^2 - 8Bv^2}{4D} \tag{15.108}$$

$$B = \frac{3}{64\pi^2v^4}(2m_W^4 + m_Z^4 - 4m_t^4) \tag{15.109}$$

$$\lambda(T) = \lambda - \frac{3}{16\pi^2v^4}\left(2m_W^4 log\frac{m_W^2}{A_BT^2} + m_Z^4 log\frac{m_Z^2}{A_BT^2} - 4m_t^4 log\frac{m_t^2}{A_FT^2}\right) \tag{15.110}$$

Notice that this expression does not converge to the bare potential wenn $T \to 0$ - this is due to a high-temperature expansion performed in the derivation! (see [9])

We are interested in the Higgs VEV at the critical temperature, therefore we evaluate the minima of V_{eff} at T_c. For general T, the minima are at

$$\phi_0(T) = 0 \tag{15.111}$$

$$\phi_m(T) = \frac{3ET}{2\lambda} + \frac{\sqrt{9E^2T^2 - 8D(T-T_0)^2\lambda}}{2\lambda}. \tag{15.112}$$

At the critical temperature now, both minima are degenerate:

$$V_{eff}(\phi_m(T_c)) = V_{eff}(\phi_0(T_c)) = 0 \tag{15.113}$$

$$\Rightarrow T_c = \sqrt{\frac{\lambda(T_c)DT_0^2}{\lambda(T_c)D - E^2}} \tag{15.114}$$

Plugging this back into eqn. 15.112, we get

$$\phi_m(T_c) = \frac{2ET_c}{\lambda(T_c)} \tag{15.115}$$

where E (here, E is a parameter (eqn. 15.107) - not the energy!) is determined by the experimental data

$$\frac{2}{3}E = \frac{2}{3}\frac{2m_W^3 + m_Z^3}{4\pi v^3} \approx 9.5 \times 10^{-3} \tag{15.116}$$

Recall now the condition for $\phi(T_c)$ we derived in sec. 4.7

$$\frac{\phi(T_c)}{T_c} > 1.3 \text{ or } > 1.0. \tag{15.117}$$

With $m_h^2 = 2\lambda v^2$, eq. 15.115 and eq. 15.116, this turns into condition a for the Higgs mass

$$m_h \leq 42GeV \text{ or } 48GeV. \tag{15.118}$$

Which is far too small, considering the experimental data from the LHC!

6 Validity of perturbative expansion

We concluded, that according to our calculation, the experimentally obtained value for the Higgs mass of about $\sim 125GeV$ rules out a 1^{st} order phase transition in the SM. Still, there is the question whether the validity of the perturbative treatment still holds at high temperature like those at the EW phase transition (see also [9]).

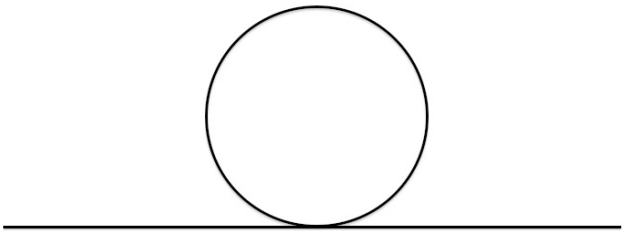

Figure 15.8: One loop contribution to the self energy (for the scalar theory).

The diagram shown fig. 15.8 is quadratically divergent and behaves like $\sim \lambda T^2$.
If we attach additional loops like shown in fig. 15.9 we obtain a behavior like

$$\lambda^{n+1}\frac{T^{2n+1}}{M^{2n-1}} = \lambda^2\frac{T^3}{M}\left(\frac{\lambda T^2}{M^2}\right)^{n-1} \tag{15.119}$$

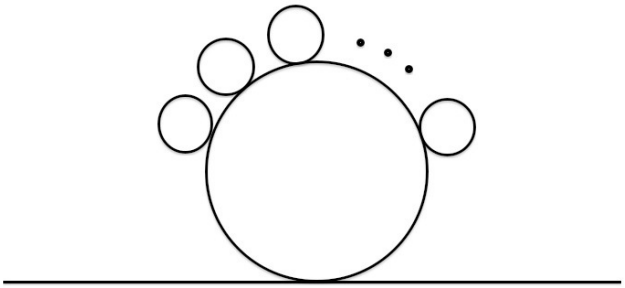

Figure 15.9: n-loop contribution to the self energy (for the scalar theory).

where M is a mass scale to rescale the additional powers of temperature.
We see that every additional loop yields an additional factor of

$$\alpha = \lambda \frac{T^2}{M^2} \tag{15.120}$$

which gives a condition for the validity of perturbative expansion:

$$\alpha << 1 \tag{15.121}$$

We see that the perturbative treatment loses its validity when $T \sim \frac{M}{\sqrt{\lambda}}$.

6.1 Simulation on the lattice

To overcome the problems associated with a perturbative treatment, it is possible to investigate the behavior of the theory by directly solving the corresponding path integral on a discretized space-time lattice. A detailed discussion of lattice gauge theory would be far beyond the scope of this report (for a short introduction, see for instance [4]), so I restrict myself to briefly dicuss one specific simulation by F. Csikor et. al. [10].

Here, the simulation was performed for pure SU(2) + Higgs theory, and later (perturbatively) extrapolated to the SM. The lagrangian was discretized as follows:

$$\begin{aligned} S[U_\mu, \phi] = \beta_s \sum_{sp} \left(1 - \frac{1}{2}\operatorname{Tr} U_{pl}\right) + \beta_t \sum_{tp} \left(1 - \frac{1}{2}\operatorname{Tr} U_{pl}\right) \\ + \sum_x \frac{1}{2}\operatorname{Tr}(\phi_x^+ \phi_x) + \lambda \left[\frac{1}{2}\operatorname{Tr}(\phi_x^+ \phi_x) - 1\right]^2 \\ -\kappa_s \sum_{\mu=1}^{3} \operatorname{Tr}(\phi_{x+\hat{\mu}}^+ U_{x,\mu} \phi_x) - \kappa_t \operatorname{Tr}(\phi_{x+\hat{4}}^+ U_{x,4} \phi_x) \end{aligned} \tag{15.122}$$

Where $U_{x,\mu}$ are the gauge links at point x in the direction μ; U_{pl} is the gauge invariant Wilson plaquette and $\kappa_s \kappa_t = \kappa^2$, $\beta_s \beta_t = \beta^2$ are the hopping parameters.

To keep it short, I shall just briefly scetch how to the simulation is performed:

- Start out with an arbitrary field configuration.
- Update Higgs- and gauge filelds at a random point (with Metropolis, Heatbath, ... algorithm).
- With each local update, measure the corresponing value of the Higgs field to get statistics.

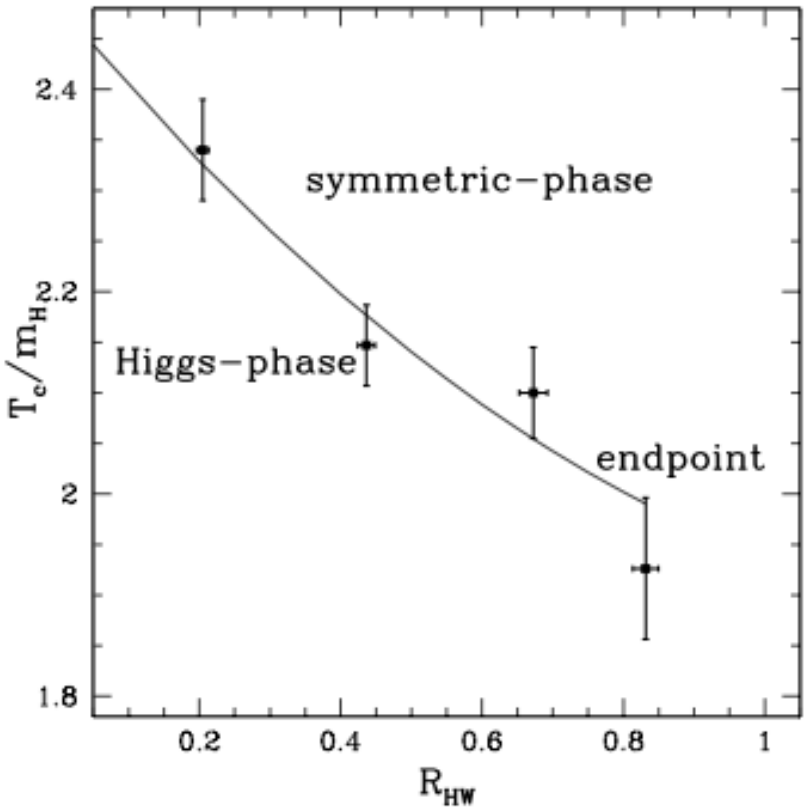

Figure 15.10: Lattice simulation of $SU(2)$ + Higgs theory. Quadratic fit of phase-transition line. 1^{st} order PT until endpoint at $R_{HW} = \frac{M_H}{M_W} = 0.827 \pm 0.017$ (see [10])

- Decrease the lattice spacing and extrapolate to the continuum limit.

It is very hard to determine the type of the phase transition by simply looking at the behavior of the "measured" Higgs expectation value. A possible solution can be found in terms of the so-called **Lee-Yang-Zeros**, which is also discussed in [10].

When looking at fig. 6.1, one sees that the endpoint for the 1^{st} order PT lies at a Higgs mass of $M_H = (66.5 \pm 1.4)GeV$, with SM-extrapolation at $M_H = (72.4 \pm 1.7)GeV$. Since the Higgs mass was experimentally found to be $M_H \approx 125GeV$, the lattice simulation does not change the conclusion we got from the perturbative calculations.

7 Conclusion & Outlook

Both perturbative (see sec. 5.3) and non-perturbative (sec. 6.1) calculations show that the Standard Model is not capable to describe the observed Baryon asymmetry we encounter today. This is another strong indice that the SM is not the ultimate theory to describe our Universe, and different models are needed!

One candidate would of course be Supersymmetry, and it is shown in [9] that a minimal supersymmetric extension of Standard Model (MSSM) may indeed fulfill the necessary requirements. A modest problem here is the lack of experimental data that would support the theory.
Another way to solve the problem would be the consideration of the physics of grand unified theories (GUTs) (like discussed in [7]). Here, Baryon number violating perturbative processes, out-of equilibrium decays and different CP-violating terms would provide new possibilities to explain the Baryon asymmetry of our universe.

Bibliography

[1] N.S. Manton F.R. Klinkhamer. *Phys. Rev.*, D30:2212, 1984.

[2] R. Singleton Jr. M. Dine, P. Huet. Baryogenesis at the electroweak scale. *Nuclear Physics*, B375:625–648, 1992.

[3] O. Philipsen. The sphaleron rate in the "symmetric" electroweak phase. *Phys. Lett.*, B358:210–216, 1995.

[4] M. Walzl G. Münster. Lattice gauge theory a short primer. Technical report, 2000.

[5] Koichi Funakubo et al. Cp-violating profile of the electroweak bubble wall. *Progress of Theoretical Physics*, 94(5):845–859, November 1995.

[6] A. Pitch. The standard model of electroweak interactions. Technical report, Departament de Física Teòrica and IFIC, Universitat de València, Dr. Moliner 50, E-46100 Burjassot, València, Spain, November 1994.

[7] M. S. Turner E. W. Kolb. *The Early Universe*. Westview, 1990.

[8] J. S. Langer. Statistical theory of the decay of metastable states. *Annals of physics*, 54:258–275, 1969.

[9] Mariano Quiros. Finite temperature field theory and phase transitions. Technical report, Instituto de Estructura de la Materia (CSIC), Madrid, 1998.

[10] J. Heitger F. Csikor, Z. Fodor. Endpoint of the hot electroweak phase transition. *Phys. Rev. Lett.*, 82, 1999.

[11] Mark Trodden. Electroweak baryogenesis. *Rev. Mod. Phys.*, 71:1463–1500, 1999.

[12] C. Jarlskog. A basis independent formulation of the connection between quark mass matrices, cp violation and experiment. *Zeitschrift für Physik C*, 29:491–497, 1985.

[13] James M. Cline. Baryogenesis. Technical report, McGill University, Dept. of Physics, Montreal, Qc H3A 2T8, Canada, 2006.